Endoplasmic Reticulum Membrane Contact Sites: Roles in Phospholipid Synthesis and Cell Polarity

by

SHABNAM TAVASSOLI

B.Sc., The University of Tehran, 2005

A THESIS SUBMITTED IN PARTIAL FULFILLMENT OF

THE REQUIREMENTS FOR THE DEGREE OF

DOCTOR OF PHILOSOPHY

in

THE FACULTY OF GRADUATE STUDIES

(Cell and Developmental Biology)

THE UNIVERSITY OF BRITISH COLUMBIA

(Vancouver)

August 2013

ABSTRACT

Membrane contact sites between the endoplasmic reticulum (ER) and other organelles are present in all eukaryotic cells. Their roles in calcium signaling and transport between the ER and the plasma membrane (PM) or the ER and mitochondria are quite well understood, but the molecular mechanisms underlying their roles in lipid synthesis and transport remains unknown. In order to identify the importance of organelle-ER contact sites, I used Saccharomyces cerevisiae - a model organism that has proven to be a particularly informative for studying lipid-related cellular processes. Previously, we found a role for an ER anchor protein, Scs2, being important for PM-ER contact sites. Further, *SCS2* interacts genetically with *ICE2*, an ER gene with unknown function. In *Chapter 2*, I investigated a role for PM–ER contact sites in regulating phosphatidylcholine (PC) synthesis and I found that *Δscs2Δice2* cells are choline auxotrophs and PM–ER contacts are required for PC synthesis. Osh2 and Osh3, the oxysterol-binding protein homologues in yeast, rescued the choline auxotrophy phenotype of *Δscs2Δice2* cells but did not restore pmaER, indicating that they may function with Opi3 in PC synthesis. In search for regulators of pmaER, we identified the phosphatidic acid phosphohydrolase Pah1 that seems to be involved in establishing pmaER, independent of its enzymatic activity. Finally, we proposed that PE to PC synthesis by Opi3 happens *"in trans"* at PM-ER contacts. In *Chapter 3*, I aimed to discover novel genes involved in PE synthesis/traffic from ER to mitochondria. By doing a genome-wide screen for *CHO2*, we identified genetic interactions between *CHO2* and Emc proteins indicating that Emc proteins are important for PE metabolism and we proposed that Emc facilitates PS transfer from the ER to mitochondria for PE synthesis. In *Chapter 4*, I investigated for roles of *SCS2* in polarized growth. I found a physiologically important function of the ER diffusion barrier, which is to restrict diffusion of the spindle from mother to bud until M phase. Scs2 interacts directly with the spindle capture protein Num1 and it prevents Num1 from diffusing from the mother into the bud during S and G2 phases.

PREFACE

1. The work in Chapter 2 was published as:

Tavassoli, S., Chao, J.T., Young, B.P., Cox, R.C., Prinz, W.A., de Kroon, A.I., and Loewen, C.J. (2013). Plasma membrane-endoplasmic reticulum contact sites regulate phosphatidylcholine synthesis. EMBO Rep

Contributions: S.T. and C.J.R.L. conceived, designed and analyzed the experiments and S.T., B.P.Y. and C.J.R.L wrote the manuscript. S.T. performed all the experiments except:

- B.P.Y. performed the Δ*scs2*Δ*ice2* suppressor screen and the *in vivo* PE methylation assays in Fig. 2.2 A-B-C-D, Fig. 2.5 B-C, and Fig 2.6 E-D.
- J.C.T. performed experiments in Fig. 2.4 D, Fig 2.5 D, Fig. 2.9 A-B-C-D-E-F, Fig. 2.10 E and Fig. 2.11 .
- W.A.P developed the *in vivo* PE methylation assays.
- C.R.C. and A.I.P.K. designed and performed the *in vitro* "*in trans"* methylation assays in Fig. 2.10 A-B-C-D.

2. The work in Chapter 3 was submitted for publication as:

A Conserved ER-Membrane Complex Facilitates Phospholipid Exchange Between the ER and Mitochondria. Lahiri, S.,* Chao, J.T.,* Tavassoli, S.,* Wong, A.K.O., Young, B.P., Loewen, C.J., Prinz, W.A.

* These authors contributed equally to this work.

Contributions: S.T. performed:

- *CHO2* and *EMC6* SGA screens in Fig 3.1 A-B-C-D., Fig 3.2 A-B-C-D and identified the EMC and TOM5 genes from *CHO2* SGA.
- Table 3.2, Table 3.3, and Table 3.4, which were related to *CHO2* and *EMC6* SGA screens.
- Tagging EMC genes with GFP and examined the complex organization in Fig. 3.3 A-C-D.

Others performed other experiments of this chapter and this work is in preparation for publication. The section of the manuscript contains S.T. results was written by S.T. and C.J.R.L.

3. A more complete version of the work in Chapter 4 has been submitted for publication as:

Polarization of the Endoplasmic Reticulum is mediated by an ER-Septin Tethering Complex. Chao, J.T., Wong, A.K.O., Tavassoli, S., Young, B.P., Chruscicki, A., Fang, N.N., Howe, L.J., Mayor, T., Foster, L.J., and Loewen, C.J.

Contributions: J.T.C performed majority of the experiments, which were not presented in *chapter 4* but will be the mail body of the manuscript. S.T. performed Fig. 4.3, Fig. 4.4 and Fig. 4.5 A-B-D. S.T. and C.J.R.L wrote the results presented in *chapter 4* for the manuscript version of this chapter.

TABLE OF CONTENTS

LIST OF TABLES

LIST OF FIGURES

LIST OF ABBREVIATIONS

ALS amyotrophic lateral sclerosis

Δ gene deletion

3D three dimensional

PA phosphatidic acid

PC phosphatidylcholine

PE phosphatidylethanolamine

PI phosphatidylinositol

PL phospholipid

PS phosphatidylserine

PIPs phospoinosides

pmaER PM-associated ER

cecER central cisternal ER

PAM PM-associated membranes

MAM Mitochondria-associated membrane

CL cardiolipin

DAG diacylglycerol

DTT dithiothreitol

ER endoplasmic reticulum

ERAD endoplasmic reticulum-associated protein degradation

EM electron microscopy

EMC ER-membrane protein complex

ERMES ER mitochondria encounter structure

FM4-64 Fei Mao dye 4-64

Fld fatty liver dystrophy

GFP green fluorescence protein

GST glutathione S-transferase

GlcCer glucosylceramide

CDP-DAG cytidine diphosphate-diacylglycerol

CRAC Ca^{2+} release-activated Ca^{2+}

DMSO dimethylsulfoxide

MAM Mitochondria-associated membrane

HPLC high-performance liquid chromatography

IP3 inositol trisphosphate

µg microgram

µL microliter

µm micrometer

M molar

µCi microcurie

NSF N-ethylmaleimide-sensitive factor

mg milligrams

LTPs lipid transfer proteins

w/v weight/volume

Dex glucose

Gal galactose

NBD Nitro-2-1,3-BenzoxaDiazol-4-yl

OPI1 over production of inositol

ORD OSBP related domain

ORP OSBP related protein in humans

OSBP Oxysterol binding protein

OSH OSBP homologues in *Saccharomyces cerevisiae*

PCR polymerase chain reaction

PCA protein complementation assay

PME phosphatidylmonomethylethanolamine

RFP red fluorescent protein

RT room temperature

SD synthetic defined

SM sphingomyelin

SOCE store-operated Ca^{2+} entry

SC synthetic complete media

TAG triacylglycerol

TLC thin layer chromatography

ts temperature sensitive

TGN trans-Golgi Network

VAP VAMP associated protein

YFP yellow fluorescent protein

YNB yeast nitrogen base

UPR unfolded protein response

VDAC voltage dependent anion selective channel

Genetics Nomenclature:

Wild type alleles of *S.cerevisiae* are represented by capitalized and italicized letters (e.g. *SCS2*). Mutant alleles are denoted by lower cased italics indicating a deletion (e.g. Δ*scs2*), point mutation (e.g. C1513A, esp1 C1531A) or conditional allele (e.g. *mmm1-1*). Genes are under their endogenous promoter unless another is indicated (e.g. GAL1, GAL1/10). Gene products have their first letter capitalized and are non-italicized (Scs2). Plasmids/vectors are in dictated by the little "p" and are italicized (*pSCS2).*

ACKNOWLEDGMENTS

My greatest thank to my PhD supervisor, Chris Loewen, who introduced me to the fascinating world of lipids. I could not finish this endeavor without his guidance and support and it has been an honor to be his first PhD student. I would also like to thank my committee members: Dr. Lacey Samuels, Dr. Vivien Measday and Dr. Robert Nabi for their time, advice and critique of my research.

Thanks to all members of the Loewen lab for making our lab such a great place to be at. Thanks for all the discussions on science, and especially for many fun times. To all my lab mates from the Allan, Bamji, and Tanentzapf labs, thanks for making our shared space a wonderful place. I truly enjoyed the work environment at the Life Sciences Institute for having outstanding research groups that I have greatly benefited from.

I would like to acknowledge the University of British Columbia Graduate Fellowship Research award that I received during my PhD.

I would like to thank my parents Roshanak and Aliakbar and my brother Alireza who have supported me in every decision I have made and have been encouraging, loving, accepting and much more. Finally, I would like to thank Peiman Amini for his love and support, and for making me see myself in a different, better way.

1. INTRODUCTION

1.1. THE STRUCTURE AND FUNCTION OF ENDOPLASMIC RETICULUM (ER)

The endoplasmic reticulum (ER) is the organelle primarily responsible for both the synthesis and folding of secreted and membrane proteins and is the site of lipid biosynthesis. It also functions as one of the main cellular calcium stores. The eukaryotic ER has perhaps one of the most complex organelle structures, consisting of morphologically distinct domains: i) the nuclear envelope (NE), surrounds the nucleus and is comprised of two large, flat membrane bilayers; ii) an extensive network of both highly inter-connected fenestrated tubular membranes that are linked by three-way junctions and flat cisternal sheets which all referred to peripheral ER (Baumann and Walz, 2001; Fehrenbacher et al., 2002). The shape of the peripheral ER is variable among different eukaryotes, reflecting specialized functional requirements.

Historically, the ER was classified, based upon its appearance under an electron microscope, into the rough endoplasmic reticulum (rER) and the smooth endoplasmic reticulum (sER) (Shibata et al., 2006). The rER is occupied by ribosomes, and is therefore actively involved in synthesis of proteins. The rER has also been associated with posttranslational processes such as N-linked protein glycosylation and protein quality control (Ellgaard and Helenius, 2003; Helenius and Aebi, 2004). The sER is mainly involved in Ca^{2+} signaling in neurons and muscle cells and different detoxification processes in liver cells (Rossi et al., 2008; Voeltz et al., 2002). Cells that are specialized for lipid metabolism are enriched for sERs (Baumann and Walz, 2001) and vesicle budding occurs from a part of the sER called transitional ER (Rossi et al., 2008; Voeltz et al., 2002). Simply put, the morphological distinction between the two type of ER are that the rER is usually made of ribosome-covered sheets (cisternae), whereas the sER usually appears as a tubular network devoid of bound ribosomes (Shibata et al., 2006). This classification came from the comparison of the EM images of ER structure in secretory cells, such as those in the pancreas that are filled extensively with ER cisternae covered with ribosomes, to muscle cells occupied entirely by tubular ER free of ribosomes (Porter and Palade, 1957). However, in addition to regular ER sheets, there are fenestrated ER sheets, which were described originally by Palade (Palade, 1956). Fenestrated ER sheets have high curvature

membranes and varying amount of ribosomes (Novikoff et al., 1983; Palade, 1956; Porter and Palade, 1957; Rambourg et al., 2001).

For a long time, the molecular mechanisms underlying the formation of sheets and tubules of the ER and consequently rough and smooth ER were have been elusive. In an *in vitro* assay, it was shown that the cytoskeleton is not required for the shape of the tubular ER, rather there should be factors present within the ER membrane itself that determine its shape (Dreier and Rapoport, 2000). A few years later, it was shown that a class of evolutionarily conserved ER proteins called reticulons (Rtns) and DP1/Yop1 are important for ER tubule formation (Voeltz et al., 2006). Rtns are notable for their signature RHD (reticulon homology domain) and localization to regions of high membrane curvature in the ER, such as the tubules and edges of cisternae, to the exclusion of membrane domains that lack curvature, for example the nuclear envelope and the plane of the cisternae (Zurek et al., 2011).

Very little was known about how cisternae are shaped until it was recently shown that Climp-63 is a sheet-inducing factor in mammalian cells (Shibata et al., 2010). The authors suggested that the coiled-coil domain of Climp-63 serves as a spacer between the sheets in the ER lumen, likely by forming bridges, and is not found in high-curvature areas (e.g. ER tubules) (Shibata et al., 2010). Climp 63, along with the translocon complex, localizes to ER sheet to generate the rER, while DP1 and reticulons partition to the edges of sheets and ER tubules to induce a high degree of curvature. Additional factors that determine the morphology of peripheral ER sheet may exist in mammalian cells. Climp-63 has no homologue in *S. cerevisiae* and the abundance of the reticulons and Yop1 might determine the ratio of ER sheets and tubules in yeast (Shibata et al., 2010). It is plausible that sheet-inducing proteins exist similarly in yeast; however, the current view is that curvature-stabilizing proteins are the major players in yeast peripheral ER morphology.

1.1.1. ER morphology of Saccharomyces cerevisiae

In spite of this heterogeneity and compartmentalization of biological activities, fascinatingly, the ER is one contiguous organelle that is capable of exchanging information between regions. Using budding yeast, which has multiple ER domains (cisternae and tubules,

rough and smooth), as a model for understanding ER structure and biogenesis, a recent paper by the Voeltz group has used EM and tomographic three dimensional (3D) reconstruction to significantly advanced our knowledge of ER structure (Fig. 1.1) (West et al., 2011). Similarly to animals, the structure of the ER in budding yeast consists primarily of the nuclear envelope and the peripheral ER (Preuss et al., 1991; Prinz et al., 2000; Voeltz et al., 2002). The recent 3D EM reconstruction revealed that the yeast peripheral ER can be divided into three distinct domains: (i) pmaER, the PM-associated ER (previously referred to as the cortical ER, as it forms a meshwork-like structure beneath the PM), (ii) cecER, central cisternal ER, which had not been described before, and (iii) tubER, corresponding to individual cytoplasmic ER tubules (West et al., 2011).

(i) pmaER, the PM-associated ER: The pmaER has previously been recognized as the cortical ER, described as a tubular network structure underlying the PM (Prinz et al., 2000; Voeltz et al., 2002). However, consistent with the most recent and comprehensive study of the yeast peripheral ER by the Voeltz group (West et al., 2011), I will refer to it as pmaER. This recent 3D structural analysis with ~ 4 nm resolution revealed that the pmaER contains both tubular and cisternal elements. A unique aspect of the peripheral ER in yeast is the existence of approximately 1100 contact sites between ER and PM in an average series of sections done by three-dimensional image reconstruction (Pichler et al., 2001; West et al., 2011) (see Section *1.1.4.4.* for membrane contact sites). The pmaER is completely excluded from the bud neck and is not inherited through the neck. The pmaER membrane that faces the PM is devoid of ribosomes, consistent with what has been observed for mitochondria-ER and Golgi-ER contact sites, whereas the cytoplasmic face of pmaER has the highest ribosome density (West et al., 2011).

ii) cecER, central cisternal ER: The cecER had not been described before, primarily due to its resemblance to ER tubules in 2D electron micrographs – a resemblance that led researchers to assume only one structure (tubER) traversed the cytoplasm. However, a 3D rendering of the ER revealed a large, flat sheet occupied by ribosomes pointing out from the nuclear ER in the mother towards the bud, a structure that came to be referred to as cecER (West et al., 2011). The orientation of cecER suggests that it likely provides a major source of ER for the growing bud. The ribosome density of yeast cecER is similar to pmaER.

(iii) tubER, tubular ER: The nuclear ER and pmaER are connected by only a few individual linear ER tubules (Fehrenbacher et al., 2002). The tubER has less ribosome than cecER and pmaER, and is found throughout the cytoplasm. It functions to connect the nuclear envelope to the cecER, the cecER to the pmaER, and pmaER domains. tubER is also seen forming contacts with other organelles.

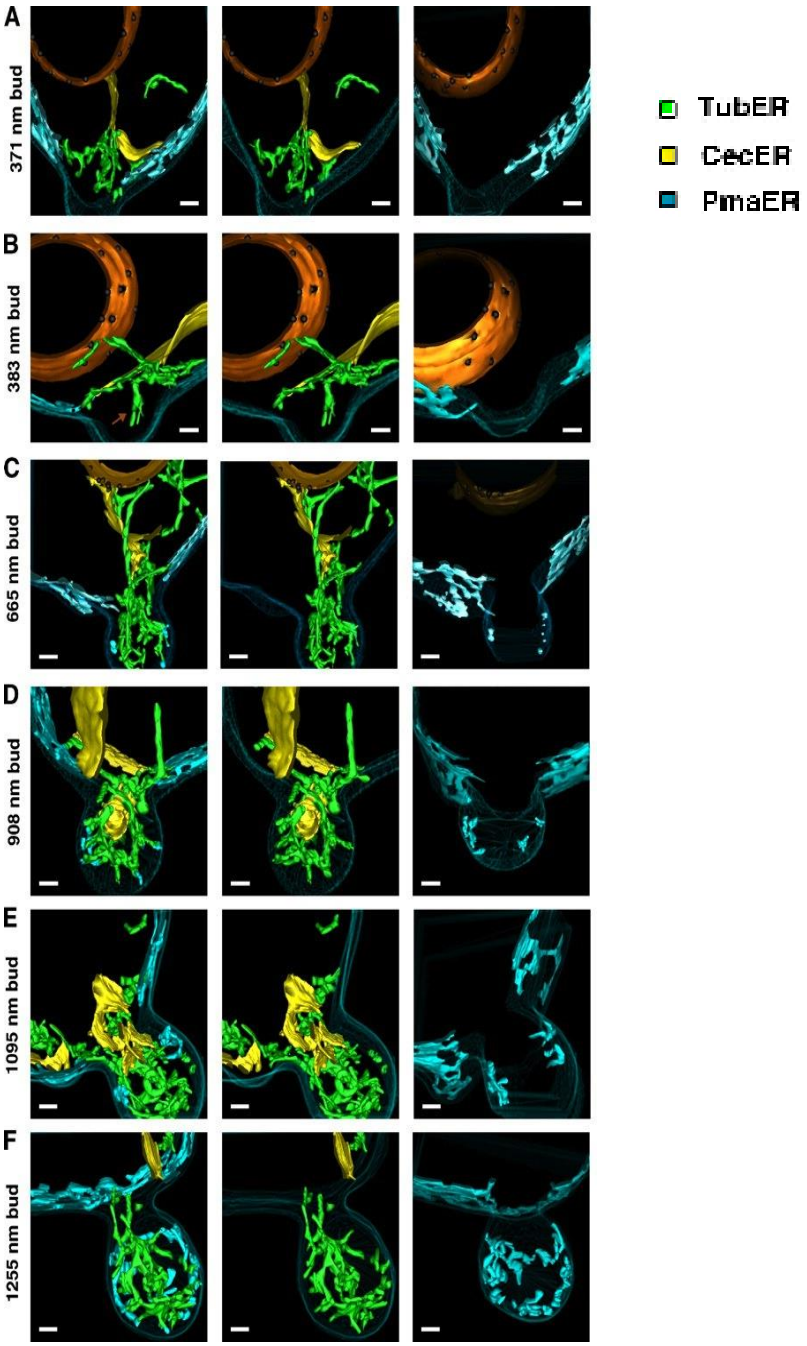

Figure 1.1: Different ER domains and their organization in the mother and bud cells during budding.

(A–F) 3D models derived from 200-nm-thick section serial tomograms in six different wide type cells ordered by increasing bud sizes. Panels show domain distribution of all ER domains (left), cecER and tubER (yellow and green domains in middle), and pmaER alone (blue on right) (adapted from (West et al., 2011)).

1.1.2. Inheritance of ER in Saccharomyces cerevisiae

Many organelles, such as the ER are essential for viability; therefore, it is essential that new daughter cells inherit a fraction of ER during cell division. During the budding process in yeast, the nuclear envelope and peripheral ER use distinct mechanisms for inheritance into the new daughter cell. The nuclear envelope uses a microtubule-dependent mechanism (Heil-Chapdelaine et al., 2000; Schwartz et al., 1997), referred to as "nuclear migration", in which it is segregated with the nucleus during anaphase (see Section *4.2.2.*). The inheritance of the peripheral ER, on the other hand depends primarily on the actin cytoskeleton in yeast (Du et al., 2004; Estrada et al., 2003; Prinz et al., 2000).

In animal cells, ER tubules align along the microtubules, as evidenced by the inhibition of their movement using nocodazole, a drug which disrupts microtubule organization (Waterman-Storer and Salmon, 1998). By contrast, in yeast, formation and maintenance of ER structure does not depend on microtubules, as nocodazole does not influence either the structure or dynamics of the ER. In yeast, the maintenance of the ER structure instead depends on actin filaments, which also play a role in ER dynamics (Prinz et al., 2000). When actin polymerization is blocked using latrunculin A, the number and movement of ER tubules are reduced (Estrada et al., 2003; Prinz et al., 2000). Moreover, defects in ER inheritance have been identified in yeast, carrying a temperature sensitive allele of actin genes (Du et al., 2004). During polarized growth in yeast, the actin cytoskeleton undergoes rearrangement throughout the cell cycle. During G1 and S phase, actin cables are oriented towards the growing bud and cortical actin patches are polarized in this direction (Madden and Snyder, 1998). As a consequence of actin polarization, particular exocytic vesicles (Johnston et al., 1991) and mRNAs (Aronov et al., 2007) are transported along the actin cables into the daughter cell. Additionally, the yeast PM and the ER

are both compartmentalized into a mother and a bud domain during polarized growth by the formation of a diffusion barrier at the bud neck. This barrier is created by the septin ring, which is a membrane-associated cytoskeletal structure (Barral et al., 2000; Luedeke et al., 2005). Such compartmentalization might function in retaining the localized mRNAs and their protein products in the bud for establishment of cell polarity. Septin involvement in compartmentalization of the ER domains between mother and bud suggests that septins might restrict diffusion of ER proteins through the neck and create an "ER diffusion barrier". In yeast, the ER diffusion barrier has been found to be dependent on the septin Shs1 and on two components of the polarisome, Bud6 and Pea2 (Luedeke et al., 2005). Similar to yeast, in neurons, the ER in dendritic spines and at dendritic branch points is compartmentalized (Cui-Wang et al., 2012). This compartmentalization is again dependent on septins (Tada et al., 2007), suggesting that a similar diffusion barrier is present in the ER in metazoans. It has been proposed that direct contact between the ER and septins creates the ER diffusion barrier (Luedeke et al., 2005), although the molecular nature of this relationship is not known.

The yeast ER is asymmetric during mitosis, with respect to some mRNAs (Shepard et al., 2003). One of the best-characterized examples of the asymmetric mRNA localization in yeast is ASH1 mRNA. Ash1 is a transcription inhibitor that specifically suppresses the expression of the HO endonuclease. This nuclease catalyzes the recombination of genomic DNA at the *MAT* locus, thereby promoting the mating-type switch in haploid yeast cells (Cosma, 2004). The motor protein Myo4 travels along actin filaments towards the bud tip while it is attached to its adapter protein She3. For mRNA transport, She3 binds to the RNA binding protein She2 and the complex of all three proteins together with the mRNA is transported towards the bud (Aronov et al., 2007; Estrada et al., 2003; Munchow et al., 1999; Takizawa et al., 2000). Additionally, the mRNAs of two ER resident proteins involved in lipid biosynthesis, Erg2 and Lcb1, were co-fractionated with the ASH1 mRNA (Shepard et al., 2003; Takizawa et al., 2000). These observations are consistent with these mRNAs being translated on the surface of the ER and suggest that subfraction of these mRNAs probably contributes to *de novo* synthesis and expansion of the ER in the bud (Ouellet and Barral, 2012). Together, ER asymmetry and movement of bud-specific mRNAs into the bud ensures the asymmetric partition of ER-associated factors (Ouellet and Barral, 2012).

Inheritance of ER is initiated in early S-phase. ER tubules are inherited first as previously suggested (Du et al., 2004; Estrada et al., 2003). Previous works suggested that these ER tubules

are captured at the bud tip, which then branch out to form junctions in multiple directions with the PM to make the reticular network that is the pmaER (Du et al., 2004; Estrada et al., 2003; Fehrenbacher et al., 2002). However, West et al. have found that the source of an inherited ER is from both cecER and ER tubules domains and not from the pmaER (West et al., 2011). In this elegant work, authors showed that ER tubules and cecER move along the mother-bud axis on polarized actin cables and are subsequently depleted from the mother cell as the bud grows. ER tubules form a 'nexus' near the center of the bud, not at the bud tip, and projects radially outward toward the bud cortex. The pmaER is completely excluded from the bud neck and is reestablished in the bud as it grows (West et al., 2011). It is possible that the pmaER is not inherited because it is attached to the PM and/or because it cannot traverse the septin ring located at the bud neck (Luedeke et al., 2005).

Several genes have been identified to be involved in inheritance of the ER in yeast, acting at different stages in the process. Besides their function in mRNA transport, Myo4 and She3 are also responsible for the inheritance of the ER as they are required for the orientation of ER tubules from mother to daughter cells. This transport is independent of She2 but functions in parallel to mRNA transport (Estrada *et al.* 2003). The Aux1 (Swa2), exocyst (Sec3, Sec8), translocon (Sec61, Seb1, Sss1), reticulons (Rtn1, Rtn2, Yop1), Ice2 and Scs2 proteins are important for formation of the pmaER and anchoring the ER tubules in the bud. Aux1 is a J-domain containing protein whose loss causes a delay in the transport of pmaER elements into the new bud and accumulation of abnormal ER structures throughout the cytoplasm, through its exact molecular impact on ER inheritance is still unclear (Du et al., 2001). Sec8 and Sec3 are two subunits of a vesicle-tethering complex known as the exocyst. Δ*sec8* show both a lack of ER membrane formation as well as early Golgi cisternae (Toikkanen et al., 2003; Wiederkehr et al., 2003) while Δ*sec3* cells have an aberrant distribution of ER. It has been suggested that Sec3 is required as an anchor for ER tubules that move to the daughter cell in addition to its role in polarized exocytosis, likely through its physical interaction with the translocon complex (Du et al., 2004; Wiederkehr et al., 2003). The Sec61 translocon complex (Sec61, Sbh1, and Sss1) interacts physically and genetically with the exocyst complex, thus providing an additional molecular bridge between ER and PM (Du et al., 2004; Wiederkehr et al., 2003). Reticulons are involved in shaping the membrane bilayer of ER tubules (see Section *1.1.*) in multiple eukaryotes, including animals, plants, and yeast (Voeltz et al., 2006). In *S. cerevisiae*, reticulons stabilize and maintain membrane curvature of ER tubules. Rtn1 co-purifies with the exocyst

component, Sec6 (De Craene et al., 2006) and Sbh1 that is not part of the translocon complex (Feng et al., 2007). Rtns/Yop1 and membrane curvature control the amount of pmaER that covers the PM. In the absence of reticulons and Yop1, the mother cell pmaER appears as a single large ER cisternae that is lacking any ER fenestration. Deletion of Rtn1/2 and Yop1 proteins in *S. cerevisiae* dramatically changes the peripheral ER into a flat cisternal shape structure, leading to a loss of cecER and pmaER cisternal fenestrations (West et al., 2011). Moreover, in these mutants, the peripheral ER adapts a higher degree of association with PM, possibly due to a loss in ER membrane. *ICE2* is a fungal gene encoding an ER protein but with unknown molecular function. Deletion of *ICE2* causes defects in the morphology of the ER tubular network indicating that Ice2 contributes to forming and maintaining the pmaER network in budding yeast (Estrada de Martin et al., 2005). Ice2 has an aggravating genetic interaction with *SCS2*, an integral ER membrane protein that appears to function in the attachment of ER to PM (Loewen et al., 2007). In cells lacking *SCS2*, although ER tubules are delivered into the bud and appear normal, Δ*scs2* cells show reduced pmaER, especially in buds. Cells lacking both *SCS2* and *ICE2*, however, have more severed defects in pmaER structure, consistent with the genetic interaction between these genes (Loewen et al., 2007) (see Section *1.4.* for more details on Scs2). In general, with the exception of cells lacking *SCS2*, there are no serious ER defects in the single-gene deletion mutants mentioned above. In all of these mutants, ER defects are not observed in mother cells or large buds, for all intensive purposes appearing normal other than a delay in ER delivery. Since most of the proteins discussed above are localized to the bud tip, they likely play a role in transport or capture of ER tubules during budding, but not in formation of the pmaER network. Many aspects of the molecular components and underlying mechanisms of how pmaER is made and distributed in the new bud are still unknown.

1.1.3. ER stress

Environmental disturbance such as glucose deprivation, hypoxia, dysregulation of calcium homeostasis, anoxia, infection by viruses, and accumulation of misfolded proteins can cause ER stress (Kaufman, 2002; Lai et al., 2007; Schubert et al., 2000). Two major pathways that deal with ER stress are the UPR (Unfolded Protein Response) and ERAD (ER Associated Degradation) will briefly be described here. It has been shown that both ERAD and the UPR are

critical for maintaining efficient protein degradation and minimizing ER stress. Chronic ER stress has been linked to various pathophysiological states including cancer (Tsai and Weissman, 2010), neurodegenerative diseases (Bernales et al., 2012) and inflammation due to obesity or diabetes (Hummasti and Hotamisligil, 2010). Recently, it has been shown that dysregulation of lipid homeostasis can also cause ER stress (Basseri and Austin, 2012). The UPR and ERAD may play a critical role in regulation of different lipid classes such as phospholipids, sphingolipids and sterols in the ER (Raychaudhuri et al., 2012).

1.1.3.1. Unfolded protein response, UPR

To cope with the accumulation of unfolded proteins in the ER, cells evolved an adaptive mechanism called the UPR (Bernales et al., 2006). The UPR is an evolutionary conserved response was discovered originally in budding yeast (Shamu et al., 1994) and is one of the major signaling pathways controlling ER homeostasis. In yeast, an integral ER protein Ire1 (Inositol-requiring protein 1) is the sole UPR sensor, serving to initiate the UPR pathway. Ire1 has a luminal dimerization domain and a cytosolic domain with serine/threonine kinase and RNAse activities (Ron and Walter, 2007). In response to unfolded proteins, Ire1 both dimerizes and undergoes autophosphorylation in order to induce activity, leading to splicing of the *HAC1* mRNA. This posttranscriptional modification of *HAC1* mRNA yields expression of the active Hac1 – a transcription factor protein capable of inducing expression of UPR-associated genes leading to their induction and ER membrane expansion (Ron and Walter, 2007). In yeast, inositol availability dynamically regulates phospholipid synthesis (see Section *1.2.2.1*) and interestingly inositol deficiency induces the UPR (Cox et al., 1997). The UPR massively expands the amount of ER membrane by upregulating lipid synthesis and increases expression of protein chaperones and other enzymes involved in protein folding to increase the protein folding capacity of the ER (Schuck et al., 2009).

Similar to yeast IRE1/HAC1, mammals have the IRE1/XBP1 UPR cascade. Activated Ire1 splices XBP1 mRNA (Yoshida et al., 2001) and activated XBP1 binds to promoter elements of UPR target genes to activate them. Unlike yeast, two additional UPR branches exist in mammals: i) PERK, protein kinase RNA-like ER kinase, the ER-localized transmembrane protein that phosphorylates and inactivates a translation initiation factor eIF2a and ii) ATF6,

activating transcription factor 6, which upon ER stress is transported to the Golgi to be cleaved to form a soluble transcription factor fragment "f". ATF6f, then moves to the nucleus to activate UPR targeted genes (Kimata and Kohno, 2011; Ron and Walter, 2007). In mammals, Ire1 induces multiple cellular events (Hetz and Glimcher, 2009), increasing the complexity of their UPR when compared to *S. cerevisiae*. Moreover, there is cross talk between the three UPR signaling pathways IRE1, PERK and ATF6, further compounding the intricacy of the response.

1.1.3.2. Endoplasmic reticulum-associated degradation, ERAD

The UPR is coordinated with another quality control pathway, known as ERAD (Travers et al., 2000). One important consequence of the UPR is the up-regulation of ERAD. The ERAD pathway eliminates aberrant proteins from the secretory pathway, a function that becomes essential if the concentration of misfolded proteins becomes too high and/or if the induction of the UPR simultaneously compromised (Ng et al., 2000; Travers et al., 2000). ERAD can be broken down into four steps: substrate recognition, ubiquitination, retro-translocation to the cytosol, and proteasome-mediated degradation. Though it is not currently known how substrates are retro-translocated from the ER, the ERAD substrates may be present either in the ER lumen, ER membrane, or cytoplasm, which influences the types of chaperones with which they interact (Brodsky, 2007).

Yeast have at least three different ERAD pathways for removing misfolded proteins. These pathways are known as ERAD-L, which responds to misfolded soluble or membrane bound proteins in the ER lumen, ERAD-M, responsible for misfolded ER membrane proteins and ERAD-C, coordinating the response to misfolded proteins in the cytosol (Vashist and Ng, 2004). Briefly, in ERAD-L, the substrate is recognized luminally by Yos9 and Hrd3 of the Hrd1 complex. The substrate is passed across a translocon pore that is likely composed of Sec61 proteins and subsequent ubiquitination is mediated by Ubc7 and Hrd1. In ERAD-M, unneutralized polar/charged residues of substrate transmembrane segments are recognized by the polar face of the Hrd1 transmembrane domain. Ubiquitination and extraction then coordinate similarly to ERAD-L (Xie and Ng, 2010). In ERAD-C, misfolded cytosolic domains of membrane substrates are recognized by cytosolic chaperones and the RING cytosolic domain of Doa10. Again, the E2 enzyme Ubc7 promotes ubiquitination, and extraction is mediated by the

Cdc48 complex (Xie and Ng, 2010). In contrast to yeast, as many as 16 ubiquitin ligases have so far been implicated in mammalian ERAD (Claessen et al., 2012), including Hrd1, Gp78 (also called AMFR) and TEB4 (orthologous to Doa10). This level of complexity likely reflects an evolutionary adaptation in response to a more complex metazoan proteome. Together, the UPR and ERAD ensure that proper quality control is maintained throughout protein synthesis.

1.1.4. Membrane contact sites or organelle-ER associated membrane

The ER contacts many other membrane-bound compartments in the cell. Regions of the ER that are in close apposition to other organelles being called membrane contact sites (Levine, 2004; Levine and Loewen, 2006; Vance, 1991). Membrane contact sites are thought to be important sites of lipid exchange and signaling yet how they form and are regulated remain important questions. Association of the ER with the Golgi apparatus, mitochondria, peroxisomes, vacuoles and PM has been detected by electron microscopy (Achleitner et al., 1999; Ladinsky et al., 1999; Pan et al., 2000; Pichler et al., 2001) and biochemical studies (Achleitner et al., 1999; Pichler et al., 2001) (Fig. 1.2). In most cases, fusion between membranes of the ER with these organelles is not seen; however, these membranes have very close apposition (from 10 to 50 nm) (Achleitner et al., 1999; Pichler et al., 2001). Physical contacts between the ER and other organelles have many different names in literature. For example, in the case of the contacts between the ER and the PM, names include triads (Wagenknecht et al., 2002), dyads (Bassot and Nicolas, 1987), PM-associated membranes (PAM) (Pichler et al., 2001), peripheral couplings (Treves et al., 2004) and PM-ER junctions (Levine, 2004) exist. For simplicity, I will use the term PM-ER contacts and, in case of other ER contact sites, the most common name used in literature, for example NVJs, which are described in the next section.

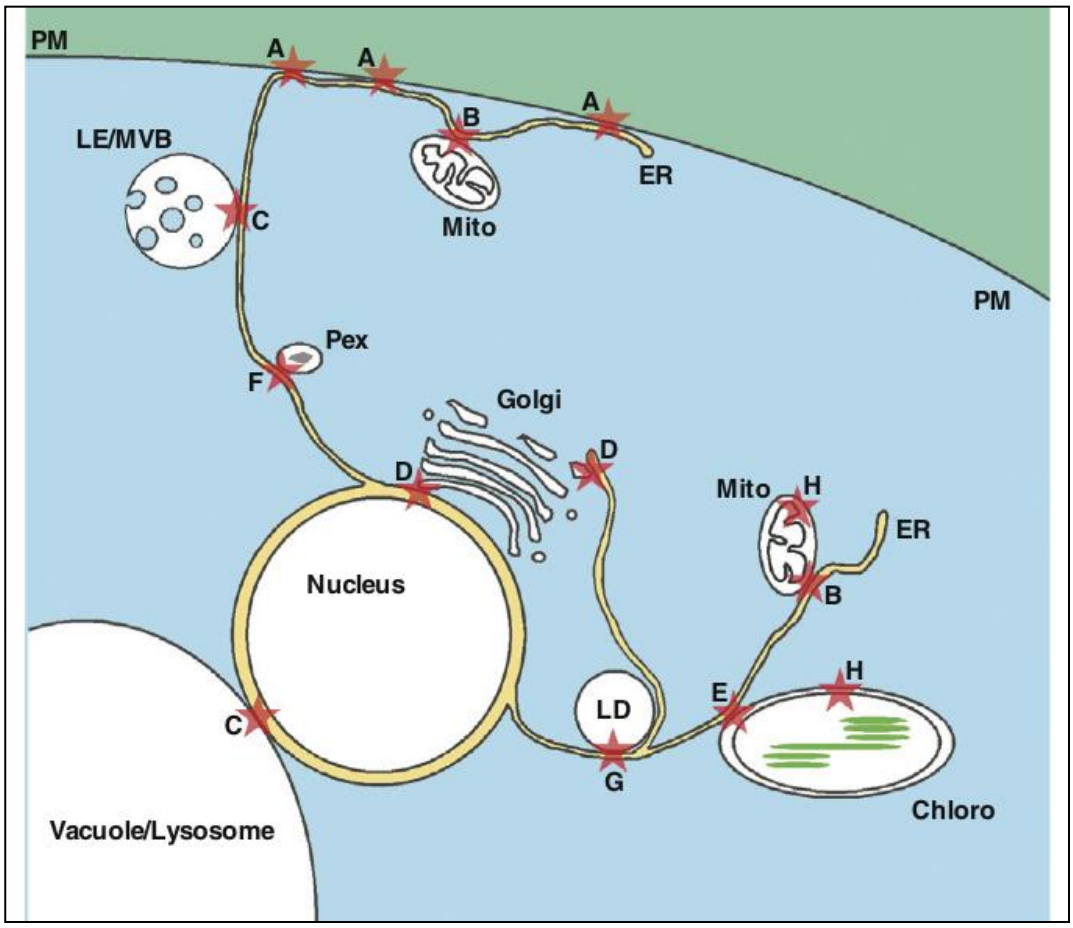

Figure 1.2: Various contact sites between membranes of the ER and other organelles.

(A) PM-ER (B) Mitochondria-ER (C) Late endosome (LE)/multivesicular bodies (MVB)-ER. In yeast there are contacts between the nucleus and vacuole (NVJ). (D) Golgi-ER (E) chloroplast (chloro)-ER. (F) Peroxisome (Pex)-ER (G) Lipid droplets (LD)-ER. (H) Contact sites between the inner and outer membranes of mitochondria and chloroplasts (Adapted from (Toulmay and Prinz, 2011)).

1.1.4.1. Nucleus–vacuole junctions (NVJs)

NVJs are the only contact sites with known protein structure and they lie between the vacuole (equivalent to the lysosome in animal cells) and the nuclear envelope in yeast cells. A NVJ is established by direct binding of Vac8, a vacuolar membrane protein, to Nvj1, a type I

integral ER membrane protein of the nuclear envelope. In yeast NVJs facilitate degradation of portions of the nucleus through an autophagic process (Pan et al., 2000). Osh1, an oxysterol binding protein (see Section *1.3.3.2.* for more details on Osh proteins) and Tsc13, which catalyzes the last step of very long chain fatty acid elongation, are both targeted to NVJs, implicating a role for this ER junction/contact sites in lipid metabolism (Kvam and Goldfarb, 2006). Moreover, the NVJs are sites of PMN (piecemeal microautophagy of the nucleus), a unique form of selective autophagy that targets nonessential portions of the yeast nucleus (Roberts et al., 2003). In response to nutrient depletion, PMN structures arise through the exvagination of the nucleus membrane into an invagination of the vacuole membrane, forming a nuclear 'bleb'. Ultimately, the bleb is pinched off from the nucleus as a free vesicle, released into the vacuole lumen, and degraded by vacuolar hydrolases (Krick et al., 2009; Kvam and Goldfarb, 2007). Osh1 itself is not required for the formation of NVJs or PMN function (Kvam and Goldfarb, 2004), while Tsc13 is required for efficient PMN (Kvam et al., 2005). However, Osh1 and Tsc13 enrichment at NVJs may contribute to the normal biogenesis of PMN vesicles and whether additional proteins reside in the NVJs are still far from understood.

1.1.4.2. Golgi-ER contact sites

Based on electron tomography studies, association of the ER with the trans Golgi network (TGN) has been observed (Ladinsky et al., 1999). It has been proposed that contact sites between TGN and ER are required for sphingomyelin (SM) synthase through the ceramide transfer protein (CERT) in mammalian cells (see Section *1.3.3.2.* for more details on CERT). Moreover, the cholesterol-esterifying enzyme ACAT is enriched in ER-Golgi membrane contact sites and ERC (early recycling compartments) perhaps allowing efficient transport of cholesterol from these cholesterol-rich membranes to the locale of ACAT for esterification (Khelef et al., 2000).

1.1.4.3. Mitochondria-associated membrane, MAM

Morphological evidence for the physical association between the mitochondria and the ER emerged in the 1960s. Such contact sites have since been observed between mitochondria and ER in rat liver (Lewis and Tata, 1973; Morre et al., 1971) and rat hepatocytes (Franke and Kartenbeck, 1971). Subsequent studies led to this ER-like fraction being called MAM (for mitochondria-associated membrane). MAM was identified in mammalian rat liver (Vance, 1990) mouse liver (Ardail et al., 1991) and yeast (Achleitner et al., 1999), and is enriched in functionally diverse enzymes involved in lipid metabolism compared with the bulk of ER. For example, both mammalian PS synthases are enriched in MAM (Vance and Steenbergen, 2005) and it has been shown that the *in vitro* traffic of PS from the ER to mitochondria for PE biosynthesis (see Section *1.2.1.1.* for phospholipid synthesis) is independent of cytosolic factors and ATP. However, treatment with proteinase K decreased the rate of the transport up to 50%, which indicates that transport through mitochondria-ER contact sites is mediated by proteins (Achleitner et al., 1999), In rat liver, there are two PE methyltransferase (PEMT) enzymes. PEMT1 appears to be localized to the ER whereas PEMT2 is enriched in MAM (Vance et al., 1997). PE is also likely to be made from lyso-PE, which has only one acyl chain, in the MAM fraction via the acyl-CoA- dependent acyltransferase, Ale1, which is also enriched in MAM in yeast (Riekhof et al., 2007). Moreover, MAM might be involved in ceramide biosynthesis (Bionda et al., 2004) and its nonvesicular traffic (see Section *1.3.3*. for nonvesicular traffic) between ER and mitochondria (Ardail et al., 2003; van Meer and Lisman, 2002).

In addition to lipid metabolism, MAM is involved in calcium signaling. Calcium is an important second messenger in numerous signal transduction pathways. The supply of Ca^{2+} to mitochondria is vital for many physiological events such as ATP production by the TCA cycle, activation of many hormones and neurotransmitter receptors, and apoptosis (Hayashi and Su, 2007). Uptake of calcium released from the ER or the sarcoplasmic reticulum (SR) in muscle cells likely to be facilitated by MAM (Poburko et al., 2004). Briefly, phospholipase C (PLC) activation by signaling cascades results in the production of inositol 1, 4, 5-triphosphate (IP3) which binds to the IP3 receptor in the ER membrane to release Ca^{2+} from the ER. Ca^{2+} released upon the activation of IP3 receptors at the ER is taken up into mitochondria via the voltage dependent anion selective channel (VDAC) of the mitochondrial outer membrane relatively rapid and very efficient. Ca^{2+} released from IP3 receptor at the MAM creates microdomains of

high Ca^{2+} concentrations that, in turn, activate the Ca^{2+} uniporter for Ca^{2+} uptake into the mitochondrial matrix (Rizzuto et al., 2004). Rizzuto et al. have shown that although the Ca^{2+} uniporter has a surprisingly low affinity for Ca^{2+}, the close contact between mitochondria and the ER results in the exposure of the mitochondrial uniporter to a ~ 20 fold greater amount of Ca^{2+} than the overall cytoplasmic level, which could explain the high efficiency of uptake (Rizzuto et al., 1998).

It is only recently that the proteins involved in the formation of contact sites between ER and mitochondria have been identified. Two sets of interactions have been reported. The Scorrano group showed that ER-localized mitofusin2 tethers mitochondria to the ER by homotypic and heterotypic interactions with mitochondrially-localized mitofusin2 or mitofusin1 (de Brito and Scorrano, 2008). These contacts are critical for IP3 generated calcium flux from the ER into mitochondria. The Walter group discovered a tethering complex in *S. cerevisiae* by screening for yeast mutants that were unable to grow on non-fermentable carbon sources without an artificial mitochondria-ER tether (Kornmann et al., 2009). This complex was ultimately named the ERMES for the endoplasmic reticulum-mitochondria encounter structure and it proposed to have four subunits: i) Mmm1, ii) Mdm10, iii) Mdm12 and iiii) Mdm34 (Kornmann et al., 2009). Mdm12 is localized to the outer membrane of mitochondria and defective Mdm12 mutants are incapable of growing on a non-fermentable carbon source (Berger et al., 1997). Mdm12 binds to two mitochondrial proteins, Mdm10 and Mdm34, and a fourth protein called Mmm1, which is an ER-integral protein. ERMES forms one to five discrete focal structures per cell as judged by confocal microscopy of GFP-tagged ERMES subunits (Kornmann et al., 2009). Interestingly, all subunits of the ERMES complex have reduced CL levels, a mitochondria-specific phospholipid, as well as two- to five fold reductions in PS-to-PC conversion (Kornmann et al., 2009), consistent with earlier work indicating tethering is required for mitochondrial lipid metabolism.

1.1.4.4. PM-ER contacts (PAM or PM-ER junctions)

Contacts between the ER and PM were first reported in muscle (Porter and Palade, 1957), and subsequent studies confirmed their existence in neurons (Rosenbluth, 1962). Since these contacts were discovered by biochemical means, it was named PAM for plasma membrane-

associated membrane, a subfraction of the ER that is close to the plasma membrane. I will use PM-ER contacts to refer to contact sites between pmaER and the PM. A detailed analysis of lipid composition of PM-ER contacts in yeast showed enrichment of PS synthase and PI synthase activity relative to the bulk of ER (Pichler et al., 2001; Schnabl et al., 2005), suggesting these contacts might play an important role in the supply of specific lipids to the PM. 3D electron microscopy reconstruction of yeast cells demonstrated the presence of an extensive number of contacts (>1100 ER-PM contacts per cell) (Pichler et al., 2001), suggesting an important role for PM-ER contacts in cell physiology. In contrast to the MAM, the protein composition of the PM-ER contacts is not well understood.

The best-understood PM-ER contacts are in mammalian muscle cells; the invagination of the PM and the terminal cisternae of sarcoplasmic reticulum (SR) creates a structure known as triad junctions or dyads, a type of contact required for intracellular calcium signaling in muscles (Takeshima et al., 2000). Junctophilin, an ER/SR membrane protein contributes to the formation of the triad junctions, but its binding partner at the PM has not been described. Another example of physical interactions between PM and ER proteins are those between an ER-resident protein STIM and a PM protein ORAI in immune cells for store-operated Ca^{2+} entry (SOCE) mediated by Ca^{2+} release-activated Ca^{2+} (CRAC) channels. STIM functions as a dynamic sensor of Ca^{2+} within the ER lumen and ORAI tetramers are the pore-forming units of CRAC channels (Carrasco and Meyer, 2010; Hogan et al., 2010). Production of IP3 upon phospholipase C (PLC) activation, releases Ca^{2+} from the ER. Upon Ca^{2+} release and depletion of the ER Ca^{2+}, STIM proteins undergo a conformational change and multimerize in the ER membrane, which allows them to bind ORAI in the PM at PM-ER contact sites to activate the CRAC channels (Carrasco and Meyer, 2010). Both STIM and ORAI are widely expressed in many tissues in both human and mice consistent with the widespread prevalence of SOCE and CRAC channel currents in many cells types (Feske, 2010).

In yeast, Ist2 is an ER transmembrane protein, that localizes to PM-ER contacts, and has a lipid- binding domain that recognizes PI (4, 5) P2 and other anionic lipids (Maass et al., 2009). Recently, it has been shown that Ist2 plays roles in the association of ER and PM (Wolf et al., 2012). Deletion of *IST2* resulted in an increased distance between ER and PM and allowed access of ribosomes to the space between the two membranes (Wolf et al., 2012). Interestingly, when Ist2 is expressed in mammalian cells, it promotes the formation of a structure resembling the yeast pmaER (Lavieu et al., 2010). As previously discussed, pmaER of yeast is not a known

feature of the peripheral ER of most mammalian cells. Considering the smaller size of a yeast cell and identifying more than 1000 contacts between pmaER and PM in yeast, confirmed by electron microscopy (Pichler et al., 2001), it is expected that a significantly higher surface density of the ER is in contact with the PM in yeast than would be expected in mammalian cells. In yeast, PM-ER contacts sites have primarily been studied in relation to lipid metabolism rather than Ca^{2+} signaling. Studies in yeast suggest that the essential role of these contacts is in ergosterol and possibly other types of lipid synthesis. However, very little is known about the structural components and regulatory mechanisms of forming and maintaining these contacts in yeast or higher eukaryotes.

1.2. PHOSPHOLIPIDS

The major lipid components of all eukaryotic cell membranes are glycerolipids (e.g., phospholipids and triacylglycerol), sphingolipids, and sterols (Fig.1.3 A). Phospholipids are important structural components of all biological membranes. They consist of a glycerol backbone with fatty acids bound through ester bonds at the *sn*-1 and *sn*-2 positions and a phosphate group on the *sn*-3 position. One exception is cardiolipin (CL), in which a single headgroup is shared by two glycerol backbones with a total of four fatty acyl chains. Phosphatidylcholine (PC), phosphatidylethanolamine (PE), phosphatidylinositol (PI) and phosphatidylserine (PS) are the major phospholipids of all membranes, while phosphatidylglycerol (PG) and CL are present in mitochondrial membranes (Fahy et al., 2005; Voelker, 1991) (Fig. 1.3 B). Phospholipids have diverse physical and chemical properties. Phospholipids adopt different molecular shapes including cone (e.g., PE), inverted cone (e.g., lyso-PC), or cylinder (e.g., PC). These shapes are determined by the lipid headgroup and its ratio to the acyl chains (Cullis et al., 1986; Sprong et al., 2001).

PC, because of its cylindrical shape, is a bilayer-forming lipid and is one of the most abundant phospholipids, comprising approximately 40-50% of total cellular phospholipids. In mammals, PC is the major phospholipid in bile, plasma lipoproteins, and lung surfactants, which plays a critical role as a second messenger in signal transduction (Kanno et al., 2007). In the brain, PC is an essential precursor for the biosynthesis of the cholinergic neurotransmitter acetylcholine from choline (Li and Vance, 2008). Coupling of PC hydrolysis and acetylcholine

synthesis in the brain has been proposed (Blusztajn et al., 1987). PE makes up 15-25% of membrane phospholipids and the smaller size of the ethanolamine headgroup allows it to assume a conical shape. This shape gives PE the tendency to adopt non-bilayer structures, which are proposed to be essential for vesicular budding and fusion/fission (van Meer et al., 2008). PE is more abundant in mitochondria (80% of total lipid) than in other organelles, consistent with the high level of fusion and fission taking place in this organelle. PS, which has a cylindrical shape, exists at relatively low levels in eukaryotic organelles (2–10 %) and is more abundant in membranes such as the ER and PM. PS is essential for the regulation of several important biological processes, such as activation of platelets in the blood coagulation cascade and the maturation of sperm cells (Gadella and Harrison, 2000). At the PM, the externalization of PS to outer leaflets is a signal for the engulfment and clearance of apoptotic cells by macrophages (Vance and Steenbergen, 2005). PI and its derivatives make up less than 10% of total cellular lipids and are key regulators of multiple cellular processes including signal transduction, vesicular trafficking, apoptosis, cytoskeletal organization, transcription and cell proliferation (Fruman et al., 1998).

A

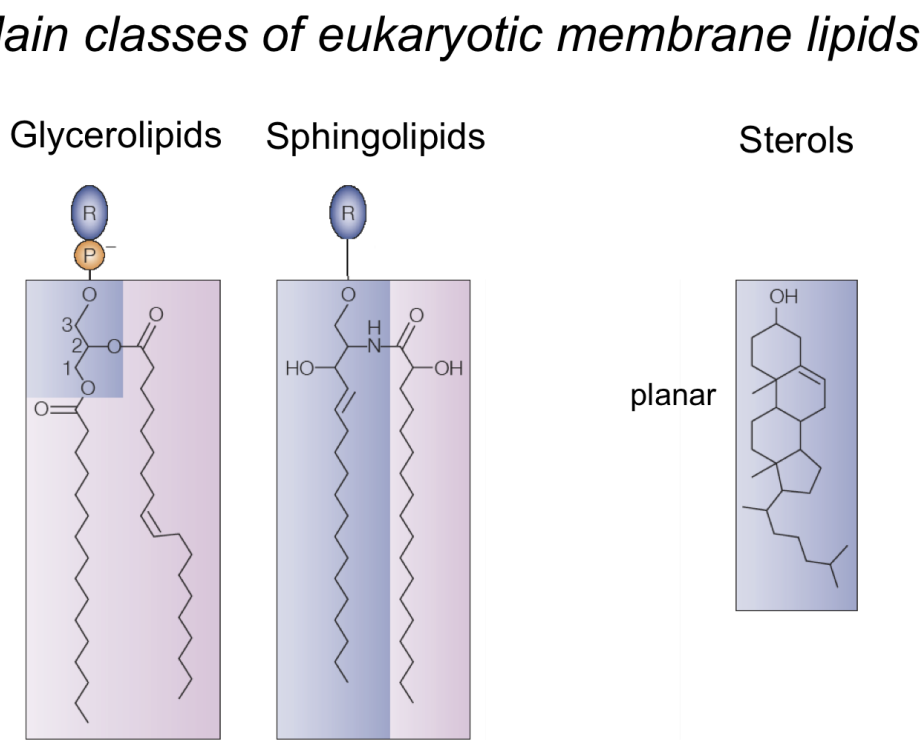

B

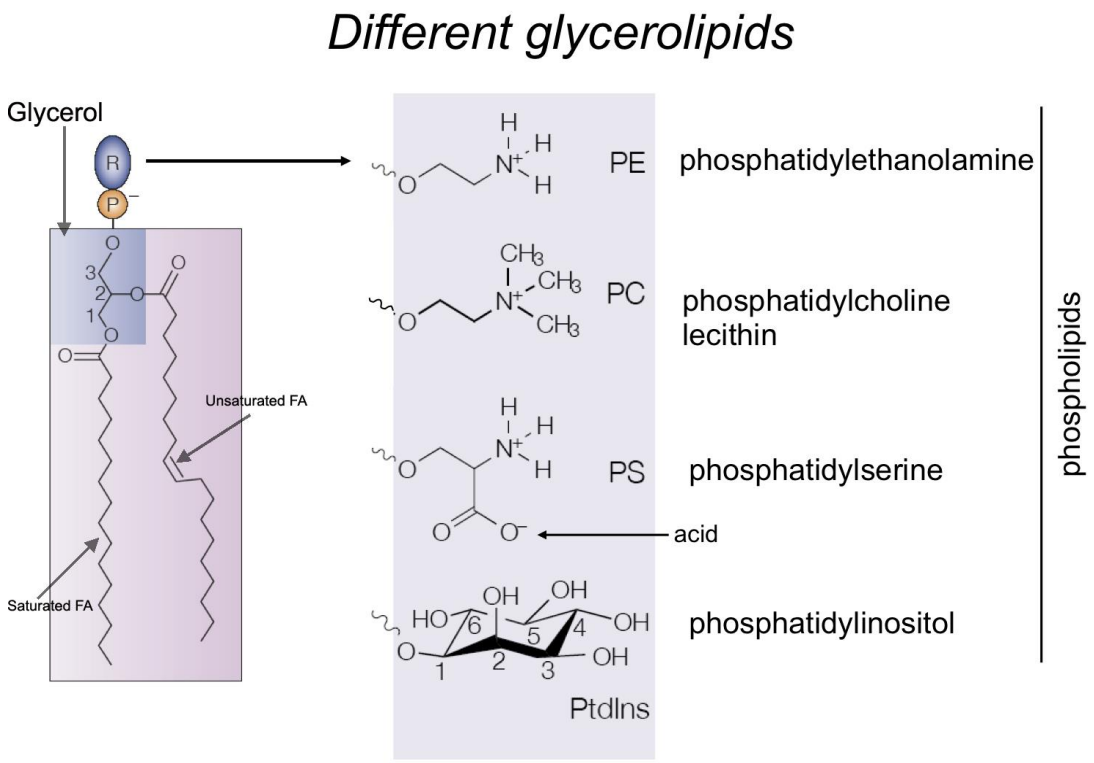

Figure 1.3: The three main classes of eukaryotic membrane lipids.

A) Glycerolipids are based on glycerol (blue shading) with two C16–C18 fatty-acid chains (pink shading) linked at sn-1 and -2, which forms DAG. A cis-double bond is usually present in the fatty acid that is linked at sn-2, which causes a kink in the acyl chain and decreases the packing density of the lipid. B) A phosphate (P) can be attached at sn-3 which forms phosphatidic acid (PA) and this phosphate can carry a head group (R) that is either neutral which produces PS or PI and gives a net acidic charge, or basic which forms PE or PC and gives a neutral or zwitterionic lipid (Adapted from (Holthuis and Levine, 2005)).

1.2.1. Phospholipid biosynthesis in Saccharomyces cerevisiae

Phospholipid biosynthesis is a complex process that includes many branch points and which is regulated by multiple factors. Pathways for making phospholipids in yeast and higher

eukaryotes are very similar (Carman and Han, 2009; Carman and Henry, 1999), and in this section I will review the synthesis and functions of PC in yeast and make comparisons to mammalian cells. Both yeast and mammals use two redundant pathways for PC synthesis, called the methylation pathway and the salvage or Kennedy pathway. In yeast, plants and mammals there is an alternative pathway to make PC via a lyso-PC route (Larsson et al., 2007; Riekhof et al., 2007) (Lands and Merkl, 1963) which is critical for phospholipids remodeling.

1.2.1.1. The methylation pathway

The methylation pathway is the primary route of *de novo* synthesis of PC in yeast in the absence of choline or ethanolamine and is the major route for PC biosynthesis in hepatic cells in mammals (Carman and Han, 2009; Carman and Henry, 1999) (Fig. 1.4). In yeast, phospholipid synthesis is initiated by transfer of a fatty acid from acyl-CoA to the *sn*-1 position of glycerol-3-phosphate (Gly-3-P) to form lysophosphatidic acid, lyso-PA (Athenstaedt and Daum, 1999). Ale1 or Slc1, two acyltransferases, further acylate lyso-PA to form PA (Riekhof et al., 2007). PA is then converted into CDP-diacylglycerol (CDP-DAG), a central intermediate for making all phospholipids. Biosynthesis of the four major phospholipids in yeast, PS, PE, PC and PI, begins with CDP-DAG, and is the reason for the *de novo* pathway sometimes being referred to as the CDP-DAG pathway.

PI is synthesized from CDP-DAG and inositol by PI synthase, encoded by the *PIS1* gene in yeast. Pis1 is an ER-associated enzyme (Nikawa and Yamashita, 1997) essential for growth in *S. cerevisiae.* Therefore, PI is essential, but probably not for its structural contribution to bilayers. Rather, PI is likely critical to cell viability due to its role in cell signaling, where it functions as a precursor of the phosphoinositides (Wera et al., 2001). PS is a minor component of total cell phospholipids, but is an essential intermediate metabolite in the *de novo* synthesis of the two major yeast phospholipids, PE and PC. One important difference arises between yeast and mammalian cells in the synthesis of PS. In mammals, PS synthesis occurs both by transfer of one serine molecule to CDP-DAG and by an exchange reaction between PE and serine, while in yeast, PS is made only from CDP-DAG by PS synthase encoded by the *CHO1* gene. PS synthase has been found to be located in the cytosolic leaflet of the ER in both yeast and mammals, and additionally, in the outer mitochondrial membrane in mammals (Vance and Steenbergen, 2005).

PS made in the MAM, mitochondria-associated ER membrane (Section *1.2.3.3.*) is decarboxylated by Psd1 in the inner mitochondria membrane (in both yeast and mammals) (Vance, 2003) and Psd2 (only in yeast) in the Golgi/vacuolar membranes to make PE (Wu and Voelker, 2001). Approximately, 80% of the total PE is made by Psd1. Δ*psd1* cells have significantly less PE in their mitochondria and exhibit a greater tendency to produce petite cells, which have little or no mitochondrial DNA and lead to the formation of small anaerobic colonies when grown on media (Trotter and Voelker, 1995). Although Psd2 only accounts for ~ 5 - 10 % of the cellular PS decarboxylase activity, it was suggested that it could synthesize enough PE to support the growth of Δ*psd1* cells (Trotter and Voelker, 1995). PE produced in mitochondria and Golgi/vacuoles then migrates back to the ER and undergoes three sequential methylations by two methyltransferases, Cho2 and Opi3 resulting in production of PC. Cho2 catalyzes the rate-limiting first methylation step, and the second and third methylations are catalyzed by Opi3 (Kodaki and Yamashita, 1987). Opi3 can also perform the first methylation, but not as efficiently as Cho2. In mammals, all three methylations are catalyzed by the Opi3 orthologous, PEMT (Walkey et al., 1999), as there is no known Cho2 orthologous. In yeast, the Δ*cho2*Δ*opi3* double mutant is auxotrophic for choline, suggesting that PC is essential for the growth of yeast (Summers et al., 1988). The *pemt* -/- mouse develops liver failure and steatohepatitis when fed a choline-deficient diet, likely due to a decreased ratio of PC to PE (Li et al., 2006; Li et al., 2005). In most mammalian tissues, PC made by the methylation pathway contributes little, if at all. However, in the liver, 5-40% of PC can be provided through the methylation pathway to provide hepatic cells with adequate amount of PC to regulate the synthesis of serum lipoproteins and bile (Kent and Carman, 1999).

1.2.1.2. The Kennedy pathway

The Kennedy pathway is the major route of synthesis of PC in all mammalian cells (DeLong et al., 1999) (Fig. 1.4). In yeast cells, in the presence of exogenous choline or ethanolamine, PC and PE are primarily synthesized via the Kennedy pathway in a series of reactions nearly identical to mammals (Choi et al., 2004). The Kennedy pathway can be divided into two branches, one that uses choline to synthesize PC, the so-called CDP-choline pathway, and the other using ethanolamine to synthesize PE, known as the CDP-ethanolamine pathway.

Both branches of the Kennedy pathway consist of three metabolic steps. The formation of PC by the CDP-choline branch starts with the phosphorylation of choline by the choline kinase, Cki1 in the cytosol (Carman and Han, 2007). Second, phospho-choline is converted to CDP-choline in a rate-limiting manner by Pct1. Pct1 is a membrane-associated enzyme localized to ER and nuclear membranes. Finally, Cpt1, the cholinephosphotransferase, forms PC from CDP-choline and DAG (Carman and Han, 2007; Morash et al., 1994). The localization of Cpt1 is unknown, but likely is localized in the ER and/or Golgi. Similarly, in the CDP-ethanolamine pathway, *EKI1*-encoded ethanolamine kinase, *ECT1*-encoded ethanolamine-P cytidylyltransferase, and *EPT1*- encoded ethanolamine phosphotransferase catalyze reactions that lead to the formation of PE in a similar manner as PC (Carman and Han, 2007). The DAG utilized for the making of PC and PE by the CDP-choline and CDP-ethanolamine branch originates from the dephosphorylation of PA, a reaction catalyzed by the PA phosphatase, Pah1 (see Section *1.2.2.2* for Pah1).

In yeast, the Kennedy pathway can compensate for defects in the methylation pathway. For example, Δ*cho1* and Δ*psd1*Δ*psd2* mutants, that are defective in the synthesis of PS and PE respectively, are ethanolamine and choline auxotrophs. Similarly, Δ*cho2*Δ*opi3* double mutants are auxotrophic for choline, and each null mutant on its own shows poor growth in media lacking choline (Kersting et al., 2004). In yeast, even in the absence of exogenous choline, the Kennedy pathway contributes to the synthesis of PC because choline is produced from the phospholipase D-mediated turnover of PC produced by the methylation pathway (Patton-Vogt et al., 1997). The ethanolamine branch of the Kennedy pathway can also use ethanolamine provided by sphingolipid catabolism to produce PE, which can then be converted into PC by the methylation pathway (Schuiki et al., 2010).

1.2.1.3. Lyso-PC route

In addition to the aforementioned pathways, PC can also be made by acylation of lyso-PC through a pathway called Land's cycle, in which phospholipids are deacylated and reacylated in liver (Lands and Merkl, 1963). Recently, it was found that yeast cells are capable of making PC and PE by phospholipid remodeling in a pathway named lysolipid metabolism (ELM) (Riekhof et al., 2007). Lyso-PC can be generated itself via PC deacylation or made by acylation

of glycerophosphocholine (GPC) (Stalberg et al., 2008). Subsequently, lyso-PC can be acylated by Ale1, the acyltransferase in the ER, to produce PC (Riekhof et al., 2007). Rather than being responsible for the bulk of PC synthesis in cells, this route's primary purpose is likely for the recycling and remodeling of PC, although not much else is currently known about the mechanisms responsible for PC remodeling. Similarly, in plant cells the incorporation of acyl groups from acyl-CoA into lyso-PC/lyso-PE occurs at PM-ER contact sites (See section *1.1.4.4.* for PM-ER contact sites) (Larsson et al., 2007) and PC and PE delivered to the PM independent of the secretory pathway (Larsson et al., 2007). In mammalian cells, in the Lands' cycle phospholipases make lysophospholipids and fatty acids, while lysophospholipids are converted to phospholipids in the presence of acyl-CoA by acyltransferases as occurs in yeast and plant cells (Lands and Merkl, 1963).

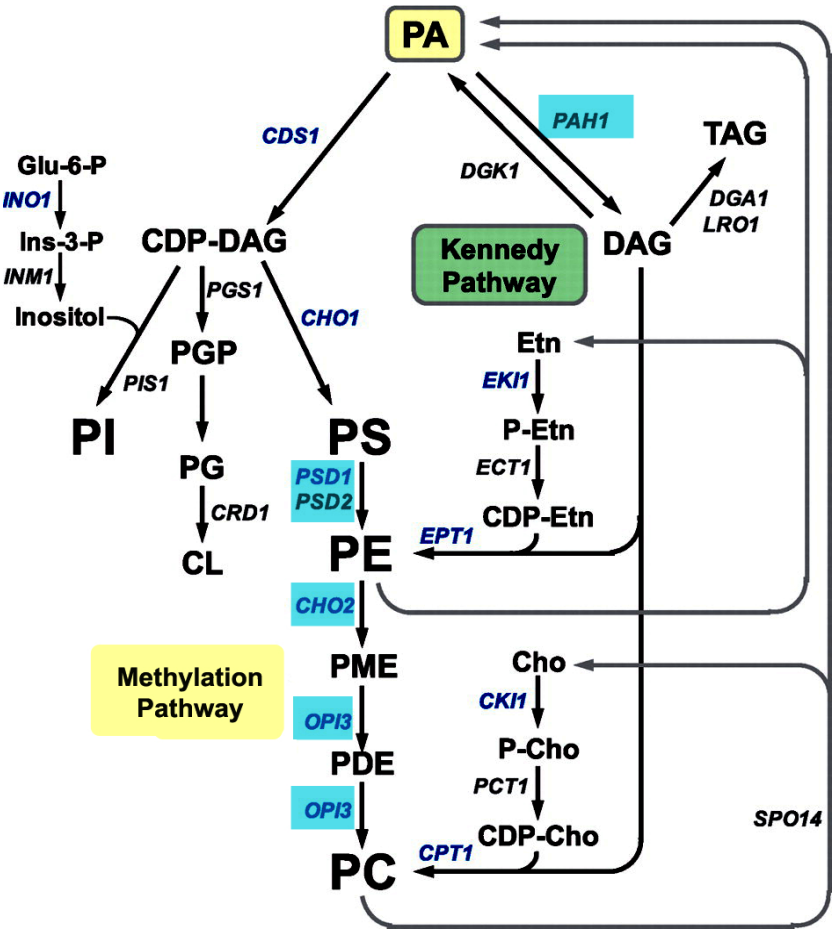

Figure 1.4: Phospholipid synthesis in *S. cerevisiae.*

The pathways shown for the synthesis of phospholipids include the relevant steps for the Kennedy and methylation pathways. Psd1/Psd2: PS decarboxylases, Cho2: PE methyltransferase, Opi3: phosphatidylmonomethylethanolamine (PME) and phosphatidyldimethylethanolamine (PDE) methyltransferase leading to the formation of PC in the methylation pathway, Cki1: choline kinase, Pct1: choline-P cytidylyltransferase, and Cpt1: choline phosphotransferase leading to the formation of PC by the CDP-choline branch of the Kennedy pathway, Eki1: ethanolamine kinase, Ect1: ethanolamine-P cytidylyltransferase, and Ept1: ethanolamine phosphotransferase leading to the formation of PE by the CDP-ethanolamine branch of the Kennedy pathway. DAG, diacylglycerol, *PAH1*-encoded phosphatidate phosphatase enzymes. The genes that are discussed throughout this dissertation are highlighted in blue boxes (adapted from a review (Carman and Han, 2009)). The synthesis of PE and PC from lysoPE and lyso-PC, respectively, is not shown in the figure.

1.2.2. Phospholipid regulation in Saccharomyces cerevisiae

In yeast, the phospholipid metabolism is regulated by multiple factors, including phospholipid precursors (inositol, choline, ethanolamine), pH, temperature, nucleotides (e.g. ATP and CTP), lipids (e.g. PA and CDP-DG), growth phase, phosphorylation, and zinc availability as well the post-translational regulation (Carman and Han, 2011; Henry et al., 2012). Here, the regulatory impact of both inositol and Pah1 in lipid metabolism will briefly be addressed.

1.2.2.1. Transcriptional Regulation by Inositol

Many genes involved in the methylation and Kennedy pathways contain a cis-element in their promoter region that is referred to as an upstream activating sequence inositol responsive element (UAS_{INO}) (Henry and Patton-Vogt, 1998). Genes containing UAS_{INO} element are *INO1* (encoding inositol-3-phosphate synthase), *CDS1*, *CHO1*, *PSD1*, *CHO2*, *OPI3*, *EKI1*, *EPT1*, *CKI1*, *CPT1*, *HNM1*, and *ITR1* (Carman and Han, 2011). Inositol supplementation is capable of

repressing the expression of these genes, while inositol starvation upregulates them (Carman and Han, 2011). However, these genes are variable in their transcriptional response to inositol. For example, *INO1* is the most regulated gene in response to inositol whereas *OPI3* is the least regulated one (Jesch et al., 2005). Inositol's effect on transcription on genes containing the UAS_{INO} is dependent on the activator heterodimer complex, Ino2-Ino4, and the repressor, Opi1 (Carman and Han, 2011; Gaspar et al., 2007) (Fig. 1.5). Opi1 is capable of binding to a PA pool in the ER and the ER protein Scs2 via the FFAT motif in Opi1, which also exists in variety of lipid binding/transferring proteins (Loewen et al., 2003) (see Section *1.3.3.1.*).

Briefly, during inositol starvation, Opi1 binds PA and Scs2 at the ER, which blocks its repressor function in the nucleus allowing the Ino2-Ino4 complex to bind to the UAS_{INO} element of these genes and activate their transcription. During inositol supplementation, the PA pool in the ER is consumed for the synthesis of PI leading to the translocation of Opi1 from the ER to the nucleus where it binds to Ino2 at the promoters of these genes and inhibits their transcription. Deletion of *OPI1* causes constitutive expression of *INO1* and leads to overproduction of inositol as a consequence of overactivation of the Ino1 enzyme (hence the name 'opi'). Therefore, inositol inhibits phospholipid synthesis in both the methylation and Kennedy pathways resulting in less PS- derived PE and PC (Kelley et al., 1988). Interestingly, in many cases the repressive effects of inositol are enhanced by the presence of ethanolamine or choline in growth media, while choline itself only has a limited effect (Jesch et al., 2005).

A) Inositol depletion and exponential phase

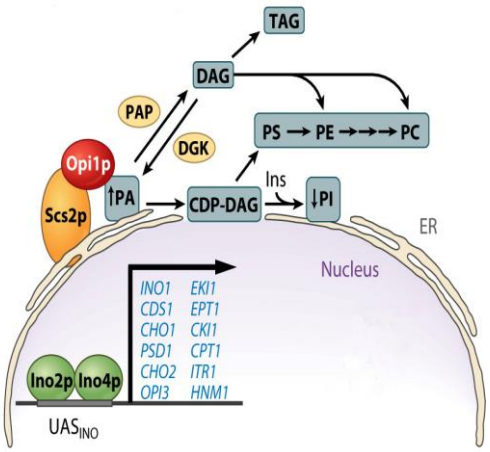

B) Inositol supplementation and stationary phase

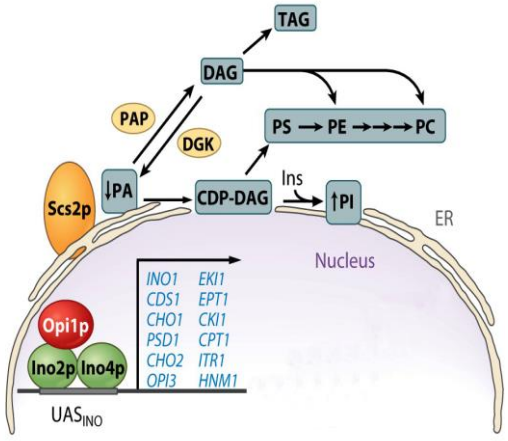

Figure 1.5: **Models for the phosphatidate (PA)-mediated regulation of UAS_{INO}-containing phospholipid synthesis genes.**

(A) Under growth conditions whereby the levels of PA are increased, the Opi1 repressor is tethered to the nuclear ER membrane via interactions with Scs2 and PA, allowing the maximal expression (bold arrow) of UAS_{INO}-containing genes (blue) by the Ino2-Ino4 activator complex. (B) Under growth conditions whereby the levels of PA are reduced, Opi1 is dissociated from the nuclear ER membrane and enters into the nucleus, where it binds to Ino2 and attenuates (thin arrow) the transcriptional activation by the Ino2-Ino4 complex. CDP-DAG, CDP-diacylglycerol; PC, phosphatidylcholine; PE, phosphatidylethanolamine; PS, phosphatidylserine; TAG, triacylglycerol; UAS_{INO}, inositol-responsive element (Adapted from (Carman and Han, 2011)).

1.2.2.2. Pah1, phosphatidic acid phosphatase

Among the enzymes that contribute to PC biosynthesis, *PAH1*-encoded PA phosphatase has been identified as one of the key regulators of PA content. PA acts as a precursor in the methylation pathway and is converted into CDP-DAG by CDS1-encoded CDP-DAG synthase (Shen and Dowhan, 1996). DAG needed for the biogenesis of PE and PC via the Kennedy pathway, is derived from PA by the PAH1-encoded PA phosphatase (Fig. 1.4). DAG has been recognized as an essential factor for protein trafficking from the Golgi to the PM (Baron and Malhotra, 2002), and as a second messenger in signal transduction via activation of protein kinase C (Merida et al., 2008). It has a conical shape similar to PE, which can induce membrane bending and facilitate membrane fusion and fission events (Baron and Malhotra, 2002). Therefore, Pah1 activity can dictate to cells whether make phospholipids from DAG via the Kennedy pathway or from CDP-DAG via the methylation pathway, as well as control key signal transduction pathways. There are two classes of PA phosphatase (PAP) enzymes present in both yeast and mammals; those that are Mg^{2+} - dependent and those that are Mg^{2+} - independent. In *S.cerevisiae*, *PAH1* encodes for the Mg^{2+} - dependent PAP activity (Han et al., 2007; Han et al., 2006), while *DPP1* and *LPP1* encode the Mg^{2+} - independent activities. Pah1 has been localized to both the cytosolic and membrane fractions of yeast by biochemical methods (Han et al., 2006). Δ*pah1* cells showed an increase of ~150% in cellular PA levels, a reduction in PC by ~

43 %, and increase in PE and PI by ~ 50 % and 80 % respectively (Han et al., 2006). Deletion of *PAH1* also results in a massive expansion of the nuclear ER membrane (Santos-Rosa et al., 2005). Because Δ*pah1* cells have altered phospholipid composition, it may change the physical properties of lipid bilayers and membranes.

Pah1 has sequence homology with mammalian lipin1 (Fig. 1.6). The DxDxT catalytic domain near the middle of the protein is required for the phosphatase function (Csaki and Reue, 2010; Siniossoglou, 2009). Lipin1 was identified as gene mutated in the fatty liver dystrophy (fld) mouse, characterized by a dramatic reduction of the adipose tissue and cellular lipid droplet content (Csaki and Reue, 2010). Mammalian lipin1 can be found in the nucleus of hepatocytes (Bou Khalil et al., 2010) and adipocytes, where it regulates the expression of fatty acid oxidation and adipogenic genes (Peterfy et al., 2005). These findings indicate that lipins regulate lipid metabolism by multiple mechanisms (Reue and Brindley, 2008). Interestingly, lipin1 is strikingly upregulated during phospholipid biosynthesis, which leads to ER and Golgi expansion during differentiation of B-lymphocyte into antibody-secreting cells (Reviewed by (Siniossoglou, 2009)). This suggests that yeast and mammalian lipins could have roles in the biogenesis of membrane-bound organelles, although the molecular mechanisms involved in yeast and mammals may differ. Pah1 is inactivated via phosphorylation by the cyclin-dependent kinase Cdc28 (also known as Cdk1), and activated through dephosphorylation by the Nem1–Spo7 phosphatase complex (Santos-Rosa et al., 2005). It has been recently shown that the enzymatic activity of Pah1 is essential for fusion of vacuole membranes in yeast consistent with the roles of DAG and PA in promoting membrane fusion (Sasser et al., 2011).

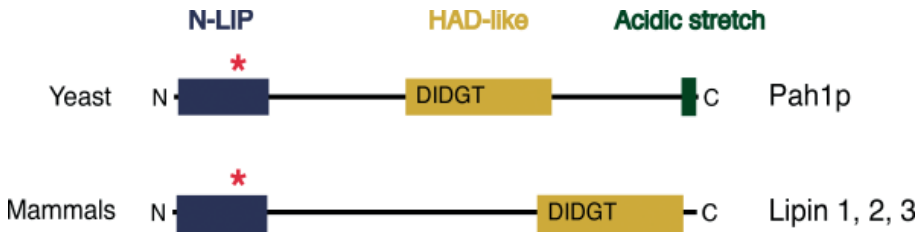

Figure 1.6: Pah1, a yeast lipin.

All members of the lipin family have a conserved N-terminal domain (N-LIP) of unknown function and a C-terminal catalytic domain that contains a HAD-like phosphatase motif (DIDGT). Within these two domains, the sequence identity between the yeast and the three mammalian orthologous is about 45%. Pah1p and lipins from other yeast species also contain a C-terminal acidic stretch. The red star indicates the position of the mutation of the conserved glycine residue (G84R, corresponding to G80 in Pah1) identified in the *fld* mouse that causes lipodystrophy (Adapted from (Siniossoglou, 2009)).

1.2.3. Compartmentalization of lipid biosynthesis

In all eukaryotic cells there is compartmentalization of lipid biosynthetic pathways. This means that enzymes responsible for lipid synthesis, remodeling and turnover have differential localization to different membrane compartments. This is true for the synthesis of all three major classes of bilayer lipids; phospholipids, sphingolipids and sterols. Compartmentalization of these pathways makes it necessary to be able move the newly made lipids within the cell in a timely manner. Organelles along the endocytic pathways are connected by bidirectional vesicular transport to maintain their distinct membrane composition, while also allowing lipids could move anterograde and retrograde between ER and Golgi. Sterol and sphingolipid content increases progressively through the compartments of the secretory pathway, and this gradient facilitates membrane protein sorting (Bankaitis et al., 2012). Sterols and sphingolipids enrichment in TGN vesicles relative to the ER suggested the existence of sorting mechanisms for biogenesis of TGN-derived vesicles (Surma et al., 2011). Yet not all lipids are moved along the secretory pathways (see Section 1.3), and vesicular trafficking cannot explain lipid transport to mitochondria, peroxisomes, and chloroplasts. These organelles originate from formerly autonomous microscopic organisms, and do not seem to be connected by vesicular transport.

1.2.3.1. Compartmentalization of phospholipid biosynthesis

As previously discussed for phospholipid synthesis, in the methylation pathway PS is made in the ER/MAM while PE is made in either Golgi/vacuole by Psd2 or in mitochondria by Psd1 (see Section *1.2.1.*) and will be converted to PC by the methyltransferase enzymes in the ER, Cho2 and Opi3 (Carman and Han, 2009; Voelker, 2005) (Fig. 1.7). Although vesicular trafficking can explain the transport of PS for Psd2 to the Golgi, it cannot explain how PE moved to mitochondria to be converted to PC by Psd1. Genetic screens and biochemical assays have identified few components that are important for interorganelle phospholipid traffic. In yeast, Met30, a substrate recognition subunit of a multicomponent ubiquitin ligase, required for transport of PS from the ER/MAM into mitochondria for PE synthesis (Choi et al., 2005; Voelker, 2009). The major substrate of Met30 is the transcription factor Met4 which, when is inactivated by ubiquitination, results in more PS moving from the ER to the mitochondria. Activation of Met4, on the other hand, inhibits PS transfer to the mitochondria. The mechanism by which Met4 negatively regulates lipid transport is unknown (Voelker, 2009). It is not yet clear if Met30 ubiquitinates a substrate directly on the ER and/or mitochondria or has a role independent of its function in the ubiquitin ligase complex. PS made in the ER is also transported to the Golgi to be converted to PE. Genetic studies suggested that Stt4, a PI-4-kinase in the PM, is required for PS transport to Psd2, but it is not clear how Stt4 function regulates PE synthesis (Voelker, 2005). PM, lysosomes, and endosomes appear essentially incapable of synthesizing PC, PE, PS, and PI. Thus, both the biogenesis and the maintenance of these membranes require phospholipid transport. However, our understanding of how phospholipids are trafficked within cells is still very limited.

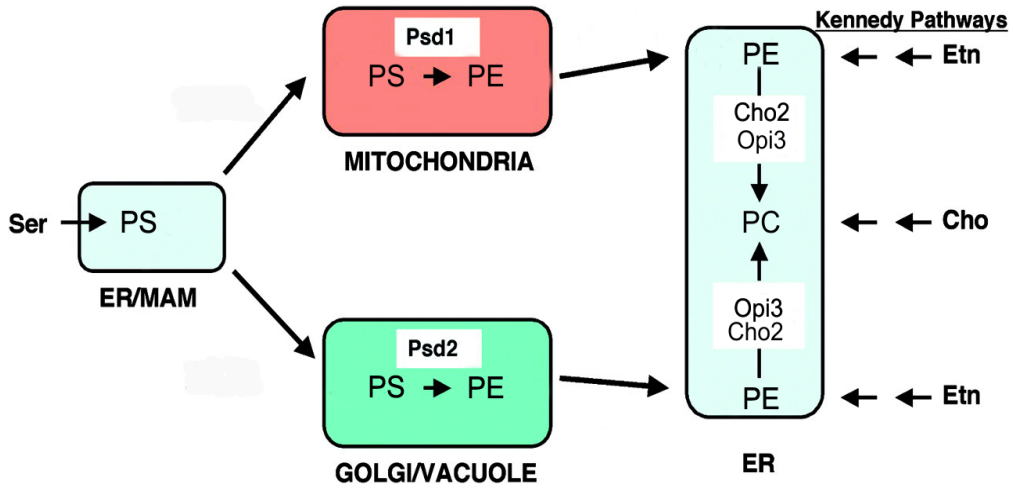

Figure 1.7: **Compartmentalization of phospholipid synthesis in eukaryotes.**

PS made in the ER and mitochondria-associated membrane (MAM) is transported to the mitochondria or the Golgi-vacuole (only in yeast). The PE either retained or exported to other organelles. PE is methylated to form PC by the methyltransferase enzymes (Cho2 and Opi3). In mammals, only the mitochondrial Psd1 has been described. Eukaryotes can also synthesize PE and PC in via the Kennedy pathways (see Section *1.2.1.2.*).

1.3. NONVESICULAR LIPID TRAFFIC

In addition to vesicular transport, three other possibilities have been considered for the transport of lipids. These are: (1) lateral diffusion, (2) transbilayer flip-flop, and (3) monomeric lipid exchange. Monomeric lipid exchange may occur via lipid binding/transfer proteins and/or spontaneous diffusion through the aqueous compartment and these events are thought to occur at membrane contact sites (Holthuis and Levine, 2005; Lev, 2010; van Meer et al., 2008) with or without lipid transfer proteins (Fig. 1.8).

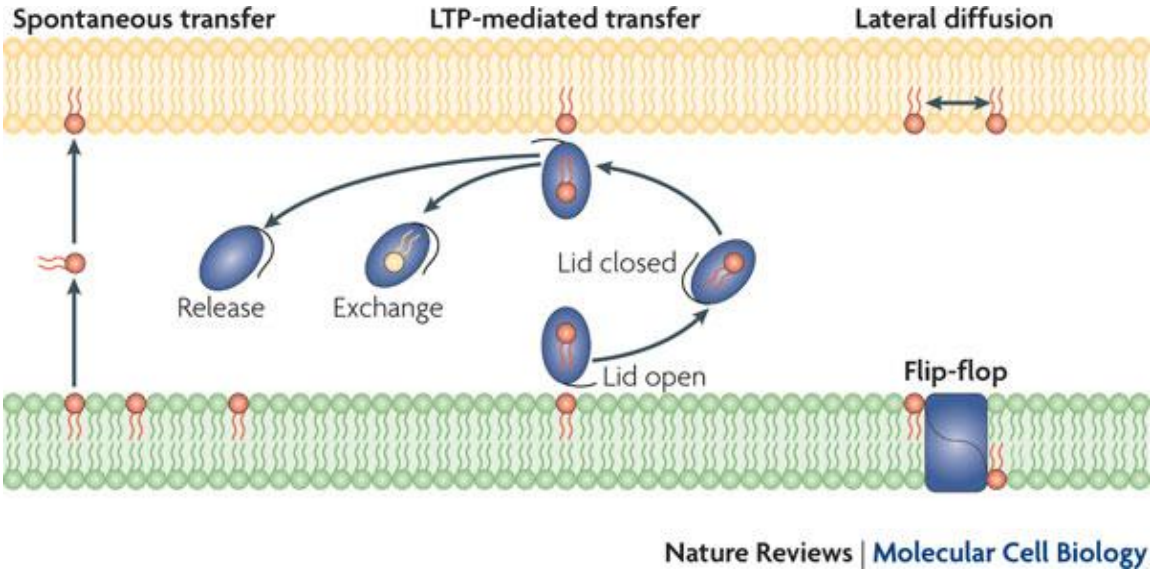

Figure 1.8: Lipid transport processes via multiple routes.

There are three mechanisms involved in nonvesicular lipid transport: 1) monomeric lipid exchange, either spontaneous or mediated by lipid-transfer proteins (LTPs), 2) lateral diffusion and 3) transbilayer flip-flop. Transbilayer flip-flop can be either spontaneous (not shown) or mediated by proteins (adapted from (Lev, 2010)).

1.3.1. Lateral diffusion

One possible mechanism of lipid trafficking is the lateral diffusion by which lipids move in the two-dimensional plane of the membrane bilayer. This diffusion could be influenced by different membrane parameters such as polypeptides, proteins, extracellular domains of membrane proteins, or cholesterol-enriched rafts capable of exerting an effect. The diffusion coefficients for lipids are 10–100-fold greater than most membrane proteins (Murase et al., 2004). There is a correlation between the microviscosity of the headgroup region and upper hydrophobic part of the phospholipids and their lateral diffusion rate (Venable et al., 1993). Previously, the rate of lateral diffusion of phospholipids in erythrocyte microvesicles was measured to be 2×10^{-12} m^2/s at 36 ^{o}C (Gawrisch et al., 1986).

1.3.2. Transbilayer movement or flip-flop

The ER possesses a transversally symmetrical lipid composition and the enzymes involved in lipid formation are asymmetrically localized to the two membrane leaflets (Sprong et al., 2001). On the other hand, in many eukaryotic cells, differences in lipid composition of the inner and outer leaflet of their membranes are observed. For example, the outer (exoplasmic) leaflet of the PM is enriched in PC and sphingolipids, while the inner (cytoplasmic) leaflet is primarily composed of PE, PS and less abundant lipids such as PI and PA. This asymmetry of inner and outer leaflet lipids is an important characteristic of the eukaryotic PM (Zachowski, 1993). The three classes of proteins that maintain asymmetry or symmetry of the cell membrane by translocating lipids across the membranes are: i) scramblases, ii) flippases and iii) floppases (Daleke, 2003). The movement of lipids between the two membrane leaflets is known as transbilayer movement, an event that occurs either independent of ATP hydrolysis (scramblases) or through an enzyme-catalyzed mechanism (flippases and floppases).

Scramblases mediate ATP-independent, bidirectional lipid movement with little specificity (Daleke, 2003). They are involved in the calcium-dependent transbilayer movement of phospholipids, which tends to eliminate their asymmetric distribution across the membranes. Scramblase activity is essential in red blood cells and platelets for PS exposure on the surface of the cell, and stimulation of blood clotting as a consequence of calcium influx (Daleke, 2003). In humans, four related phospholipid scramblases, called PLSCRs, have been identified (Wiedmer et al., 2000). PLSCR1, 3 and 4 are expressed in a variety of tissues including heart, kidney, pancreas, spleen, prostate, colon while the expression of PLSCR2 is restricted to the testes (Wiedmer et al., 2000). The proteins responsible for scramblase activity are unknown in yeast.

Flippases are transbilayer lipid translocators that catalyze the lipid movement from the outer leaflet to the inner leaflet of the membranes (Contreras et al., 2010; Voelker, 2009). Type 4 P-type ATPases (P4-ATPases) are believed to have flippase activity. The human genome contains 14 genes encoding P4-ATPases, while *C. elegans* genome has 6 and *Drosophila melanogaster* containing at least that many as well (Tanaka et al., 2011). In *S. cerevisiae*, five flippases (Dnf1, Dnf2, Dnf3, Drs2, and Neo1) have been identified so far (Tanaka et al., 2011). Dnf1 and Dnf2 are present on the PM and are most likely to be responsible for the flippase activity at the PM (Graham et al., 2003). Lem3, a yeast Cdc50 family protein, forms a

heterodimeric complex with Dnf1 or Dnf2 and regulates Dnf1-Dnf2 activity (Saito et al., 2004). Drs2 and Dnf3 primarily reside in the trans-Golgi network (TGN). Like Lem3, Crf1 is a potential noncatalytic subunit that associates with Dnf3 (Furuta et al., 2007) and Cdc50 is crucial for the catalytic activity of Drs2 (Lenoir et al., 2009). Neo1 was implicated in the retrograde transport pathway from the Golgi to the ER although it remains to be precisely determined in which pathway it functions (Wicky et al., 2004).

Floppases are transbilayer lipid translocators that catalyze the lipid inward movement towards the outward monolayer in an ATP-dependent manner. The most well characterized lipid floppase activities are those catalyzed by ABC lipid transporters, although not all ABC lipid transporters are floppases. The human genome encodes 48 ABC transporter genes and mutations in most have been linked to diseases (Linton et al., 2011). A number of ABC transporters have been identified in yeast. The most well characterized yeast ABC lipid transporters are Yor1 (yeast oligomycin resistance 1) and Pdr5 (pleiotropic drug resistance 5), which are involved in the movement of NBD-PE across the PM (Decottignies et al., 1998). To date, no data has demonstrated any endogenous lipid transport reactions for Yor1 or Pdr5. Two other ABC transporters located in the yeast PM, Aus1 and Pdr11, were recently found to facilitate sterol influx when sterol biosynthesis was compromised (Wilcox et al., 2002), and they likely mediate sterol movement from the PM to the ER in a non-vesicular manner (Li and Prinz, 2004).

1.3.3. Monomeric Lipid Exchange

Vesicular traffic, which has been intensively studied for decades (Bonifacino and Glick, 2004), has long been believed to be the only route by which the ER communicates with other organelles. However, recent studies found that some lipids are not solely distributed via the secretory pathway. The third mechanism of transfer of lipid monomers could be via the cytosol, which could occur either by spontaneous diffusion or by protein-facilitated transport via lipid binding/transferring proteins (D'Angelo et al., 2012; Holthuis and Levine, 2005).

1.3.3.1. Diffusion through the aqueous compartment

A passive and random migration of a lipid molecule from one membrane to another cannot be efficient and such traffic is extremely slow for the majority of lipids. However, a few studies have shown that some lipid monomers are able to move effectively between membranes, though the speed at which it occur depends on the monomer's composition (Massey et al., 1984; Nichols and Pagano, 1981). For example, for lyso-PC this process could occur faster when compared to PC, which has two acyl chains with 16 or more carbons. The kinetics of the transport of lipid is influenced by membrane curvature as well as lipid aqueous-phase solubility (Lev, 2010; McLean and Phillips, 1981). Cholesterol can spontaneously move between bilayers unassisted by any proteins (Frolov et al., 1996) but cholesterol transfer between lipid membranes occurs with a characteristic half-time of 2–3 hours (Bar et al., 1986) which is relatively slow compared to the rates at which sterols are trafficked within the cell ($t^{1/2}$ = 10 min) (DeGrella and Simoni, 1982). For phospholipids, the spontaneous movement is extremely slow with a half-time of at least 12 hours and it decreases with increasing chain length which is not probably physiological (Dawidowicz, 1987). Therefore, diffusion via the cytosol cannot explain how lipids are trafficked between organelles.

1.3.3.2. Lipid transfer proteins (LTPs) and lipid binding proteins

There is growing evidence that the disrupting vesicular trafficking in budding yeast and mammalian cells does not disturb the traffic from the ER for some lipids. These include ceramide (Funato and Riezman, 2001; Hanada et al., 2003), sterols (Baumann et al., 2005; Urbani and Simoni, 1990) and phospholipids (Raychaudhuri and Prinz, 2008; Vance et al., 1991; Wu and Voelker, 2001). Moreover, some semi-autonomous organelles such as mitochondria (Vance et al., 1991), peroxisomes (Raychaudhuri and Prinz, 2008) and plastids (Benning et al., 2006) do not obtain their lipids through the secretory pathway. Therefore, there is considerable evidence accumulating to support a significant role for traffic of lipids independent of vesicles, which can function in parallel with vesicular traffic (Voelker, 2009).

The hydrophobic nature of lipids in most cases limits the spontaneous movement of lipids through the cytosol from a thermodynamic point of view. The existence of families of

soluble proteins with specific domains capable of binding different lipids suggested that these proteins may mediate a lipid trafficking mechanism that was independent of vesicles (D'Angelo et al., 2008). Historically, these soluble proteins were named lipid transfer proteins (LTPs) as they were originally identified by their ability to transport lipids between donor and acceptor vesicles *in vitro*. In these assays, LTPs can directly bind to specific lipids in donor membranes, extract them, and then deliver their cargo molecules to acceptor membranes in an ATP-independent manner (Fig. 1.9). LTPs are grouped, by sequence similarity of their lipid-binding domains, into different families, including START, SEC14/PITP, GLTP, OSBP/ORPs, and SCP-2 (non-specific LTPs) (D'Angelo et al., 2008). The most well characterized LTPs are: (i) CERT, for the ceramide transport from ER to trans Golgi (TGN), in mammalian cells, (ii) *OSH4/Kes1* (member of the OSBP binding protein family) for sterol transporter in yeast, and (iii) PITPs, phosphatidylinositol transfer proteins, in *Drosophila* and yeast.

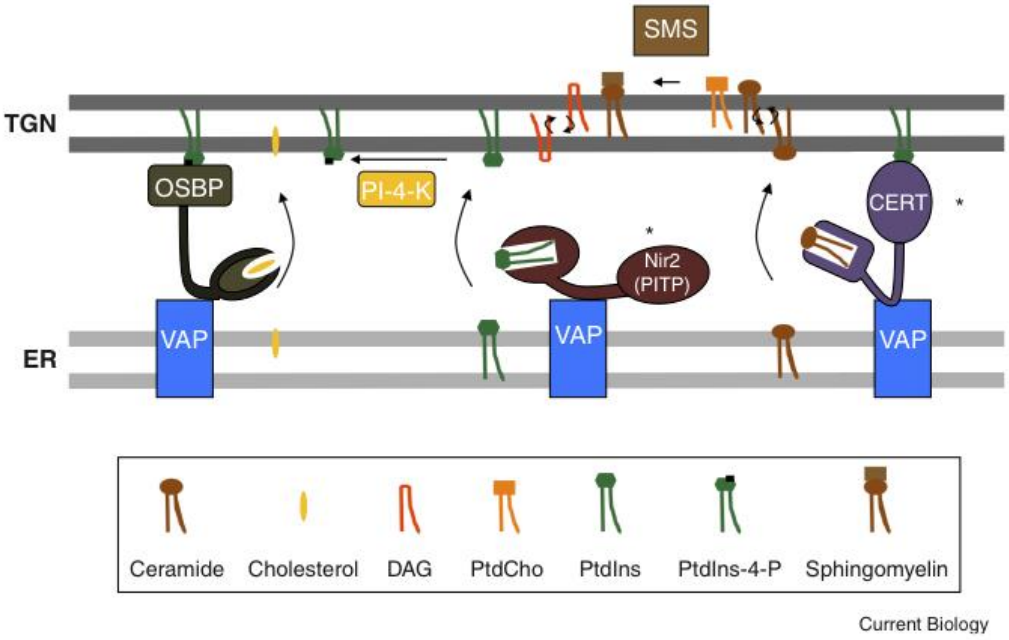

Figure 1.9: Lipid transfer proteins.

OSH/ORPs, rdgB/Sac14 and CERT, and are proposed to facilitate lipid trafficking out of the ER of sterols, PI4P, and ceramide, respectively. The ER protein VAP/Scs2 binds the FFAT motifs of OSH/ORPs, rdgB/Sec14 and CERT (modified from (Bankaitis et al., 2012)) (see text below for more information).

1.3.3.3. Ceramide transfer protein (CERT) or StAR-related lipid transfer protein

Perhaps the most well studied nonvesicular lipid transport system at the molecular level is the transport of ceramide in mammalian cells, one of the few cases in which the lipid transfer activity of the lipid binding protein has been established in the cellular context. Ceramide is synthesized in the cytosolic surface of the ER through a series of reactions (Hanada et al., 2007; Watanabe et al., 2002) and is transported to the Golgi for conversion to both sphingomyelin (SM) and glucosylceramide (GlcCer) (van Meer and Holthuis, 2000). Transport of ceramide from the ER occurs by both ATP-dependent vesicular trafficking (Fukasawa et al., 1999) and ATP-independent nonvesicular mechanisms. The nonvesicular trafficking of ceramide is mediated by an LTP called CERT (Hanada et al., 2003). CERT has four domains: a C-terminal START domain responsible for ceramide transfer between membranes, a pleckstrin homology (PH) domain, which recognizes phosphatidylinositol 4-monophosphate (PI4P) at the Golgi; a highly conserved short amino acid motif called the FFAT motif (two phenylalanines in an acidic tract); and a serine-rich domain. The FFAT motif binds to a highly conserved ER integral membrane protein of the VAP family (the human homologue of yeast Scs2) (Hanada et al., 2007), allowing CERT to access ceramide in the ER. The PH domain targets CERT to the Golgi. Yeast cells synthesize inositolphosphoceramide (IPC) from phytoceramide instead of SM and phytoceramide transport form the ER to the Golgi occurring through both vesicular and non-vesicular pathways (Funato and Riezman, 2001). However, CERT orthologs have not been detected in yeast by homology searches, suggesting yeast use a distinct mechanism for phytoceramide transport (Dickson, 2008).

1.3.3.4. OSBP-related proteins (ORPs)

Sterols are major components of all eukaryotic PM and are primarily made in the ER, which contains relatively low levels of sterols because of their rapid sterol traffic to the PM. In general, sterol transport seems to involve multiple pathways. For example, cholesterol can be delivered to the PM via the secretory pathway for glycoprotein secretion in mammalian cells, (Kaplan and Simoni, 1985; Urbani and Simoni, 1990) or receptor-mediated endocytosis of low-

density lipoproteins (LDLs) from early endosomes to late endosomes/lysosomes and later on to the ER and the PM (Brown and Goldstein, 1999).

In mammalian cells, newly synthesized cholesterol traffics from the ER to the PM, in an ATP-dependent manner, with a half-life of 10 minutes (DeGrella and Simoni, 1982). In theory, cholesterol could be trafficked by vesicles; however, it has been shown that this is not the primary pathway by which they are transported. Treating cells with brefeldin A, which inhibits protein secretion, does not dramatically inhibit the transport of newly synthesized cholesterol from the ER to PM (Holtta-Vuori and Ikonen, 2006; Urbani and Simoni, 1990). OSBP was identified as the first protein having affinity for oxysterols (oxygenated derivatives of cholesterol) (Kandutsch and Thompson, 1980). The OSBP-related domain (ORD), which demonstrates sterol-binding and/or sterol-transfer activities, was also found in additional proteins. In humans, 11 OSBP homologues have been identified and named ORPs, OSBP-related proteins (Lehto and Olkkonen, 2003). The ORP family is present in all eukaryotes and is proposed to mediate nonvesicular traffic of sterols (Ridgway, 2010). Additional domains also present in CERT are found in ORP family proteins, including PH domains and FFAT motifs. Eight of the human ORPs; OSBP, ORP1– 4, ORP6, ORP7 and ORP9, have the FFAT motif and have dual targeting for the ER and other membranes (Ridgway, 2010).

Yeast cells do not have classical receptor-mediated endocytosis of sterols due to the lack of LDL-receptors. Extensive studies of mutants of *SEC18*, which encodes a yeast homologues of N-ethylmaleimide-sensitive factor (NSF) that is required for most if not all vesicular trafficking, suggested that vesicular trafficking is not the sole route for transporting of newly synthesized ergosterol between the ER and the PM (Baumann et al., 2005; Schnabl et al., 2005). In the *S.cerevisiae* genome, seven ORPs, called Osh proteins (OSBP-homologue) exist. Deletion of any of the seven Osh proteins or several in combinations is not lethal. However, the deletion of all seven is inviable suggesting there is an overlapping function for all Osh proteins (Beh et al., 2001). Osh1, Osh2, and Osh3 contain the FFAT motif, which binds Scs2 (Loewen et al., 2003). Osh1 is localized to the Golgi and NVJs (see Section *1.1.4.1.* for NVJ*)*, and its NVJ localization is dependent on its binding to Scs2 (Loewen et al., 2003). Osh2 and Osh3 are localized to the pmaER in a Scs2-dependent fashion since mutations in their FFAT motif or deletion of the entire motif prevents their peripheral localization (Loewen et al., 2003).

The most abundant Osh protein is Osh4, which localizes to the TGN/endosomal membranes by binding to PI4P pool (Li et al., 2002). Osh4 is the focus of many yeast ORPs studies, as it can binds phospoinosides (PIPs) as well as sterols. It has been shown previously that Osh4 can transfer sterols between liposomes, an artificially-prepared vesicle composed of a lipid bilayer, *in vitro*, with transfer stimulated in the presence of PIPs (Raychaudhuri et al., 2006). Although Osh4 lacks a PH domain, its ORD is capable of binding to PIPs. The crystal structure of Osh4 revealed that the ORP domain has a central hydrophobic pocket in which one sterol molecule can be bound. Upon sterol binding, the protein changes its conformation to cover the pocket with a flexible lid that will shield the lipid during its transit through the hydrophilic cytosol (Im et al., 2005; Raychaudhuri et al., 2006; Schulz and Prinz, 2007). Thus, this data suggests that Osh4 is capable of extracting and transferring sterols between membranes within cells.

Does Osh4 transfer sterol in a nonvesicular fashion *in vivo*? Previous studies suggested that the Osh family also regulates the vesicular transport required for polarized growth in yeast (Kozminski et al., 2006) and some new data argues that Osh proteins in general do not transport sterol *in vivo* (Beh et al., 2012; Georgiev et al., 2011). New studies challenged the role for Osh4 in sterol transfer between the ER and the PM, as it was demonstrated to be essentially unaltered in Osh-deficient cells (Georgiev et al., 2011). Additionally, Osh4 mutants that cannot bind to sterol are more toxic to yeast than Osh4 when both are overexpressed (Mousley et al., 2012). This very recent study by the Bankaitis group (Mousley et al., 2012) suggests that Osh4 is more involved in the sensing of sterols in membranes, rather than their actual transfer. Osh4 has a dual-binding activity for sterol and PI4P, which allows Osh4 to bind to the TGN/endosomal PI4P pool. The Bankaitis group found that increased levels of Osh4 impaired trafficking through the TGN/endosomes, which is toxic to the cell. Interestingly, the sterol-binding mutant form of Osh4 binds the TGN/endosomal membrane with higher affinity than the wild type form of Osh4 resulting in inhibition of cell growth and decreased trafficking. Binding to sterol is essential for the release of Osh4 from PI4P in the TGN/endosomal membrane. Thus, they proposed that Osh4 is recruited to membranes by its ability to bind to PI4P and binding to sterols at the TGN/endosomal membranes releases it (Mousley et al., 2012). This data suggested that Osh4 is a sterol sensor in the TGN/endosomal system, rather than an LTP, which clearly contradicts previous models that propose a role for Osh4 in nonvesicular sterol transfer (Schulz et al., 2009).

1.3.3.5. Phosphatidylinositol transfer proteins (PITP)

PITPs were originally discovered by their ability to transfer PI derivatives and PC between biological membranes *in vitro* (Cockcroft, 2001). PITPs are divided into two major classes: metazoan PITPs and Sec14-like proteins. These two classes lack sequence homology with each other, although they have functional redundancy (Griac, 2007).

In *Drosophila*, rdgB (so called since mutations in this gene cause retinal degeneration type B) has a PITP domain. In photoreceptor cells the activity of phospholipase C enzymes results in conversion of PI(4,5)P2 in the PM to I(1,4,5)P3 and DAG in response to light. PI(4,5)P2 can then be replaced by the sequential phosphorylation of PI, which must be trafficked out of the ER. Therefore, an adequate supply of PI to the PM is essential to maintaining optimal levels of PI(4,5)P2 for phototransduction. rdgB appears to be required for re-supplying the PM with PI as a precursor for PI(4,5)P2 synthesis, directly from the ER by nonvesicular traffic in these cells (Trivedi and Padinjat, 2007). rdgB has a FFAT motif that interacts with VAP on the ER (Loewen et al., 2003) but the mechanism by which rdgB targets the PM is unknown. Although mutations in the PITP transfer domain of rdgB cause photoreceptor degeneration, it is not clear if rdgB is associated with true monomeric phospholipid traffic; only one study has addressed the specific role of PI transfer in the rdgB phenotype (Milligan et al., 1997). There is an obvious lack of correlation between the *in vitro* PI transfer function and its ability to rescue the phenotype *in vivo*. The mammalian homologues of rdgB are Nir2 (rdgB1) and Nir3 (rdgB2), all of which contain the PITP domain. Nir1 is a third homologue of ridge, though it lacks the PITP domain (Lev, 2004). All three Nir proteins have the FFAT motif that can bind VAP on the ER (Loewen et al., 2003).

In yeast, Sec14 is the major PITP that couples PC metabolism with PI4P production (Schaaf et al., 2008). Sec14 originally was discovered in a genetic screen for yeast mutants that were defective in secretion of invertase (Bankaitis et al., 1989). Sec14 was later found to be an essential gene required for transport from the yeast Golgi complex (Bankaitis et al., 1990; Cleves et al., 1991). Sec14 was originally considered to act as an LTP to provide the PI 4-kinase in the Golgi with its substrate after extracting PI from the ER membranes. However, there was poor evidence for Sec14 acting as an LTP *in vivo*. There are many complexities associated with *sec14* phenotypes, but studying ‘bypass Sec14’ mutants revealed that Sec14 regulates lipid metabolism

in yeast Golgi membranes as well as the secretory function of this organelle (Bankaitis et al., 2010). Genetic data also showed that deletion of Sec14 is compensated by deletion of Osh4 (Fang et al., 1996). As previously discussed, Osh4 binds PI4P and acts antagonistically to Sec14 in modulating the Golgi localized PI 4-kinase, Pik1 (Fairn et al., 2007). Similarly, PC is intrinsically toxic to Sec14-dependent Golgi secretory function as genetic studies showed that deletion of Kennedy pathway genes suppressed the *sec14-ts* phenotype (Cleves et al., 1991). While a comprehensive discussion of physiological roles of Sec14 is beyond the scope of this section, the newest model for Golgi PI4P is that Sec14 has a tug of war with Osh4 to regulate multiple aspects of lipid metabolism, such as sphingolipid signaling, PI4P and sterol at multiple levels (Bankaitis et al., 2010; Mousley et al., 2012; Villasmil et al., 2012), Sec14 functions as a lipid sensor rather than in the monomeric nonvesicular transfer of PI.

1.3.4. Membrane contact sites and nonvesicular traffic

Membrane contact sites are genuine, specialized domains that are more than just the ubiquitous structures observed by electron microscopy (see Section *1.1.4.*). Coordination of lipid biosynthesis and traffic at contact sites between membranes is an attractive hypothesis and there is increasing evidence to support this idea. Although, it is likely that some LTPs function *in vivo* by diffusing between membranes across large cytoplasmic distances, especially if these proteins lack specific membrane targeting signals, the alternative hypothesis is that LTPs act at membrane contact sites. In theory, LTPs acting at contact sites eliminates the diffusion step, which should dramatically increase the efficiency of lipid transfer between organelles (Fig. 1.10). For instance, CERT localizes to Golgi-ER contact sites through binding of its FFAT motif to VAP on the ER and its PH domain on Golgi membranes, which may dramatically increase the efficiency of ceramide transfer (Levine and Loewen, 2006).

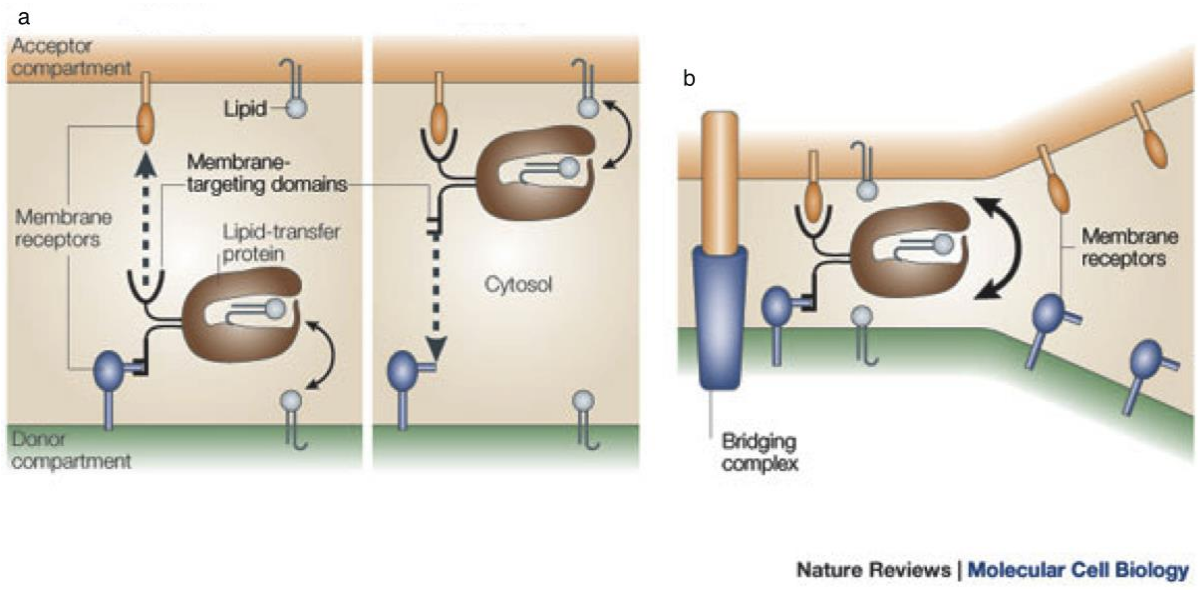

Figure 1.10: A hypothetical example of nonvesicular lipid traffic at membrane contact sites by an LTP.

(A) An LTP shuttling across contact sites. The two potential states of an LTP are shown, and its diffusion across the cytosolic gap is indicated by dashed arrows. Lipid is exchanged at both membranes (curved arrows), which allows transport down a concentration gradient. (B) If an LTP can interact with both of its membrane receptors simultaneously at contact sites, this will increase the avidity of membrane binding. The absence of a diffusion step would increase the efficiency of lipid transfer (larger curved arrow) (adapted from (Holthuis and Levine, 2005)).

1.3.5. Membrane contact sites and the "in trans" model

The model that LTPs transport lipids at contacts does not seem to be supported by all *in vivo* studies (except for CERT) and it appears unlikely that all LTPs perform this function *in vivo*. As previously discussed (see Section *1.3.3.2.*), genetic analyses and the localization of enzymes involved in lipid biosynthesis as well as lipid binding proteins to membrane contact sites (see Section *1.1.4.*) suggest that these structures are important for regulating lipid metabolism. However, it remains an open question how lipids move between membranes. Another alternative is that membrane contact sites can regulate lipid synthesis through

controlling the localization of enzymes and substrates in a way that there is no need for lipids to be actually trafficked.

Consistent with this idea, it has been shown that the PI 4-phosphatase, Sac1 regulates PI4P levels "*in trans"* in the PM (Stefan et al., 2011). Sac1 also controls PI4P levels in the ER and Golgi *in cis* (Baird et al., 2008; Manford et al., 2010). The "*in trans*" model predicts that the substrate PI4P is localized in a different membrane than that in which, the enzyme resides. Stefan et al. have shown that Sac1, which is an integral ER protein in yeast localizes to PM-ER contacts where Osh3, a soluble lipid binding protein of the OSBP family, acts as a sensor of PI4P levels at the PM and subsequently activates the Sac1 PI phosphatase at the ER (Stefan et al., 2011). Moreover, they have shown that cells lacking yeast Scs2 display elevated levels of PI4P at the PM (Stefan et al., 2011), suggesting that Scs2 may bind to and activate Osh3 at PM-ER contacts to control PM PI4P levels. Scs2 may also indirectly modulate the activity of Sac1 by mediating PM-ER contact site formation (Loewen et al., 2007). It has been proposed that Osh3 may act as a noncatalytic subunit of Sac1 at PM-ER contacts to activate its phosphatase activity *in trans.*

PEMT enzymes may also act "*in trans"* in the synthesis of PC from PE. In several previous enzymological studies, PEMT substrates were added in the form of sonicated lipid suspensions and it was unclear how phospholipid substrates became methylated by PEMT enzymes located in the microsomal membranes (Gaynor and Carman, 1990; Kodaki and Yamashita, 1987). More recently, the possibility of PEMTs acting *in trans* was investigated using subcellular membrane fractions isolated from Δ*cho2* and Δ*opi3* yeast PEMT mutants (see Section *1.2.1.1.* for PEMTs)(Janssen et al., 2002). It was found that in this *in vitro* assay, Opi3 on microsomes converted PMME on liposomes to PDME and PC (Janssen et al., 2002) indicating catalysis likely occurred *in trans*. It should also be noted that the first bacterial phospholipid methyltransferase enzyme discovered is in fact a soluble protein without any transmembrane domains (Arondel et al., 1993). Since then more prokaryotic phospholipid methyltransferases have been found that are soluble enzymes (Aktas and Narberhaus, 2009). Thus, in prokaryotes PEMT enzymes likely act "*in trans"*. Finally, the soluble PS synthase and PE methyltransferase enzymes in *E.coli* (Ishinaga and Kito, 1974) are capable of acting on their lipid substrates in membranes suggesting that "*in trans"* catalysis may be widespread in biology.

1.4. SCS2

Scs2 is a highly conserved tail-anchored ER protein that was originally discovered as a high copy suppressor of choline sensitivity of inositol auxotrophy of the yeast Δ*hac1* and Δ*cse1* mutants (Nikawa et al., 1995). The *CSE1* gene was never cloned in yeast and *HAC1* was later found to encode a transcription factor that activates expression of UPR target genes in yeast (see Section *1.1.3.1.* for UPR). The majority of studies of Scs2 have been focused on its role in the regulation of inositol synthesis (see Section *1.2.2.1.*). Deletion of *SCS2* causes slight inositol auxotrophy, since it can no longer sequester Opi1 in the ER and therefore *INO1* expression is constitutively repressed by Opi1(Kagiwada and Zen, 2003) (Fig. 1.5). Additionally, Scs2 interacts with a short FFAT peptide motif (two phenylalanines in an acidic tract) of which the conserved core sequence is: EFFDAxE (Loewen et al., 2003). The FFAT motif is present in multiple families of lipid binding/transfer proteins and is important for their function in accessing lipids in the ER (see Section *1.3.3.1.*).

Our lab previously found a novel role for Scs2 in the attachment of the ER to the PM and the formation of PM-ER contacts (Loewen et al., 2007). Cells lacking *SCS2* demonstrated normal nuclear ER structure as well as normal ER tubule delivery into the bud. However, these mutants showed reduced amount of pmaER, especially in small budded cells (Loewen et al., 2007). We also found that *ICE2,* a gene encoding an ER protein previously found to be involved in inheritance of pmaER (Estrada de Martin et al., 2005), but with unknown molecular function, had an aggravating genetic interaction with *SCS2* (Loewen et al., 2007). Δ*scs2*Δ*ice2* cells have almost a complete loss of pmaER, multiple buds and formed defective septin rings at the bud neck. Together, the loss of pmaER in Δ*scs2*Δ*ice2* cells and the genetic interaction between *ICE2* and *SCS2* suggested that they function in parallel or partially redundant pathways in ER biogenesis. Uniquely among ER proteins, Scs2 is enriched within the ER at sites of polarized growth, and localizes to these sites even when its C-terminal transmembrane domain is deleted. Thus, the polarized localization of Scs2 is likely mediated by interactions with components of the PM, since this protein is no longer physically tethered to the ER (Loewen et al., 2007). These results suggested a role for Scs2 in ER polarization during cell division. Interestingly, VAP, the human homologue of Scs2, expressed in yeast, also localized to the bud tip, indicating that these interactions are highly conserved (Loewen et al., 2007). Mutations in the MSP domain of VAP-B cause amytrophic lateral sclerosis (ALS) (Nishimura et al., 2004), however, the molecular

mechanism of disease is not yet know. This suggests that defects in ER inheritance or phospholipid metabolism at membrane contact sites may be a contributing factor to ALS pathology. The major focuses of this dissertation are: defining the molecular functions for Scs2 in the formation of pmaER and PM-ER contact sites, roles for ER contacts in phospholipid metabolism specifically PS to PE traffic/synthesis at mitochondria-ER contacts and Scs2's role in the polarized growth in yeast.

In *Chapter 2*, I investigated a role for PM–ER contact sites in regulating phosphatidylcholine (PC) synthesis in budding yeast. I found that Δscs2Δice2 cells are choline auxotrophs and PM–ER contacts are required for PC synthesis. We showed that the addition of choline or overexpression of Opi3, the enzyme that catalyzes the second and third methylation steps of PC biosynthesis, rescued growth defect of Δscs2Δice2 cells. Interestingly, localization of the Opi3 to pmaER seems to have a crucial role in regulating the activity of the protein. Osh2 and Osh3, the oxysterol-binding protein homologues in yeast, rescued the choline auxotrophy phenotype of Δscs2Δice2 cells but did not restore pmaER, indicating that they may function with Opi3 in PC synthesis. In search for regulators of pmaER, we identified the phosphatidic acid phosphohydrolase Pah1 that seems to be involved in establishing pmaER, independent of its enzymatic activity. Finally, we proposed that PE to PC synthesis by Opi3 happens "in trans" at PM-ER contacts to control rapid PC requirements of the PM. This work demonstrates the capability for de novo lipid synthesis at membrane contact sites.

In *Chapter 3*, I aimed to discover novel genes involved in PE synthesis/traffic from ER to mitochondria. Initially, we found a genetic interaction between Psd1, the mitochondrial PS decarboxylase, and Cho2, which catalyzes the first methylation of the PE. By doing a genome-wide screen for *CHO2*, we identified genetic interactions between *CHO2* and Emc proteins indicating that Emc proteins are important for PE metabolism. We found that mitochondria-ER tethering requires two complexes, EMC and ERMES, which has previously been shown to act as a tether between mitochondria and ER. We found that cells missing both complexes are not viable and ER to mitochondria lipid transport is blocked. Both phenotypes were completely corrected by the expression of an artificial ER-mitochondria tethering protein, demonstrating for the first time that tethering and lipid exchange between the ER and mitochondria are essential processes. We proposed that Emc facilitates PS transfer from the ER to mitochondria for PE synthesis.

Interestingly, Scs2 is a polarized protein and localizes to sites of polarized growth even in the absence of its transmembrane domain. Thus, the polarized localization of Scs2 is likely mediated by interactions with components of the PM, since this protein is no longer physically tethered to the ER (Loewen et al., 2007). These results suggested a role for Scs2 in ER polarization during budding. In *Chapter 4*, I investigated for roles of SCS2 in polarized growth. Jesse Chao from our lab found that there is a tether between ER and septin created by a direct interaction between the septin Shs1 and Scs2 (unpublished data). I found a physiologically important function of the ER diffusion barrier, which is to restrict diffusion of the spindle from mother to bud until M phase. Scs2 interacts directly with the spindle capture protein Num1 and it prevents Num1 from diffusing from the mother into the bud during S and G2 phases.

The final chapter of this dissertation, *Chapter 5*, summarizes results and discusses the significant of my work and future directions.

2. PLASMA MEMBRANE – ENDOPLASMIC RETICULUM CONTACT SITES REGULATE PHOSPHATIDYLCHOLINE SYNTHESIS

2.1. SYNOPSIS

Synthesis of phospholipids, sterols and sphingolipids is thought to occur at contact sites between the ER and other organelles because many lipid-synthesizing enzymes are enriched in these contacts. In only a few cases have the enzymes been localized to contacts in vivo and in no instances have the contacts been demonstrated to be required for enzyme function. Here, we show that plasma membrane (PM) - endoplasmic reticulum (ER) contact sites in yeast are required for phosphatidylcholine (PC) synthesis and regulate the activity of the phosphatidylethanolamine N-methyltransferase enzyme, Opi3. Opi3 activity requires Osh3, which localizes to PM-ER contacts where it may facilitate in trans catalysis by Opi3. Thus, membrane contact sites provide a structural mechanism to regulate lipid synthesis.

2.2. INTRODUCTION

The structure of the ER of *Saccharomyces cerevisiae* is somewhat unique amongst eukaryotes, in that its reticular network, a characteristic of all eukaryotic cells, lies just beneath the PM. Reconstruction of total yeast ER in individual cells by 3D electron tomography (West et al., 2011) has revealed that PM-associated ER (pmaER) consists of ER tubules and flattened fenestrated ER sheets that are in close apposition to the cytosolic leaflet of the PM. Regions of pmaER that are apposed to the PM are devoid of ribosomes (West et al., 2011),consistent with these being sites of physical contact between ER and PM (Pichler et al., 2001). PM-ER contacts likely play important roles in all eukaryotic cells (Levine, 2004) and in yeast, pmaER is enriched in lipid synthesizing enzymes (Pichler et al., 2001), suggesting PM-ER contacts are important for lipid metabolism. Protein families with lipid related functions have been found specifically localized at PM-ER contact sites (Loewen et al., 2003; Schulz et al., 2009; Toulmay and Prinz, 2012) where they are thought to play roles in non-vesicular lipid transport between PM and ER, although the role for the contacts themselves has not been directly demonstrated. Recently, it has

been found that localization of the integral ER phosphatidylinositol phosphate phosphatase, Sac1, to PM-ER contacts regulates phosphatidylinositol 4-phosphate (PI4P) levels in the PM *in trans* (Stefan et al., 2011). *In trans* catalysis by Sac1 requires interaction with Osh3, a soluble lipid binding protein of the oxysterol binding protein (OSBP) family that localizes to PM-ER contacts (Loewen et al., 2003), and may present PI4P in the PM to the ER-localized Sac1 (Stefan et al., 2011). Consistent with a role for contacts in regulating Sac1, a mutant with reduced pmaER has increased levels of PI4P (Manford et al., 2012).

We previously found that two genes with roles in ER biogenesis in yeast, *SCS2* and *ICE2*, exhibit an aggravating genetic interaction, and Δ*scs2*Δ*ice2* double mutants appear to have greatly reduced pmaER by confocal microscopy (Loewen et al., 2007). This suggests that pmaER and possibly PM-ER contacts perform an essential function required for cell growth. Ice2 is an integral ER protein that is required for inheritance of pmaER, but its molecular function is unknown (Estrada de Martin et al., 2005). Scs2 is a highly conserved tail-anchored protein of the VAP family that localizes proteins containing FFAT motifs to the ER (Loewen et al., 2003) and regulates yeast phospholipid synthesis (Loewen et al., 2004). Scs2 localizes both Osh2 and Osh3, two of seven yeast OSBP homologues that contain FFAT motifs to PM-ER contacts (Loewen et al., 2003; Schulz et al., 2009), which is also required for regulation of in trans Sac1 activity (Stefan et al., 2011). Here, we show that like Sac1, the yeast phosphatidylethanolamine (PE) N-methyltransferase (PEMT) enzyme, Opi3, likely acts *in trans* at PM-ER contact sites to synthesize PC.

2.3. MATERIALS AND METHODS

2.3.1. Plasmids and yeast strains

The *pGAL-OSH1*, *OSH2* and *OSH3* multicopy plasmids (pOSH1, -2, -3) used in this study were a kind gift from C. Beh (Kozminski et al., 2006) and express the native untagged protein under control of the galactose promoter (GAL1-10). pGST-*PAH1* was isolated from the GST-ORF yeast array (Sopko et al., 2006) and confirmed by sequencing. It expresses Pah1 tagged at the N-terminus under control of the galactose promoter. HA-tagged Pah1 (pPAH1) and the catalytically dead D398E variant (pPAH1 D398E; containing the D398E mutation in the

Pah1 coding sequence) were a kind gift from G. Carman (Han et al., 2007). The *pOPI3* plasmid is based on pRS416 (CEN, URA3) (Sikorski and Hieter, 1989) and expresses the Opi3 protein with an N-terminal myc tag (MEQKLISEEDL) under control of the constitutive portion of the *PHO5* promoter and was constructed by amplifying the *OPI3* coding sequence from yeast genomic DNA and cloning the PCR product into the Bgl2 (5') and SacI (3') restriction sites. *pSCS2* was constructed as *pOPI3* except that the *SCS2* gene was inserted. *pCHO2* was obtained from the MoBY-ORF collection (Ho et al., 2009) and contains the *CHO2* gene with its endogenous promoter and terminator cloned into a centromere-based vector. RFP-ER contains the C-terminal transmembrane domain of Scs2 fused to monomeric DsRed in pRS416 (CEN, URA) under control of the *PHO5* promoter (Loewen et al., 2007).

All yeast strains were based on S288C. Deletion strains were obtained from freezer stocks of the haploid yeast deletion collection (BY4741, MAT a, KanMX), a gift from C. Boone. All deletion strains were confirmed by PCR. GFP-tagging of endogenous proteins was done by homologous recombination of PCR-generated fragments in haploids at the C-terminus of the endogenous protein using the pKT128 (SpHIS5) plasmid (Sheff and Thorn, 2004) in the BY7043 background (Tong and Boone, 2006). Gene deletion strains were constructed in BY4741 using PCR-generated fragments from pKT127 (KanMX) (Sheff and Thorn, 2004) or in BY7092 using p4339 (NatR) Tong, 2006 #2555}. Double and triple deletion strains were generated by standard yeast genetic techniques.

2.3.2. Yeast growth assays

10- fold serial dilutions of log phase cells were spotted using a pin-frogger (Sigma) onto agar plates containing synthetic defined (SD) media with the appropriate amino acid dropout mix and either 2% glucose or 2% galactose as indicated. Ethanolamine, choline or monomethylethanolamine were added to SD media to a final concentration of 1 mM. All growth assays were performed at 30°C for at 24-48 hours.

2.3.3. Array-based genome-wide suppressor screen

The array-based genome-wide suppressor screen for the Δ*scs2*Δ*ice2* mutant was performed by modifying the synthetic genetic array (SGA) method (Tong and Boone, 2006) and using the GST-ORF collection (Open Biosystems) in place of the deletion mutant array (Sopko et al., 2006). GST-ORFs are expressed under control of the GAL1/10 promoter and tagged at the N-terminus with GST. The GST-ORF collection was arrayed using a RoToR HDA robot (Singer Instruments) at a density of 1536 spots per plate onto SD media containing glucose. This array was crossed with a Δ*scs2::*NatMX Δ*ice2*::KanMX mutant query strain (Y7092 background) grown on SD media containing choline and diploids were selected on medium also containing choline prior to sporulation for 5 days. Haploid Δ*scs2*Δ*ice2* double mutant progeny containing the GST-ORF plasmids were recovered on media lacking His, Arg, Lys, and containing canavanine, thialysine, G418, and Nat. The final pinning step was to media containing 2% galactose and lacking choline. Suppressors were identified by visual inspection of plates and GST-ORF plasmids were recovered and sequenced to confirm the identity of the suppressors.

2.3.4. Confocal microscopy

Yeast strains expressing GFP-tagged proteins were grown to log phase and imaged by squashing 1-5 µl of live yeast in media between a slide and cover slip. Yeast were examined at room temperature using a Zeiss LSM-5 Pascal confocal microscopy system equipped with a Zeiss 100X objective (Plan-neofluar, 1.3) and images were acquired with Zeiss Pascal software. All confocal microscopy images within a given experiment were taken with identical microscope settings to enable direct comparison between images and samples. Image brightness was adjusted uniformly for the entire image using Adobe Photoshop software. Quantification of Opi3-GFP from confocal images was done using Image J software (NIH) by drawing a line across the nuclear ER and determining the maximum pixel intensity from the resulting plot. Two separate measurements were taken per cell and averaged and a minimum of 20 cells per strain was analyzed.

2.3.5. Quantification of PM-ER contact sites by transmission electron microscopy

For thin-section electron microscopy, cells were prepared essentially as described previously (Prinz et al., 2000). Briefly, log-phase cells growing in SD media with galactose and choline were harvested. Cells were washed twice with water and incubated in freshly prepared potassium permanganate solution (1.5%) twice for 30 min at 4°C. The cells were washed several times in water, and dehydrated with increasing concentrations of acetone and embedded in Spurr's resin. Sections approximately 50 nm thick were cut with a Leica UCT microtome and stained with 4% uranyl acetate for 20 minutes, followed by Reynold's lead citrate at room temperature for 6 min. Thin sections were viewed on a Hitachi H7600 transmission electron microscope (located at the UBC Bioimaging Facility). To quantify PM-ER contacts in each cell we identified sections of ER, which are electron-dense linear structures, within 60 nm of and parallel to the PM in TEM images at 80,000 x magnification (approximately 5-10 images per cell). PM-ER contact length was measured by tracing each segment using ImageJ software (National Institutes of Health). The whole-cell perimeter was measured from a single 20,000 X magnification image for each cell by tracing the PM. Contact length was calculated as the average of the lengths of the contacts for a given cell. The ER:PM ratio was calculated as the sum of the length of the contacts divided by the length of the PM perimeter for each cell. The contact frequency (per μm) was calculated by dividing the number of contacts in a given cell by the perimeter of that cell. A minimum of 15 budded cells, were analyzed per condition. Measurements were assumed to fit a gaussian distribution and P values were calculated using an unpaired Student's one-tailed t-test.

2.3.6. In vivo methylation assay

To monitor conversion of PE to PC, 100 ml of cells were grown in synthetic defined media containing 2% raffinose and 2% galactose (SD-RG) to an OD_{600} of 0.5. For the experiments shown in Fig. 2.2 A and Fig. 2.2 C, SD-RG media was supplemented with 1 mM choline to support growth of the Δ*cho2* and Δ*scs2*Δ*ice2* mutants. Cells were collected by centrifugation, washed once in 0.67% Yeast Nitrogen Base (YNB) then resuspended in 12 ml YNB + 2% raffinose, 2% galactose (YNB-RG). After addition of 24 μCi of [^{3}H]-ethanolamine,

cells were shaken at 37 °C for 1 h. Cells were then collected by centrifugation, washed once in 1.6 ml YNB-RG, resuspended in 120 mL SD-RG (without choline) and shaken at 30 °C. Aliquots of 20 ml were removed every hour, collected by centrifugation, washed once in 1 ml water, and then frozen for subsequent analysis. After thawing cell pellets and washing once in 1 ml water, cells were resuspended in 200 µl water and glass beads added to the top of the meniscus. Cells were lysed by three 30 s cycles of agitation in a Precellys 24 tissue homogenizer. The lysate was collected by washing the beads twice with 800 µl water and transferred to a glass tube. Lipids were extracted by the addition of 6 ml 2:1 methanol:chloroform and vortexed once, followed by addition of 2 ml of 0.9% w/v NaCl and vortexing once more [10]. Phase separation was achieved by centrifugation at 1500 g for 1 min. The upper aqueous phase was discarded and the lower organic phase transferred to a clean tube. The solvent was evaporated under a stream of nitrogen and the resultant lipid film resuspended in 60 µl chloroform containing 2 mg/ml PS/PE/PC standards. Following addition of 140 µl of HPLC buffer (90:3:1 acetonitrile:methanol:phosphoric acid) (Voss et al., 2012), the entire sample was injected into a GE Healthcare AKTA FPLC system and lipids separated on a LiChrospher 60 Si column. Fractions corresponding to the PE and PC peaks were collected and activity determined by scintillation counting. The extent of conversion of PE to PC was calculated as the ratio of PC counts divided by PE counts after subtracting a background reading corresponding to column flow-through between the PE and PC fractions.

2.3.7. In vitro Opi3 methylation assay

Microsomes containing Opi3 were isolated from wild type strain D273-10B as described (de Kroon et al., 2003). [^{3}H]-PME-loaded mitochondria from a Δ*opi3* strain SH414 prepared as described (de Kroon et al., 2003) were subjected to lipid extraction. The dried mitochondrial lipid extract was hydrated in buffer (50 mM Tris-HCl pH 7.5, 0.6 M sorbitol), and large unilamellar vesicles (liposomes) were obtained by extrusion through 200 nm pore-size polycarbonate filters after 10 freeze-thaw cycles (Hope et al., 1985). Microsomes at 1 mg protein/ml were incubated with [^{3}H]-PME-loaded liposomes at 0.4 mM phospholipid-phosphorous in buffer supplemented with 5 mM S-adenosyl-L-methionine at 30 °C for 2 h. Lipids were extracted before or after separating liposomes from microsomes on a 20% (w/v)

sucrose cushion in buffer also containing 1 mM EDTA by centrifugation at 175,000 g for 1 h (SW41 rotor, Beckman). The conversion of [^{3}H]-methyl-PME was quantitated after thin layer chromatography as described (Janssen et al., 2002). Lipid extraction was performed according to (Bligh and Dyer, 1959), and phospholipids were quantitated according to (Rouser et al., 1970). Protein concentrations were determined using the BCA method (Pierce) with 0.1% (w/v) SDS added and BSA as a standard.

2.3.8. NBD-PC, NBD-PE and FM4-64 cellular uptake assays

The assays were performed essentially as described (Pomorski et al., 2003). Briefly, stock solutions of NBD-PE and NBD-PC (10 mM; Avanti Polar Lipids) were prepared in DMSO. Log phase cells were pre-incubated at 4^{o}C and NBD-lipids were added to a final concentration of 100 μM, vortexed thoroughly, and incubated at either 4^{o}C or room temperature for the indicated length of time. After incubation, cells were washed in ice-cold media without glucose, containing 2% sorbitol and 20 mM NaN_3. Cells were then mounted on a microscope slide for confocal microscopy. For FM4-64 labeling, log phase cells were incubated either at 4^{o}C or room temperature with 40 μm FM 4-64 for 15 and 60 minutes. Cells were then washed twice in ice-cold media and mounted on a microscope slide for confocal microscopy.

2.4. RESULTS

2.4.1. SCS2 and ICE2 are required for making PC via the methylation pathway

To uncover clues about PM-ER contact site function we examined the yeast global genetic interaction network (Costanzo et al., 2010), which is a comprehensive map of pairwise genetic interactions in which genes with similar functions form coherent clusters. We noticed that *SCS2* and *ICE2* were found in a cluster that was enriched for genes involved in phospholipid metabolism (Fig. 2.1 A). These included genes required to make phosphatidylcholine (PC) by the Kennedy pathway and a salvage pathway that synthesizes PC and PE from the lipid precursors choline, ethanolamine and diacylglycerol (DAG) (Fig. 2.1 B)(Carman and Han,

2011). The cluster containing *SCS2* and *ICE2* showed predominately aggravating genetic interactions with a gene cluster containing both PEMT enzymes, encoded by *CHO2* and *OPI3,* which synthesize PC from PE by the methylation pathway (Fig. 2.1 A & B). Also in this cluster were *INO2* and *INO4,* which encode both subunits of the transcription factor that activates expression of over thirty phospholipid synthesis genes, including *OPI3* (Carman and Han, 2011). *ICE2* was also present in this cluster, further suggesting a role for this gene in the methylation pathway. We found that choline, but not ethanolamine rescued the Δ*scs2*Δ*ice2* slow growth phenotype (Fig. 2.1 C), indicating that the Δ*scs2*Δ*ice2* mutant likely had a defect in the synthesis of PC. We found that overexpression of *OPI3* in the Δ*scs2*Δ*ice2* mutant rescued its growth defect (Fig. 2.1 D) whereas overexpression of *CHO2* did not (Fig. 2.1 E), suggesting Opi3 function was compromised in the mutant. Addition of monomethylethanolamine, which is converted into phosphatidylmonomethylethanolamine (PME) by the Kennedy pathway and bypasses the requirement for Cho2, did not rescue growth of Δ*scs2*Δ*ice2* cells (Fig. 2.1 F) consistent with loss of Opi3 function.

Cho2 performs the first PE methylation step, whereas Opi3 is primarily responsible for the second and third methylations (Fig. 2.1 B), although Opi3 can also perform the first methylation at a reduced rate (Kodaki and Yamashita, 1987). Because of this redundancy, Δ*cho2* cells grow poorly on media lacking choline, but are not obligate choline auxotrophs, whereas Δ*cho2*Δ*opi3* cells are obligate auxotrophs and are rescued by overexpression of Opi3, but not Cho2 (Kodaki and Yamashita, 1987). The aggravating genetic interaction between Scs2 and Cho2 and the alleviating interaction between Scs2 and Opi3 observed in the gene cluster (Fig. 2.1 A), suggested that Scs2 might modify Opi3 function directly. Consistent with Scs2 regulating Opi3, we found that Δ*scs2*Δ*cho2* cells were obligate choline auxotrophs (Fig. 2.1 G), and overexpression of Scs2 rescued the choline auxotrophy of the Δ*cho2* mutant (Fig. 2.2 H). The function of *ICE2* was less clear, however, we did uncover a genetic interaction with *PSD1* that was rescued by ethanolamine (Fig. 2.2 I), further supporting a role for Ice2 in the methylation pathway as implied by the gene cluster.

2.4.2. Opi3 function was compromised in Δscs2Δice2 cells

To measure Opi3 function in the Δ*scs2*Δ*ice2* mutant, we pulse-labelled cells with [^{3}H]-ethanolamine and monitored conversion of radiolabelled PE into PC. In both wild type and mutant cells, the rate of incorporation of label into PC was linear for at least the first three hours of the assay (Fig. 2.2 A). As expected, we found that the rate of PC synthesis in a Δ*cho2* mutant control was significantly reduced (Fig. 2.2 A). Consistent with decreased Opi3 function, PC synthesis was also reduced in the Δ*scs2*Δ*ice2* mutant (Fig. 2.2 B). Overexpression of Opi3 increased the rate of PC synthesis back to levels similar to wild type (Fig. 2.2 C & D). Thus, reduced synthesis of PC in the Δ*scs2*Δ*ice2* mutant likely accounted for the choline auxotrophy of the mutant. Finally, the Δ*scs2*Δ*ice2* mutant was sensitive to dithiothreitol (Fig. 2.2 E), indicating increased ER stress, also consistent with decreased Opi3 function (Thibault et al., 2012).

2.4.3. Δscs2Δice2 cells have altered pmaER

Loss of Opi3 function in the Δ*scs2*Δ*ice2* mutant suggested that Opi3 functioned at PM-ER contacts. Using an endogenous type I integral ER protein Pho88 tagged with GFP we verified our previous findings that Δ*scs2*Δ*ice2* cells had normal ER tubules and nuclear ER, but greatly diminished ER at the cell cortex (Fig. 2.3 A). To characterize PM-ER contacts, we used a specific marker that is an integral ER membrane protein that localizes to PM-ER contacts by interacting directly with the PM (Toulmay and Prinz, 2012). As previously found, Tcb3-GFP localized only to the pmaER domain at the cell cortex, but not the nuclear ER or ER tubules (Fig. 2.3 B). Consistent with 3D electron tomography showing that pmaER forms distinct domains in the bud and mother and is absent from the bud neck (West et al., 2011), Tcb3-GFP was discontinuous through the neck and otherwise localized to pmaER throughout the cell cycle (Fig. 2.3 C). In the Δ*scs2*Δ*ice2* mutant, Tcb3-GFP localization was clearly disrupted. pmaER defects were pronounced in small and medium-sized buds, in which Tcb3-GFP often failed to localize to the bud periphery and instead localized to ER tubules near the center of the bud (Fig. 2.3 D). In mothers, Tcb3-GFP also mislocalized to the nuclear ER.

Now, we examined the localization of the endogenous Opi3 enzyme tagged with GFP, which appeared functional (Fig. 2.4 A). In wild type cells Opi3-GFP localized throughout the ER

(Fig. 2.4 B). We observed some additional diffuse staining in the vacuole that was likely a result of turnover of Opi3-GFP. In the Δ*scs2*Δ*ice2* mutant, localization of Opi3-GFP to the nuclear ER remained intact, however, it was almost completely absent from pmaER (Fig. 2 4 B). Quantification of Opi3-GFP in the nuclear ER revealed no change in its expression level (Fig. 2.4 C), indicating that loss of Opi3 function likely resulted from the defect in pmaER in the mutant. Consistent with this, Opi3 overexpression did not appear to rescue pmaER (Fig. 2.4 D).

2.4.4. Yeast oxysterol-binding proteins regulated Opi3 function at PM-ER contacts

Scs2 localizes both Osh2 and Osh3 to PM-ER contacts (Loewen et al., 2003), and we tested for their roles in regulating Opi3. Overexpression of Osh2 partially restored growth of the Δ*scs2*Δ*ice2* mutant, whereas Osh3 fully rescued (Fig. 2.5 A). In contrast, Osh1, which is localized to the nucleus-vacuole junction by Scs2 (Loewen et al., 2003), did not rescue, and in fact impeded growth (Fig. 2.5 A). Osh3 overexpression restored PC synthesis in the Δ*scs2*Δ*ice2* mutant (Fig. 2.5 B & C), consistent with rescue of growth of the mutant. However, Osh3 did not rescue pmaER in Δ*scs2*Δ*ice2* cells (Fig. 2.5 D), but it did restore growth of the Δ*cho2* mutant (Fig. 2.5 E), suggesting Osh3 regulated Opi3 function at contacts.

2.4.5. PAH1 overexpression rescued PC defect and PM-ER contacts.

We now exploited the choline auxotrophy phenotype of the Δ*scs2*Δ*ice2* mutant in a screen to identify regulators of PM-ER contact structure. We identified a suppressor plasmid carrying the *PAH1* gene (Fig. 2.6 A), which encodes a highly conserved phosphatidic acid (PA) phosphatase enzyme of the lipin family that catalyzes the conversion of PA into DAG in the Kennedy pathway (Fig. 2.1 B) (Han et al., 2006). Surprisingly, a catalytically inactive mutant of Pah1, D398E (Han et al., 2007) also rescued the choline auxotrophy of the Δ*scs2*Δ*ice2* mutant (Fig. 2.6 B), arguing against rescue via the Kennedy pathway. Consistent with this, Pah1 still rescued a Δ*pct1*Δ*scs2*Δ*ice2* triple mutant with an inactivated Kennedy pathway (Fig. 2.6 C). Overexpression of Pah1 rescued PC synthesis in the Δ*scs2*Δ*ice2* mutant (Fig. 2.6 D & E),

indicating Pah1 rescued Opi3 function. However, it did not rescue the Δ*cho2* mutant (Fig. 2.6 E), suggesting Pah1 did not regulate Opi3 directly.

These results suggested that Pah1 might rescue pmaER in the Δ*scs2*Δ*ice2* mutant. In contrast to Opi3 and Osh3, overexpression of GST-Pah1 appeared to restore Tcb3-GFP localization to pmaER (Fig. 2.6 F), and Pah1 also restored Opi3-GFP to pmaER (Fig. 2.6 G). Therefore, we performed an ultrastructural analysis of PM-ER contacts using transmission electron microscopy. We quantified ER segment length, frequency, and the overall ratio of PM-ER contacts to PM perimeter (Fig. 2.7 and Fig. 2.8 A). In the Δ*scs2*Δ*ice2* mutant we found that contacts were decreased to ~7% in buds and ~ 3% in mothers, compared to ~25% of the cell periphery in wild type (Fig. 2.8 B). In buds, the decrease resulted from both a decrease in contact site length (Fig. 2.8 C) and frequency (Fig. 2.8 D). In mothers, the decrease resulted only from reduced frequency since contact site length was unaffected.

Overexpression of both Pah1 and D398E Pah1 in the Δ*scs2*Δ*ice2* mutant restored contacts to near wild type levels in both buds and mothers (Fig. 2.8 B). Rescue resulted from increased contact length and frequency in buds (Fig. 2.8 C & D), indicating Pah1 rescued the defect in formation of pmaER in the bud. In wild type cells, Pah1 increased contacts to ~40% of the cell periphery, a result of increased frequency, supporting a physiological role for Pah1 in initiating contacts. Finally, Pah1 rescued the dithiothreitol (DTT) sensitivity of the Δ*scs2*Δ*ice2* mutant, which did not require activation of the unfolded protein response (Fig. 2.8 E), further supporting that Pah1 directly rescued the defect in PM-ER contacts by a mechanism that was independent of activation of general stress response pathways.

2.4.6. NP-40 sensitivity suggests PME accumulated in the PM of Δ*scs2*Δ*ice2 cells.*

Our results suggest that PM-ER contacts provide a spatial mechanism to regulate synthesis of PC by the yeast PEMT enzyme, Opi3. A consequence of altered Opi3 activity at contacts could be altered PM stability, as has been found in the livers of PEMT -/- mice, which have increased PE:PC in their PM (Li et al., 2006). Yeast mutants with increased PE:PC in the PM are sensitive to nonionic detergents, which destabilize the bilayer (Schuller et al., 2007). We found that Δ*lem3/ros3* cells, which have a buildup of PE in the PM due to decreased PE flippase

activity, (Kato et al., 2002; Saito et al., 2007) were sensitive to NP-40 (Fig. 2.9 A). We also found that Δ*opi3* cells, which have increased PME (Bilgin et al., 2011), were NP-40 sensitive (Fig. 2.9 B), suggesting that PME accumulated in the PM. The Δ*scs2*Δ*ice2* mutant was similarly NP-40 sensitive, which was suppressed by Opi3 (Fig. 2.9 C). Importantly, D398E Pah1 also suppressed, consistent with rescue of PM-ER contacts and reconstitution of Opi3 function by Pah1 (Fig. 2.9 D). Loss of Osh3 also caused NP-40 sensitivity, further supporting its role in regulating Opi3 at contacts (Fig. 2.9 E). This function for Osh3 was independent of its role in regulating PI4P levels in the PM (Stefan et al., 2011), because Δ*sac1* cells were insensitive to NP-40 (Fig. 2.9 E). NP-40 sensitivity was not due to decreased PE flippase activity, because Δ*scs2*Δ*ice2* cells were insensitive to cinnamycin (Ro09-0198), which binds PE located in the outer leaflet of the PM and lyses cells (Kato et al., 2002; Saito et al., 2007) whereas Δ*lem3/ros3* cells were highly sensitive (Fig. 2.9 F).

2.4.7. Opi3 methylation of PME in trans

Previous work suggested that Opi3 could act *in trans* by catalyzing the methylation of PME located in a juxtaposed membrane (Janssen et al., 2002). Hence, the role for PM-ER contacts might be to provide Opi3 access to PE/PME located in the PM for *in trans* methylation. We tested this possibility using an *in vitro* assay. We incubated liposomes containing tritiated PME with ER microsomes containing Opi3 and monitored synthesis of PC (Fig. 2.10 A). Mixing of liposomes and microsomes resulted in conversion of ~35% of the PME into PDE and PC (Fig. 2.10 B). Recovery of the liposomal fraction, which contained the majority of the radiolabel (Fig. 2.10 C), revealed a similar lipid distribution with ~30% of the PME converted to PDE and PC (Fig. 2.10 D), Thus, accumulation of PDE and PC in the liposomal fraction was consistent with *in trans* Opi3 activity. We did not detect defects in endocytosis or uptake of NBD-PE/PC in the Δ*scs2*Δ*ice2* mutant (Fig. 2.10 E & 2.11), indicating lipid transport between PM and ER was likely not disrupted, further supporting that Opi3 functioned *in trans* at contacts.

2.5. DISCUSSION

The ER is an intricate network of tubules and cisternae making contacts with the PM in plants, yeast, and mammals yet how the ER is attached to the cell cortex and maintain its highly reticulated architecture remain largely unknown. Here, we showed that two ER genes in budding yeast, *SCS2* and *ICE2,* which had a negative genetic interaction (Loewen et al., 2007) were required for the formation of PM-ER contacts and consequently PC synthesis via the methylation pathway of phospholipid biogenesis. Scs2 is a highly conserved integral ER protein belonging to the vesicle-associated membrane protein-associated protein (VAP) family and Ice2 was previously identified as required for the proper ER morphology although its functions were not clear (Estrada de Martin et al., 2005). We previously found that *SCS2* and *ICE2* were synthetic lethal only when the double mutants were grown on synthetic defined media (SD), containing a carbon source and salts that supply nitrogen, phosphorus, and trace metals, but not on YP, a rich media of yeast extract, peptone and a carbon source which is commonly used for growing yeast under nonselective conditions (Loewen et al., 2007). It was not clear what was behind this media-dependent negative genetic interaction.

By interrogating the known global genetic interaction network in yeast (Costanzo et al., 2010), we hypothesized that *SCS2* and *ICE2* must somehow be required for PC synthesis by the methylation pathway. We found that Δ*scs2*Δ*ice2* cells were choline auxotrophs, which is a phenotypic manifestation of yeast mutants defective in PC synthesis (Fig. 2.1 C). This observation led us to discover a defect in incorporation of PE to PC in Δ*scs2*Δ*ice2* cells measured by our *in vivo* assay (Fig. 2.2 A). Rescuing the choline auxotrophy and PE to PC conversion by overexpression of Opi3, the phospholipid N-methyltransferase, confirmed our initial hypothesis. By using the confocal microscopy, we examined the morphology of total ER and pmaER and we found a dramatic reduction of pmaER in Δ*scs2*Δ*ice2* cells. Indeed, ultrastructural analyses by TEM revealed that pmaER segments were shorter and made fewer contacts with the PM, resulting in a lower ratio of ER to PM in Δ*scs2*Δ*ice2* cells. The absence of Opi3-GFP from the pmaER in Δ*scs2*Δ*ice2* cells, suggested that Opi3 in nuclear ER and ER tubules could not supply cells with sufficient amount of PC. These findings suggested that: 1) PM-ER contacts were not properly formed in Δ*scs2*Δ*ice2* cells; 2) Defective PE to PC incorporation observed in Δ*scs2*Δ*ice2* cells was the physiological consequence of Opi3 malfunction. Recent studies showed that Ist2, Tcb proteins, and Scs2 are required for tethering

the pmaER to the PM at contact sites and the collapse of pmaER leads to elevated levels of a phosphoinositide lipid at the PM and an unexpected induction of the UPR in the ER (Manford et al., 2012). Similarly, we found that Δ*scs2*Δ*ice2* cells were sensitive to dithiothreitol suggesting the importance of PE:PC ratio on cell growth, viability, and lipid composition.

As an alternative approach to address which novel enzymes and perhaps lipid transfer proteins maybe involved in PC synthesis, we further performed a high copy suppressor screen to identify genes that when over-expressed, could rescue the choline auxotrophy phenotype of Δ*scs2*Δ*ice2* cells. The crux of the matter lies in the assumption that PC synthesis at the ER requires PE resupply from the mitochondria or Golgi/endosomes – the compartments where PE is synthesized. We found Pah1, the PA phosphatase (Han et al., 2006), as the sole suppressor of the Δ*scs2*Δ*ice2* choline auxotrophy phenotype (Fig 2.6 A). Overexpression of Pah1 rescued defective PE to PC incorporation in Δ*scs2*Δ*ice2* cells similar to overexpression of Opi3. It should be noted that initially the rescue by Pah1 was believed to come from the overproduction of DAG by Pah1, which is the substrate for Cpt1 and Ept1 enzymes for synthesizing PE and PC via the Kennedy pathway (Carman and Han, 2011). However, by deleting *PCT1*, the rate –limiting enzyme in the CDP-choline branch of the Kennedy pathway (Skinner et al., 1995), we showed that Δ*scs2*Δ*ice2*Δ*pct1* cells were rescued by Pah1 which argued against an enzymatic role for Pah1 (Fig. 2.6 C). In this regard, rescue of growth and PE to PC conversion by the catalytically dead version of Pah1, D398E, led to investigating a structural role for Pah1. We found that Pah1 and Pah1 D398E rescued the length of pmaER segments, frequency of PM-ER contacts, and the overall ratio of the PM-ER contacts in Δ*scs2*Δ*ice2* cells. Our genetic data indicated that Osh3 is required for Opi3 activity and PC synthesis at PM-ER contacts. PC is considered a bilayer forming lipid while PE can form nonbilayer structures under physiological conditions (Cullis et al., 1986). Maintaining the balance of bilayer and nonbilayer lipids in PM is important for the cell growth and viability. Sensitivity of Δ*lem3,* Δ*scs2*Δ*ice2,* Δ*osh3,* and Δ*opi3* cells to NP-40 suggested that the lipid composition of the PM was altered in these mutants. Since Δ*sac1* cells, which demonstrated an increase of PI4P levels 13-fold above wild type (Stefan et al., 2011) were not sensitive to NP-40, we conclude that an accumulation of PME was a result of Opi3 malfunction and altered PE:PC ratio.

We hypothesized that by restricting the localization of Osh3 to PM-ER contact sites and by providing the lipid substrate *in trans*, Opi3 activity can be restricted to PM-ER contacts and PC can be synthesized directly in the PM. Similar to its proposed role in regulation of Sac1

(Stefan et al., 2011), Osh3 may present PME or PE in the PM to Opi3 located at PM-ER contact sites. *In trans* methylation by Opi3 may enable cells to rapidly adjust the PME/PE:PC ratio of the PM, affecting the physical properties of the bilayer. *In trans* methylation by Opi3 requires that PME is available in the PM. Lipidomic analysis of subcellular fractions of yeast organelles identified PME in the Golgi, but not in any other compartments, including ER microsomes or PM (Schneiter et al., 1999). This suggests that PME is a constituent of the secretory pathway and is trafficked to the PM, where it rapidly is converted to PDE and PC by Opi3. The active site of all eukaryotic PEMTs resides on the cytoplasmic face of the ER membrane and is therefore accessible to the PM. As well, prokaryotic PEMTs are soluble enzymes that lack transmembrane domains (Shields et al., 2003a) and hence must associate with the PM peripherally. Together, this suggests that PM-ER contacts control PC synthesis by regulating access of PEMT enzymes to PE/PME located in the PM for *in trans* catalysis and additionally, these contacts likely constrain localization of many peripheral proteins and enzymes throughout the cellular cortex.

Figure 1

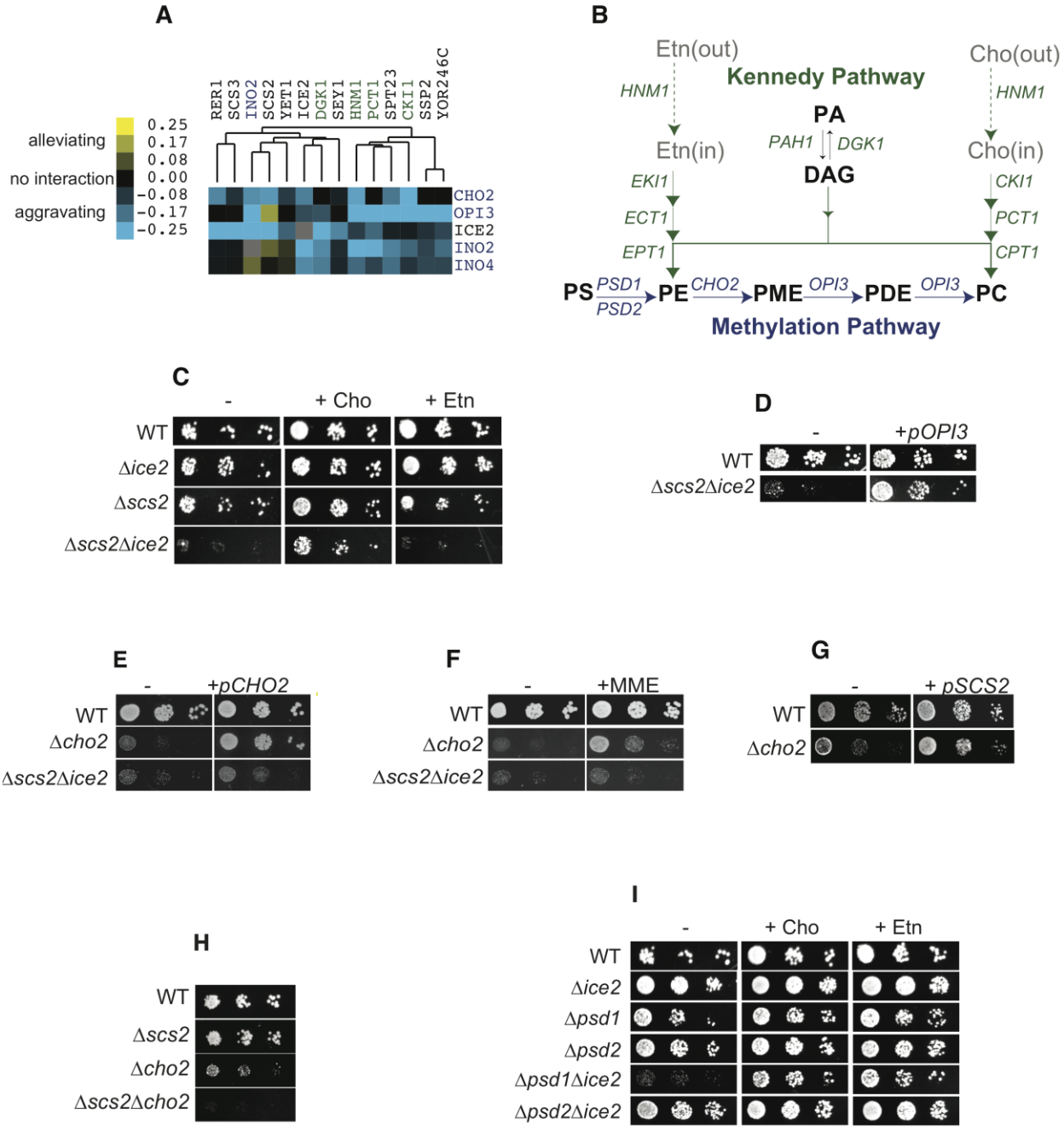
A
RER1
SCS3
INO2
SCS2
YET1
ICE2
DGK1
SEY1
HNM1
PCT1
SPT23
CKI1
SSP2
YOR246C
alleviating
no interaction
aggravating
0.25
0.17
0.08
0.00
−0.08
−0.17
−0.25
CHO2
OPI3
ICE2
INO2
INO4
B
Etn(out)
Kennedy Pathway
Cho(out)
HNM1
HNM1
PA
Etn(in)
PAH1
DGK1
Cho(in)
DAG
EKI1
CKI1
ECT1
PCT1
EPT1
CPT1
PS
PSD1
PSD2
PE
CHO2
PME
OPI3
PDE
OPI3
PC
Methylation Pathway
C
-
+ Cho
+ Etn
WT
Δice2
Δscs2
Δscs2Δice2
D
-
+pOPI3
WT
Δscs2Δice2
E
-
+pCHO2
WT
Δcho2
Δscs2Δice2
F
-
+MME
WT
Δcho2
Δscs2Δice2
G
-
+ pSCS2
WT
Δcho2
H
WT
Δscs2
Δcho2
Δscs2Δcho2
I
-
+ Cho
+ Etn
WT
Δice2
Δpsd1
Δpsd2
Δpsd1Δice2
Δpsd2Δice2

Figure 2.1: *SCS2* and *ICE2* are involved in making PC by the methylation pathway.

(A) Gene clusters containing *SCS2* and *ICE2* revealed a potential role for PM-ER contacts in phospholipid metabolism. Genes are color coded according to pathways in (B). Data was clustered from (Costanzo et al., 2010). (B) Major pathways for phospholipid synthesis in S. cerevisiae. Genes encoding enzymes required for each step are shown in italics. Cho, choline; Etn, ethanolamine; PA, phosphatidic acid; DAG, diacylglycerol; PS, phosphatidylserine; PE, phosphatidylethanolamine; PME, phosphatidylmonomethylethanolamine; PDE, phosphatidyldimethylethanolamine; PC, phosphatidylcholine. (C) Ten-fold serial dilutions of the indicated mutant yeast strains grown on SD media (-) or SD supplemented with either choline (+Cho) or ethanolamine (+Eth). (D) WT and Δ*scs2*Δ*ice2* yeast grown on SD media transformed with either a plasmid expressing Opi3 *(+ pOPI3*) or a control plasmid (-). (E) Yeast growth assays of mutants containing either a plasmid expressing Cho2 *(+pCHO2*) or empty vector (-) on SD media lacking choline. (F) Yeast growth assays of mutants on SD media in the absence (-) or presence of 1 mM monomethylethanolamine (+MME). (G) Mutant yeast grown on SD media without choline. (H) Yeast grown on SD media transformed with either a plasmid expressing Scs2 *(+ pSCS2*) or a control plasmid (-). (I) Yeast growth assays of indicated mutants on SD media without choline or ethanolamine (-), with choline (+Cho) or with ethanolamine (+Etn).

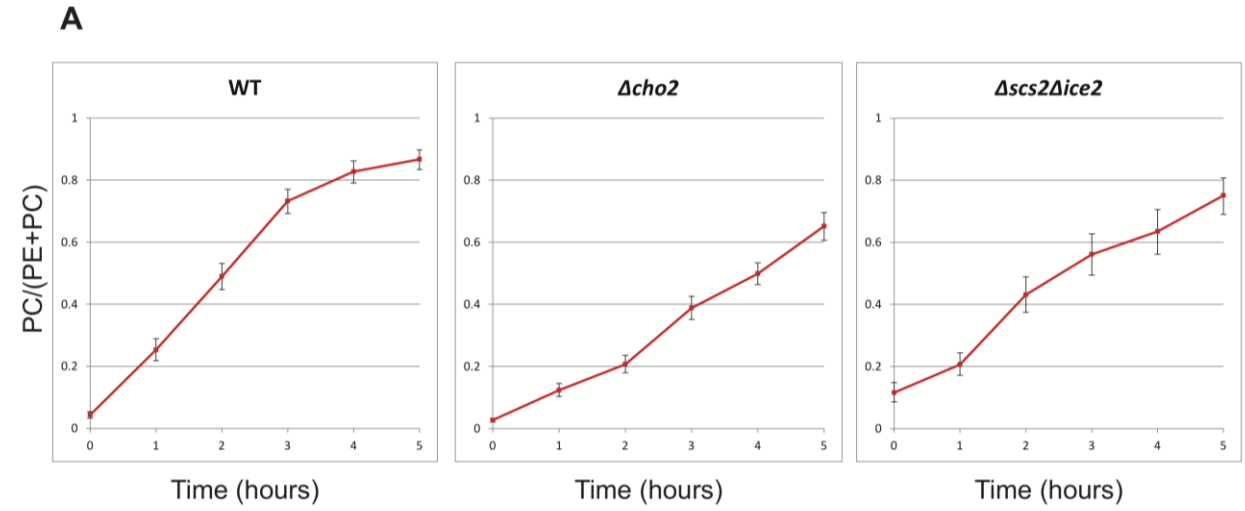
A
WT
Δcho2
Δscs2Δice2
PC/(PE+PC)
Time (hours)
Time (hours)
Time (hours)

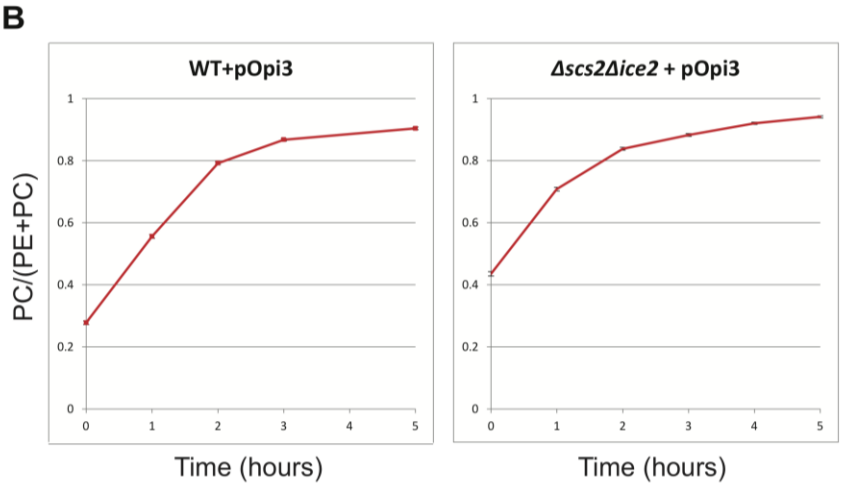
B
WT+pOpi3
Δscs2Δice2 + pOpi3
PC/(PE+PC)
Time (hours)
Time (hours)

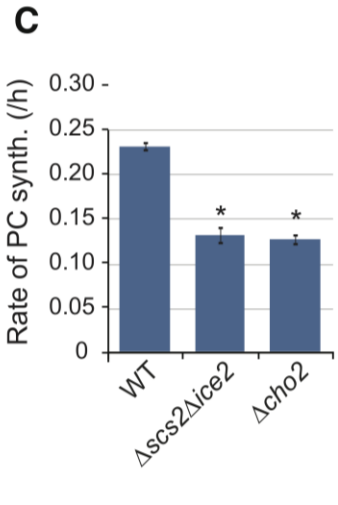
C
Rate of PC synth. (/h)
WT
Δscs2Δice2
Δcho2

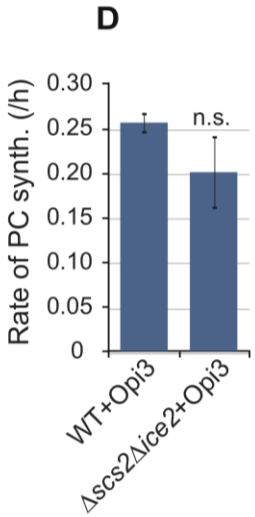
D
Rate of PC synth. (/h)
n.s.
WT+Opi3
Δscs2Δice2+Opi3

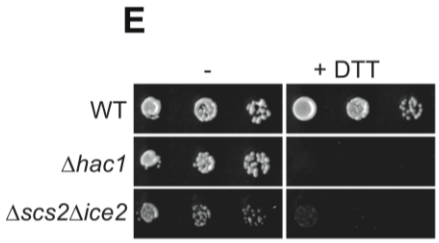
E
-
+ DTT
WT
Δhac1
Δscs2Δice2

Figure 2.2: Δ*scs2*Δ*ice2* mutant has a defect in the synthesis of PC and increased ER stress.

(A) Incorporation of [^{3}H]-ethanolamine into PC over time in wild type, Δ*cho2* and Δ*scs2*Δ*ice2* yeast grown in the presence of choline. Plotted is the fraction of counts in PC out of total PE+PC counts at each time point. (B) Incorporation of [^{3}H]-ethanolamine into PC over time in wild type and Δ*scs2*Δ*ice2* cells expressing Opi3 from a plasmid grown in the absence of choline. Plotted is the fraction of counts in PC out of total PE+PC counts at each time point. Error bars = SD. (C) *In vivo* PE methylation assay. Log phase yeast were pulse-labelled with [^{3}H]-Etn and the rate of PC synthesis was determined by measuring conversion of PE into PC over time. Error bars, SEM. Asterisks, $P < 0.005$ vs. WT. (D) PE methylation assay for indicated strains expressing Opi3 from a plasmid (n.s., not significant vs. WT). (E) Yeast grown on SD media containing choline with 1 mM diothiothreitol (+DTT) or without (-).

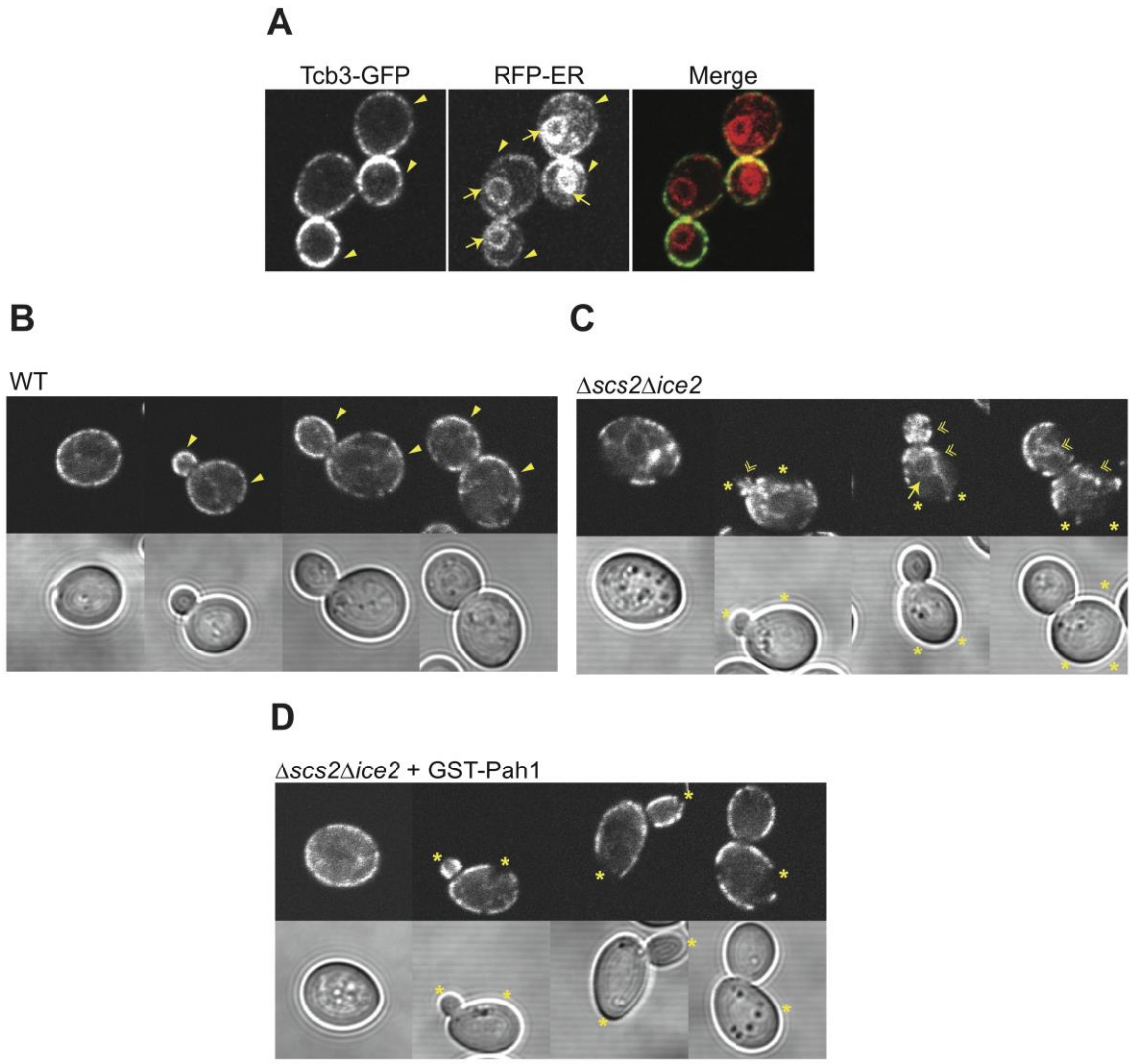

Figure 2.3: Δ*scs2*Δ*ice2* cells have an altered pmaER structure.

(A) Images of yeast cells expressing endogenous Pho88-GFP. Arrows indicate nuclear ER, arrowheads indicate pmaER, and asterisks indicate absence of pmaER. (B) Yeast expressing endogenous Tcb3-GFP (green) and RFP-ER (red) expressed from a plasmid. (C&D) Yeast expressing Tcb3-GFP staged throughout the cell cycle. Double arrowheads indicate mislocalization of Tcb3-GFP to ER tubules and asterisks indicate absence of pmaER.

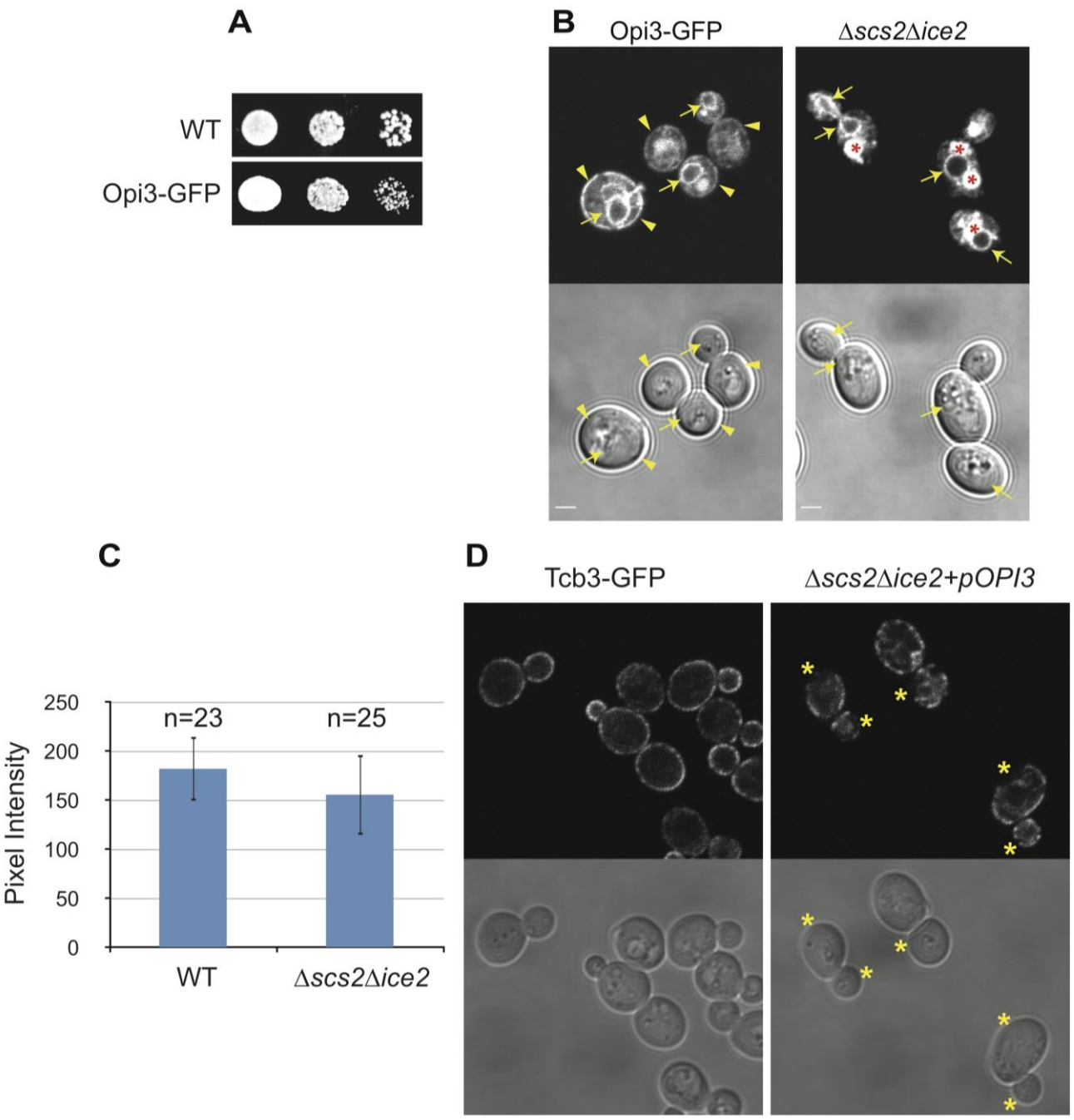
A
WT
Opi3-GFP
B
Opi3-GFP
Δscs2Δice2
C
Pixel Intensity
250
200
150
100
50
0
n=23
n=25
WT
Δscs2Δice2
D
Tcb3-GFP
Δscs2Δice2+pOPI3

Figure 2.4: Opi3 localization to the nuclear ER remains intact, however, it was almost completely absent from pmaER.

(A) Yeast growth assays of WT and Opi3-GFP yeast on SD media lacking choline. (B) Yeast expressing endogenous Opi3-GFP. Asterisks indicate vacuoles. All scale bars = 2 μm. (C) Quantification of Opi3-GFP in the nuclear ER of WT and Δ*scs2*Δ*ice2* mutant yeast (n = number of cells; error bars = SD). (D) Images of WT and Δ*scs2*Δ*ice2* yeast cells (transformed with the *pOPI3*) expressing endogenous Tcb3-GFP grown on SD media containing galactose. Asterisks indicate regions with disorganized pmaER in the mutants. Scale bars = 2 μm.

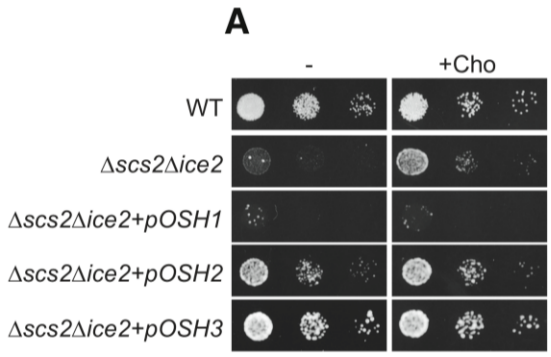
A
-
+Cho
WT
Δscs2Δice2
Δscs2Δice2+pOSH1
Δscs2Δice2+pOSH2
Δscs2Δice2+pOSH3

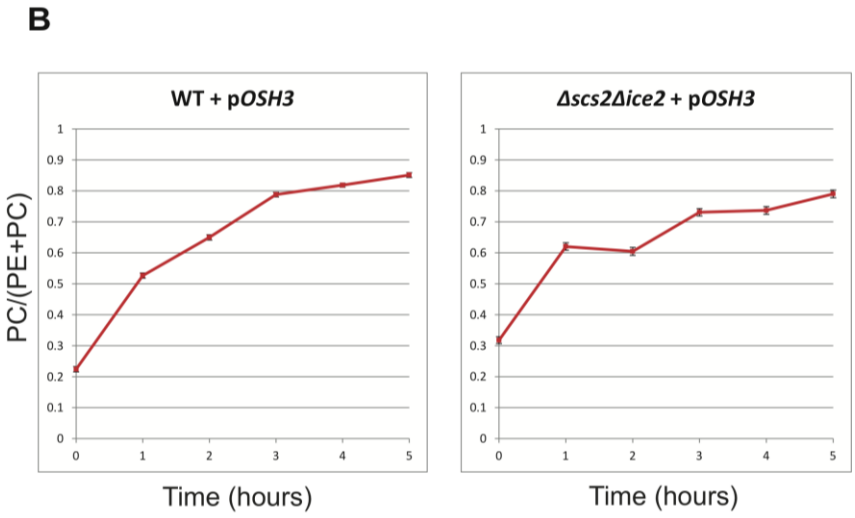
B
WT + pOSH3
Δscs2Δice2 + pOSH3
PC/(PE+PC)
Time (hours)
Time (hours)

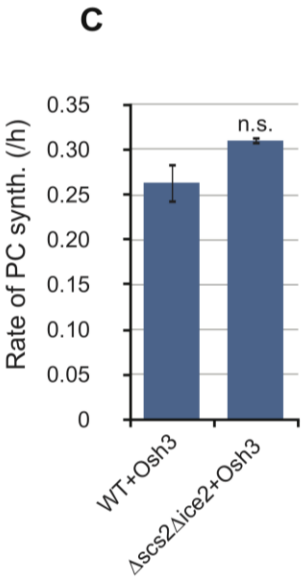
C
Rate of PC synth. (/h)
n.s.
WT+Osh3
Δscs2Δice2+Osh3

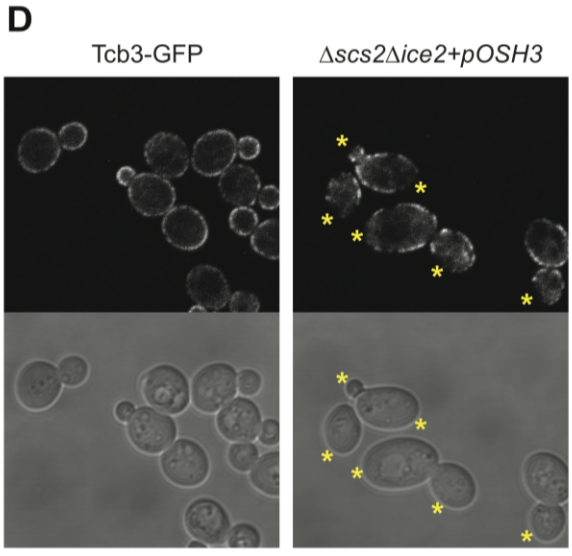
D
Tcb3-GFP
Δscs2Δice2+pOSH3

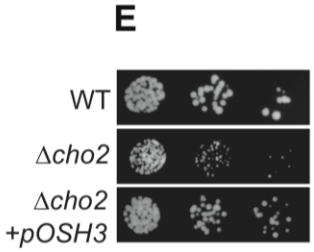
E
WT
Δcho2
Δcho2
+pOSH3

Figure 2.5: Yeast oxysterol-binding proteins regulate Opi3 function at PM-ER contacts.

(A) Growth of WT and Δ*scs2*Δ*ice2* yeast overexpressing Osh proteins from plasmids grown on SD media containing galactose in the absence (-) or presence (+Cho) of choline. (B) Incorporation of [^{3}H]-ethanolamine into PC over time in wild type and Δ*scs2*Δ*ice2* cells expressing Osh3 from a plasmid grown in the absence of choline. Plotted is the fraction of counts in PC out of total PE+PC counts at each time point. Error bars = SD. (C) PE methylation assay for indicated strains expressing Osh3 from a plasmid. (D) Images of WT and Δ*scs2*Δ*ice2* yeast cells (transformed with *pOSH3*) expressing endogenous Tcb3-GFP grown on SD media containing galactose. Asterisks indicate regions with disorganized pmaER in the mutants. Scale bars = 2 μm. (E) Growth assays of WT and Δ*cho2* mutant yeast overexpressing Osh3 from a plasmid grown on SD media containing galactose in the absence of choline.

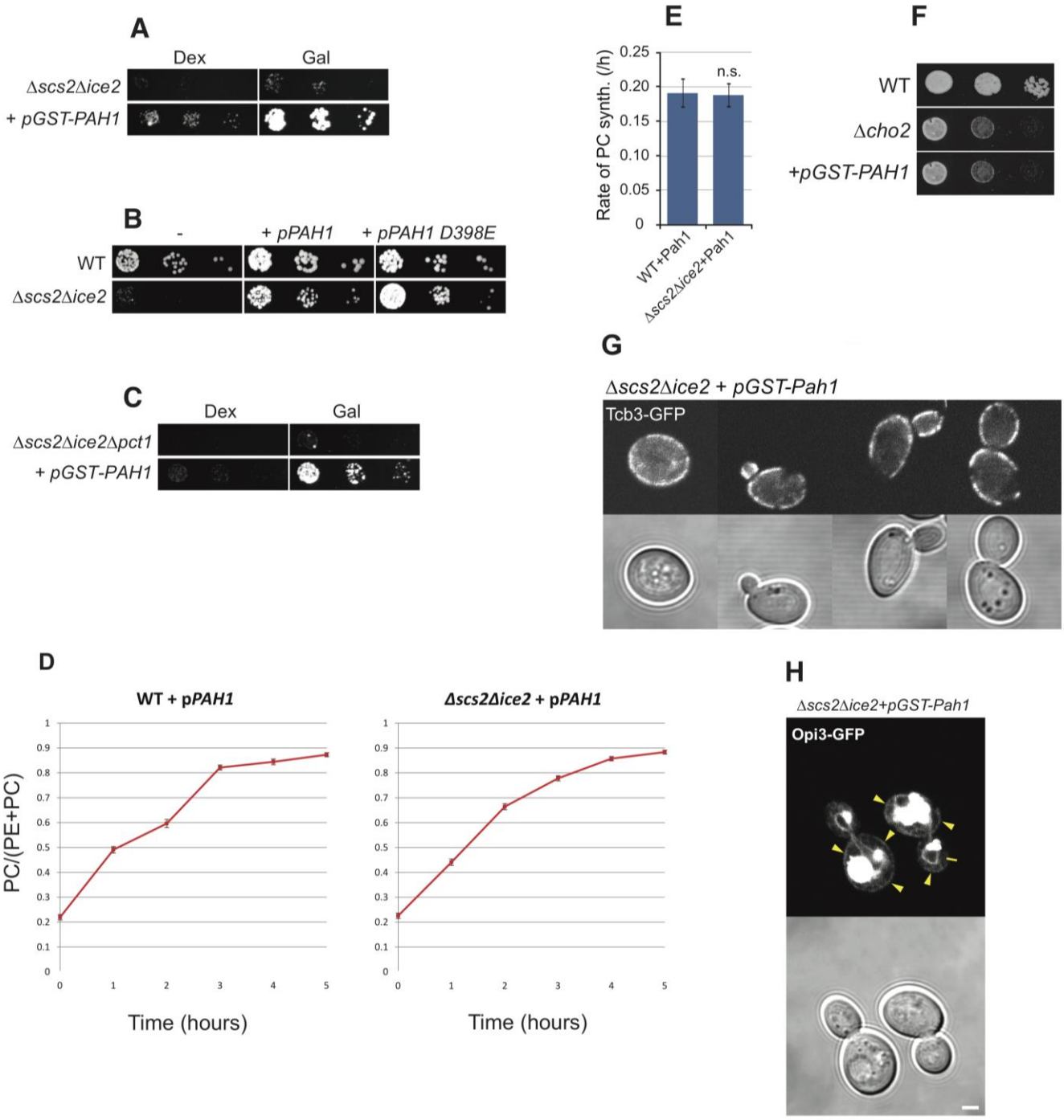
A
Dex
Gal
Δscs2Δice2
+ pGST-PAH1
B
-
+ pPAH1
+ pPAH1 D398E
WT
Δscs2Δice2
C
Dex
Gal
Δscs2Δice2Δpct1
+ pGST-PAH1
D
WT + pPAH1
Δscs2Δice2 + pPAH1
PC/(PE+PC)
Time (hours)
Time (hours)
E
Rate of PC synth. (/h)
n.s.
WT+Pah1
Δscs2Δice2+Pah1
F
WT
Δcho2
+pGST-PAH1
G
Δscs2Δice2 + pGST-Pah1
Tcb3-GFP
H
Δscs2Δice2+pGST-Pah1
Opi3-GFP

Figure 2.6: Pah1 regulates PM-ER contacts.

(A & C) Serial dilutions of (A) Δ*scs2*Δ*ice2* and (C) Δ*scs2*Δ*ice2*Δ *pct1* yeast overexpressing GST-Pah1 from a plasmid under control of the galactose promoter (+pGST-PAH1) on SD media containing either glucose (Dex) or galactose (Gal). (B) Yeast expressing either HA-Pah1 or the catalytically inactive D398E mutant from a plasmid grown on SD media lacking choline. (D) Incorporation of [^{3}H]-ethanolamine into PC over time in wild type and Δscs2Δice2 cells expressing GST-Pah1 from a plasmid grown in the absence of choline. Plotted is the fraction of counts in PC out of total PE+PC counts at each time point. Error bars = SD. (E) Opi3 methylation assay for wild type and Δ*scs2*Δ*ice2* cells overexpressing GST-Pah1 (n.s., not significant vs. WT). (F) Growth assays of wild type and Δ *cho2* yeast expressing GST-Pah1 from a plasmid grown on SD media containing galactose and lacking choline. (G) Images of Tcb3-GFP in Δscs2Δice2 yeast overexpressing GST-Pah1. Scale bar = 2 μm. (H) Images of Δscs2Δice2 yeast expressing endogenous Opi3-GFP and transformed with a plasmid expressing GST-Pah1 grown on SD medium containing galactose and lacking choline. Scale bar = 2 μm.

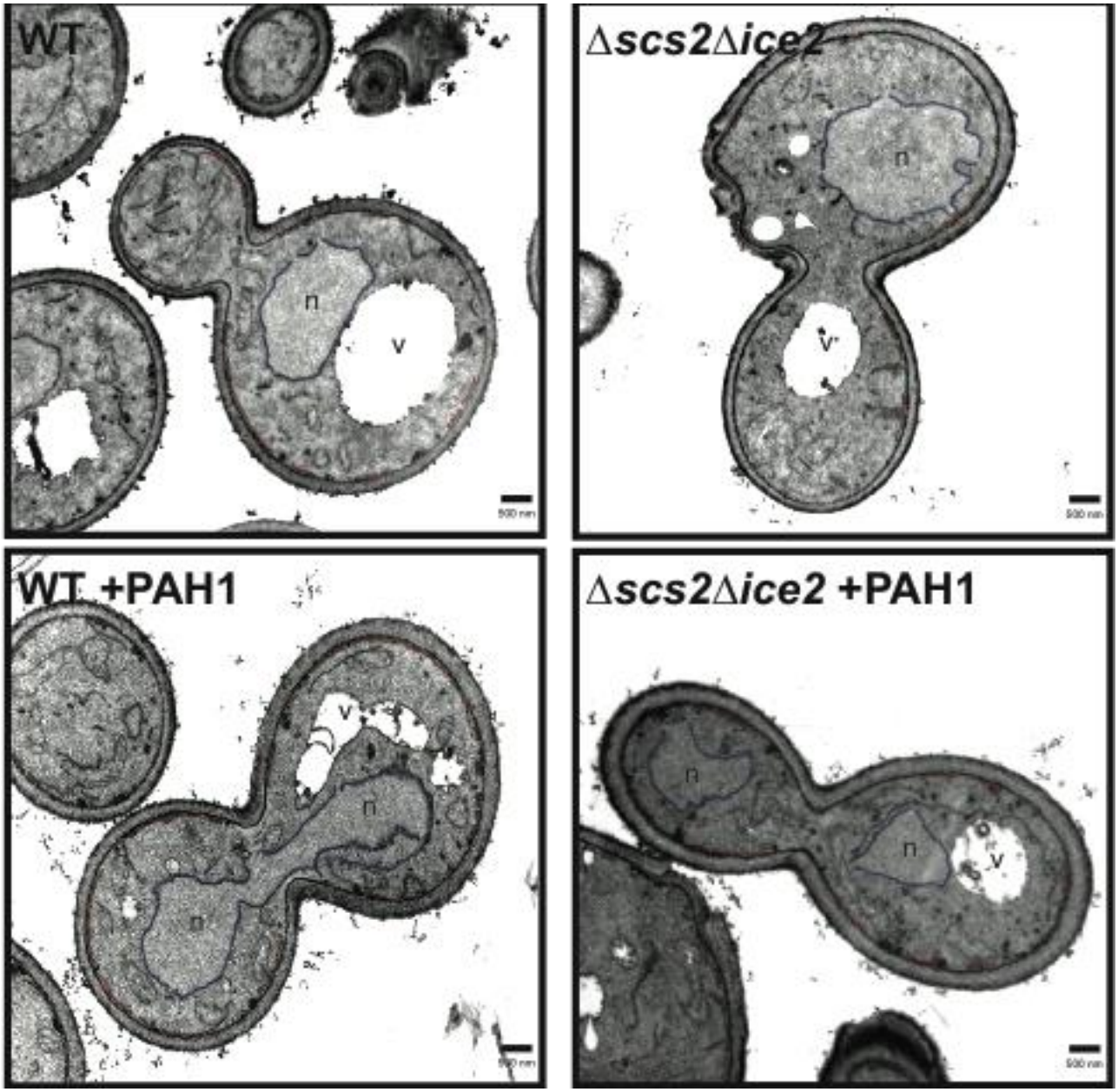

Figure 2.7: Representative transmission electron microscopy images.

Representative transmission electron microscopy images of wild type and Δ*scs2*Δ*ice2* yeast expressing GST-Pah1 from a plasmid (+PAH1) grown on SD media containing galactose and choline. pmaER has been indicated on the images by tracing in red and nuclear ER has been traced in blue. n, nucleus; v, vacuole. Scale bars = 500 nm.

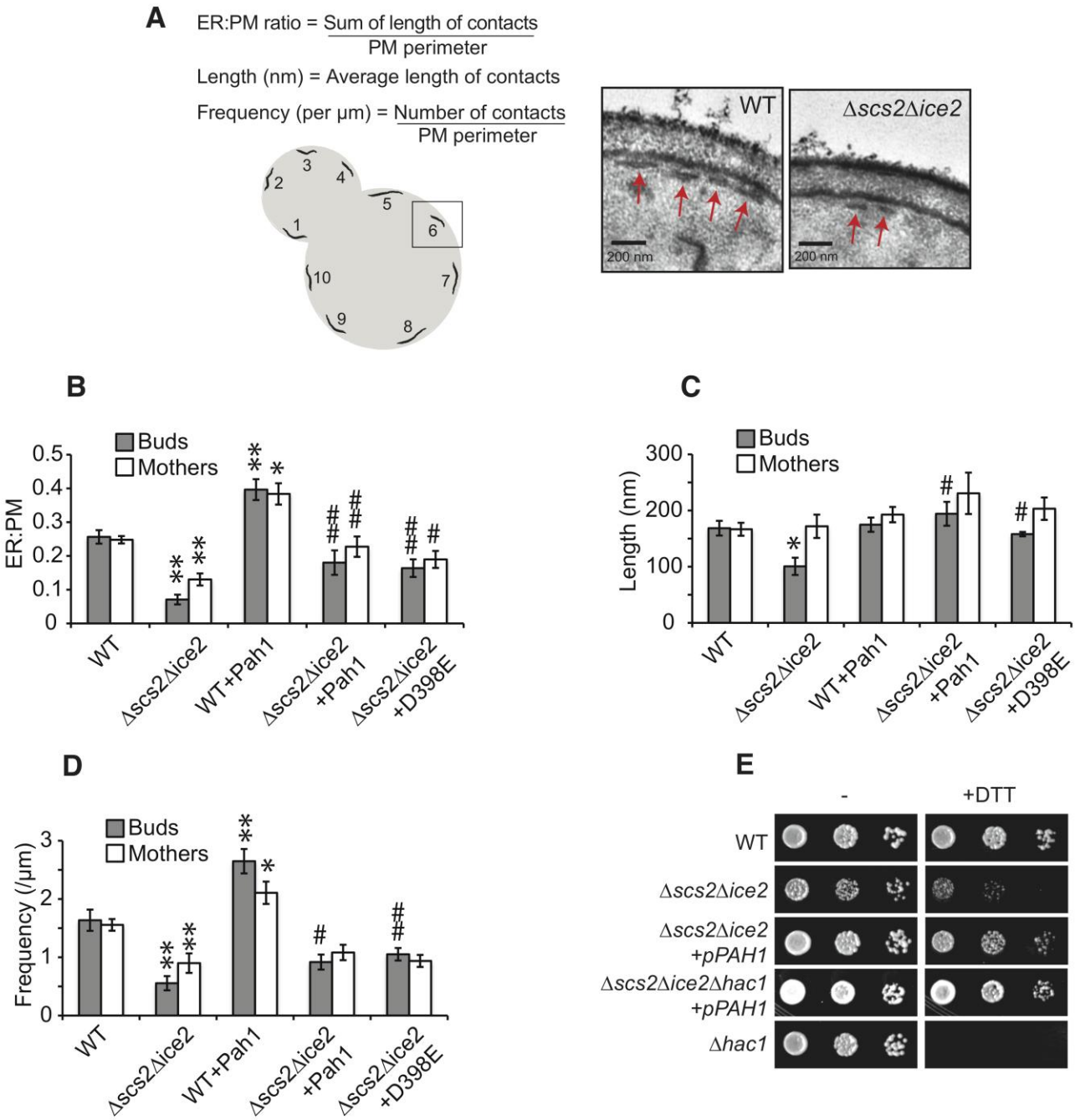
A
ER:PM ratio = Sum of length of contacts / PM perimeter
Length (nm) = Average length of contacts
Frequency (per μm) = Number of contacts / PM perimeter
1
2
3
4
5
6
7
8
9
10
WT
Δscs2Δice2
200 nm
200 nm
B
Buds
Mothers
ER:PM
0.5
0.4
0.3
0.2
0.1
0
WT
Δscs2Δice2
WT+Pah1
Δscs2Δice2 +Pah1
Δscs2Δice2 +D398E
C
Buds
Mothers
Length (nm)
300
200
100
0
WT
Δscs2Δice2
WT+Pah1
Δscs2Δice2 +Pah1
Δscs2Δice2 +D398E
D
Buds
Mothers
Frequency (/μm)
3
2
1
0
WT
Δscs2Δice2
WT+Pah1
Δscs2Δice2 +Pah1
Δscs2Δice2 +D398E
E
-
+DTT
WT
Δscs2Δice2
Δscs2Δice2 +pPAH1
Δscs2Δice2Δhac1 +pPAH1
Δhac1

Figure 2.8: Pah1 overexpression rescues the defect in PM-ER contacts.

(A) Schematic of ultrastructural assay and representative TEM images illustrating PM-ER contacts (arrows). (B) Ratio of PM-ER contacts to PM perimeter. **, P <10-4 vs. WT; *, P <0.001 vs. WT; ##, P <0.01 vs. Δscs2Δ ice2, #, P <0.05 vs. Δscs2Δice2. (C) PM-ER contact length. *, P < 0.005 vs. WT; #, P < 0.005 vs. Δscs2Δice2. (D) Frequency of PM-ER contacts. **, P < 0.005 vs. WT; *, P <0.05 vs. WT; ##, P <0.005 vs. Δscs2Δice2; #, P <0.05 vs. Δscs2Δice2. Error bars, SEM. (E) Yeast grown on SD media with Cho (-) and with Cho and 1 mM diothiothreitol (+DTT).

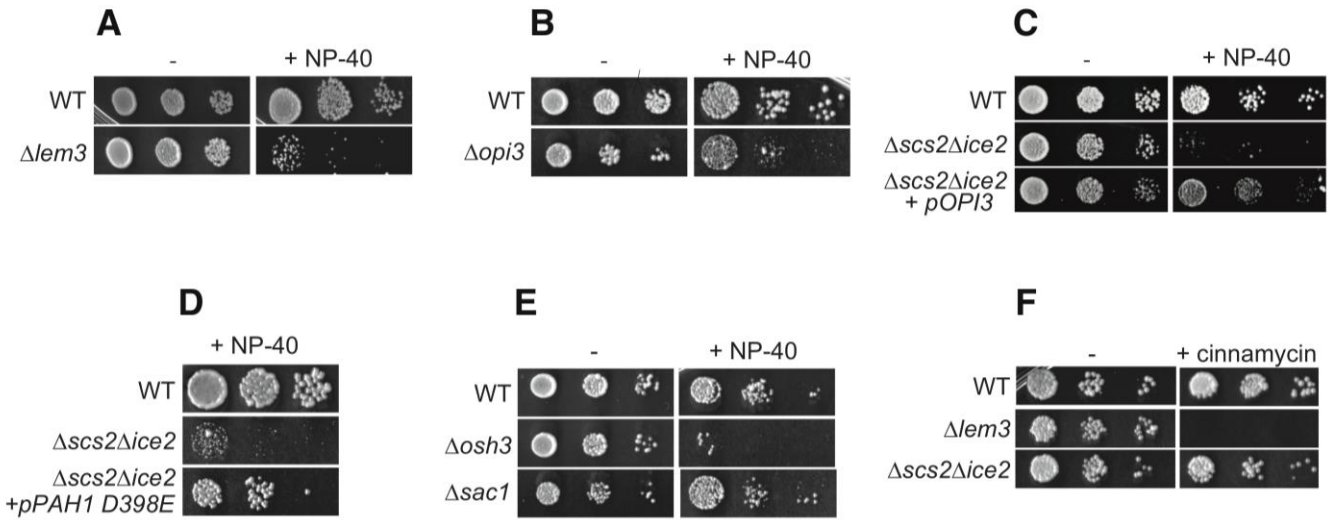

Figure 2.9: PM-ER contacts affect PM stability.

(A-E) Yeast growth assays done in the absence (-) or presence of 0.1 % NP-40 (+NP-40) on SD media containing choline. (F) Yeast growth assays done in the absence (-) or presence of cinnamycin (+) on SD media containing choline.

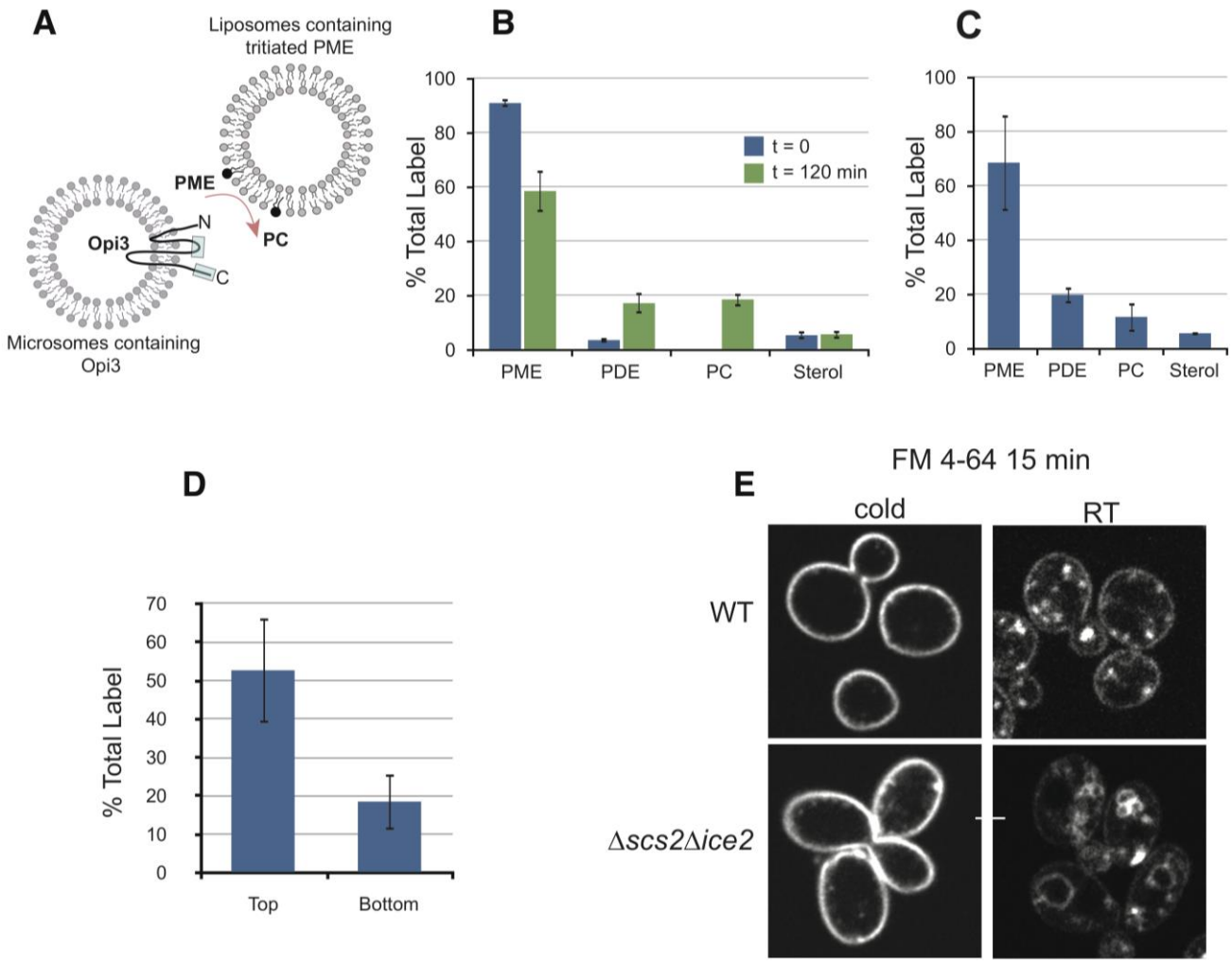

Figure 2.10: Opi3 methylates PME *in trans.*

(A) Schematic of in vitro trans-methylation assay. Opi3 topology is based on mammalian PEMT and boxes indicate regions containing catalytic sites (Shields et al., 2003a) (B) Distribution of label before and 120 min after mixing. (C) Distribution of label in the liposomal fraction 120 min after mixing. Error bars, SD. (D) Lipid radiolabel recovered after separation of liposomes and microsomes in the *in vitro* Opi3 assay. Radiolabel recovered from the top and bottom of the sucrose cushion after sedimentation is plotted as a percentage of total label before sedimentation. Note that ~30% of total label was not recovered after sedimentation. (E) Endocytosis assay. Uptake of FM 4-64 dye at 4°C (cold) or room temperature (RT) for 15 minutes in the indicated strains. Note that at 4°C the FM 4-64 dye remained in the plasma membrane whereas at RT it was endocytosed and labelled internal membranes.

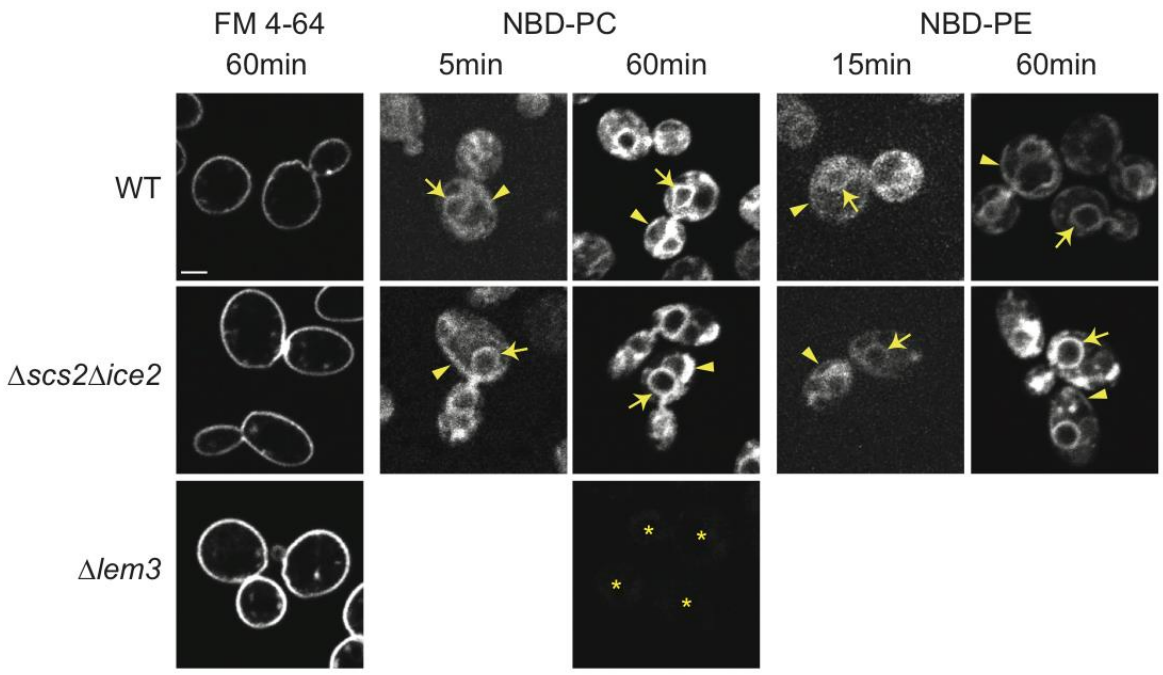

Figure 2.11: Δ*scs2*Δ*ice2* cells shows no lipid transport defect.

The indicated strains were labelled with either NBD-PC or NBD-PE for the indicated times at 4°C and imaged. Cells were additionally labeled with FM 4-64 under the same conditions to ensure endocytosis was blocked for the duration of the assay. Δlem3 cells were used as a control to show specificity of uptake of NBD-labelled lipids by the non-endocytic lysolipid transport pathway (Riekhof et al., 2007). Asterisks mark unlabeled cells in the Δ*lem3* control. Note that during the time course of the assay, FM 4-64 remained in the plasma membrane whereas NBD lipids were transported in a Lem3-dependent manner to internal membranes that included pmaER (arrows) and the nuclear ER (arrowheads). No differences in transport of NBD-PC or NBD-PE to the ER in the Δ*scs2*Δ*ice2* mutant were observed. Scale bars = 2 μm.

3. A CONSERVED ER-MEMBRANE COMPLEX FACILITATES PHOSPHOLIPID EXCHANGE BETWEEN ER AND MITOCHONDRIA

3.1. SYNOPSIS

Mitochondrial membrane biogenesis and lipid metabolism require phospholipid transfer from the endoplasmic reticulum (ER) to mitochondria. Transfer is thought to occur at regions of close contact of these organelles and to be nonvesicular, but the mechanism is not known. Here we show that a *S. cerevisae* strain missing multiple components of the conserved ER-membrane protein complex (EMC) have decreased phosphatidylserine (PS) transport from the ER to mitochondria. Cells lacking EMC proteins and a protein that is a member of the ER-mitochondria tethering complex called ERMES (the ER mitochondria encounter structure) were not viable and PS transfer to mitochondria was dramatically reduced. These defects were corrected by expression of a protein that artificially tethers the ER to mitochondria. Our findings suggest that the EMC facilitates ER to mitochondria PS transport by promoting ER-mitochondria tethering and that phospholipid exchange between the ER and mitochondria and tethering of these organelles are essential processes.

3.2. INTRODUCTION

Mitochondria are critical cellular components that are needed for energy production, lipid metabolism, calcium regulation, and apoptosis. Most proteins and lipids necessary for mitochondrial biogenesis are not synthesized in mitochondria and must be imported. Although protein import into mitochondria is relatively well understood, much less is known about phospholipid transfer to mitochondria. Phospholipid synthesis occurs largely in the ER and mitochondria acquire phospholipids from the ER at regions of close contact between these organelles (Prinz, 2010; Voelker, 2009). Zones of close contact between organelles, often called membrane contact sites, are regions where lipids, small molecules, and other signals are transferred between organelles (Elbaz and Schuldiner, 2011; Toulmay and Prinz, 2011). Contacts between the ER and mitochondria are not only important for lipid exchange and signaling

between these organelles but have also been proposed to play a role in calcium signaling, apoptosis, Alzheimer's disease pathology, and viral replication (Area-Gomez et al., 2012; Raturi and Simmen, 2013; Williamson, 2012). Protein complexes proposed to mediate ER-mitochondria contacts have been identified in mammalian cells and in *S. cerevisiae* (de Brito and Scorrano, 2008; Giorgi et al., 2009; Kornmann et al., 2009; Szabadkai and Duchen, 2009).

The only such complex that has been found in yeast to date is called ERMES, which contains an integral ER glycoprotein (Mmm1), a cytosolic protein (Mdm12) and two proteins in the outer mitochondrial membrane (Mdm10 and Mdm34) (Kornmann et al., 2009). The ERMES complex may play a role in phospholipid exchange between the ER and mitochondria. The study that identified this complex found that phospholipid exchange between the ER and mitochondria decreases 2-5 fold in cells missing this complex. However, two subsequent studies found that the transfer of PS from the ER, where it is produced (Zinser et al., 1991) to mitochondria did not significantly slow in cells lacking the ERMES complex (Nguyen et al., 2012). These findings suggest that protein complexes in addition to ERMES mediate ER mitochondria tethering since lipid exchange between these organelles probably occurs only at contacts and may be required for cell viability. Consistent with this, cells lacking ERMES proteins are viable (Kornmann and Walter, 2010). The mechanism of phospholipid exchange between the ER and mitochondria at sites of contact between these organelles is not well understood, but is thought to be nonvesicular in nature (Osman et al., 2011). PS transport from the ER to mitochondria is reduced ~ 2-fold in certain yeast mutants, but the proteins involved do not seem to directly mediate transfer. Met30 is a subunit of a ubiquitin ligase complex (Schumacher et al., 2002) that ubiquitinates the transcription factor Met4, which, in turn, regulates PS transport to mitochondria (Voelker, 2009). Cells missing the ERMES complex and proteins needed to shape the ER have a similar ~ 2-fold defect in ER to mitochondria PS transfer (Voss et al., 2012). Why lipid exchange slows in these mutants, however, is not understood.

PS transport to mitochondria is required for the synthesis of phosphatidylethanolamine (PE) in mitochondria (Osman et al., 2011). PE is critical for mitochondrial function (Gohil and Greenberg, 2009) and although PE can be made outside mitochondria, for unknown reasons this PE is not efficiently transported to mitochondria (Burgermeister et al., 2004). Failure to import PE may explain why all cells from yeast to humans have an enzyme that converts PS to PE in the mitochondrial matrix. In yeast, this protein is called PS decarboxylase 1 or Psd1 (Fig. 3.1 A) (Clancey et al., 1993; Trotter et al., 1993). PE produced in mitochondria by Psd1 can be

transferred back to the ER and converted to phosphatidylcholine (PC) by the methyltransferases Cho2 and Opi3 (Fig. 3.1 A). There is a second PS decarboxylase in yeast, called Psd2, which resides in the Golgi complex, endosomal system or vacuole (Trotter and Voelker, 1995). PE can also be synthesized from CDP-diacylglycerol (DAG) and ethanolamine, a metabolic pathway known as the Kennedy pathway (Fig. 3.1 A) (Henry et al., 2012). The Kennedy pathway can also produce PC from CDP-DAG and choline (Fig. 3.1 A). In this study we used a novel genetic screen to identify genes required for phospholipid exchange between the ER and mitochondria. We found that mutants missing multiple proteins of the ER-membrane protein complex (EMC) have dramatic defects in PS transport to mitochondria. This complex is thought to contain six conserved proteins, called Emc1-6 (Jonikas et al., 2009). The EMC has previously been suggested to play roles in the cellular response to ER stress, in membrane protein folding, or the unfolded protein response in the ER (Bircham et al., 2011; Christianson et al., 2012; Jonikas et al., 2009) but its function is not known. Our findings indicate that the EMC mediates lipid transfer from the ER to mitochondria by facilitating close contacts between these organelles.

3.3. MATERIALS AND METHODS

3.3.1. Strains, plasmids, and growth media

Strains and plasmids used in this study are listed in the Table 3.1. Media used were: YPD (1% yeast extract, 2% peptone, 2% glucose), YPGly (1% yeast extract, 2% peptone, 3% glycerol), and SC (2% glucose, 0.67% yeast nitrogen base without amino acids, and amino acid dropout mix from BIO101). Where indicated, ethanolamine or choline was added to a concentration of 5 mM. 5-fluoroorotic acid was added at a concentration of 1 mg/ml. Single deletion strains were obtained from freezer stocks of the haploid yeast deletion collection (BY4741, Mat a, KanMX, a gift from C. Boone) unless otherwise stated. Other gene deletions were constructed using the PCR method with the heterologous markers *S. pombe HIS5* (pKT128), *K. lactis URA3* (pKT209) or *NatR* (p4339). Double deletion strains were derived from the meiotic products of heterozygous diploids with at least three spores of each genotype being compared.

All yeast cells expressing GFP fusion proteins were tagged endogenously in haploids unless otherwise indicated. C-terminally tagged GFP strains were constructed by standard methods involving single-step gene replacement using the pKT128 (SpHIS5) plasmid (Sheff and Thorn, 2004) in the wild type Y7043 background and crossed to the indicated single deletion mutants (BY4741; kanMX). Mdm12-RFP was created similarly to C-terminal GFP fusions except using pMRFP-NAT in BY4741. For PCA, the plasmids used for C terminal genomic tagging were created as follows: Venus-YFP fragments F1 and F2 were amplified by PCR from p413-TEF-Zip-linker-Venus YFP-F1 and p415-TEF-Zip linker-Venus YFP-F2 (gift of S. Michnick (Tarassov et al., 2008)) and cloned into plasmids pKT128 and pKT209 (Sheff and Thorn, 2004) respectively, replacing yEGFP and including a myc tag (MEQKLISEEDL) in the linker region to give pHVF1CT (pFA6amyc-VF1-HIS5) and pUVF2CT (pFA6a-myc-VF2-URA3). For N-terminal integrations, plasmid pHVF1NT (HIS5-PHO5-VF1) was created by replacing eGFP in plasmid pTLHPG (HIS5-PHO5-GFP; gift of T. Levine) with the Venus F1 PCR fragment. To create the Tom5ΔTM-VF1 strain the C-terminal 21 amino acids of endogenous *TOM5* were replaced in-frame by VF1.

3.3.2. Synthetic genetic array (SGA) analysis for CHO2 and EMC6

SGA analysis was performed according to established protocols (Tong and Boone, 2006) essentially as previously described (Young et al., 2010) using a Singer RoToR Colony Arraying robot (Singer Instruments). Δ*cho2*::*URA*3 and Δ*emc6*::*URA3* query strains were constructed using standard techniques in strain background Y7092 and crossed to the yeast haploid deletion mutant array using a Singer RoToR HAD robot. Following diploid selection, spots were replicated three times and sporulated for 5 days. Haploids were germinated on SD-media lacking histidine, arginine and lysine supplemented with thialysine and canavanine (both at 100 µg/ml). Control sets of single deletion strains were generated by plating on media containing 5-fluoroorotic acid to counter-select for the Δ*cho2*::*URA3* or Δ*emc6*::*URA3* alleles and G418 sulfate (200 µg/ml) to select for the DMA strain; while double mutants were selected for by plating on media lacking uracil and containing G418 sulfate. A further round of selection was performed on the same media. For the *CHO2* SGA screen in the presence of choline, all plates additionally contained 1 mM choline. Arrays were imaged using a flatbed scanner.

Balony software (http://code.google.com/p/balony/) was used to measure spot sizes, determine cut-off values for genetic interactions and define strains the showed statistically significant changes in growth rate. Cut-off values for genetic interactions were defined for each screen by determining three standard deviations from the mean of the ratios of the double mutant to single mutant growth rates. Double mutant strains that met the cut-off and showed significant changes in growth relative to the corresponding single mutant control (one-tailed students' t-test; $p < 0.05$; n=3), were considered as genetic interactions. For the *CHO2* SGA screen, aggravating genetic interactions identified in the screen done in the absence of choline were considered rescued if they were no longer identified as genetic interactions according to the above criteria in the screen done in the presence of choline. Gene ontology analysis was performed using Funspec (http://funspec.med.utoronto.ca) and Cytoscape (http://www.cytoscape.org) (Cline et al., 2007; Robinson et al., 2002).

3.3.3. Protein subcellular localization by confocal microscopy

Log phase live yeast cells were imaged using a Zeiss LSM-5 Pascal confocal microscope and Zeiss Pascal software. Unless otherwise stated, all proteins were tagged at the C-terminus of the endogenous protein. Optical slices were taken through the center of each cell and images being directly compared were captured with identical microscope settings on the same day.

3.3.4. Protein-fragment complementation assay (PCA)

The Venus-YFP variant of PCA was used to examine protein-protein interactions in live yeast. Unless otherwise stated, endogenous proteins were tagged in haploid yeast by the PCR method with either VF1 or VF2 in the BY4741 and Y7043 strains, respectively. Correct integration and expression was confirmed by colony PCR and Western blot analysis with anti-myc antibodies (Sigma) for each fusion protein. The VF1 and VF2 strains to be assayed were then crossed, and haploid meiotic progenies with both alleles were recovered by random spore analysis or tetrad dissection. Finally, the PCA was visualized in log phase yeast by confocal microscopy.

3.3.5. In vivo labeling with [^{3}H]serine.

Cells were labeled with L-[3-3H]serine (American Radiolabeled Chemicals) as described (Raychaudhuri and Prinz, 2008) with the following modifications. About 2 OD600 units of cells from a saturated culture were added to 25mL of SC medium and incubated at 30^{o}C. When the cultures reached an OD600 of about 0.3, 10 μg/mL myriocin (SigmaAldrich, stock = 500 μg/mL in methanol) was added to the medium, the cells were grown for 30 minutes, and 10 μg/mL cerulenin (SigmaAldrich, stock = 5 mg/mL in dimethyl sulfoxide) was added to the medium. About 5 minutes later, 50 μCi of [^{3}H]serine was added to the medium and the cells were grown for an additional 30 minutes. The culture was then added to an equal volume of ice-cold water and it was washed once with ice-cold water. Cells were lysed in a Mini-BeadBeater-8 (BioSpec). Lipids were extracted as described (Parks et al., 1985) separated by HPLC (Wang et al., 2003) and the fractions containing PS, PE, and PC were collected and analyzed by liquid scintillation counting.

3.3.6. Mitochondrial extracts and in vitro [^{3}H]serine labeling

Crude mitochondria were prepared as described (Voss et al., 2012). Briefly cells were grown in YPD medium to an OD600 of ~0.3, washed once with water, and incubated in 1 mL 0.1 M Tris-SO4 (pH 9.4) containing 10 mM DTT for 10 minutes at 30ºC. They were washed once with spheroplast buffer (1.2 M sorbitol, 20 mM Tris pH 7.4) and resuspended in 1.5 mL of the same buffer containing 1 mg/mL zymolyase 20T (Seikagaku Biobusiness, Japan). After incubation for 60 min at 30ºC, cells were pelleted (5 min, 500 x *g*) and washed twice with spheroplast buffer. Cells were resuspended in ice-cold lysis buffer (0.6 M mannitol, 2 0mM Tris pH 7.4, 1 mM EDTA, 1mM PMSF and protease inhibitors, [Roche]) and lysed with a dounce using a B-pestle. The extract was centrifuged twice for 5 min at 3000 x *g* to remove unlysed cells and debris. The supernatant was centrifuged at 9,600 x *g* for 10 min and the pellet containing crude mitochondria was resuspended in lysis buffer using a dounce (B-pestle). The method of labeling crude mitochondria with [^{3}H]serine was adapted from (Achleitner et al., 1999)1-2 mg of crude mitochondria in 1mL of lysis buffer were heated to 30^{o}C and 0.6 μM $MnCl_2$ and 10 μCi of L-[3-^{3}H]serine (American Radiolabeled Chemicals) were added. After 20 minutes, 0.5 mM serine and 5 mM EDTA were added. Samples of 200 μl were taken after 0, 5, 10, and 15 minutes

and added to 6 mL of chloroform:methanol (1:2). Lipids were extracted, separated by HPLC, and extracted as described in the previous section.

3.3.7. Mitochondrial purification and determination of mitochondrial steady state lipid

About 2 OD600 units of cells from a saturated culture were washed with water, resuspended in 50 mL of fresh SC medium containing 200 μCi of [^{3}H]acetate (American Radiolabeled Chemicals), and grown at 30^{o}C for at least 3-4 generations. Crude mitochondria were purified as described in the previous section and further purified by equilibrium centrifugation using density gradients made from OptiPrep (Axis-Shield, Oslo, Norway) as described (Nunnari et al., 2002). Lipids were extracted and separated by one-dimensional TLC as described by (Vaden et al., 2005). TLC plates were scanned on a RITA Star Thin Layer Analyzer (Raytest).

3.3.8. Psd assay

Psd assay were performed as described (Raychaudhuri and Prinz, 2008) except that the concentration of the substrate, 1-oleoyl-2- (12-[(7-nitro-2-1, 3-benzoxadiazol-4-yl) amino] dodecanoyl)-*sn*-glycero-3-phosphoserine (Avanti Polar Lipids), was 500 μM.

3.4. RESULTS

3.4.1. Genetic screen for components that mediate transport of phospholipids between ER and Mitochondria

In a prior synthetic genetic array (SGA) screen for the *PSD1* gene we uncovered an aggravating genetic interaction with the *CHO2* gene. We found that the growth defect of cells missing Psd1 and Cho2 was rescued by the addition of ethanolamine or choline to the medium (Fig. 3.1 B), which allows cells to make PE and PC via the Kennedy pathway (Fig. 3.1 A). We reasoned that genes required for transport of PS from ER to mitochondria and PE from

mitochondria to ER would similarly have negative genetic interactions with *CHO2* that would be rescued by ethanolamine or choline. Therefore, we performed an SGA screen for the *CHO2* gene in the absence and presence of choline to identify genes that function in lipid transport between ER and mitochondria. The results of this genome-wide screen are shown in Fig. 3.1 C, in which we plotted the growth of double mutants in the absence of choline versus their growth in its presence. We identified 191 double mutants that exhibited slow growth phenotypes whose growth was significantly improved by choline addition (Fig. 3.1 C and Table 3.2). We found significant enrichment for various functional classifications for this set of genes and these are shown in Fig. 3.1 D and Table 3.3. Membrane-associated functions were highly represented among these groups and included ER, vacuole, and endosomal compartments.

3.4.2. Genetic interactions reveal that the EMC functions in the phospholipid synthesis

In the Cellular Component category, we noticed almost thirty-fold enrichment in EMC proteins, a conserved, uncharacterized ER membrane protein complex (Fig. 3.1 D). In our screen, genes encoding the six subunits of the EMC showed strong aggravating genetic interactions with *CHO2* that were rescued by choline addition (Fig. 3.2 A). We verified these genetic interactions and their rescue by choline by spot assay (Fig. 3.2 D). Interestingly, these interactions were not rescued by ethanolamine, suggesting that the EMC has a function distinct from PE production by Psd1.

To uncover additional functional information about the EMC we examined the global genetic interaction network, which is a comprehensive map of pairwise genetic interactions in which genes with similar functions form coherent clusters (Costanzo et al., 2010). We noticed that all EMC genes except for *EMC5*, which was not present in the global network, formed a discrete cluster, suggesting EMC genes share similar functions (Fig. 3.2 B). Interestingly, also in this cluster were *CHO2* and *OPI3*, which encode the two methyltransferases that convert PE to PC (Fig. 3.1 A), further supporting a role for EMC genes in phospholipid metabolism. EMC genes showed primarily aggravating genetic interactions with a cluster of genes that contained *INO2* and *INO4*, which encode both subunits of the Ino2/4 transcriptional activator complex required for expression of gene involved in phospholipid synthesis, including *CHO2* and *OPI3*.

Next, we performed an SGA screen for one of the EMC genes, *EMC6*, to further define functions for the EMC complex. We identified 36 aggravating and 41 alleviating genetic

interactions with *EMC6* (Table 3.4). Genetic interactions with *EMC6* revealed enrichment for functions associated with lipid metabolism, mitochondria, membrane traffic, cell polarity and morphogenesis, cell signaling and chromatin (Fig. 3.2 C). Although EMC genes have links to the ER unfolded protein response (UPR) (Bircham et al., 2011; Christianson et al., 2012; Jonikas et al., 2009), we did not find significant enrichment for ER stress response functions and *EMC6* did not interact genetically with either *HAC1* or *IRE1*, two key factors required for induction of the UPR. Our screen did uncover genetic interactions with key regulators of phospholipid metabolism, *INO2, INO4* and *SCS2*, as well as *CHO2* (Fig. 3.2 C), further supporting a role for EMC proteins in phospholipid synthesis. We also did not observe aggravating genetic interactions between *EMC6* and any of the remaining EMC genes (Table 3.3 and 3.4).

3.4.3. EMC proteins form a complex in the ER

EMC proteins 1-6 were first identified by their ability to interact in an affinity purification experiment (Jonikas et al., 2009). We now examined their individual localizations by tagging the endogenous proteins with GFP and imaging by confocal microscopy. We found that each of Emc1-6 localized throughout the yeast ER and were expressed at similar levels (Fig. 3.3 A). Next we verified interactions between each EMC protein by Protein-Fragment Complementation Assay (PCA) in which we tagged each endogenous Emc protein with one half of the Venus fluorescent protein. Shown in Fig. 3.3 B is the matrix containing all pair-wise interactions between the EMC proteins. We observed PCA interactions in the ER between most EMC proteins and there was no single EMC protein that failed to interact with any of the EMC proteins, suggesting that all six EMC proteins did indeed form a complex within the ER. Interestingly, we did not detect interactions between Emc1 and Emc3 or Emc 1 and Emc4, whereas as all other EMC proteins interacted, suggesting that Emc1 was organized distinctly within the complex. To test the functional interdependence of the EMC proteins we examined the localization of GFP-tagged EMC proteins in various *emc* deletion mutant strains. We found that deletion of *EMC6* resulted in a dramatic reduction of Emc2-5 in the ER, whereas the localization of Emc1 was unaffected (Fig. 3.3 C). This indicated an important role for Emc6 in complex organization and further suggested that Emc1was distinct within the complex. All EMC proteins except Emc2 contain predicted transmembrane domains. Therefore, Emc2 must be peripherally associated with the ER. Consistent with a central role for Emc6 in complex

organization, Emc6 was primarily responsible for localizing Emc2 to the ER (Fig. 3.3 D). Together, the PCA interaction data between EMC proteins and their functional interdependence for ER localization indicated that EMC proteins form a complex within the ER.

3.4.4. ER to mitochondria PS transport decreases in cells missing multiple Emc proteins.

To determine if the EMC plays a role in phospholipid exchange between the ER and mitochondria we used an in vivo assay to measure PS import into mitochondria from the ER. After synthesis in the ER, PS can be transported to mitochondria and converted to PE by Psd1 (Henry et al., 2012). Thus, the conversion of newly synthesized PS to PE has been used to estimate the amount of PS transfer from the ER to mitochondria (Voelker, 2009). We metabolically labeled cells with [^{3}H]serine, which is used for PS production in the ER (Zinser et al., 1991). Previously, we have shown that, using the labeling conditions described in Experimental Procedures, cells produce PS and PE at linear rates and that little of the radiolabeled PE is converted to PC (Raychaudhuri and Prinz, 2008). Strains were labeled with [^{3}H]serine for 30 minutes and the ratio of [^{3}H]PS to [^{3}H]PE calculated. In a wild-type strain, this ratio was 2.5. Cells missing either Psd1 or Psd2 had a significant decrease in the [^{3}H]PS to [^{3}H]PE ratio and this ratio was close to zero in a strain missing both proteins (Fig. 3.4 A).

Using this assay we determined the amount of PS converted to PE in cells missing any one of the Emc proteins. Surprisingly, we found that the amount of PS converted to PE did not decrease significantly in these strains (Fig. 3.4 A and data not shown). We speculated that the Emc proteins might have redundant functions and therefore measured ER to mitochondria PS transport in cells missing multiple Emc proteins. A strain lacking Emc2 and Emc6 had a ~25% decrease in the ratio of [^{3}H]PS to [^{3}H]PE compared to wild type. Cells missing additional Emc proteins had more substantial transport defects; a strain missing Emc1, Emc2, Emc3, and Emc6 *(4x-Δemc)* or one missing these proteins and Emc5 *(5x-Δemc)* had ~50% reduction in the ratio of [^{3}H]PS to [^{3}H]PE (Fig 3.4 A). These strains contain Psd2, which is outside mitochondria and converts a significant fraction of newly synthesized PS to PE (Fig. 3.4 A). Since the amount of PS to PE conversion in 4xemc and 5-emc cells is about the same as that of cells lacking Psd1, our findings suggest that very little PS to PE conversion occurs in the mitochondria of these strains. To test this, we sought to make a *5x-Δemc Δpsd2* strain to measure PS to PE conversion only in mitochondria. However, we found that 5x-emc *Δpsd2* cells were not viable. We

transformed *5x-Δemc* cells with a plasmid containing *PSD2* and *URA3* and then deleted *PSD2* on the chromosome. The resulting strain was not able to grow on medium with 5- fluoroorotic acid (5-FOA), which is toxic to *URA3* strains and selects against the plasmid with *URA3* and *PSD2* (Fig 3.4 B). This data confirms that loss of *PSD2* in *5x-Δemc* cells is lethal. Together, these findings suggest that ER to mitochondria PS transport is dramatically reduced in cells missing multiple EMC proteins. It is possible that *5x-Δemc Δpsd2* was not viable because it was unable to produce sufficient PE. However, adding ethanolamine to the medium, which can be used to make PE by the Kennedy pathway (Fig. 3.1 A), did not restore viability to *5x-Δemc Δpsd2* cells (Fig. 3.4 B). This strain probably has defects in lipid metabolism in addition to a significant reduction in PS transport to mitochondria. To rule out that the decrease in PS to PE conversion in 5x-emc cells was caused by a reduction in Psd1 activity or mislocalization of Psd1, we determined the amount of Psd activity in mitochondria derived from *5x-Δemc* cells. An *in vitro* Psd assay was performed using a fluorescent PS analog [7-nitro-2–1,3-benzoxadiazol-4-yl]-PS (NBDPS). We found mitochondrial Psd activity was not reduced in mitochondria from *5x-Δemc* cells compared to those from wild-type cells but rather was significantly increased for unknown reasons (Fig 3.4 C). These findings suggest that 5x-emc cells have a significant decrease in the transfer of PS from the ER to mitochondria.

3.4.5. Mitochondria in 5x-emc cells are nonfunctional and have abnormal phospholipid levels.

Because 5x-emc cells have reduced PS transport from ER to mitochondria, we wondered if mitochondria from 5x-emc cells have reduced amounts of PS and PE. To measure phospholipid levels, wild type and 5x-emc cells were labeled with [^{3}H]acetate for at least 3-4 generations and the relative abundance of the major phospholipids in purified mitochondria was determined. We found that PS levels in the mitochondria of *5x-Δemc* cells were about 50% lower than those in wild-type mitochondria (Fig 3.5 A). Therefore, reduced ER to mitochondria PS transport in 5x-emc cells results in decreased steady-state PS levels in mitochondria. Notably, PE levels were also reduced about 50%. This reduction is probably caused by the defect in ER to mitochondria PS transport in *5x-Δemc* cells since most PE in mitochondria, is generated from PS by Psd1 (Burgermeister et al., 2004). Thus, a reduction in PS levels in mitochondria probably results in lower levels of PE in mitochondria. Interestingly, the relative abundance of other phospholipids was increased in *5x-Δemc* mitochondria, particularly phosphatidic acid (PA) and

cardiolipin (CL) (Fig. 3.5 A). These changes may reflect a mechanism by which cells compensate for low levels of mitochondrial PE, which is thought to be critical for proper mitochondrial function (Gohil and Greenberg, 2009).

Because the lipid profile of mitochondria in *5x-*Δ*emc* cells was dramatically altered, we wondered if the mitochondria were functional. Yeast strains with nonfunctional mitochondria cannot grow on media containing nonfermentable carbon sources such as glycerol. We found that *5x-*Δ*emc* cells and other strains missing multiple EMC proteins cannot grow on the glycerol-containing medium YPGly, as has previously been shown for cells lacking the ERMES component Mmm1 (Fig. 3.5 B and data not shown) (Dimmer et al., 2002). Therefore cells missing multiple EMC proteins do not have functional mitochondria, probably because of the abnormal levels of phospholipids in the mitochondria of these strains. Interestingly, *5x-*Δ*emc* cells had a substantial growth defect even on the glucose, containing medium YPD (Fig 3.5 B) and had abnormal morphology with many cells having multiple buds (Fig. 3.5 C).

3.4.6. 5x-emc cells have a reduced rate of ER to mitochondria PS transfer in vitro

Since we found that 5x-emc cells have reduced ER to mitochondria PS transport in vivo, we wondered if a similar defect could be detected in vitro. We used a previously established two-step assay to monitor the transfer of newly synthesized PS from the ER to mitochondria (Achleitner et al., 1999; Voss et al., 2012). In the first step, crude mitochondria are incubated for 20 minutes with [^{3}H]serine and Mn^{2+}. We have shown that crude mitochondria have tightly associated ER-derived membranes that contain PS synthase (Voss et al., 2012). The presence of Mn^{2+} is required by PS synthase but inhibits the conversion of [^{3}H]PS to [^{3}H]PE by Psd1 (Achleitner et al., 1999). Thus, in the second step of the reaction, Mn^{2+} is chelated by EDTA and the PS to PE conversion rate was determined. Since Psd2 is not active in this assay (Voss et al., 2012), all PS to PE conversion in this assay is mediated by Psd1 and indicates that PS synthesized in ER derived membranes has been transferred to mitochondria. Using mitochondria derived from wild-type cells, we found that about 1 % [^{3}H]PS synthesized was converted to PE per minute (Fig 3.6 A). When mitochondria from 3x-emc (missing Emc2, Emc5, and Emc6) and *5x-*Δ*emc* cells were used, this rate decreased about 2-fold and 3-fold respectively (Fig 3.6 A). It should be noted that for all the strains tested the rate of PS to PE conversion was linear ($R2 > 0.9$). Since mitochondria derived from 5x-emc cells have Psd activity that is not lower than those

from wild type (Fig. 3.4 C), these finding indicate that the rate of ER to mitochondria PS transfer is significantly reduced in crude mitochondria derived from 5x-emc cells.

3.4.7. The EMC and ERMES complex are required for viability and ER to mitochondria PS transport

Because the ERMES complex tethers the ER and mitochondria, we wondered whether PS transfer would be slower in crude mitochondria missing Emc proteins and the ERMES complex. As disruption of a single ERMES component causes disassembly of the whole complex (Kornmann et al., 2009), we sought to delete one of the four genes encoding the ERMES proteins in *5x-*Δ*emc* cells. However, we were unable to delete *MMM1* in *5x-*Δ*emc* cells, probably because the resulting strain would not be viable. Therefore we introduced the conditional *mmm1-1* allele into *5x-*Δ*emc* cells. This strain is not viable at the non-permissive temperature of 37^{o}C (Fig. 3.6 B). We found that when 5x-emc *mmm1-1* cells were shifted to restrictive temperature (37^{o}C), they stopped growing after 4 hours. Therefore, we isolated crude mitochondria from *5x-*Δ*emc mmm1-1* cells 3 hours after shift to 37^{o}C. In these mitochondria, the rate of PS to PE conversion was reduced ~5-fold (Fig. 3.6 B). Because mitochondria derived from *5x-*Δ*emc mmm1-1* cells have equivalent Psd activity to those from wild type cells (Fig. 3.4 C), these findings indicate that PS transfer from ER to mitochondria is almost abolished in *5x-*Δ*emc mmm1-1* cells at non-permissive temperature. It should be noted that PS to PE transfer slowed only modestly in mitochondria derived from *mmm1-1* cells (Fig. 3.6 B), indicating that the effects of *mmm1-1* and *5x-*Δ*emc* mutations on ER to mitochondria PS transfer were additive.

3.4.8. An artificial ER-mitochondria tether restores PS transfer in cells missing multiple Emc proteins and ERMES proteins

The decrease in ER to mitochondria PS transfer in cells missing EMC proteins could be caused by a decreased ability to transport PS or by inefficient tethering of the ER and mitochondria. To distinguish between these possibilities, we determined if artificially tethering the ER and mitochondria corrects the PS transport defect in mitochondria derived from 5x-emc and *5x-*Δ*emc mmm1-1* cells. For these studies we used a fusion protein called ChiMERA, which has previously been shown to tether the ER and mitochondria (Kornmann et al., 2009). When

this fusion protein was expressed in 5x-emc and *5x-Δemc mmm1-1* cells, it corrected the ER to mitochondria PS transport defect in mitochondria derived from these strains (Fig. 3.6 C). It also restored the ability of *5x-Δemc mmm1-1* cells to grow at elevated temperature (Fig. 3.6 B). These findings suggest that inefficient tethering of the ER and mitochondria probably causes the defect in ER to mitochondria PS transfers in 5x-emc and *5x-Δemc mmm1-1* cells.

3.4.9. The EMC interacts with Tom5 at ER-mitochondria contact sites

Our findings suggested that EMC may play a role in ER-mitochondrial tethering, a conclusion that was further supported by the genetic interactions we uncovered between *EMC6* and genes with mitochondria-related functions. Therefore, we searched for genes identified in the *CHO2* SGA screen that encoded mitochondrial outer membrane proteins. We identified one gene, *TOM5* that showed a strong genetic interaction with *CHO2* that was rescued by choline (Table 3.2). *TOM5* encodes a small integral membrane protein in the outer membrane of mitochondria that is a subunit of the of the transporter outer membrane (TOM) complex, which imports proteins into mitochondria (Dudek et al., 2013). Thus, Tom5 was a good candidate for interacting with the EMC and we tested for a physical interaction using PCA.

We found that both Emc1 and Emc2 interacted with Tom5 in punctae (Fig. 3.7 A and B) that were suggestive of the localization of the ERMES complex (Kornmann et al., 2009). Interestingly, when we deleted the transmembrane domain of Tom5, Tom5ΔTM now interacted with Emc2 on the ER (Fig. 3.7 C), indicating that localization of Tom5 to the outer mitochondrial membrane was not required for its interaction with the EMC. This also suggested that proximity of ER to mitochondria would regulate binding of the EMC to Tom5 located in the mitochondrial outer membrane. To verify that the EMC interacted with Tom5 at ER-mitochondria contacts, we co-localized the PCA interaction between Emc1 and Tom5 with the ERMES subunit Mdm12, tagged endogenously with RFP. We found that in 100% of the cells we examined, the Emc1-Tom5 PCA punctate co-localized with ERMES foci (Fig. 3.7 D). This indicated that the EMC-Tom5 interaction likely formed a tether between ER and mitochondria at the same contact sites as defined by ERMES. We did not detect an interaction between Tom5 and another integral ER protein, Ale1, using PCA (Fig. 3.8 B), even though Ale1-GFP localized throughout the ER similar to EMC proteins (Fig. 3.8 C). Ale1 has a cytoplasmically oriented C-terminus, which should be accessible to Tom5 on mitochondria (Pagac et al., 2011). Deletion of

individual EMC genes also had no effect on the localization of Mdm34-RFP indicating the EMC likely did not regulate ERMES complex assembly (Fig. 3.9). These findings support a specific role for the EMC at contacts between ER and mitochondria

Next we examined the functional relevance of the EMC-Tom5 interaction. We did not observe growth defects of the Emc2-Tom5 PCA strain grown on fermentable or nonfermentable carbon sources (Fig. 3.10 A), indicating that mitochondrial function was likely normal. However, we found that the PCA between Emc2 and Tom5ΔTM caused this strain to grow poorly on both media types (Fig. 3.10 A), suggesting that recruitment of Tom5ΔTM to the ER by the EMC interfered with normal mitochondrial function. Since loss of EMC function in the *5x-*Δ*emc* mutant lead to decreased PS transfer and impaired mitochondrial function, this suggested that the interaction between the EMC and full length Tom5 at contacts might be important for PS transfer. Therefore we measured PS transfer between ER and mitochondria in cells expressing Tom5ΔTM-VF1, Emc2-VF2, or both proteins. Expression of both proteins in the same cell caused a dramatic decrease in the amount of [^{3}H]PS converted to [^{3}H]PE (Fig. 3.10 B). It should be noted that Psd2 may mediate much of the PS to PE conversion in this strain and that PS transfer to mitochondria is probably severely compromised. Together, these findings suggest that Tom5 and the EMC interact at sites of close contact of the ER with mitochondria and that blocking this interaction dramatically reduced PS transfer between these organelles.

3.5. DISCUSSION

Lipid exchange between the ER and mitochondria is critical for mitochondrial membrane biogenesis and lipid metabolism. Here we used a novel genetic screen to identify mutants with defects in these processes. We found that cells missing multiple components of a conserved protein complex of the ER, called EMC, had dramatic reductions in the amount of PS transferred from the ER to mitochondria both in vitro and in intact cells. This leads to a reduction in the amount of PS and PE in mitochondria. A role for the EMC in phospholipid metabolism was further supported by our unbiased global genetic analyses. We found that the EMC proteins localize to the ER where they form a complex, consistent with previous findings (Jonikas et al., 2009). The EMC interacts with the mitochondrial outer membrane protein Tom5 at sites of close contact between the ER and mitochondria. The ERMES complex is also found at these sites,

which are thought to be regions of lipid exchange between these organelles. A PCA interaction between Emc2 and the cytosolic portion of Tom5 (Tom5ΔTM) reduced PS transfer to mitochondria, suggesting that the EMC interaction with full length Tom5 is important for lipid transfer at contact sites. Together, these findings indicate that the EMC localizes to sites of ER to mitochondria contact where it facilitates PS transfer from the ER to mitochondria.

Our data suggest that the EMC may perform a tethering function at ER-mitochondria contact sites. Using our in vitro PS transport assay we found that the rate of transport was decreased almost 70% in the *5x-*Δ*emc* mutant and was almost completely abolished in combination with the ERMES mutation, *mmm1-1*. Strikingly, this transport defect was entirely ameliorated in the *5x-*Δ*emc mmm1-1* cells that expressed ChiMERA. We previously showed that synthesis of PE in this assay results from transport of PS from ER that remains associated with mitochondria, since transport cannot occur between donor membranes from Δ*psd1* cells, which cannot synthesize PE and wild type acceptor membranes (Voss et al., 2012). PE synthesis by mitochondria with associated ER was also unaffected by dilution (Voss et al., 2012), indicating that tethering rather than the presence of soluble transport factors is critical for in vitro transport, consistent with previous studies (Achleitner et al., 1999; Schumacher et al., 2002). Thus, the decreased PS transfer to mitochondria *in vitro* in the EMC mutants and rescue by an artificial tethering protein, strongly support a role for the EMC in tethering. Although unlikely, it is also possible that expression of ChiMERA artificially bypasses the requirement for membrane-associated lipid transporters or that it enhances the transport activity of mutated, but partially functional EMC complex by increasing ER-mitochondria contacts. However, a direct role for the EMC in lipid transport is unlikely since EMC proteins do not contain known lipid binding or transport domains. Further support for a tethering function for the EMC comes from genetic interactions between the EMC and ERMES. Similar to ERMES mutants, we found that disruption of the EMC complex interfered with mitochondrial respiration, indicating that mitochondrial function was compromised in the absence a functional EMC. This may be a result of decreased mitochondrial PE in these mutants, similar to Δ*psd1* cells. However, some growth of EMC mutants was observed on fermentable carbon sources, suggesting that contacts between ER and mitochondria were not completely lost.

Consistent with this, we did not observe defects in ERMES in EMC mutants. Strikingly, additional inactivation of ERMES in the EMC defective strain resulted in synthetic lethality, even on fermentable carbon sources, suggesting that contacts were completely lost in this mutant. Consistent with lethality arising from loss of ER-mitochondrial tethering, expression of

ChiMERA completely rescued growth of the *5x-Δemc mmm1-1* cells. Thus, these data indicate that the EMC and ERMES, together, are likely responsible for tethering of ER to mitochondria, a process which we now show is essential for cell growth. Although our initial genetic screen was designed to identify proteins with specific functions in mediating lipid transport between ER and mitochondria, our data supports a more general role for the EMC in ER-mitochondrial tethering. We found that *5x-Δemc Δpsd2* cells are not viable and do not grow even when supplemented with ethanolamine. Since *Δpsd1Δpsd2* cells can grow if ethanolamine is in the medium, *5x-Δemc Δpsd2* cells must have other defects in lipid metabolism or other essential processes in addition to altered PS transport to Psd1 in mitochondria. Genetic interactions with *EMC6* revealed functional links to vesicular transport and the Golgi complex, consistent with a role for Psd2 in Golgi/vacuole compartments. It is unclear how ER-mitochondria tethering might affect the secretory pathway. However, the EMC might have additional roles in ER stress and quality control in the ER, which are important for secretion (Bircham et al., 2011; Christianson et al., 2012; Jonikas et al., 2009).

Additionally, Emc6 contains a putative Rab5-interacting protein domain that may also explain its functions in the secretory pathway. Similarly, the ERMES tethering complex has functions in addition to tethering (Kornmann and Walter, 2010). Finally, the synthetic lethality observed between the EMC and ERMES mutants indicates that physiological defects more widespread than PE synthesis result from abolishing ER-mitochondrial tethering. These could include defective calcium homeostasis, mitochondrial protein import and inheritance of mitochondrial DNA. The nature of this synthetic lethality will need to be investigated further to better understand additional functions for ER-mitochondrial tethering beyond phospholipid synthesis. Even though the EMC appears to be a complex in the ER, loss of individual Emc proteins had little effect on PS transfer. This suggests that proteins in the EMC have overlapping tethering functions and that assembly of tethering complexes containing EMC proteins may not require all of the proteins. However, we did detect a modest, but significant 25% decrease in PS transport in cells expressing a non-mitochondrial version of Tom5 lacking its C-terminal transmembrane domain. Additionally, in Emc2 x Tom5ΔTM PCA cells transport was reduced even further, suggesting that this interaction interfered with tethering. We also found that all six EMC proteins interacted with full length Tom5 at ER-mitochondria contacts by PCA (data not shown), providing a possible explanation for the lack of transfer defects in individual EMC mutants. It therefore seems likely that multiple EMC proteins interact with Tom5 to tether ER to

mitochondria and that loss of individual EMC components is not sufficient to disrupt this tethering.

Tom5 is a tail-anchored membrane protein that is one of three small subunits of the translocase of the outer mitochondrial membrane (TOM) complex that is responsible for import of most, if not all mitochondrial proteins across the outer membrane (Neupert and Herrmann, 2007). The two other small subunits, Tom6 and Tom7 are similar in length and topology, but share no sequence homology with each other or Tom5. However, all these proteins perform an overlapping essential function since the triple deletion mutant interferes with import and is lethal, whereas the individual deletions have only minor effects (Alconada et al., 1995; Honlinger et al., 1996). It may be that Tom6 and Tom7 can compensate for loss of Tom5 function in ER-mitochondria tethering, explaining why we only see a partial defect in PS transfer in Tom5ΔTM cells. In summary, we have shown that the EMC plays an important role in mediating tethering and lipid trafficking between the ER and mitochondria, which we demonstrate for the first time, are essential processes. Understanding how the EMC facilitates tethering and how tethering makes possible lipid exchange and signaling between the ER and mitochondria are important topics for future studies.

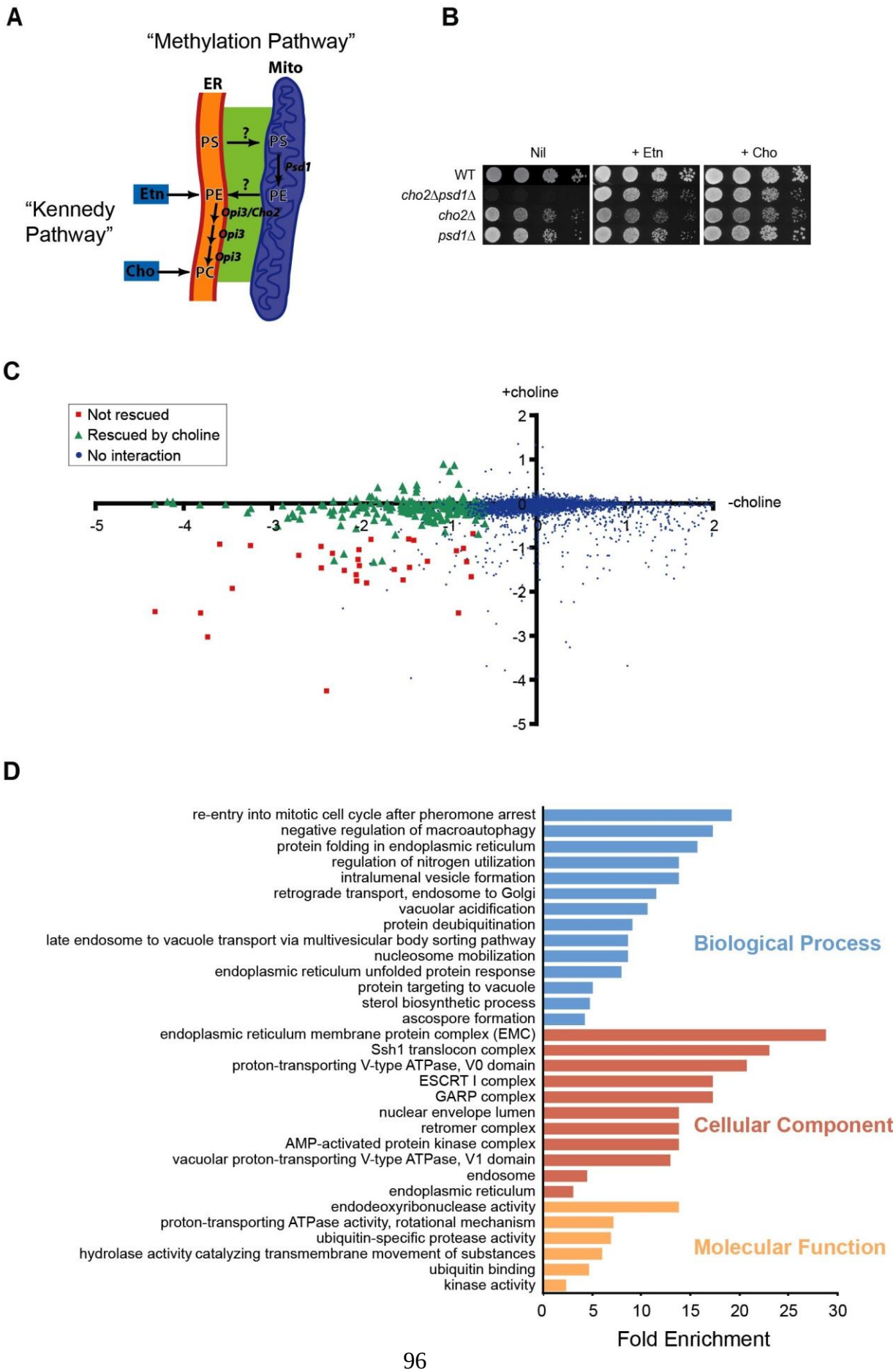
A
"Methylation Pathway"
Mito
ER
PS
?
PS
Psd1
Etn
PE
?
PE
"Kennedy Pathway"
Opi3/Cho2
Opi3
Opi3
Cho
PC
B
Nil
+ Etn
+ Cho
WT
cho2Δpsd1Δ
cho2Δ
psd1Δ
C
Not rescued
Rescued by choline
No interaction
+choline
-choline
2
1
0
-1
-2
-3
-4
-5
-5
-4
-3
-2
-1
0
1
2
D
re-entry into mitotic cell cycle after pheromone arrest
negative regulation of macroautophagy
protein folding in endoplasmic reticulum
regulation of nitrogen utilization
intralumenal vesicle formation
retrograde transport, endosome to Golgi
vacuolar acidification
protein deubiquitination
late endosome to vacuole transport via multivesicular body sorting pathway
nucleosome mobilization
endoplasmic reticulum unfolded protein response
protein targeting to vacuole
sterol biosynthetic process
ascospore formation
endoplasmic reticulum membrane protein complex (EMC)
Ssh1 translocon complex
proton-transporting V-type ATPase, V0 domain
ESCRT I complex
GARP complex
nuclear envelope lumen
retromer complex
AMP-activated protein kinase complex
vacuolar proton-transporting V-type ATPase, V1 domain
endosome
endoplasmic reticulum
endodeoxyribonuclease activity
proton-transporting ATPase activity, rotational mechanism
ubiquitin-specific protease activity
hydrolase activity catalyzing transmembrane movement of substances
ubiquitin binding
kinase activity
Biological Process
Cellular Component
Molecular Function
0
5
10
15
20
25
30
Fold Enrichment

Figure 3.1: Phospholipid synthesis in the methylation pathway is compartmentalized between ER and mitochondria.

(A) PS synthesized in the ER is transported to mitochondria for conversion into PE and transport back to the ER for conversion to PC. The Kennedy pathway synthesizes PE and PC from ethanolamine (etn) and choline (cho) independent of lipid transport between ER and mitochondria. (B) Yeast growth assays for the indicated mutants in the absence (nil) or presence of ethanolamine (+ etn) or choline (+ cho). *Cho2psd1* was rescued by choline and ethanolamine. (C) Results of SGA screen for *CHO2* in the absence (-) and presence (+) of choline. Genetic interactions are plotted as the log2 of the ratio of growth of single versus double mutants with Δcho2 in the absence and presence of choline. Interactions rescued by choline (green triangles) predominately clustered on the X axis, whereas interactions not rescued (red squares) were present on the diagonal. (D) Enrichment of functional groups for the genes that showed interactions that and were rescued by choline in (C). Fold enrichment represents the frequency of a given term in our dataset relative to the frequency of that term in the whole genome.

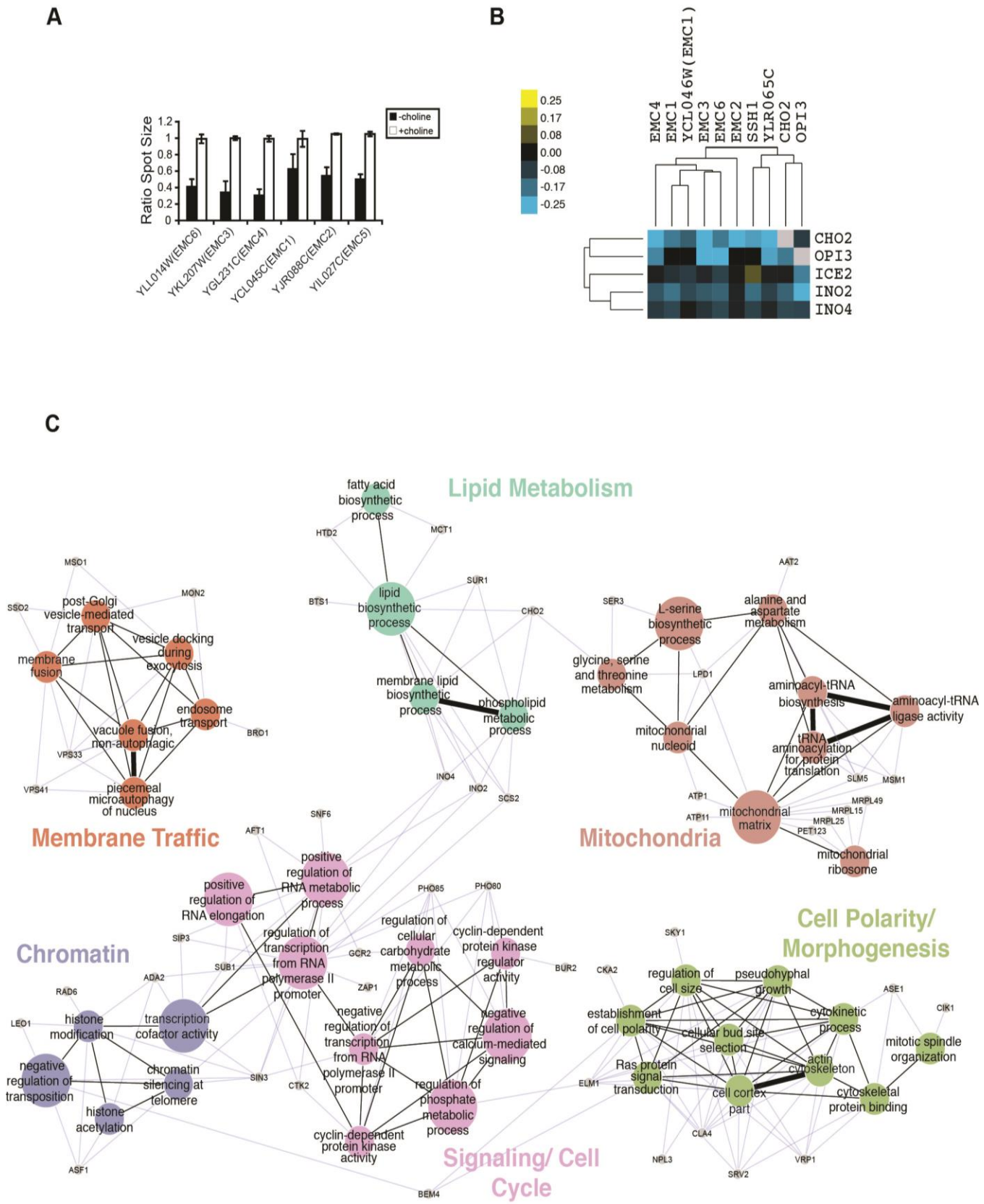
A
Ratio Spot Size
1.2
1
0.8
0.6
0.4
0.2
0
-choline
+choline
YLL014W(EMC6)
YKL207W(EMC3)
YGL231C(EMC4)
YCL045C(EMC1)
YJR088C(EMC2)
YIL027C(EMC5)
B
0.25
0.17
0.08
0.00
-0.08
-0.17
-0.25
EMC4
EMC1
YCL046W(EMC1)
EMC3
EMC6
EMC2
SSH1
YLR065C
CHO2
OPI3
CHO2
OPI3
ICE2
INO2
INO4
C
Lipid Metabolism
fatty acid biosynthetic process
HTD2
MCT1
SUR1
BTS1
lipid biosynthetic process
CHO2
membrane lipid biosynthetic process
phospholipid metabolic process
INO4
INO2
SCS2
MSO1
SSD2
post-Golgi vesicle-mediated transport
MON2
vesicle docking during exocytosis
membrane fusion
endosome transport
BRO1
vacuole fusion, non-autophagic
VPS33
VPS41
piecemeal microautophagy of nucleus
Membrane Traffic
SNF6
AFT1
AAT2
SER3
L-serine biosynthetic process
alanine and aspartate metabolism
glycine, serine and threonine metabolism
LPD1
aminoacyl-tRNA biosynthesis
aminoacyl-tRNA ligase activity
mitochondrial nucleoid
tRNA aminoacylation for protein translation
SLM5
MSM1
ATP1
ATP11
mitochondrial matrix
MRPL49
MRPL15
MRPL25
PET123
mitochondrial ribosome
Mitochondria
positive regulation of RNA metabolic process
positive regulation of RNA elongation
PHO85
PHO80
regulation of cellular carbohydrate metabolic process
cyclin-dependent protein kinase regulator activity
SIP3
GCR2
BUR2
SUB1
regulation of transcription from RNA polymerase II promoter
ZAP1
ADA2
RAD6
LEO1
histone modification
transcription cofactor activity
negative regulation of transcription from RNA polymerase II promoter
negative regulation of calcium-mediated signaling
negative regulation of transposition
chromatin silencing at telomere
SIN3
CTK2
histone acetylation
ASF1
regulation of phosphate metabolic process
cyclin-dependent protein kinase activity
BEM4
Chromatin
Signaling/ Cell Cycle
Cell Polarity/ Morphogenesis
SKY1
CKA2
regulation of cell size
pseudohyphal growth
ASE1
CIK1
establishment of cell polarity
cellular bud site selection
cytokinetic process
mitotic spindle organization
Ras protein signal transduction
actin cytoskeleton
ELM1
cell cortex part
cytoskeletal protein binding
CLA4
NPL3
SRV2
VRP1

D

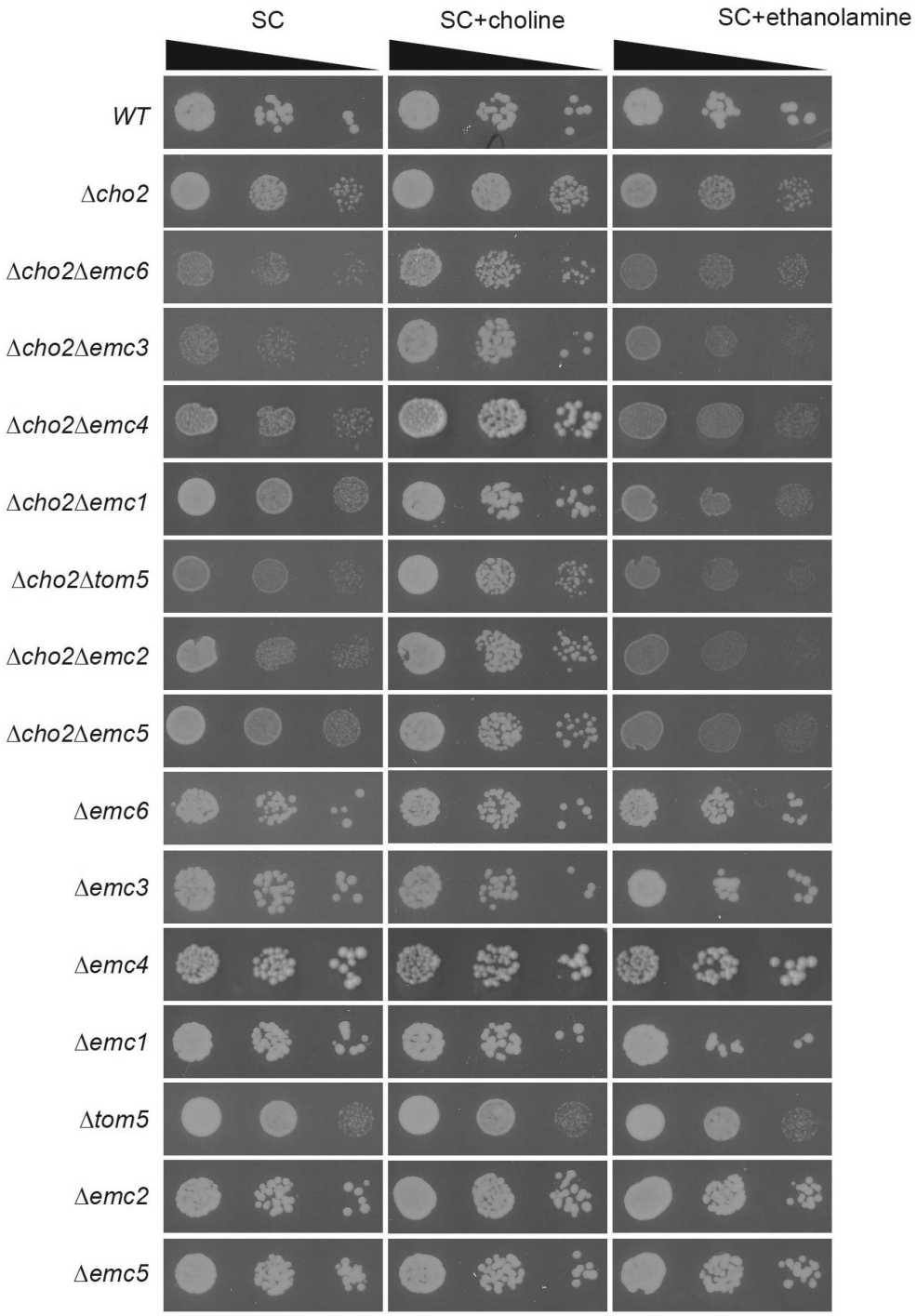
SC
SC+choline
SC+ethanolamine
WT
Δcho2
Δcho2Δemc6
Δcho2Δemc3
Δcho2Δemc4
Δcho2Δemc1
Δcho2Δtom5
Δcho2Δemc2
Δcho2Δemc5
Δemc6
Δemc3
Δemc4
Δemc1
Δtom5
Δemc2
Δemc5

Figure 3.2: EMC genes function in phospholipid metabolism.

Genetic interactions identified between EMC genes and CHO2. Plotted is the ratio of spot size of the single EMC mutants versus the corresponding double mutants with Δcho2 in the absence and presence of choline. (B) Serial dilutions of the indicate strains were spotted onto agar plates containing synthetic complete media (SC) or with or without ethanolamine or choline (C) EMC gene cluster identified in the global genetic interaction map (Costanzo et al., 2010) and aggravating genetic interactions with a cluster of genes that function in the methylation pathway of phospholipid synthesis. Aggravating interactions have negative values and alleviating interactions have positive values. (D) Yeast growth assays of mutants identified in the CHO2 SGA screen, related to Figure 3.1. Serial dilutions of the indicate strains were spotted onto agar plates containing synthetic complete media (SC) or with or without ethanolamine or choline.

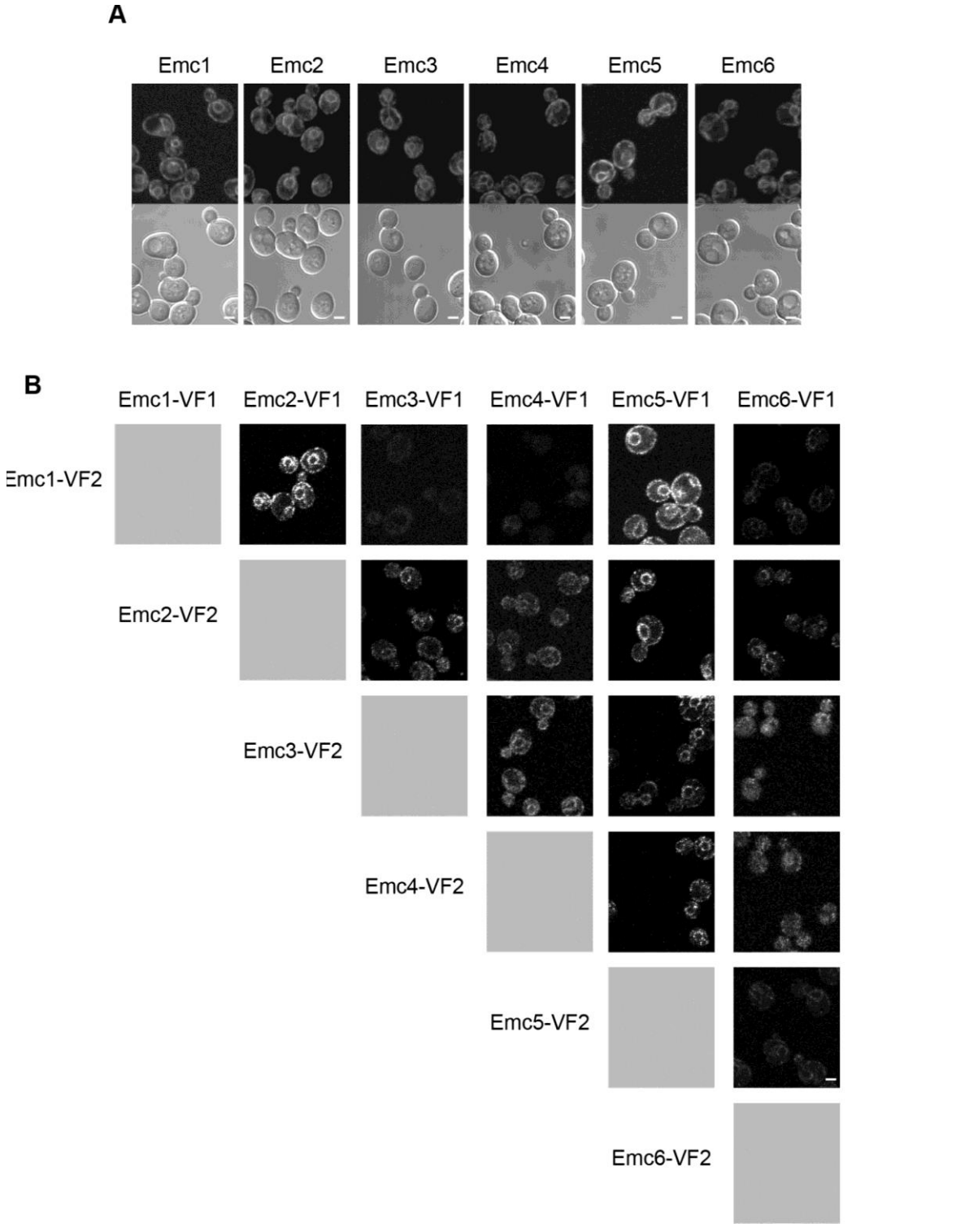
A
Emc1
Emc2
Emc3
Emc4
Emc5
Emc6
B
Emc1-VF1
Emc2-VF1
Emc3-VF1
Emc4-VF1
Emc5-VF1
Emc6-VF1
Emc1-VF2
Emc2-VF2
Emc3-VF2
Emc4-VF2
Emc5-VF2
Emc6-VF2
C emc6Δ cells
Emc1-GFP
Emc2-GFP
Emc3-GFP
Emc4-GFP
Emc5-GFP
D Emc2-GFP
emc1Δ
emc3Δ
emc4Δ
emc5Δ

Figure 3.3: EMC proteins form a complex in the ER.

(A) Yeast expressing EMC proteins endogenously tagged with GFP imaged by confocal microscopy. (B) Interactions between EMC proteins in the ER imaged using Venus PCA. Images on the bottom half of the matrix are copies of the top half and have been included for clarity. (C) Localization of EMC proteins tagged with GFP in *emc6*Δ cells. (D) Emc2 tagged with GFP imaged in EMC mutants. All scale bars 2 μm.

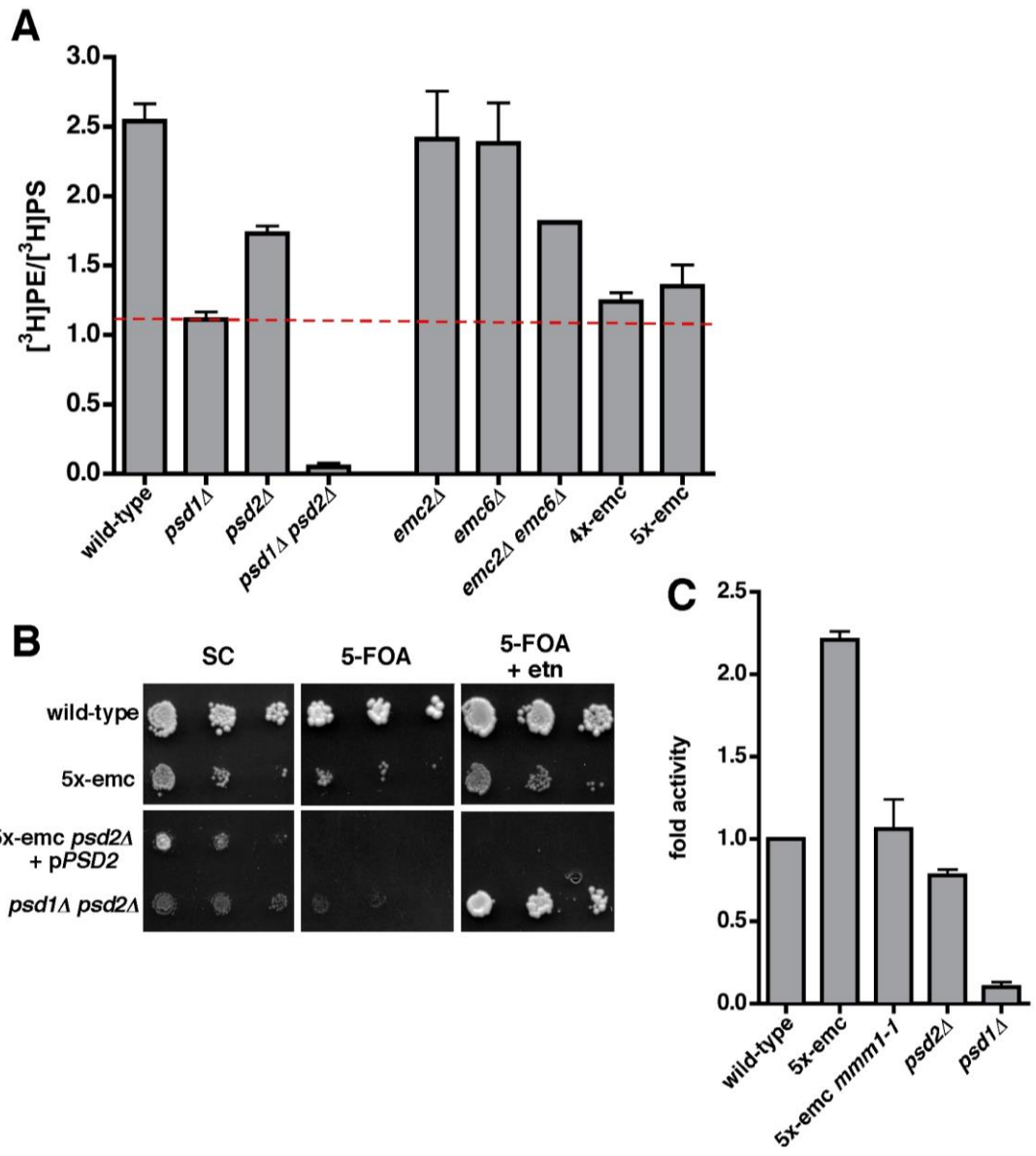

Figure 3.4: Cells missing multiple EMC proteins have defects in PS transfer from the ER to mitochondria and dysfunctional mitochondria.

(A) Cells with the indicated genotypes were labeled with [^{3}H]serine for 30 minutes and the ratio of [^{3}H]PS converted to [^{3}H]PE determined (mean + sad, n = 2-5 independent experiments). The dashed red line indicates the amount of conversion that occurred in *psd1Δ* cells. * = $p < 0.05$ compared to wild-type, two-tailed t-test. (B) 10-fold serial dilutions of cultures of the indicated strains were spotted onto SC medium with or without 5-FOA and ethanolamine. The plates were incubated at 30^{o}C for four days. (C) PSD of crude mitochondria incubated with NBD-PS for 1 hour at 30^{o}C. PSD activity was normalized to that of wild type crude-mitochondria (mean + Sc.D., n = 2-3 independent experiments). * = $p < 0.05$ compared to wild-type, two-tailed t-test.

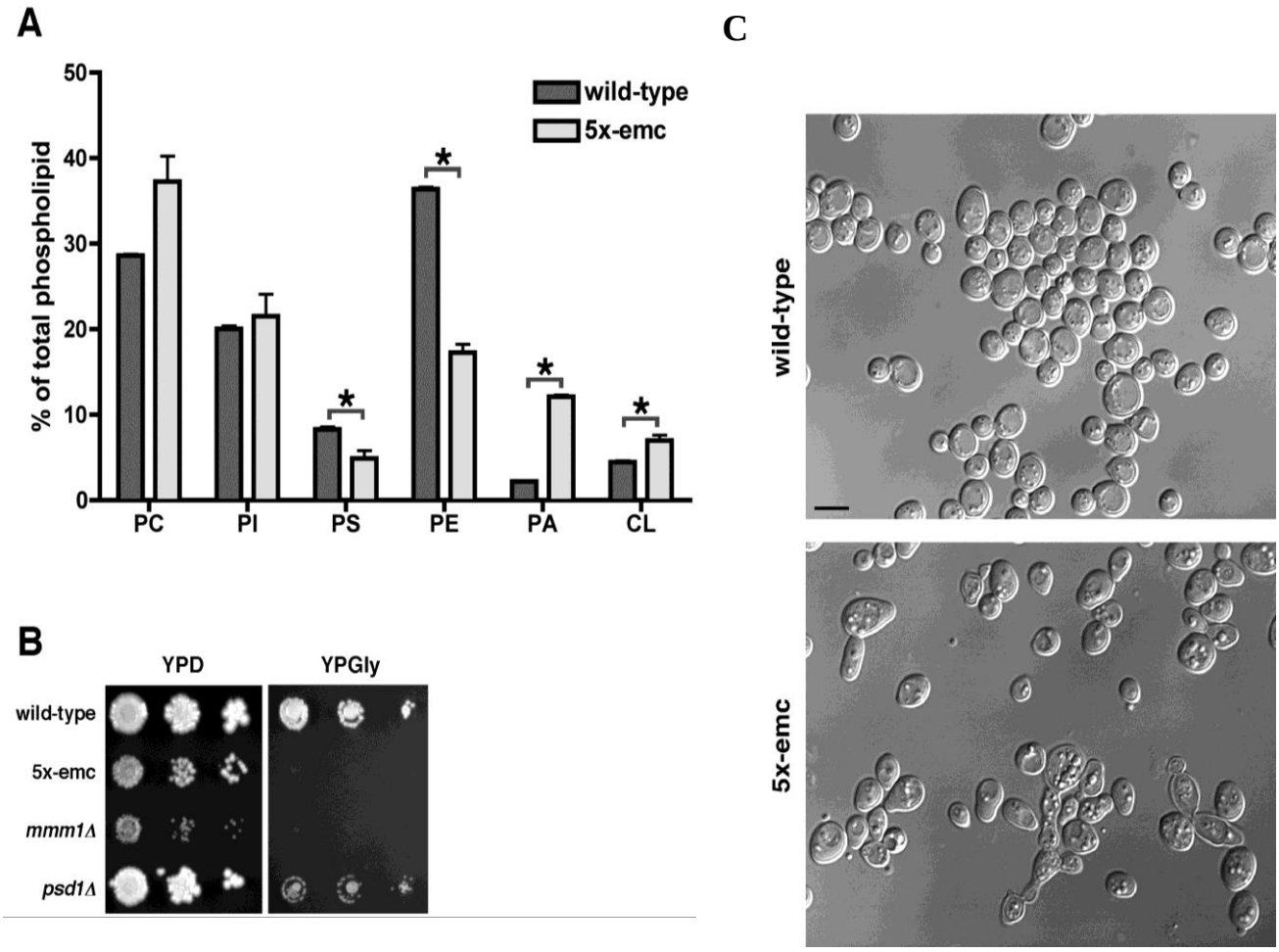

Figure 3.5: Mitochondria from cells missing Emc proteins have reduced levels of PS and PE.

(A) Wild-type and 5x-emc cells were grown for at least three generations in medium containing [^{3}H]acetate and the amount of the six major phospholipids in purified mitochondria was determined (mean + s.d., n = 3 independent experiments). * = $p < 0.05$, two-tailed t-test. (B) 10-fold serial dilutions of the indicated strains on YPD and YPGly plates. The plates were incubated at 30^{o}C for three days. (C) DIC images of wild type and 5-emc cells in mid-logarithmic growth phase showing that 5x-emc cells have abnormal shapes. Bar = 5 μm.

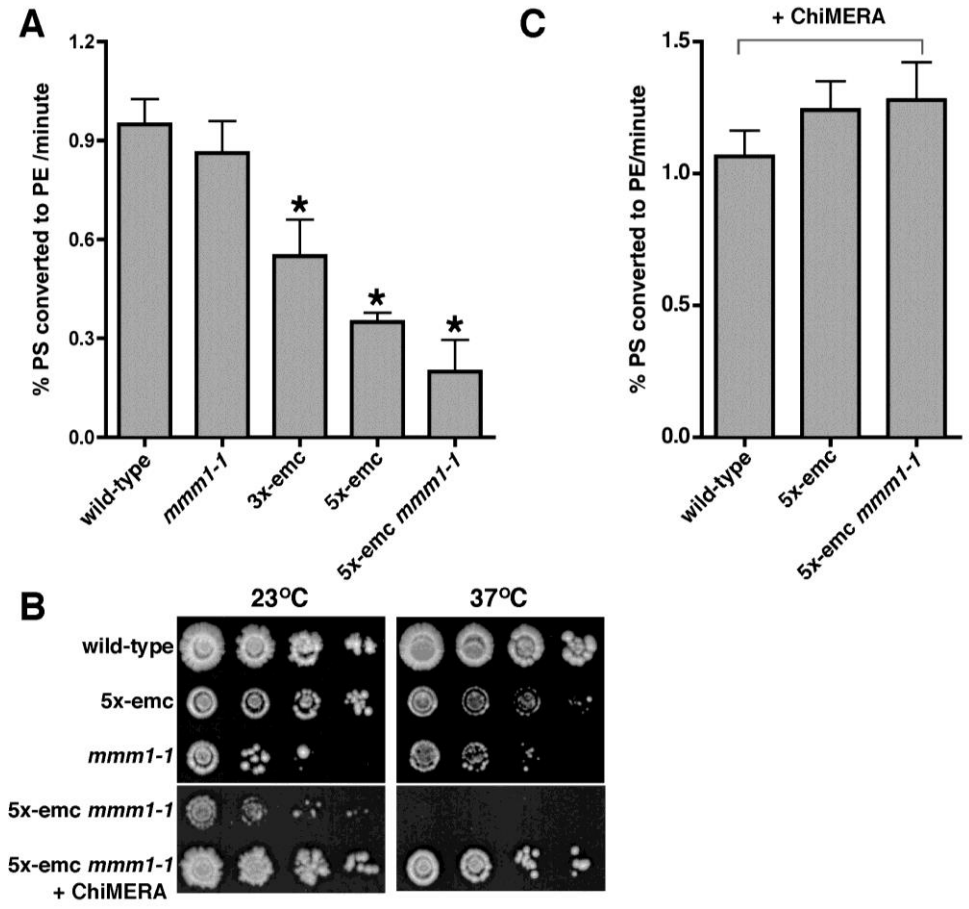

Figure 3.6: The rate of ER to mitochondria PS transfer is significantly reduced in crude mitochondria derived from 5x-emc cells.

(A) Crude mitochondria were incubated with [^{3}H]serine and Mn^{2+}. After 20 minutes at 30°C, an excess of unlabeled serine and EDTA were added; chelation of Mn^{2+} by EDTA inhibits PS synthase and allows Psd1p to function. The samples were collected over 15 minutes and the rate of [^{3}H]PS to [^{3}H]PE conversion per minute was calculated (mean + s.d., n = 3-5 independent experiments). * = $p < 0.05$ compared to wild-type, two-tailed t-test. (B) Cultures of strains with the indicated genotypes were grown at 23°C and 10-fold serial dilutions were spotted on to YPD plates and incubated at 23°C or 37°C for 4 days. (C) The rate of PS to PE conversion of strains expressing ChiMERA was determined as in Fig 3.5 (mean + s.d., n = 3 independen experiments).

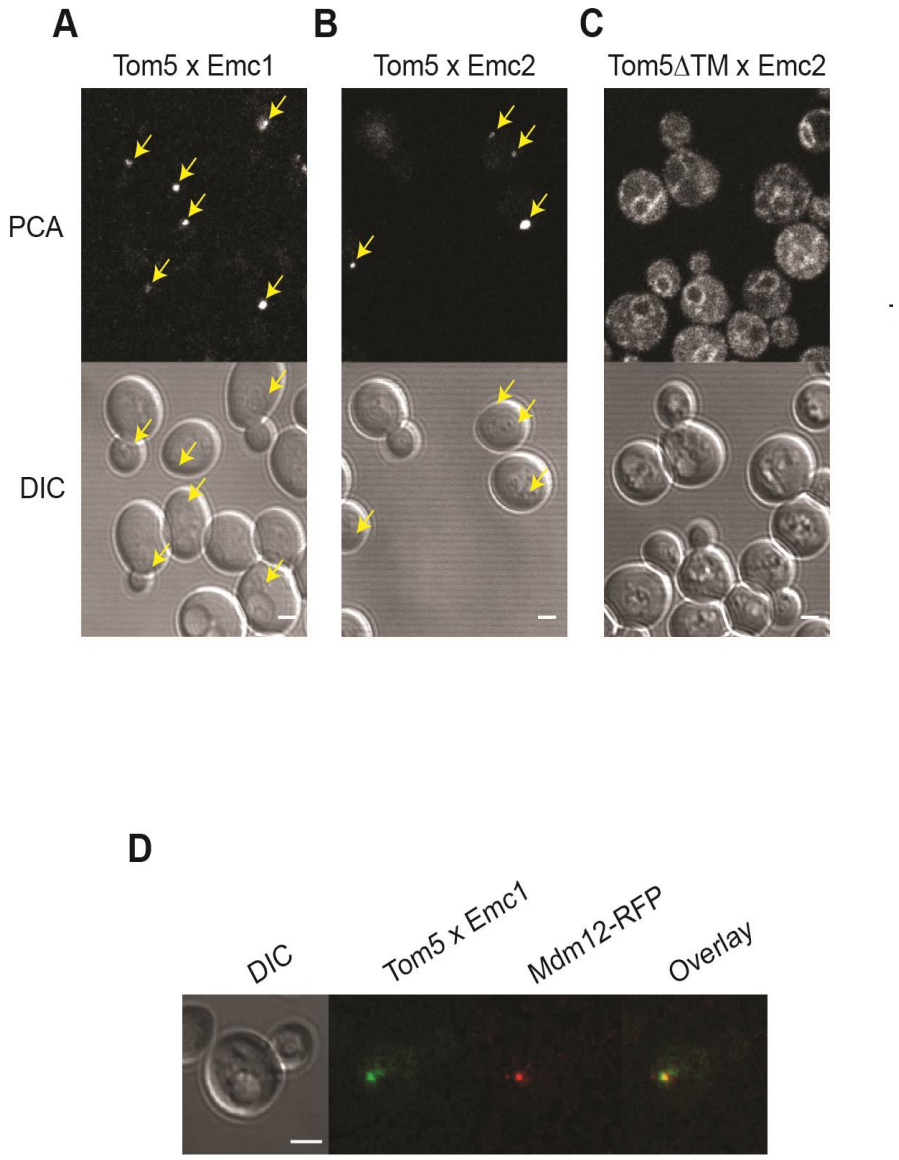

Figure 3.7: The EMC interacts with Tom5 at ER-mitochondria contacts.

(A&B) Interactions between Tom5 and Emc1 (A) and Emc2 (B) proteins imaged by Venus PCA. (C) Interaction between Tom5ΔTM and Emc2 by PCA. (D) Co-localization of the Tom5-Emc interaction and Mdm12-RFP of the ERMES complex.

A

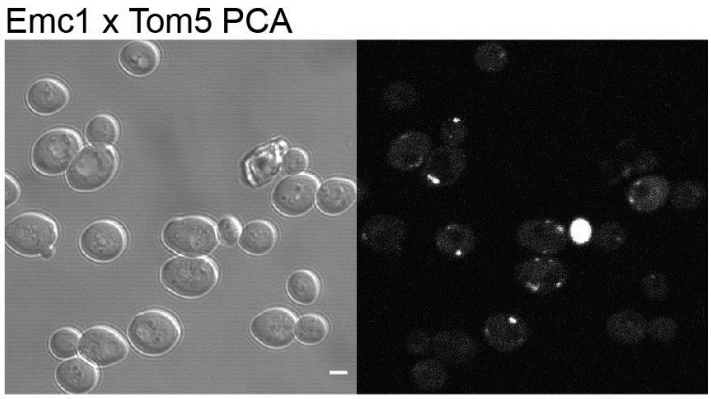

B

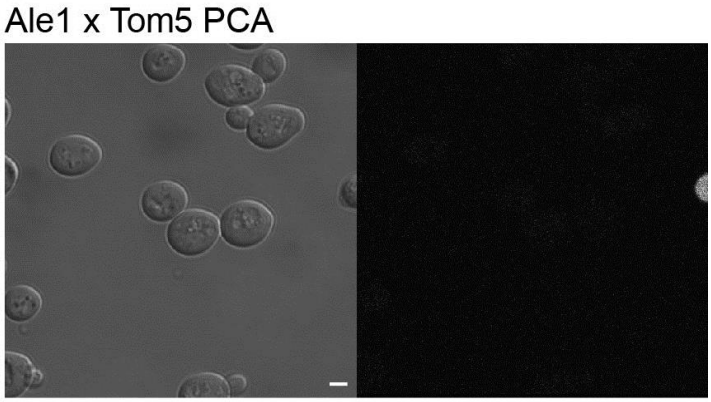

C

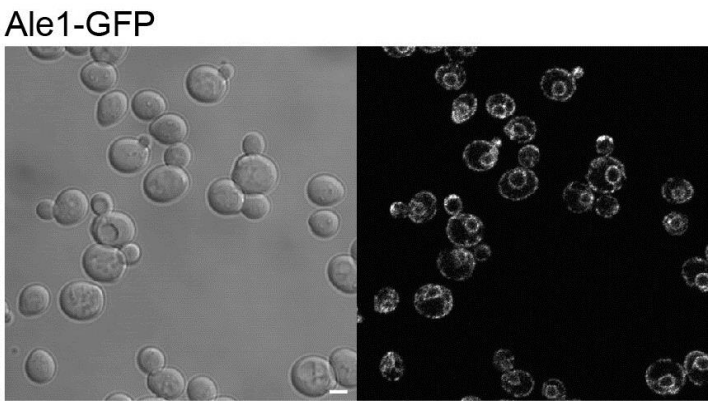

Figure 3.8: Ale1 control for PCA between the EMC and Tom5.

(A) Emc1 x Tom5 PCA in diploids. (B) Ale1 x Tom5 PCA in diploids captured with identical microscope settings as in (A). (C) Ale1 tagged at the endogenous gene locus with GFP. All scale bars; 2µm.

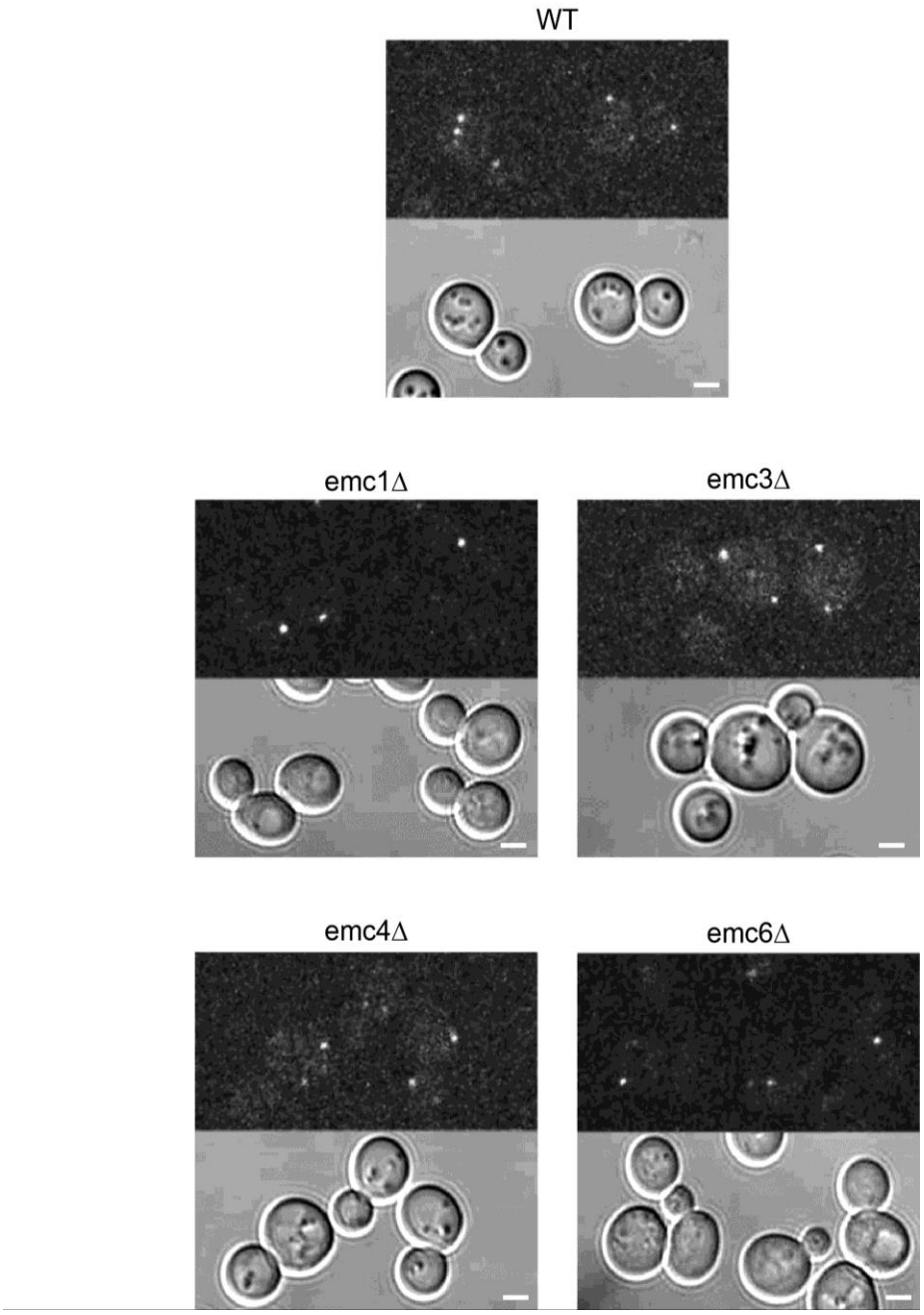

Figure 3.9: Localization of ERMES subunit Mdm34 is not disrupted in EMC mutants.

Mdm34-RFP tagged at the endogenous locus was imaged in various EMC deletion mutants using confocal microscopy. Scale bars = 2 μm.

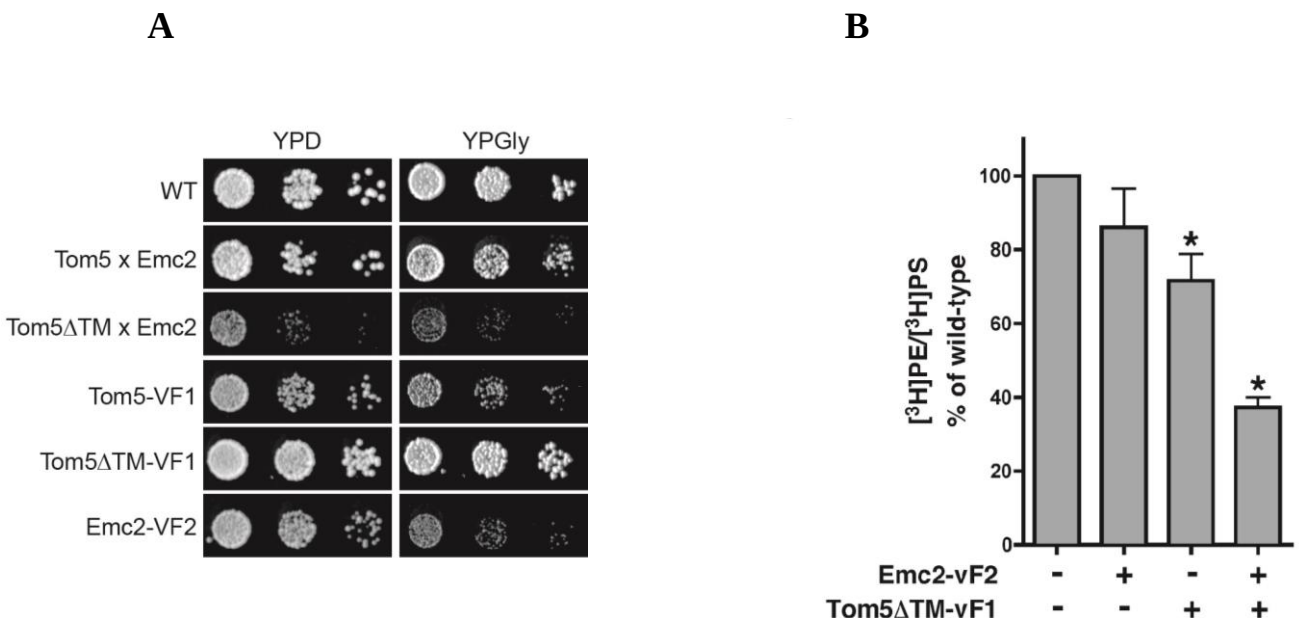

Figure 3.10: Emc2 and full length Tom5 interaction at contacts is important for PS transfer.

(A) Yeast growth assays for the indicated strains on media containing glucose (YPD) or glycerol (YPGly). Tom5 x Emc2 and Tom5ΔTM x Emc2 indicate haploid strains used for PCA containing Tom5 tagged with vF1 and Emc2 tagged with vF2. (B) Cells with the indicated genotypes were labeled with [^{3}H]serine as in Fig 4 A. The ratio of [^{3}H]PS converted to [^{3}H]PE was determined and expressed as a percent of wild-type cells (mean + s.d, n = 3 independent experiments). * = $p < 0.05$ compared to wild-type, two-tailed t-test. All scale bars = 2 µm.

Table 3.1: Strains and plasmids.

Strains	Genotype	Source
Δcho2	Y7092 cho2Δ::URA3	
Δemc6	Y7092 emc6Δ::URA3	
ALE1-GFP	Y7043 ALE1-GFP::HIS5	
ALE1-VF1	Y7043 *ALE1-VF2::URA3*	
BY4741	MATa his3Δ1 leu2Δ met15Δ ura3Δ	
EMC1-GFP	Y7043 EMC1-GFP::HIS5	
EMC1-VF1	BY4741 EMC1-VF1::HIS5	
EMC1-VF2	Y7043 EMC1-VF2::URA3	
EMC2-GFP	Y7043 EMC2-GFP::HIS5	
EMC2-VF1	BY4741 EMC2-VF1::HIS5	
EMC2-VF2	Y7043 EMC2-VF2::URA3	
EMC3-GFP	Y7043 EMC3-GFP::HIS5	
EMC3-VF1	BY4741 EMC3-VF1::HIS5	
EMC3-VF2	Y7043 EMC3-VF2::URA3	
EMC4-GFP	Y7043 EMC4-GFP::HIS5	
EMC4-VF1	BY4741 EMC4-VF1::HIS5	
EMC5-GFP	Y7043 EMC5-GFP::HIS5	
EMC5-VF2	Y7043 EMC5-VF2::URA3	
EMC6-GFP	Y7043 EMC6-GFP::HIS5	
EMC6-VF1	BY4741 EMC6-VF1::HIS5	
EMC6-VF2	Y7043 EMC6-VF2::URA3	
MDM12-RFP	BY4741 MDM12-RFP::natMX	
TOM5ΔTM-VF1	BY4741 TOM5ΔTM-VF1::HIS5	
VF1-TOM5	BY4741 HIS5::PHO5p-VF1-TOM5	
Y7043	Mat alpha can1Δ::STE2pr-leu2 lyp1Δ cyh2 his3Δ leu2Δ met15Δ ura3Δ	Tong, A. H. & Boone, C. Synthetic genetic array analysis in Saccharomyces cerevisiae. Methods Mol. Biol. 313, 171–192 (2006).
Y7092	Mat alpha can1Δ::STE2pr-Sp-his5 lyp1Δ his3Δ leu2Δ met15Δ ura3Δ	Tong, A. H. & Boone, C. Synthetic genetic array analysis in Saccharomyces cerevisiae. Methods Mol. Biol. 313, 171–192 (2006).
BY4741	*MATa his3Δ1 leu2Δ0 met15Δ0 ura3Δ0*	Invitrogen
BY4742	*MATα his3Δ1 leu2Δ0 lys2Δ5 ura3Δ0*	Invitrogen
YSL1	BY4741 *emc1::HIS5*	
YSL2	BY4741 *emc2::hygMX4*	
YSL3	BY4741 *emc3::HIS5*	
YSL58	BY4741 *emc5::kanMX4*	Invitrogen
YSL59	BY4741 *emc6::kanMX4*	Invitrogen
YSL4	BY4741 *emc1::HIS5 emc5::kanMX4*	
YSL5	BY4741 *emc3::HIS5 emc6::kanMX4*	
YSL6	BY4741 *emc1::HIS5 emc2::hygMX4 emc5::kanMX4*	
YSL7	BY4742 *emc4::kanMX4*	
YSL8	BY4742 *emc3::HIS5 emc6::kanMX4*	
YSL9 (5x-emc)	BY4741 *emc1::HIS5 emc2::hygMX4 emc3::HIS5 emc5::kanMX4 emc6::kanMX4*	
YSL27 (4x-emc)	BY4741 *emc1::HIS5 emc2::hygMX4 emc3::his emc6::kanMX4*	
YSL36	BY4741 *mmm1-1:Ca-URA3*	
YSL38	YSL9 *mmm1-1: Ca-URA3*	
YSL57 (3x-emc)	BY4741 *emc2::hygMX4 emc5::kanMX4 emc6::kanMX4*	
WPY442	BY4741 psd2::kanMX4	Invitrogen
WPY461	BY4742 *psd1::kanMX4 psd2::kanMX4*	lab collection
Plasmids		
pSL8	Expresses Psd2 under *PSD2* promoter (*URA3/CEN*)	
ChiMERA	Expresses chiMERA protein (*URA3/CEN*)	Kornmann et al., An ER-mitochondria tethering complex revealed by a synthetic biology screen. Science 325, 477-
pSL13	Expresses ChiMERA protein (*LEU2/CEN*)	

Table 3.2: *CHO2* genetic interactions rescued by choline.

Aggravating genetic interactions with *CHO2* that showed significant improvement in the presence of choline are listed. Genetic interaction strength is plotted as the ratio of the growth of the double mutant with Δ*cho2* versus the single mutant in the absence of choline.

Query gene	Target gene	Strength - choline (Ratio ΔΔ/Δ)	Query gene	Target gene	Strength - choline (Ratio ΔΔ/Δ)
CHO2	ADE16	0.64	CHO2	FAR7	0.47
CHO2	AFT1	0.38	CHO2	FAT1	0.50
CHO2	AIM34	0.46	CHO2	FIT1	0.67
CHO2	AIP1	0.68	CHO2	FMC1	0.59
CHO2	ARE2	0.35	CHO2	GAL1	0.29
CHO2	AST2	0.60	CHO2	GAL83	0.54
CHO2	BNI5	0.52	CHO2	GCN5	0.22
CHO2	BUB3	0.53	CHO2	GDS1	0.44
CHO2	CDC50	0.26	CHO2	GET3	0.46
CHO2	CHA4	0.61	CHO2	GLO3	**0.62**
CHO2	CNB1	0.36	CHO2	GND1	0.50
CHO2	COG6	0.59	CHO2	GPA2	0.49
CHO2	CTK2	0.63	CHO2	GSF2	0.58
CHO2	CUE1	0.62	CHO2	GYP1	0.26
CHO2	CYB5	0.54	CHO2	GZF3	0.61
CHO2	CYM1	0.42	CHO2	HAC1	0.41
CHO2	DAP1	0.55	CHO2	HCH1	0.42
CHO2	DBF2	0.24	CHO2	HEF3	0.58
CHO2	DCV1	0.61	CHO2	HST1	0.56
CHO2	DID2	0.42	CHO2	HUR1	0.25
CHO2	DNL4	0.50	CHO2	IBI2	0.45
CHO2	DOA1	0.34	CHO2	IES1	0.39
CHO2	DOT1	0.27	CHO2	IES5	0.47
CHO2	DRS2	0.15	CHO2	INO2	0.10
CHO2	DSK2	0.41	CHO2	IRE1	0.37
CHO2	EAP1	0.46	CHO2	KCS1	0.24
CHO2	EMC1	0.25	CHO2	KEL2	0.61
CHO2	EMC3	0.34	CHO2	LCB3	0.51
CHO2	EMC4	0.30	CHO2	MAF1	0.62
CHO2	EMC5	0.50	CHO2	MED1	0.44
CHO2	EMC6	0.41	CHO2	MGA2	0.29
CHO2	ENV10	0.31	CHO2	MGR3	0.65
CHO2	ENV9	0.31	CHO2	MID1	0.41
CHO2	ERG28	0.56	CHO2	MKR1	0.25
CHO2	ERG3	0.39	CHO2	MMR1	0.37
CHO2	ERG5	0.39	CHO2	MOG1	0.17
CHO2	FAR10	0.44	CHO2	MON2	0.28
CHO2	FAR11	0.39	CHO2	MRE11	0.42
CHO2	FAR3	0.37	CHO2	MRPL36	0.43

Query gene	Target gene	Strength - choline (Ratio ΔΔ/Δ)	Query gene	Target gene	Strength - choline (Ratio ΔΔ/Δ)
CHO2	MSN5	0.49	CHO2	SWI3	0.28
CHO2	MVB12	0.57	CHO2	TEX1	0.47
CHO2	NCS2	0.27	CHO2	THR1	0.35
CHO2	NHP10	0.49	CHO2	TOM5	0.15
CHO2	NNT1	0.65	CHO2	TOS1	0.64
CHO2	NPR1	0.36	CHO2	TPK1	0.58
CHO2	NPR3	0.55	CHO2	TUM1	0.28
CHO2	NRP1	0.61	CHO2	UBC7	0.66
CHO2	OTU2	0.60	CHO2	UBI4	0.21
CHO2	PAD1	0.25	CHO2	UBP1	0.22
CHO2	PEA2	0.55	CHO2	UBP14	0.61
CHO2	PEX2	0.66	CHO2	UBP15	0.56
CHO2	PHO85	0.16	CHO2	UBP2	0.56
CHO2	PHO86	0.47	CHO2	UBX2	0.48
CHO2	PLB2	0.64	CHO2	UBX4	0.50
CHO2	PMA2	0.61	CHO2	UFD2	0.23
CHO2	PMR1	0.41	CHO2	UMP1	0.23
CHO2	PPG1	0.45	CHO2	URE2	0.28
CHO2	PPZ1	0.47	CHO2	VAM10	0.30
CHO2	PSD1	0.60	CHO2	VMA1	0.37
CHO2	PUB1	0.53	CHO2	VMA11	0.39
CHO2	RAD23	0.55	CHO2	VMA16	0.39
CHO2	RAD57	0.63	CHO2	VMA21	0.31
CHO2	RHR2	0.45	CHO2	VMA4	0.54
CHO2	RIC1	0.20	CHO2	VMA6	0.38
CHO2	ROM2	0.55	CHO2	VMA7	0.34
CHO2	RPN4	0.14	CHO2	VMA8	0.20
CHO2	RPS25A	0.63	CHO2	VMA9	0.52
CHO2	RSF1	0.38	CHO2	VPH2	0.40
CHO2	RTG3	0.35	CHO2	VPS1	0.19
CHO2	SAC7	0.42	CHO2	VPS17	0.54
CHO2	SAK1	0.45	CHO2	VPS24	0.28
CHO2	SBH2	0.54	CHO2	VPS29	0.43
CHO2	SCS2	0.20	CHO2	VPS4	0.40
CHO2	SCW10	0.54	CHO2	VPS52	0.55
CHO2	SEC66	0.35	CHO2	VPS53	0.55
CHO2	SHP1	0.44	CHO2	VPS60	0.49
CHO2	SHR5	0.57	CHO2	VPS61	0.21
CHO2	SIC1	0.66	CHO2	VPS63	0.15
CHO2	SKS1	0.54	CHO2	VPS64	0.49
CHO2	SKY1	0.58	CHO2	WHI2	0.56
CHO2	SLA1	0.36	CHO2	YBL081W	0.57
CHO2	SLT2	0.50	CHO2	YBR242W	0.50
CHO2	SLX5	0.57	CHO2	YDL206W	0.47
CHO2	SMA1	0.62	CHO2	YDR186C	0.18
CHO2	SNF1	0.09	CHO2	YER084W	0.46
CHO2	SNF12	0.30	CHO2	YET1	0.65
CHO2	SNF6	0.21	CHO2	YGL081W	0.52
CHO2	SPO11	0.46	CHO2	YHR033W	0.65
CHO2	SPO7	0.53	CHO2	YJL027C	0.62
CHO2	SPT23	0.48	CHO2	YKL077W	0.57
CHO2	SRC1	0.50	CHO2	YNR021W	0.36
CHO2	SRN2	0.43	CHO2	YPL041C	0.55
CHO2	SSH1	0.50	CHO2	YPR114W	0.55
CHO2	SSK1	0.67	CHO2	YPT6	0.20
CHO2	SSP2	0.25	CHO2	YSA1	0.55
CHO2	SUM1	0.43			

Table 3.3: Functional group enrichment for genes identified in the *CHO2* SGA screen.

Only genes whose interactions were rescued by choline (Table 3.2) were used in the analysis.

Type	Category	p value	Genes
Biological Process	re-entry into mitotic cell cycle after pheromone arrest	2.20E-06	VPS64 FAR7 FAR10 FAR3 FAR11
Biological Process	negative regulation of macroautophagy	0.004806	SIC1 PHO85
Biological Process	protein folding in endoplasmic reticulum	7.71E-06	EMC1 EMC4 KRE27 AIM27 EMC6
Biological Process	regulation of nitrogen utilization	0.007858	NPR1 URE2
Biological Process	intralumenal vesicle formation	0.007858	VPS24 VPS4
Biological Process	retrograde transport, endosome to Golgi	7.52E-06	VPS52 VPS29 VPS53 RIC1 YPT6 VPS17
Biological Process	vacuolar acidification	4.23E-07	VMA1 VMA8 VMA7 DBF2 VMA16 VPH2 VMA6 VMA11
Biological Process	protein deubiquitination	0.000161	UBP14 UBP1 UBI4 UBP15 UBP2
Biological Process	late endosome to vacuole transport via multivesicular body sorting pathway	0.004322	VPS60 DID2 VPS4
Biological Process	nucleosome mobilization	0.00094	NHP10 IES1 SNF6 SNF12
Biological Process	endoplasmic reticulum unfolded protein response	0.0055	HAC1 SLT2 IRE1
Biological Process	protein targeting to vacuole	0.001047	VPS64 MVB12 VPS1 DID2 SRN2 MON2
Biological Process	sterol biosynthetic process	0.009146	ERG28 ERG3 ERG5 CYB5
Biological Process	ascospore formation	0.00118	SPO7 SHP1 GPA2 UBI4 ADE16 MRE11 SSP2
Cellular Component	ER membrane protein complex	1.13E-07	EMC1 EMC4 KRE27 AIM27 EMC6
Cellular Component	Ssh1 translocon complex	0.00245	SSH1 SBH2
Cellular Component	proton-transporting V-type ATPase, V0 domain	0.000228	VMA16 VMA6 VMA11
Cellular Component	ESCRT I complex	0.004806	MVB12 SRN2
Cellular Component	GARP complex	0.004806	VPS52 VPS53
Cellular Component	nuclear envelope lumen	0.007858	SNF1 GAL83
Cellular Component	retromer complex	0.007858	VPS29 VPS17
Cellular Component	AMP-activated protein kinase complex	0.007858	SNF1 GAL83
Cellular Component	vacuolar proton-transporting V-type ATPase, V1 domain	0.001199	VMA1 VMA8 VMA7
Cellular Component	endosome	2.29E-06	SLA1 CDC50 VPS52 VPS60 MVB12 VPS29 VPS53 VPS24 DID2 SRN2 MON2 VPS17 DAP1 VPS4
Cellular Component	endoplasmic reticulum	4.39E-10	SPO7 FAT1 SEC66 SSH1 EMC1 GET3 UBP1 VPS64 SBH2 ERG28 SCS2 EMC4 VMA21 IRE1 KRE27 PHO86 LCB3 YET1 VPH2 AIM27 EMC6 ERG3 FAR10 UBX2 GSF2 ERG5 UBC7 FAR3 CUE1 SCW10 CYB5 MID1 ARE2 YNR021W SHR5 YPR114W VPS4
Molecular Function	endodeoxyribonuclease activity	0.007858	VMA1 MRE11
Molecular Function	proton-transporting ATPase activity, rotational mechanism	0.000148	VMA1 VMA8 VMA7 VMA16 VMA6 VMA11
Molecular Function	ubiquitin-specific protease activity	0.002285	UBP14 UBP1 UBP15 UBP2
Molecular Function	hydrolase activity, acting on acid anhydrides, catalyzing transmembrane movement of substances	0.003902	DRS2 VMA1 PMR1 PMA2
Molecular Function	ubiquitin binding	0.003947	SLA1 RAD23 MVB12 DOA1 BUB3
Molecular Function	kinase activity	0.002471	GAL1 KCS1 SNF1 SAK1 DBF2 THR1 SLT2 YHR033W IRE1 TPK1 SKY1 NPR1 SKS1 PHO85

Table 3.4: Genetic interactions with EMC6.

Aggravating and alleviating interactions are listed along with the strength of the interactions plotted as the ratio of the growth of the double mutant with Δ*emc6* versus the single mutant.

Query gene	Target gene	Type	Strength (Ratio ΔΔ/Δ)				
EMC6	AAH1	aggravating	0.63	EMC6	ASE1	alleviating	1.26
EMC6	ASF1	aggravating	0.80	EMC6	ATP11	alleviating	1.23
EMC6	ATP1	aggravating	0.19	EMC6	AVO2	alleviating	1.41
EMC6	ATP25	aggravating	0.76	EMC6	BEM4	alleviating	1.24
EMC6	BUR2	aggravating	0.60	EMC6	BRO1	alleviating	1.82
EMC6	CHO2	aggravating	0.09	EMC6	BTS1	alleviating	1.22
EMC6	CIK1	aggravating	0.77	EMC6	BUB3	alleviating	1.24
EMC6	CKA2	aggravating	0.80	EMC6	CTK2	alleviating	1.77
EMC6	CLA4	aggravating	0.70	EMC6	EAP1	alleviating	1.38
EMC6	ECM3	aggravating	0.25	EMC6	GCR2	alleviating	1.22
EMC6	ELM1	aggravating	0.64	EMC6	ILM1	alleviating	1.49
EMC6	GEP4	aggravating	0.56	EMC6	INO4	alleviating	1.29
EMC6	GET1	aggravating	0.27	EMC6	LDB16	alleviating	1.44
EMC6	HTD2	aggravating	0.69	EMC6	LEO1	alleviating	1.22
EMC6	INO2	aggravating	0.55	EMC6	MON2	alleviating	1.64
EMC6	KAP123	aggravating	0.22	EMC6	MTM1	alleviating	1.48
EMC6	LPD1	aggravating	0.67	EMC6	NOP16	alleviating	1.18
EMC6	MCT1	aggravating	0.70	EMC6	OCA6	alleviating	1.43
EMC6	MDY2	aggravating	0.75	EMC6	OPI11	alleviating	1.24
EMC6	MHR1	aggravating	0.75	EMC6	PHO80	alleviating	1.55
EMC6	MRPL15	aggravating	0.57	EMC6	PHO85	alleviating	2.11
EMC6	MRPL25	aggravating	0.68	EMC6	RAD6	alleviating	2.18
EMC6	MRPL49	aggravating	0.75	EMC6	RPB9	alleviating	1.37
EMC6	MSM1	aggravating	0.69	EMC6	RPL43A	alleviating	1.29
EMC6	MSO1	aggravating	0.37	EMC6	RPS10A	alleviating	2.16
EMC6	NPL3	aggravating	0.67	EMC6	RPS19B	alleviating	2.74
EMC6	PET123	aggravating	0.71	EMC6	SAN1	alleviating	1.34
EMC6	PML39	aggravating	0.55	EMC6	SER3	alleviating	1.34
EMC6	PPA2	aggravating	0.71	EMC6	SIN3	alleviating	1.42
EMC6	SCS2	aggravating	0.81	EMC6	SKY1	alleviating	1.21
EMC6	SIP3	aggravating	0.65	EMC6	SNF6	alleviating	1.73
EMC6	SLM5	aggravating	0.69	EMC6	SSO2	alleviating	1.45
EMC6	SRV2	aggravating	0.78	EMC6	SUB1	alleviating	1.22
EMC6	UBR2	aggravating	0.72	EMC6	SUR1	alleviating	2.55
EMC6	VPS33	aggravating	0.55	EMC6	TIM18	alleviating	1.34
EMC6	VPS41	aggravating	0.75	EMC6	VPS1	alleviating	1.25
EMC6	AAT2	alleviating	1.43	EMC6	VRP1	alleviating	1.62
EMC6	ADA2	alleviating	1.76	EMC6	ZAP1	alleviating	1.24
EMC6	AFT1	alleviating	1.25				

4. The ER DIFFUSION BARRIER REGULATES SPINDLE POSITIONING AND NUCLEAR MIGRATION PATHWAYS IN BUDDIING YEAST

4.1. SYNOPSIS

Polarization of plasma membrane (PM) domains is required for establishment of cell polarity in various cell types. Polarization requires formation of molecular diffusion barriers that prevent mixing of proteins between membrane domains. Recent studies are uncovering that the endoplasmic reticulum (ER) is polarized by diffusion barriers which control cellular aging in budding yeast and glutamate signaling in the dendritic spines of neurons (Mostowy and Cossart, 2012). Septins are GTP-binding proteins that form membrane-associated cytoskeletal filament proteins that create the PM diffusion barrier in yeast. The molecular identity of the ER diffusion barrier is not known, although septins are involved. Jesse Chao a PhD student in our lab discovered a novel subunit of the polarisome called Epo1, for ER polarization. He found that Epo1 captures ER tubules at the bud cortex and the bud neck. Epo1 interacts with the ER protein Scs2 and a septin Shs1 to tether the ER to septins, thus creating the ER diffusion barrier. My work on this project uncovered a physiological role for ER polarization and the ER diffusion barrier in spindle positioning and nuclear migration in yeast. I found that the ER diffusion barrier restricts the nuclear migration protein, Num1, to the mother during S phase, which prevents premature migration of the spindle until M phase when Num1 is expressed in the bud. This thesis chapter represents my contribution to a paper under review at Cell, for which I am second author.

4.2. INTRODUCTION

4.2.1. Polarized growth in budding yeast

Establishment of cell polarity is a fundamental aspect of biology that enables cells to spatially segregate their functions and to divide. Cell polarization is most often achieved through

cytoskeleton-based directional transport of cargo to polarized domains and through the establishment of molecular diffusion barriers that compartmentalize such domains. Budding yeast is one of the best-characterized models for studying polarized growth and asymmetric cell division as it divides asymmetrically by budding. In yeast, polarization is established by Cdc42, which is responsible for polarizing the actin cytoskeleton and septins (Reviewed by (Pruyne et al., 2004)). The actin cytoskeleton mediates polarized growth in yeast and the polarisome complex helps to regulate polarization of actin cables toward the incipient bud site. The polarisome has four subunits, Pea2, Spa2, Bud6 and Bni1. Bni1 is a formin protein and nucleates actin cables in the bud and Bud6 binds to actin monomers thereby promoting the nucleating activity of Bni1 (Moseley et al., 2004). Spa2 and Pea2 are polarized coiled-coil proteins that localize Bni1 to sites of polarized growth (Ozaki-Kuroda et al., 2001) (Fig. 4.1). Type V myosin motor proteins mediate directional transport of exocytic vesicles on these cables resulting in polarized growth of the bud. Polarity establishment also requires myosin-dependent transport of mRNA, mitochondria, vacuoles, ER, trans Golgi, and astral microtubules to the growing bud.

During budding, Cdc42 also initiates the formation of a cortical diffusion barrier at the neck comprised of septins, that compartmentalizes the bud from the mother (Faty et al., 2002; Versele and Thorner, 2005). The septins are a set of cytoskeletal filaments that form a ring around the incipient bud site. As bud emerges, septins are rearranged into a collar at the mother-bud neck (Gladfelter et al., 2005). Septins are not required for bud emergence; however, they act as a scaffold to concentrate a variety of signaling molecules to shape the bud and strengthen the cell wall at the cell division site through localization of chitin synthases. Recently, septin-dependent compartmentalization was described in budding yeast. It is been shown that septins are involved in making a diffusion barrier between mother and bud to restrain the free diffusion of specific PM (Barral et al., 2000; Takizawa et al., 2000), ER (Luedeke et al., 2005), and nuclear envelope (NE) (Shcheprova et al., 2008) proteins between the mother cell and the daughter. The asymmetrical partitioning of ER-associated factors may be a regulatory mechanism for ER inheritance and biogenesis in yeast and also higher eukaryotes (see section *1.2.2.* for ER inheritance).

4.2.2. Spindle positioning and nuclear migration in budding yeast

After the establishment of the polarity axis, the mitotic spindle must be oriented properly in order to segregate duplicated chromosomes into the new daughter cell during mitosis. Yeast cells face the challenge of positioning their spindle from a random position in the mother cell to a predetermined cytokinesis site since bud-site selection in yeast occurs prior to spindle formation. At the same time the spindle has to align along the mother-bud axis. During the process of budding, the mitotic spindle must therefore move into the neck prior to mitosis. Budding yeast like other ascomycete fungi undergoes a closed mitosis; the nuclear envelope does not break down, so this process is often termed "nuclear migration" (Reviewed by (Bloom, 2001), and (Siller and Doe, 2009)). Genetic studies have revealed that spindle positioning depends on two partially redundant overlapping pathways that have been described as the early and late stages of the nuclear migration pathway (Fig. 4.2). In "the early stage", the preanaphase spindle moves towards the future site of cytokinesis at the bud neck and aligns along the mother bud axis. In the "late stage" the properly orientated spindle elongates and is pulled through the bud neck along the mother bud axis to complete mitosis.

The critical components of the "early stage" include Biml, Kar9, the type V myosin Myo2 and the kinesin-related protein Kip3 (Hwang et al., 2003). Kar9 binds to microtubules via the microtubule-binding protein Bim1 since Kar9 is lost from microtubules upon deletion of Bim1 (Lee et al., 2000; Miller et al., 2000). Concurrently, Kar9 interacts with the actin motor protein Myo2 that moves along actin cables toward the bud tip (Figure 4.2A). Kar9 bridges Myo2 to microtubules, which leads to pulling of the microtubules toward the bud through the force exerted by Myo2 (Hwang et al., 2003; Kusch et al., 2002; Liakopoulos et al., 2003). This brings the spindle close to the bud neck. Detachment of microtubules from actin cables occurs due to Kar9 degradation and disassembly of Kar9 complexes at the bud neck. In every cycle, only a small proportion of microtubule -bound Kar9 is degraded, since only Kar9 that assembles into active microtubule-guiding complexes reaches the bud neck (Liakopoulos et al., 2003). Deletion of the early stage components such as Kar9 results in misorientation of the microtubulesin the bud and (Miller and Rose, 1998).

The late stage corresponds to the movement of the anaphase nucleus through the bud neck via the actions of dynein and dynactin (Kahana et al., 1998). The dynein motor protein

travels to the tips of cytoplasmic microtubules and is anchored at the bud cortex by interaction with the cortical capture protein, Num1 (for nuclear migration protein) (Farkasovsky and Kuntzel, 1995; Heil-Chapdelaine et al., 2000). Interaction of dynein (Yeh et al., 1995) with Num1 requires the dynactin complex, which is comprised of the subunits Arp1 (Muhua et al., 1994), Nip100 (p150 Glued in humans) (Kahana et al., 1998), Jnm1 (dynamitin) (McMillan and Tatchell, 1994) and Ldb18 (p24) (Heil-Chapdelaine et al., 2000). Num1 localizes to discrete punctae at the cell cortex and its cortical localization is critical for capture of cytoplasmic microtubules, alignment of the spindle and reeling of the nucleus into the bud (Farkasovsky and Kuntzel, 1995, 2001; Tang et al., 2012). Consequently, loss of Num1, dynein or dynactin results in binucleate mother cells during mitosis, a common phenotype of cells lacking the late stage nuclear migration components. Although both early stage (Kar9 pathway) and late stage (Num1/dynein/dynactin pathway) mutants exhibit defects in spindle orientation, they are viable. However, loss of both pathways results in lethality, thus, most early stage components interact genetically with late stage components.

4.3. MATERIALS AND METHODS

4.3.1. Yeast strains, growth condition and manipulation

All yeast strains were grown at 30^{o}C with shaking for liquid culture or on 2% agar plates in synthetic defined (SD) media with the appropriate amino acid dropouts and 2% dextrose unless otherwise stated. To test for growth defects of double mutants of Δ*scs2* and late stage nuclear migration components, a Δ*scs2::NatR* (BY7092) strain was crossed to Δ*jnm1,* Δ*nip100,* Δ*ldb18,* Δ*arp1,* Δ*dyn1*, and Δ*num1* mutants from the yeast deletion collection (BY4741, *KanR*), Diploids were sporulated at 25^{0}C for 6 days on nutrient-deficient media and spores were germinated on SD-media lacking histidine, arginine and lysine; and supplemented with canavanine and thialysine to allow germination of *Mat**a*** haploid cells. Germinated cells were replica plated to SD-media lacking histidine, arginine and lysine supplemented with clonNat and G418 sulfate to recover double mutant cells.

GFP-Tub1 was made using the PCR mediated gene disruption method in BY4742 (expressing *URA3* gene as a selection marker). Num1-GFP was constructed using the PCR mediated gene disruption method. The specific primers were utilized in PCR with the *pKT128* plasmid (expressing the *S. pombe HIS5* gene as a selection marker) (Sheff and Thorn, 2004) in the BY7043 background, and colonies were plated on SD media lacking histidine. Yeast colonies were checked by PCR for the correct insertion of the cassette into the genome. To make the Num1-GFP Δ*scs2* strain, Num1-GFP yeast were crossed to Δ*scs2::G418* from the DMA (BY4741 *Mat**a***). Diploids were selected on SD media lacking histidine and having G418. Diploids were sporulated, and germinated on SD media lacking histidine and containing G418 and canavanine and thialysine to allow the germination of *Mat**a*** haploid cells. The yeast parental strains used in this study are summarized in Table A4.1.

4.3.2. Yeast growth assays

Mid-log phase grown yeast cultures (OD_{600}=0.5) were diluted in 10- fold serial dilutions and spotted onto SD media plus 2% glucose using a metal pin-frogger (Sigma). Plates were grown for 2 days at 30^{o}C.

4.3.3. Cell cycle arrest with hydroxyurea (HU)

To synchronize cells in S phase, HU was added to log phase yeast cultures grown in YPD (yeast extract and peptone plus 2% dextrose) liquid medium. The final concentration of HU used, was 0.3 M and liquid cultures were grown for 4-5 hours.

4.3.4. Spindle length quantification

Spindle length was quantified by measuring the distance between two in-focus SPBs in confocal images using ImageJ software (National Institutes of Health), in about 250 cells per strain arrested in HU for 4-5 hours.

4.3.5. DAPI staining

To stain nuclear DNA, log phase yeast cells were fixed in 70% ethanol at room temperature for 20 minutes and washed with distilled water twice. The cell pellet was re-suspended in 100 µl of 50 ng/ml DAPI solution (diluted in PBS from a 50 µg/ml DAPI stock, Sigma) at room temperature for 10 minutes. Cells were washed with distilled water to remove excess DAPI and were imaged by UV laser.

4.3.6. Confocal microscopy

Log phase live yeast cells were imaged using a Zeiss LSM-5 Pascal confocal microscope and Zeiss Pascal software. Unless otherwise stated. Optical slices were taken through the center of each cell and images being directly compared were captured with identical microscope settings on the same day.

4.3.7. Synthetic genetic array (SGA) analysis for SCS2

SGA analysis was performed according to established protocols (Tong and Boone, 2006) essentially as previously described (Young et al., 2010) using a Singer RoToR Colony Arraying robot (Singer Instruments). Δ*scs2*::URA3 query strain was constructed using standard techniques in strain background Y7092 and crossed to the yeast haploid deletion mutant array (DMA) using a Singer RoToR HAD robot. Following diploid selection, spots were replicated three times and sporulated for 5 days. Haploids were germinated on SD-media lacking histidine, arginine and lysine supplemented with thialysine and canavanine (both at 100 µg/ml). Control sets of single deletion strains were generated by plating on media containing 5-fluoroorotic acid to counter-select for the Δ*scs2*::URA3 alleles and G418 sulfate (200 µg/ml) to select for the DMA strain; while double mutants were selected for by plating on media lacking uracil and containing G418 sulfate. A further round of selection was performed on the same media. Arrays were imaged using a flatbed scanner.

Balony software (http://code.google.com/p/balony/) was used to measure spot sizes, determine cut-off values for genetic interactions and define strains the showed statistically significant changes in growth rate. Cut-off values for genetic interactions were defined for each screen by determining three standard deviations from the mean of the ratios of the double mutant to single mutant growth rates. Double mutant strains that met the cut-off and showed significant changes in growth relative to the corresponding single mutant control (one-tailed students' t-test; $p < 0.05$; n=3) were considered as genetic interactions. Gene ontology analysis was performed using Funspec (http://funspec.med.utoronto.ca) and Cytoscape (http://www.cytoscape.org) (Cline et al., 2007; Robinson et al., 2002).

4.4. RESULTS

4.4.1. Scs2 interacts genetically with S phase spindle positioning components

To uncover additional physiological roles for Scs2, I interrogated the known global genetic interaction network in yeast, which provides a functional map of the cell (Costanzo et al., 2010). This dataset contains over five million unbiased quantitative measurements of synthetic genetic interactions covering over three quarters of the yeast genome. By using this dataset and performing hierarchical clustering, one can generate gene clusters with similar genetic interaction profiles to identify genes with similar functions. I searched for *SCS2,* the major focus of my PhD dissertation and noticed that it was present in a cluster with genes that function in S phase spindle positioning, suggesting a role for Scs2 in this pathway (Fig. 4.3 A). In the S phase cluster were genes encoding the formin *BNI1*, the myosin motor *MYO2*, the microtubule guidance protein *KAR9*, and the kinesins *KIP3* and *CIN8,* which belong to early stage of nuclear migration pathway. Moreover, several microtubule associated proteins (*STU1*, *STU2*, *ASE1*) and tubulin folding cofactors (*CIN1*, *CIN2*), and the transcription factor *HCM1*, which controls S phase expression of spindle assembly factors were in this cluster. Genes in the S phase cluster formed primarily aggravating genetic interactions with a gene cluster containing M phase spindle positioning genes (Fig. 4.3 A) in the late stage of the nuclear migration pathway. The M phase cluster included the nuclear migration late stage components dynein and dynactin, its cortical capture protein Num1, and the kinesin motor and accessory proteins required to load dynein onto

the plus ends of microtubules (Huisman and Segal, 2005).

Thus, the presence of *SCS2* within the S phase cluster and its aggravating genetic interactions with genes in the M phase cluster implied a role for *SCS2* in S phase spindle positioning. To evaluate the role for Scs2 in spindle positioning, we performed our own SGA analysis. Figure 4.3 B shows gene ontology (GO) analysis for the aggravating genetic interactions identified in the screen. GO term analysis can reveal statistically significant enrichment of particular functions within a genetic interaction dataset. Our screen identified aggravating genetic interactions between *SCS2* and many of the genes involved in M phase spindle positioning and nuclear migration. I confirmed these genetic interactions between *SCS2* and dynein, dynactin and *NUM1*, and consistent with a role for Scs2 in S phase spindle positioning, these double mutants showed slow growth phenotypes (Fig. 4.3 A).

4.4.2. Scs2 plays a role in spindle positioning

To better understand the nature of *SCS2* genetic interactions with late stage component of the nuclear migration pathway, I examined spindle positioning in Δ*scs2* cells. Hydroxyurea (HU) treatment arrests yeast in S-phase, and this allowed us to assay for defects specifically in the early phase of nuclear migration, when the nucleus is anchored on the mother side of the bud neck by astral microtubules that interact with septins in the neck (Koc et al., 2004; Kusch et al., 2002). Using the mitotic spindle reporter, Tub1-GFP, I found that the spindle was predominately positioned in the mother adjacent to the neck in wild type cells (Fig. 4.4 A & B) as previously described (Yeh et al., 1995). In contrast, in Δ*scs2* cells the spindle was predominately mispositioned in the neck and in ~13% of cells it had migrated entirely into the bud, clear of the neck Fig. 4.4 A & B). I found that spindle length was normal in Δ*scs2* cells, ruling out a role for defective spindle assembly in spindle mispositioning (Fig. 4.4 C). Thus, spindle mispositioning in S phase in Δ*scs2* cells explained the aggravating genetic interactions between *SCS2* and genes in the late stage of the nuclear migration pathway.

4.4.3. Scs2 controls the localization of Num1 and the timing of nuclear migration

To provide clues into the role for Scs2 in spindle positioning, I focused on known protein interaction partners for Scs2. A previous genome-wide proteomics study identified an interaction with the spindle cortical capture protein Num1 (Gavin et al., 2002). The genetic interaction between *SCS2* and *NUM1* suggested that this physical interaction was physiologically relevant and so I turned to characterizing the role for Scs2 in localizing Num1. In wild type cells, Num1-GFP localized to the cell cortex and was absent from S and G2 phase buds, but appeared later in M phase buds (Fig. 4.5 A). Num1-GFP also appeared concentrated in patches at the distal pole of mothers and unbudded cells, adjacent to the neck in S phase cells, and at the tips of large buds. This pattern has also been observed for the native Num1 protein (Farkasovsky and Kuntzel, 1995). In Δ*scs2* cells, Num1-GFP was no longer distributed along the cell cortex and was instead concentrated in foci that corresponded to the enriched cortical patches observed in wild type cells (Fig. 4.5 B). Num1 interacts with dynein in these foci, which are cortical microtubule capture sites (Tang et al., 2012). Thus, it appeared that Scs2 localized Num1 to PM-associated ER (pmaER). Scs2 was not required to localize Num1 to microtubule capture sites.

Localization of Num1 to pmaER by Scs2 suggested that the ER diffusion barrier might play a role in restricting the entry of Num1 into S and G2 buds (Fig. 4.5 A), by preventing diffusion of Num1 from the mother along ER tubules. Therefore we examined the localization of Num1-GFP in a mutant of the septin Shs1 that lacks its C-terminal extension and has a compromised ER diffusion barrier (Jesse Chao, unpublished results). In the *shs1-cte* mutant we found that Num1-GFP was no longer restricted to pmaER in the mother and was mislocalized to pmaER in small and medium buds (Fig. 4.5 C). Localization of Num1-GFP to patches that corresponded to microtubule cortical capture sites was unaffected in the *shs1-cte* mutant. Studies using photoactivatable Num1-GFP also show that it does not freely diffuse from the mother to the bud, further supporting our results (Vorvis et al., 2008). Appearance of Num1 in M phase buds is therefore a result of its synthesis during late G2/M phase (Farkasovsky and Kuntzel, 1995), not a result of diffusion from the mother to daughter.

Thus, the ER diffusion barrier potentially controls the timing of spindle translocation to the bud by preventing premature diffusion of Num1 into the bud. In Δ*scs2* cells, Num1-GFP was no longer associated with pmaER and would therefore not be restricted from the bud by the ER

diffusion barrier. Hence, premature delivery of Num1 to the bud explains the premature spindle translocation phenotype we observed in Δ*scs2* cells. Failed cortical capture of cytoplasmic microtubules by Num1 results in binucleate cells and could conceivably also explain the spindle-positioning defect observed in Δ*scs2* cells. However, Δ*scs2* cells did not show the binucleate phenotype and Δ*scs2*Δ*num1* cells were no worse than Δ*num1* single mutant cells indicating that Scs2 is not required for cortical capture of microtubules (Fig. 4.5 D). Thus, Scs2 and the ER diffusion barrier prevented the premature migration of Num1 into the bud, which prevented migration of the spindle through the neck until M phase.

4.5. DISCUSSION

By investigating the known global genetic interaction network in yeast (Costanzo et al., 2010), I found strong genetic evidence for Scs2 functioning in spindle positioning. I found that the localization of Num1 is coordinated with the cell cycle and accurate localization requires Scs2. However, *SCS2* was only responsible for Num1-GFP localization to pmaER, as Num1-GFP remained enriched in foci which are cortical microtubule capture sites in Δ*scs2* cells (Tang et al., 2012). Therefore, I found an additional role for the ER diffusion barrier in restricting Num1 to the mother, which is required to faithfully position the spindle in the mother until nuclear migration during M phase. Thus, the ER diffusion barrier controls the timing of appearance of ER proteins in the bud and establishes cell polarity.

The ER diffusion barrier is maintained throughout the cell cycle and is also present within the nuclear ER during mitosis when the nucleus is pulled through the bud neck (Luedeke et al., 2005; Shcheprova et al., 2008). The ER diffusion barrier must therefore remain intact within the nuclear ER during nuclear migration. However, the diameter of the nucleus is much larger than that of ER tubules suggesting that the septin network at the bud neck must be remodeled during nuclear migration for the diffusion barrier to be maintained. In support of septin remodeling, Shs1 phosphorylation is cell cycle dependent and decreases in M phase (Egelhofer et al., 2008). Since Shs1 phosphorylation controls septin network formation (Garcia et al., 2011), its dephosphorylation in preparation for mitosis might remodel septins thereby enabling the nuclear ER and spindle to be pulled through without disrupting the ER diffusion barrier.

The presence of an ER diffusion barrier implies that the ER membrane is polarized between bud and mother. Polarization of ER proteins has widespread implications for ER biogenesis and function. Many lipid-synthesizing enzymes are polytopic integral ER proteins, suggesting that the diffusion barrier might also regulate membrane biogenesis. The mRNAs for two ER-localized enzymes involved in sterol and sphingolipid synthesis, Erg2 and Lcb1, are targeted to the bud (Shepard et al., 2003), suggesting a role for the ER diffusion barrier in timing the appearance of these proteins in the bud ER. The ER diffusion barrier may be particularly relevant to sterol biosynthesis because transcription of *ERG2* mRNA peaks in M phase (Spellman et al., 1998). This suggests that during bud growth in S and G2, sterols are supplied by the mother until the M phase whereupon Erg2 and the sterol biosynthetic pathway are reconstituted in the daughter. Given that the molecular mechanisms involved in asymmetrical cell division and dynein/dynactin-dependent spindle positioning is evolutionarily conserved (Gomes et al., 2005), we expect our findings to be generally applicable to higher eukaryotes.

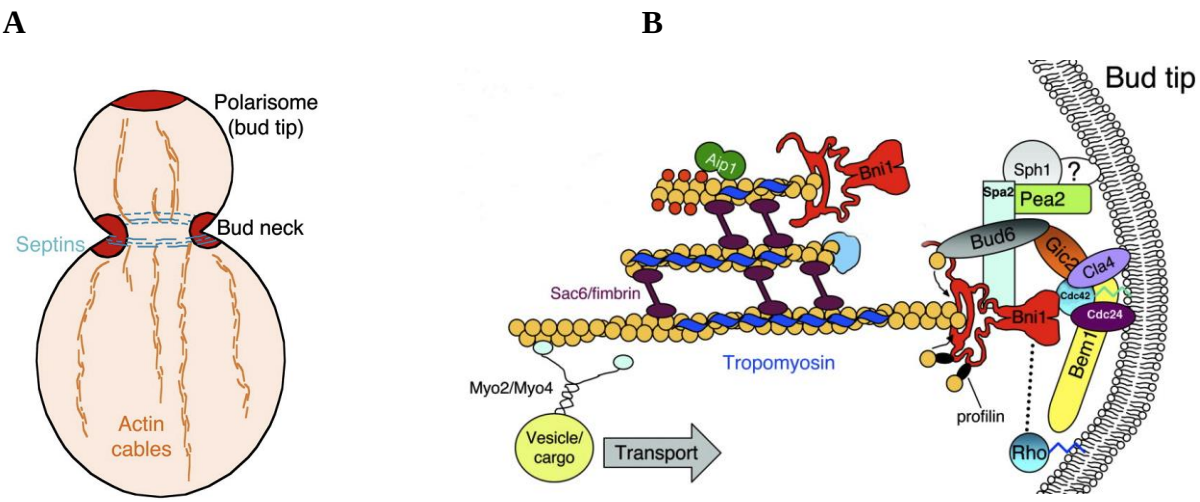

Figure 4.1: Polarisome and actin cable assembly at polarized growth.

(A) Organization of formins (red), actin cables (gold), and septin structures (blue) in a budded yeast cell. Formin proteins (Bni1, part of polarisome at the bud tip) directly nucleate actin cable formation. Septins serve as a diffusion barrier between bud and mother cell compartments and provide a scaffold for assembly of many bud neck components. **(**B) The actin cables are nucleated by Bni1 and Bud6. Bni1 activity may be regulated by interactions with Cdc42, Rho3, Rho4, Bud6, Spa2, and other factors (not pictured). Type V myosins (Myo2 and Myo4) transport vesicles, organelles, and other cargos along cables to the bud tip (Adapted from (Moseley and Goode, 2006)).

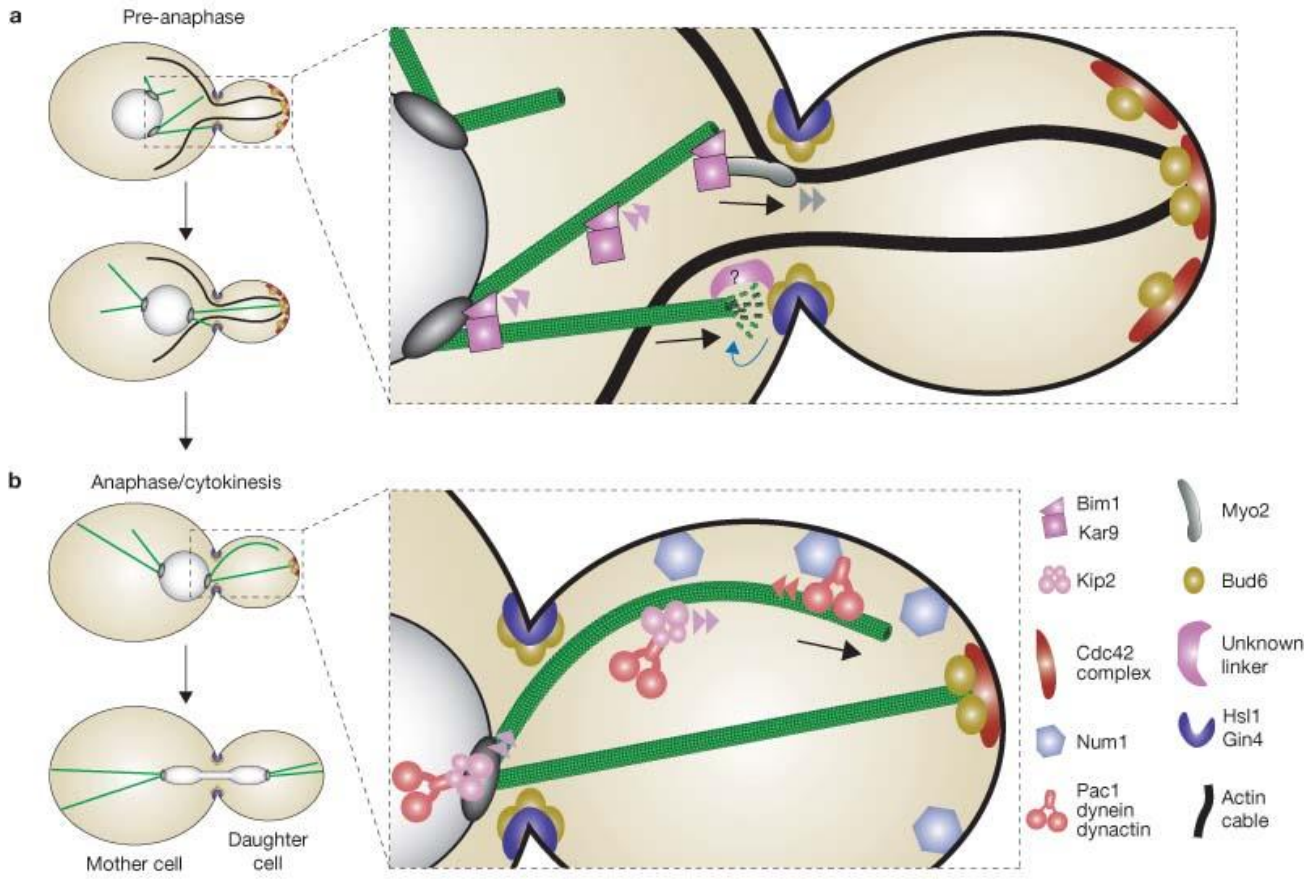

Figure 4.2: The nuclear migration pathway.

(A) The early pathway (pre-anaphase). Bim1–Kar9 are recruited to the spindle pole body (SPB), translocate to microtubule plus-ends (pink arrowheads) and associate with the myosin motor, Myo2. Myo2 motor activity (grey arrowheads) pulls attached microtubules into the bud resulting in positioning of the SPB at the bud neck. Bim1–Kar9 movement to microtubule plus-ends may require the Kip2 kinesin motor. The bud neck kinases Hsl1 and Gin4 promote microtubule shortening (blue arrow), which facilitates spindle alignment. **(**B**)** The late pathway (anaphase). The Kip2 kinesin transports the presumably inactive Pac1–dynein–dynactin complex from the SPB to microtubule plus-ends where it interacts with Num1. Cortical Num1–dynein–dynactin then pulls the daughter centrosome to the center of the bud cortex. Bold black arrows indicate the direction of the net spindle positioning force (Adapted from (Siller and Doe, 2009)).

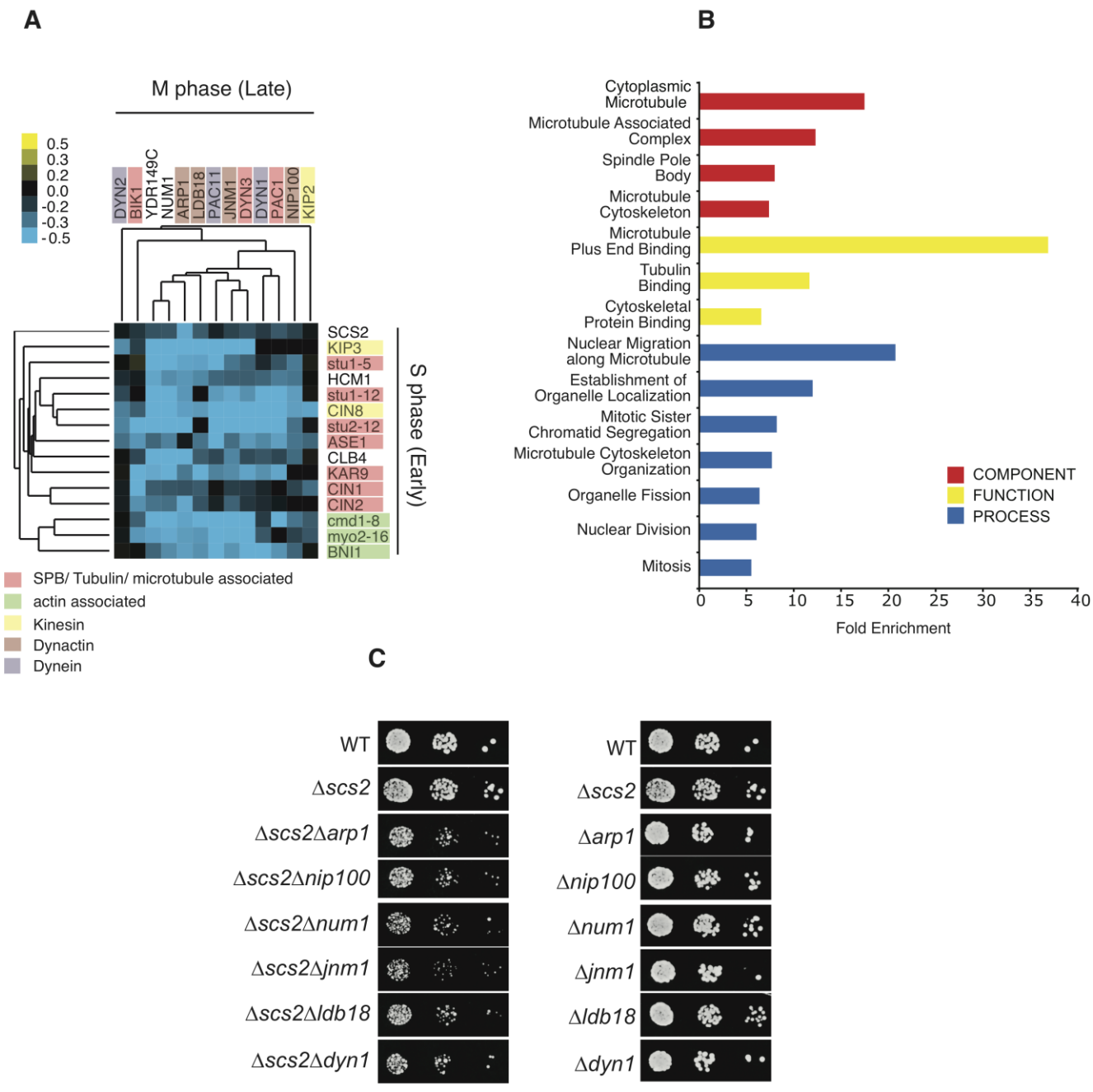
A
M phase (Late)
0.5
0.3
0.2
0.0
-0.2
-0.3
-0.5
DYN2
BIK1
YDR149C
NUM1
ARP1
LDB18
PAC11
JNM1
DYN3
DYN1
PAC1
NIP100
KIP2
SCS2
KIP3
stu1-5
HCM1
stu1-12
CIN8
stu2-12
ASE1
CLB4
KAR9
CIN1
CIN2
cmd1-8
myo2-16
BNI1
S phase (Early)
SPB/ Tubulin/ microtubule associated
actin associated
Kinesin
Dynactin
Dynein
B
Cytoplasmic Microtubule
Microtubule Associated Complex
Spindle Pole Body
Microtubule Cytoskeleton
Microtubule Plus End Binding
Tubulin Binding
Cytoskeletal Protein Binding
Nuclear Migration along Microtubule
Establishment of Organelle Localization
Mitotic Sister Chromatid Segregation
Microtubule Cytoskeleton Organization
Organelle Fission
Nuclear Division
Mitosis
COMPONENT
FUNCTION
PROCESS
0
5
10
15
20
25
30
35
40
Fold Enrichment
C
WT
Δscs2
Δscs2Δarp1
Δscs2Δnip100
Δscs2Δnum1
Δscs2Δjnm1
Δscs2Δldb18
Δscs2Δdyn1
WT
Δscs2
Δarp1
Δnip100
Δnum1
Δjnm1
Δldb18
Δdyn1

Figure 4.3: Scs2 is involved in regulation of spindle positioning.

(A) Cluster of genetic interactions between genes involved in S and M phase spindle positioning in the nuclear migration pathway (data reclustered from Costanzo et al., 2010). (B) Synthetic genetic array analysis for *SCS2*. Aggravating genetic interactions were categorized by gene ontology and fold enrichment is plotted. (C) Yeast growth assays of double mutants between *SCS2* and genes required for the late stage of nuclear migration and of single mutants.

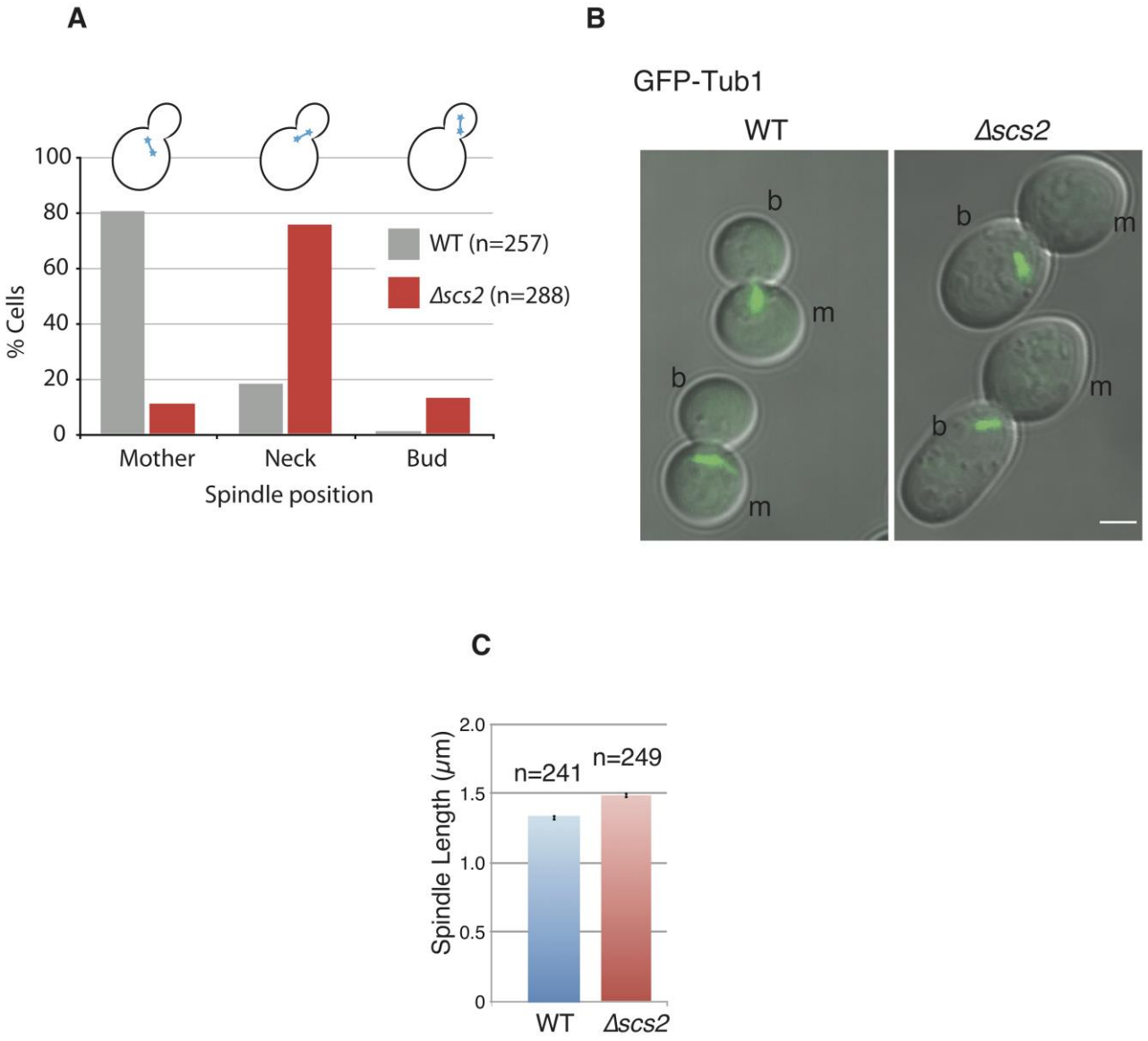

Figure 4.4: Spindle positioning defect in Δ*scs2* cells.

(A) Spindle positioning in wild type and Δ*scs2* cells synchronized in S phase with hydroxyurea by imaging GFP-Tub1. (B) WT and Δ*scs2* mutant yeast expressing endogenous Tub1 tagged with GFP synchronized in S phase with hydroxyurea. b, bud. m, mother. Scale bar, 2 μm. **(c)** Spindle length measured for cells treated in (A).

A Num1-GFP

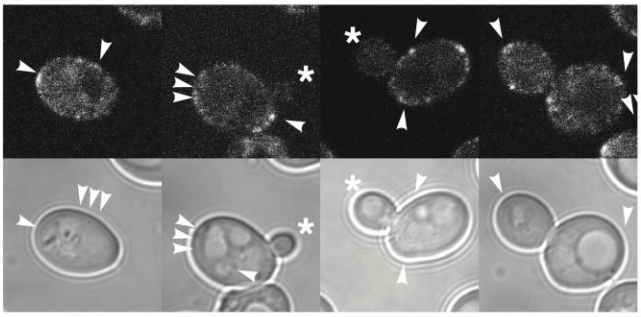

B Num1-GFP Δ *scs2*

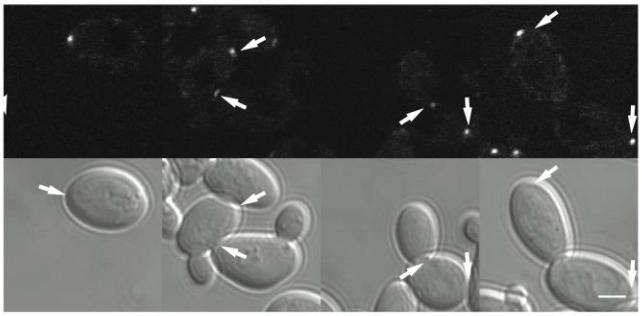

C Num1-GFP *shs1-cte*

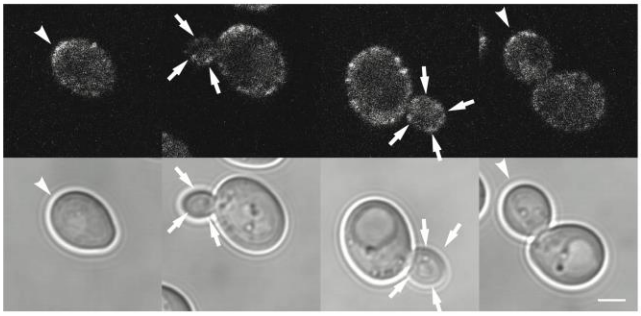

D

	Multinucleated budded cells (%)	n
WT	0	220
Δscs2	0	245
Δnum1	5.16	384
Δscs2Δnum1	5.3	189

E

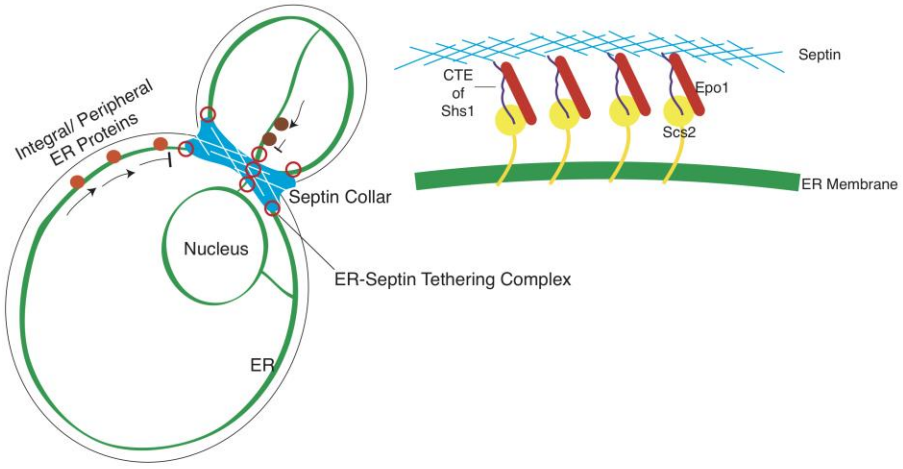

Figure 4.5: The ER Diffusion Barrier Controls Spindle Positioning.

(A-C**)** Yeast expressing endogenous Num1 tagged with GFP. Arrowheads, wild type localizations. Arrows, localizations different than wild type. Asterisks, absence of localization to the bud cortex. All scale bars, 2µm.). **(**D**)** DAPI stained wild type and mutant yeast were scored for multinucleated mother cells. **(**E**)** Model for ER polarization by the ER-septin tethering complex. Not to scale.

Table 4.1: Yeast strains used in this study.

Parental Strain	Genotype
BY4741	*MATa his3Δ1 leu2Δ0 met15Δ0 ura3Δ0*
BY7043	*MAT alpha can1Δ::STE2pr-lue2 lyp1Δ his3Δ1 leu2Δ0 ura3Δ0 met15Δ0*
BY7092	*MATα can1Δ::STE2pr-Sp_his5 lyp1Δ his3Δ1 leu2Δ0 ura3Δ0 met15Δ0*

5. DISCUSSION

Yeast Scs2 is a type II integral ER membrane protein and a member of the VAP (vesicle-associated membrane protein-associated protein) family. VAP members have multiple biological functions, including roles in membrane trafficking, lipid transport/metabolism, the unfolded protein response, and microtubule organization (see (Lev et al., 2008) for review). Major studies of Scs2 were primarily focused on how Scs2 regulates Opi1 in response to inositol and PA level, a critical event in phospholipid synthesis. Our lab has found previously that Scs2 is important for ER biogenesis and formation of membrane contact sites between the PM and ER (Loewen et al., 2007). Further, we found that *SCS2* has a negative genetic interaction with *ICE2*, another ER protein of unknown function and Δ*scs2*Δ*ice2* cells exhibited little amount of PM-ER contacts (Loewen et al., 2007). However, we know relatively little about Scs2 roles in PM-ER contact site formation and ER inheritance in yeast. Of all membrane contact sites, PM-ER contacts occupy the most significant amount of the yeast cell surface due to the unique structure of the pmaER in *S. cerevisiae.* Considering this and that Scs2 is highly conserved in eukaryotes, in this dissertation I focused on uncovering biological roles for Scs2 in budding yeast.

5.1. CHAPTER 2- PLASMA MEMBRANE – ENDOPLASMIC RETICULUM CONTACT SITES REGULATE PHOSPHATIDYLCHOLINE SYNTHESIS

5.1.1. General remarks

In *Chapter 2*, I present the crux of my PhD work - studying the Δ*scs2*Δ*ice2* yeast mutant as an invaluable tool for investigating PM-ER contacts. I found that Δ*scs2*Δ*ice2* cells exhibited a choline auxotrophy phenotype and a dramatic reduction in conversion of PE to PC, suggesting that the methylation pathway is defective in these double mutants. I found that the phospholipid-N-methyltransferase (PEMT) Opi3 was absent from pmaER in Δ*scs2*Δ*ice2* double mutant, consistent with a role for pmaER in PC synthesis. Previously, it was shown that Scs2 localizes Osh1, Osh2 and Osh3, three lipid binding proteins, to PM-ER contacts (Loewen et al., 2003). Therefore, I tested for the ability of these three proteins to rescue the choline auxotrophy of

Δ*scs2*Δ*ice2* cells. I found that the overexpression of Osh2 and Osh3 were capable of rescuing the choline auxotrophy of Δ*scs2*Δ*ice2* cells, but not Osh1. Thus, this data suggested that PM-ER contact sites provided a structural mechanism to regulate PC synthesis through controlling the localization and activity of Opi3 in pmaER and we provided evidence that Osh3 proteins localization to PM-ER contacts was needed for Opi3 function.

The active site of Opi3/PEMT is located on the cytoplasmic face of the ER membrane (Shields et al., 2003b; Shields et al., 2005), which is the binding site of S-Adenosylmethionine (SAM). SAM is the primary methyl group donor for most biological methylation reactions including the methyl groups required for PC synthesis via the methylation pathway. There are two required amino acid motifs GXG and EE that are located on the external portion of the third and fourth transmembrane helices of Opi3/PEMT, respectively. Based on the topology of Opi3 and our supporting genetic data, we proposed and tested the hypothesis that Opi3 methylates its substrates, PME and PDE in the PM *in trans.* The '*in trans'* hypothesis, which has been suggested by others, previously (de Kroon et al., 2003; Stefan et al., 2011) could explain our observations in Δ*scs2*Δ*ice2* cells. The fact that the PS synthase and PE methyltransferase of *E.coli* are both soluble enzymes (Ishinaga and Kito, 1974) supports the *in trans* model in which enzymes and their lipid substrates may be located in different membranes. Our studies provide a platform to investigate additional enzymes that may function *in trans,* similar to Sac1 (Stefan et al., 2011) and Opi3 (Janssen et al., 2002).

We discovered that the overexpression of Pah1, which belongs to the lipin family of PA phosphatases, restored the PE to PC conversion as well as PM-ER contacts in Δ*scs2*Δ*ice2* cells. Based on our genetic and ultrastructural findings, we concluded that Pah1 must have a novel role independent of its enzymatic, which is making DAG from PA. Consistent with our data, it has recently been shown that Pah1 can interact with membranes in the absence of its substrate, PA, and independent of its catalytic activity (Xu et al., 2012). These findings also suggest additional roles for Pah1 in regulating cellular membrane biogenesis. Taken together, the work presented in *Chapter 2* strengthens the hypothesis that Opi3 can act *in trans* at PM-ER contacts. The Opi3 substrate, PME, has been previously found only in endosomes (Schneiter et al., 1999), and it could be the product of the Golgi/endosome-localized PS decarboxylase Psd2, which provides further evidence that PC is synthesized in the PM by Opi3 at PM-ER contact sites

5.1.2. Significance

While the methylation pathway is the predominant method of synthesizing PC in yeast, it is primarily present in the liver in mammals, where it constitutes ~ 30 % of PC production. However, the evolutionary conservation of the methylation pathway suggests its essential role in specific functions in various cell types. For instance, PC synthesis by the methylation pathway was shown to affect membrane fluidity and function of calcium channels in the aorta, influx of Ca^{2+} and subsequent release of histamine in mast cells, polyunsaturated fatty acid metabolism in the brain, and Ca^{2+} influx in endothelial cells (see (Tehlivets et al., 2013)). We have made a significant contribution in understanding the physiological role of PM-ER contacts in phospholipid synthesis using budding yeast as a model. Our understanding of how Opi3 acts is important, as human PEMT function is associated with non-alcoholic steatohepatitis (NASH) in both humans and mice. NASH is a serious form of non-alcoholic fatty liver disease (NAFLD). *pemt* $^{-/-}$ mice have a 50% reduction in PC and a decreased PC/PE ratio in their PM, resulting in death after 3 days when subjected to a choline-deficient diet (Li et al., 2006). Recently, a new role for PEMT in insulin signaling and diabetes has been investigated. It has been demonstrated that the lack of PEMT inhibits diet-induced obesity and insulin resistance. Therefore, it is plausible to consider PEMT as a useful pharmacological target for the treatment of insulin resistance, although the side effects of down regulation of PEMT and consequently, hepatic steatosis, must also be weighed.

It has been shown that Pah1, the major PA hydrolase responsible for converting PA into DAG, is involved in vacuole homeostasis and fusion (Sasser et al., 2011), lipid droplet formation (Adeyo et al., 2011) as well as expansion of the nuclear envelope in budding yeast (Han et al., 2008). We found a novel role for Pah1 independent of its role in DAG formation. Our findings that Pah1is involved in the regulation of PM-ER contact sites is important, as yeast Pah1 shares homology with the human lipin1 protein. Lipin1 regulates fat metabolism in mammalians cells (for review see (Csaki and Reue, 2010)). Loss of lipin1 in mice results in abnormal adipose tissue development, lipodystrophy and insulin resistance while its overexpression results in obesity and insulin sensitivity (Bou Khalil et al., 2010; Reue and Brindley, 2008). Myoglobinuria, which is a rare condition resulting from the destruction of skeletal muscle fibers, is also associated with mutations in human *LPIN1* (Michot et al., 2010), which further highlights the importance of understanding the basic aspects of cell physiology that are controlled by lipins.

5.1.3. Future directions

We did not test if the presence of Osh3 affected the activity of Opi3 in the *in vitro* liposome assays. This can be addressed by repeating the *in trans* methylation assays for Opi3 in collaboration with Dr. Kroon's laboratory using microsomes from Δ*osh3* cells. Our results also predict that we will see an accumulation of PME in the PM of Δ*scs2*Δ*ice2* cells - a hypothesis that that can be tested by isolating the PM from Δ*scs2*Δ*ice2* cells and measuring the PME and PDE levels. Moreover, it will be important to define the underlying mechanism of the Osh2/Osh3 rescue of the choline auxotrophy of Δ*scs2*Δ*ice2* cells. Do Osh2 or Osh3 proteins lacking PH domains or FFAT motifs rescue the Δ*scs2*Δ*ice2* choline auxotrophy? What is the role of Pah1 in establishing pmaER? Clearly, the nature and function of contact sites between cellular membranes and role of pmaER in the control of ER stress needs further work.

Our studies provide a foundation for future efforts in dissecting the molecular mechanisms of lipid synthesis at membrane contact sites and a plausible role for "*in trans"* lipid synthesis for additional enzymes. In closing, it is important to point out that although we do not have answers for all the above questions, this work has provided insight into mechanisms of regulating PC synthesis at PM-ER contacts and it also encourages new questions such as: How does Cho2 methylate PE and where does it happen? Why does yeast have Cho2 while mammals only have Opi3? What is the function of Ice2 and why is it not conserved?

5.2. CHAPTER 3- A CONSERVED ER-MEMBRANE COMPLEX FACILITATES PHOSPHOLIPID EXCHANGE BETWEEN ER AND MITOCHONDRIA

5.2.1. General remarks

Although we know a great deal about PC and PE biosynthesis at the enzymatic level, there is still much to be learned about the inter-organelle traffic of phospholipids, particularly the movement of both PS and PE between the ER and mitochondria. In the yeast, newly synthesized PS is made in the ER, specifically at MAM or the mitochondria-ER contacts and is translocated to mitochondria for Psd1. Transport is independent of ATP and any cytosolic factors. Similarly,

in mammalian cells PS is generated by phosphatidylserine synthase (PSS) specifically at mitochondria-ER contacts and relocalizes to mitochondria in order to be decarboxylated to PE. However, in both cases it is not clear how the inner mitochondrial membrane acquires PS. In *chapter 3,* I aimed to uncover proteins responsible for moving PS from the ER to mitochondria by performing a genome-wide screen for *CHO2,* the fungal-specific PEMT, since it showed negative genetic interactions with *PSD1,* the conserved mitochondrial PS decarboxylase. The rationale for this screen was that genes demonstrating negative genetic interactions with *CHO2* might also be involved in PE/PS metabolism, similar to *PSD1*. Although we could not find any soluble lipid transfer protein involved in PS traffic, I identified genetic interactions between *CHO2* and the newly identified EMC (ER-membrane protein complex) genes (Jonikas et al., 2009). In collaboration with Dr. Prinz, we showed that EMC proteins are important for the transfer of PS between the ER and mitochondria, likely by regulating the membrane contact sites between these organelles. We showed that the deletion of multiple members of the EMC, for example the *5x-*Δ*emc* cells that lacks 5 of the 6 Emc members, dramatically reduced the transfer of PS to mitochondria both *in vivo* and *in vitro*. Rescuing the defective PS trafficking phenotype of the multiple members of the EMC by using an artificial tethering protein, ChiMERA (Kornmann et al., 2009), I found that *TOM5*, the outer mitochondrial membrane protein, showed a strong genetic interaction with *CHO2* while the Tom5 protein had a physical interaction with Emc1 and Emc2 by PCA. We showed that the EMC-Tom5 interaction likely forms a tether between the ER and mitochondria at the same contact sites defined by the ERMES (ER mitochondria encounter structure) complex (Kornmann et al., 2009) that mediates contact sites between ER and mitochondria. Further, we found that the EMC genes had negative or aggravating genetic interactions with ERMES complex genes. PS transfer from ER to mitochondria was almost abolished by mutating both EMC and the ERMES complex (*5x-*Δ*emc mmm1-1),* which was more dramatic than mutating the EMC alone. These observations suggest that EMC and ERMES, together, are likely responsible for tethering of the ER to mitochondria, a process which is essential for PS traffic and cell growth.

5.2.2. Significance

Previous studies in budding yeast suggested that loss of the EMC genes causes the

accumulation of misfolded proteins, although the precise biochemical roles of EMC genes remained unclear (Jonikas et al., 2009). Our genetic and lipid analysis data suggested that EMC genes, like the ERMES complex, are involved in tethering the ER to the mitochondria in order to regulate PS trafficking from the ER to the mitochondria, a process which can affect the overall mitochondrial dynamics and function. Recently, it has shown that PERK, the canonical ER stress sensor, establishes a physical and functional connection between the ER and mitochondria and this tethering is important for regulating inter-organellar cross-talk in reactive oxygen species (ROS)-induced cell death, a role which is not shared with other ER stress sensors, including *IRE1* (Verfaillie et al., 2012). Interestingly, TMEM85, the human homologue of Emc4, has been shown to prevent cell death in response to oxidative stress by suppressing the pro-apoptotic protein Bax (Ring et al., 2008). These findings may link EMC proteins and mitochondria-ER contact sites to stress responses and apoptosis. Another recently published study showed that EMC genes affect early secretory pathway processes rather than the UPR (Bircham et al., 2011). Intriguingly, TMEMIII, the human homologue of *EMC3*, was implicated as a disease related gene by genome-wide association studies (Nayak et al., 2009). Human TMEMIII has also been shown to be involved in ER- mediated secretory pathways, indicating that EMC genes are likely involved in regulating some aspects of ER export/retrieval processes similar to enrichment of genetic interactions of *EMC6* which was enriched important for secratery pathway.

However, the EMC might have a role in ER stress and quality control in the ER, both of which are important for secretion (Bircham et al., 2011; Christianson et al., 2012; Jonikas et al., 2009). Some studies support a role for the UPR in regulating physiological processes that are not directly related to protein misfolding including lipid metabolism (Basseri and Austin, 2012). Therefore, a possibility for crosstalk between the UPR/ERAD signaling pathways and PS/PE homeostasis in the cells may exist. The highly conserved nature of the methylation pathway and also of the EMC genes from yeast to humans, suggest that they should perform essential roles in cell physiology, and our studies on EMC proteins in yeast provide new insights into their functions.

5.2.3. Future directions

To rule out if there are indeed less mitochondria-ER contacts in cells deleted for multiple members of the EMC and ERMES (the *5x-emc mmm1-1* mutant*)*, ultrastructural analysis with TEM is required. Additionally, if ChiMERA rescues the defect in mitochondria- ER contacts, TEM analysis is capable of revealing it. It would be valuable to further define the interaction between Tom5 and Emc1/2 by systematically mutating various regions of both Ecm1 and Emc2 to identify the domains that are critical for their binding to Tom5. Emc proteins may regulate the folding and quality control of the ERMES subunit Mmm1 in the ER. Therefore, it would be helpful to examine whether the localization and stability of the ERMES subunit Mmm1 is affected by deletion of Emc proteins.

Moreover, it is unclear which Emc subunits are critical for ER-mitochondrial tethering and therefore the reduction in PE/PS ratios in *4x*-Δ*emc* and *5x*-Δ*emc* cells. It will be necessary to investigate the functional redundancy and specific functions of each Emc protein. To determine the degree of Emc protein conservation, we could directly test whether expression of mammalian Emc proteins can rescue the loss of yeast Emc subunits. The proposed experiments will enable us to learn more about the molecular mechanisms of the Emc acting at ER-mitochondria contact sites.

5.3. CHAPTER 4 -ER DIFFUSION BARRIER REGULATES SPINDLE POSITIONING AND NUCLEAR MIGRATION PATHWAY IN BUDDIING YEAST

5.3.1. General remarks

In *Chapter 4*, I found that *SCS2* interacts genetically with genes important in the late stage of nuclear migration pathway, including dynein (*DYN1)*, and dynactin (*NIP100, ARP1, LDB18, JNM1)*, its cortical capture protein Num1, and the kinesin motor and accessory proteins that are required to load dynein onto the plus ends of microtubules. These genetic interactions of *SCS2* with the late stage components lead to discovery of a spindle-positioning defect in Δ*scs2* cells. Additionally, the localization of Num1 was altered in Δ*scs2* cells. We found that "ER-

septin" tethering creates an isolated ER domain in the bud by preventing diffusion of peripheral and integral ER proteins from the mother (Jesse Chao, unpublished data), thus polarizing the bud's ER. I showed that polarization of the bud's ER is required for proper spindle positioning. This mechanism relies upon the ER-septin tether that restricts the spindle capture protein Num1 to the mother ER during the S and G2 phases of the cell cycle until it is synthesized in the bud in M phase. Spindle positioning by the ER diffusion barrier provides an unprecedented role for the ER in cell polarization. Our work represents the first description of a molecular mechanism for ER polarization in any organism, which we anticipate will have an immediate impact on the fields of cell polarity and organelle biogenesis.

5.3.2. Significance

Because the ER-septin tether is highly conserved, our insights from yeast will be relevant to higher organisms. We propose that ER-septin tethering is the primary mechanism to create ER diffusion barriers in diverse cell types. For example, in the dendritic spines of neurons, where there is restricted diffusion of ER proteins (Cui-Wang et al., 2012), septins are located in a ring at the spine base (Tada et al., 2007; Xie et al., 2007). This suggests that ER-septin tethering at the base of dendritic spines creates an ER diffusion barrier that polarizes the spine ER. Polarization of ER in spines has already been shown to be important, as the localization of the inositol trisphosphate (IP3) receptor in spines is critical for nerve transduction (Wagner et al., 2011). Septins are found at the base of many other polarized structures that contain ER, including filopodia, pseudopodia, cilia, and the cytokinetic cleavage furrow (Saarikangas and Barral, 2011). This indicates that ER-septin tethering and ER polarization may have widespread functions in biology.

It is tempting to speculate a more general role for septins in forming domain boundaries for distinct proteins and even lipids. Indeed, one remarkable example of membrane lipid asymmetry in fungus is at the tips of pheromone-induced mating projections in *Saccharomyces cerevisiae* (Proszynski et al., 2006). The polarization of sterol-rich membrane domains at these sites, are required for generating the mating projection. Additionally, Erg2 mRNA peaks in M phase (Spellman et al., 1998) suggesting that during bud growth in S and G2, sterols are supplied by mother, until M phase whereupon Erg2 and the sterol biosynthetic pathway are reconstituted

in the bud. Interestingly, it has been shown that sterol-rich domains in fission yeast *Schizosaccharomyces pombe* are localized to distinct regions of the PM in a cell-cycle-dependent manner (Wachtler et al., 2003) and appear to play multiple roles in cytokinesis (Martin and Konopka, 2004).

The mechanism of nuclear migration in neurons is very similar to the yeast nuclear migration pathway and is associated with lissencephaly, a disease in which neuronal migration to the cerebral cortex is defective (Lee et al., 2003; Xiang, 2003). Moreover, impaired dynein/dynactin function (Kieran et al., 2005; Levy and Holzbaur, 2006; Teuling et al., 2008) and mutations in human VAP (Lev et al., 2008; Nakamichi et al., 2011) are both associated with amyotrophic lateral sclerosis (ALS), a type of motor neuron disease. Consistent with this, loss of IP3 receptor polarization from dendritic spines in mice causes severe ataxia that mimics ALS (Wagner et al., 2011). These facts highlight the importance of understanding the molecular mechanisms of how Scs2/VAP functions with respect to polarized growth and cell division.

5.3.3. Future direction

Published data suggest a role for septins in forming a boundary for lipid domains during hyphal growth in *C. albicans.* Septins co-localize with ergosterol-rich membranes during hyphal growth in *C. albicans* and ergosterol-rich membranes are required for the full virulence of *C. albicans* (Martin and Konopka, 2004). Given the role for Scs2 in PM-ER contacts, its polarized localization to the ER (Loewen et al., 2007) and its role in phospholipid metabolism, there is a potential area of research to identify how Scs2/VAP may link polarized growth to lipid metabolism. By localizing lipids (e.g. filipin staining for ergosterol-rich membranes) in Δ*scs2* cells or Δ*num1* cell during the cell cycle, we may identify if the spindle defects correlate with abnormal lipid localization during the cell cycle. It would be helpful to investigate if human VAP is capable of binding to the Shs1 septin and Epo1 (Jesse Chao, unpublished work) and if overexpressing human VAP can rescue the spindle positioning defect we observed in Δ*scs2* cells. These experiments will shed some light into the molecular mechanisms of Scs2's contribution to generating the ER diffusion barrier in eukaryotes.

REFERENCES

Achleitner, G., Gaigg, B., Krasser, A., Kainersdorfer, E., Kohlwein, S.D., Perktold, A., Zellnig, G., and Daum, G. (1999). Association between the endoplasmic reticulum and mitochondria of yeast facilitates interorganelle transport of phospholipids through membrane contact. Eur J Biochem *264*, 545-553.

Adeyo, O., Horn, P.J., Lee, S., Binns, D.D., Chandrahas, A., Chapman, K.D., and Goodman, J.M. (2011). The yeast lipin orthologue Pah1p is important for biogenesis of lipid droplets. J Cell Biol *192*, 1043-1055.

Aktas, M., and Narberhaus, F. (2009). In vitro characterization of the enzyme properties of the phospholipid N-methyltransferase PmtA from Agrobacterium tumefaciens. J Bacteriol *191*, 2033-2041.

Alconada, A., Kubrich, M., Moczko, M., Honlinger, A., and Pfanner, N. (1995). The mitochondrial receptor complex: the small subunit Mom8b/Isp6 supports association of receptors with the general insertion pore and transfer of preproteins. Mol Cell Biol *15*, 6196-6205.

Ardail, D., Lerme, F., and Louisot, P. (1991). Involvement of contact sites in phosphatidylserine import into liver mitochondria. J Biol Chem *266*, 7978-7981.

Ardail, D., Popa, I., Bodennec, J., Louisot, P., Schmitt, D., and Portoukalian, J. (2003). The mitochondria-associated endoplasmic-reticulum subcompartment (MAM fraction) of rat liver contains highly active sphingolipid-specific glycosyltransferases. Biochem J *371*, 1013-1019.

Area-Gomez, E., Del Carmen Lara Castillo, M., Tambini, M.D., Guardia-Laguarta, C., de Groof, A.J., Madra, M., Ikenouchi, J., Umeda, M., Bird, T.D., Sturley, S.L., *et al.* (2012). Upregulated function of mitochondria-associated ER membranes in Alzheimer disease. EMBO J *31*, 4106-4123.

Arondel, V., Benning, C., and Somerville, C.R. (1993). Isolation and functional expression in Escherichia coli of a gene encoding phosphatidylethanolamine methyltransferase (EC 2.1.1.17) from Rhodobacter sphaeroides. J Biol Chem *268*, 16002-16008.

Aronov, S., Gelin-Licht, R., Zipor, G., Haim, L., Safran, E., and Gerst, J.E. (2007). mRNAs encoding polarity and exocytosis factors are cotransported with the cortical endoplasmic reticulum to the incipient bud in Saccharomyces cerevisiae. Mol Cell Biol *27*, 3441-3455.

Athenstaedt, K., and Daum, G. (1999). Phosphatidic acid, a key intermediate in lipid metabolism. Eur J Biochem *266*, 1-16.

Baird, D., Stefan, C., Audhya, A., Weys, S., and Emr, S.D. (2008). Assembly of the PtdIns 4-kinase Stt4 complex at the plasma membrane requires Ypp1 and Efr3. J Cell Biol *183*, 1061-1074.

Bankaitis, V.A., Aitken, J.R., Cleves, A.E., and Dowhan, W. (1990). An essential role for a phospholipid transfer protein in yeast Golgi function. Nature *347*, 561-562.

Bankaitis, V.A., Garcia-Mata, R., and Mousley, C.J. (2012). Golgi membrane dynamics and lipid metabolism. Curr Biol *22*, R414-424.

Bankaitis, V.A., Malehorn, D.E., Emr, S.D., and Greene, R. (1989). The Saccharomyces cerevisiae SEC14 gene encodes a cytosolic factor that is required for transport of secretory proteins from the yeast Golgi complex. J Cell Biol *108*, 1271-1281.

Bankaitis, V.A., Mousley, C.J., and Schaaf, G. (2010). The Sec14 superfamily and mechanisms for crosstalk between lipid metabolism and lipid signaling. Trends Biochem Sci *35*, 150-160.

Bar, L.K., Barenholz, Y., and Thompson, T.E. (1986). Fraction of cholesterol undergoing spontaneous exchange between small unilamellar phosphatidylcholine vesicles. Biochemistry *25*, 6701-6705.

Baron, C.L., and Malhotra, V. (2002). Role of diacylglycerol in PKD recruitment to the TGN and protein transport to the plasma membrane. Science *295*, 325-328.

Barral, Y., Mermall, V., Mooseker, M.S., and Snyder, M. (2000). Compartmentalization of the cell cortex by septins is required for maintenance of cell polarity in yeast. Mol Cell *5*, 841-851.

Basseri, S., and Austin, R.C. (2012). Endoplasmic reticulum stress and lipid metabolism: mechanisms and therapeutic potential. Biochem Res Int *2012*, 841362.

Bassot, J.M., and Nicolas, G. (1987). An optional dyadic junctional complex revealed by fast-freeze fixation in the bioluminescent system of the scale worm. J Cell Biol *105*, 2245-2256.

Baumann, N.A., Sullivan, D.P., Ohvo-Rekila, H., Simonot, C., Pottekat, A., Klaassen, Z., Beh, C.T., and Menon, A.K. (2005). Transport of newly synthesized sterol to the sterol-enriched plasma membrane occurs via nonvesicular equilibration. Biochemistry *44*, 5816-5826.

Baumann, O., and Walz, B. (2001). Endoplasmic reticulum of animal cells and its organization into structural and functional domains. Int Rev Cytol *205*, 149-214.

Beh, C.T., Cool, L., Phillips, J., and Rine, J. (2001). Overlapping functions of the yeast oxysterol-binding protein homologues. Genetics *157*, 1117-1140.

Beh, C.T., McMaster, C.R., Kozminski, K.G., and Menon, A.K. (2012). A Detour for Yeast Oxysterol-Binding Proteins. J Biol Chem.

Benning, C., Xu, C., and Awai, K. (2006). Non-vesicular and vesicular lipid trafficking involving plastids. Curr Opin Plant Biol *9*, 241-247.

Berger, K.H., Sogo, L.F., and Yaffe, M.P. (1997). Mdm12p, a component required for mitochondrial inheritance that is conserved between budding and fission yeast. J Cell Biol *136*, 545-553.

Bernales, S., Papa, F.R., and Walter, P. (2006). Intracellular signaling by the unfolded protein response. Annu Rev Cell Dev Biol *22*, 487-508.

Bernales, S., Soto, M.M., and McCullagh, E. (2012). Unfolded protein stress in the endoplasmic reticulum and mitochondria: a role in neurodegeneration. Front Aging Neurosci *4*, 5.

Bilgin, M., Markgraf, D.F., Duchoslav, E., Knudsen, J., Jensen, O.N., de Kroon, A.I., and Ejsing, C.S. (2011). Quantitative profiling of PE, MMPE, DMPE, and PC lipid species by multiple precursor ion scanning: a tool for monitoring PE metabolism. Biochim Biophys Acta *1811*, 1081-1089.

Bionda, C., Portoukalian, J., Schmitt, D., Rodriguez-Lafrasse, C., and Ardail, D. (2004). Subcellular compartmentalization of ceramide metabolism: MAM (mitochondria-associated membrane) and/or mitochondria? Biochem J *382*, 527-533.

Bircham, P.W., Maass, D.R., Roberts, C.A., Kiew, P.Y., Low, Y.S., Yegambaram, M., Matthews, J., Jack, C.A., and Atkinson, P.H. (2011). Secretory pathway genes assessed by high-throughput microscopy and synthetic genetic array analysis. Mol Biosyst *7*, 2589-2598.

Bligh, E.G., and Dyer, W.J. (1959). A rapid method of total lipid extraction and purification. Can J Biochem Physiol *37*, 911-917.

Bloom, K. (2001). Nuclear migration: cortical anchors for cytoplasmic dynein. Curr Biol *11*, R326-329.

Blusztajn, J.K., Liscovitch, M., and Richardson, U.I. (1987). Synthesis of acetylcholine from choline derived from phosphatidylcholine in a human neuronal cell line. Proc Natl Acad Sci U S A *84*, 5474-5477.

Bonifacino, J.S., and Glick, B.S. (2004). The mechanisms of vesicle budding and fusion. Cell *116*, 153-166.

Bou Khalil, M., Blais, A., Figeys, D., and Yao, Z. (2010). Lipin - The bridge between hepatic glycerolipid biosynthesis and lipoprotein metabolism. Biochim Biophys Acta *1801*, 1249-1259.

Brodsky, J.L. (2007). The protective and destructive roles played by molecular chaperones during ERAD (endoplasmic-reticulum-associated degradation). Biochem J *404*, 353-363.

Brown, M.S., and Goldstein, J.L. (1999). A proteolytic pathway that controls the cholesterol content of membranes, cells, and blood. Proc Natl Acad Sci U S A *96*, 11041-11048.

Burgermeister, M., Birner-Grunberger, R., Nebauer, R., and Daum, G. (2004). Contribution of different pathways to the supply of phosphatidylethanolamine and phosphatidylcholine to mitochondrial membranes of the yeast Saccharomyces cerevisiae. Biochim Biophys Acta *1686*, 161-168.

Carman, G.M., and Han, G.S. (2007). Regulation of phospholipid synthesis in Saccharomyces cerevisiae by zinc depletion. Biochim Biophys Acta *1771*, 322-330.

Carman, G.M., and Han, G.S. (2009). Regulation of phospholipid synthesis in yeast. J Lipid Res *50 Suppl*, S69-73.

Carman, G.M., and Han, G.S. (2011). Regulation of Phospholipid Synthesis in the Yeast Saccharomyces cerevisiae. Annu Rev Biochem *80*, 859-883.

Carman, G.M., and Henry, S.A. (1999). Phospholipid biosynthesis in the yeast Saccharomyces cerevisiae and interrelationship with other metabolic processes. Prog Lipid Res *38*, 361-399.

Carrasco, S., and Meyer, T. (2010). STIM Proteins and the Endoplasmic Reticulum-Plasma Membrane Junctions. Annu Rev Biochem.

Choi, H.S., Sreenivas, A., Han, G.S., and Carman, G.M. (2004). Regulation of phospholipid synthesis in the yeast cki1Delta eki1Delta mutant defective in the Kennedy pathway. The Cho1-encoded phosphatidylserine synthase is regulated by mRNA stability. J Biol Chem *279*, 12081-12087.

Choi, J.Y., Wu, W.I., and Voelker, D.R. (2005). Phosphatidylserine decarboxylases as genetic and biochemical tools for studying phospholipid traffic. Anal Biochem *347*, 165-175.

Christianson, J.C., Olzmann, J.A., Shaler, T.A., Sowa, M.E., Bennett, E.J., Richter, C.M., Tyler, R.E., Greenblatt, E.J., Harper, J.W., and Kopito, R.R. (2012). Defining human ERAD networks through an integrative mapping strategy. Nat Cell Biol *14*, 93-105.

Claessen, J.H., Kundrat, L., and Ploegh, H.L. (2012). Protein quality control in the ER: balancing the ubiquitin checkbook. Trends Cell Biol *22*, 22-32.

Clancey, C.J., Chang, S.C., and Dowhan, W. (1993). Cloning of a gene (PSD1) encoding phosphatidylserine decarboxylase from Saccharomyces cerevisiae by complementation of an Escherichia coli mutant. J Biol Chem *268*, 24580-24590.

Cleves, A.E., McGee, T.P., Whitters, E.A., Champion, K.M., Aitken, J.R., Dowhan, W., Goebl, M., and Bankaitis, V.A. (1991). Mutations in the CDP-choline pathway for phospholipid biosynthesis bypass the requirement for an essential phospholipid transfer protein. Cell *64*, 789-800.

Cline, M.S., Smoot, M., Cerami, E., Kuchinsky, A., Landys, N., Workman, C., Christmas, R., Avila-Campilo, I., Creech, M., Gross, B., *et al.* (2007). Integration of biological networks and gene expression data using Cytoscape. Nat Protoc *2*, 2366-2382.

Cockcroft, S. (2001). Phosphatidylinositol transfer proteins couple lipid transport to phosphoinositide synthesis. Semin Cell Dev Biol *12*, 183-191.

Contreras, F.X., Sanchez-Magraner, L., Alonso, A., and Goni, F.M. (2010). Transbilayer (flip-flop) lipid motion and lipid scrambling in membranes. FEBS Lett *584*, 1779-1786.

Cosma, M.P. (2004). Daughter-specific repression of Saccharomyces cerevisiae HO: Ash1 is the commander. EMBO Rep *5*, 953-957.

Costanzo, M., Baryshnikova, A., Bellay, J., Kim, Y., Spear, E.D., Sevier, C.S., Ding, H., Koh, J.L., Toufighi, K., Mostafavi, S., *et al.* (2010). The genetic landscape of a cell. Science *327*, 425-431.

Cox, J.S., Chapman, R.E., and Walter, P. (1997). The unfolded protein response coordinates the production of endoplasmic reticulum protein and endoplasmic reticulum membrane. Mol Biol Cell *8*, 1805-1814.

Csaki, L.S., and Reue, K. (2010). Lipins: multifunctional lipid metabolism proteins. Annu Rev Nutr *30*, 257-272.

Cui-Wang, T., Hanus, C., Cui, T., Helton, T., Bourne, J., Watson, D., Harris, K.M., and Ehlers, M.D. (2012). Local zones of endoplasmic reticulum complexity confine cargo in neuronal dendrites. Cell *148*, 309-321.

Cullis, P.R., Hope, M.J., and Tilcock, C.P. (1986). Lipid polymorphism and the roles of lipids in membranes. Chem Phys Lipids *40*, 127-144.

D'Angelo, G., Rega, L.R., and De Matteis, M.A. (2012). Connecting vesicular transport with lipid synthesis: FAPP2. Biochim Biophys Acta.

D'Angelo, G., Vicinanza, M., and De Matteis, M.A. (2008). Lipid-transfer proteins in biosynthetic pathways. Curr Opin Cell Biol *20*, 360-370.

Daleke, D.L. (2003). Regulation of transbilayer plasma membrane phospholipid asymmetry. J Lipid Res *44*, 233-242.

Dawidowicz, E.A. (1987). Dynamics of membrane lipid metabolism and turnover. Annu Rev Biochem *56*, 43-61.

de Brito, O.M., and Scorrano, L. (2008). Mitofusin 2 tethers endoplasmic reticulum to mitochondria. Nature *456*, 605-610.

De Craene, J.O., Coleman, J., Estrada de Martin, P., Pypaert, M., Anderson, S., Yates, J.R., 3rd, Ferro-Novick, S., and Novick, P. (2006). Rtn1p is involved in structuring the cortical endoplasmic reticulum. Mol Biol Cell *17*, 3009-3020.

de Kroon, A.I., Koorengevel, M.C., Vromans, T.A., and de Kruijff, B. (2003). Continuous equilibration of phosphatidylcholine and its precursors between endoplasmic reticulum and mitochondria in yeast. Mol Biol Cell *14*, 2142-2150.

Decottignies, A., Grant, A.M., Nichols, J.W., de Wet, H., McIntosh, D.B., and Goffeau, A. (1998). ATPase and multidrug transport activities of the overexpressed yeast ABC protein Yor1p. J Biol Chem *273*, 12612-12622.

DeGrella, R.F., and Simoni, R.D. (1982). Intracellular transport of cholesterol to the plasma membrane. J Biol Chem *257*, 14256-14262.

DeLong, C.J., Shen, Y.J., Thomas, M.J., and Cui, Z. (1999). Molecular distinction of phosphatidylcholine synthesis between the CDP-choline pathway and phosphatidylethanolamine methylation pathway. J Biol Chem *274*, 29683-29688.

Dickson, R.C. (2008). Thematic review series: sphingolipids. New insights into sphingolipid metabolism and function in budding yeast. J Lipid Res *49*, 909-921.

Dimmer, K.S., Fritz, S., Fuchs, F., Messerschmitt, M., Weinbach, N., Neupert, W., and Westermann, B. (2002). Genetic basis of mitochondrial function and morphology in Saccharomyces cerevisiae. Mol Biol Cell *13*, 847-853.

Dreier, L., and Rapoport, T.A. (2000). In vitro formation of the endoplasmic reticulum occurs independently of microtubules by a controlled fusion reaction. J Cell Biol *148*, 883-898.

Du, Y., Ferro-Novick, S., and Novick, P. (2004). Dynamics and inheritance of the endoplasmic reticulum. J Cell Sci *117*, 2871-2878.

Du, Y., Pypaert, M., Novick, P., and Ferro-Novick, S. (2001). Aux1p/Swa2p is required for cortical endoplasmic reticulum inheritance in Saccharomyces cerevisiae. Mol Biol Cell *12*, 2614-2628.

Dudek, J., Rehling, P., and van der Laan, M. (2013). Mitochondrial protein import: Common principles and physiological networks. Biochim Biophys Acta *1833*, 274-285.

Egelhofer, T.A., Villen, J., McCusker, D., Gygi, S.P., and Kellogg, D.R. (2008). The septins function in G1 pathways that influence the pattern of cell growth in budding yeast. PLoS One *3*, e2022.

Elbaz, Y., and Schuldiner, M. (2011). Staying in touch: the molecular era of organelle contact sites. Trends Biochem Sci *36*, 616-623.

Ellgaard, L., and Helenius, A. (2003). Quality control in the endoplasmic reticulum. Nat Rev Mol Cell Biol *4*, 181-191.

Estrada de Martin, P., Du, Y., Novick, P., and Ferro-Novick, S. (2005). Ice2p is important for the distribution and structure of the cortical ER network in Saccharomyces cerevisiae. J Cell Sci *118*, 65-77.

Estrada, P., Kim, J., Coleman, J., Walker, L., Dunn, B., Takizawa, P., Novick, P., and Ferro-Novick, S. (2003). Myo4p and She3p are required for cortical ER inheritance in Saccharomyces cerevisiae. J Cell Biol *163*, 1255-1266.

Fahy, E., Subramaniam, S., Brown, H.A., Glass, C.K., Merrill, A.H., Jr., Murphy, R.C., Raetz, C.R., Russell, D.W., Seyama, Y., Shaw, W., *et al.* (2005). A comprehensive classification system for lipids. J Lipid Res *46*, 839-861.

Fairn, G.D., Curwin, A.J., Stefan, C.J., and McMaster, C.R. (2007). The oxysterol binding protein Kes1p regulates Golgi apparatus phosphatidylinositol-4-phosphate function. Proc Natl Acad Sci U S A *104*, 15352-15357.

Fang, M., Kearns, B.G., Gedvilaite, A., Kagiwada, S., Kearns, M., Fung, M.K., and Bankaitis, V.A. (1996). Kes1p shares homology with human oxysterol binding protein and participates in a novel regulatory pathway for yeast Golgi-derived transport vesicle biogenesis. EMBO J *15*, 6447-6459.

Farkasovsky, M., and Kuntzel, H. (1995). Yeast Num1p associates with the mother cell cortex during S/G2 phase and affects microtubular functions. J Cell Biol *131*, 1003-1014.

Farkasovsky, M., and Kuntzel, H. (2001). Cortical Num1p interacts with the dynein intermediate chain Pac11p and cytoplasmic microtubules in budding yeast. J Cell Biol *152*, 251-262.

Faty, M., Fink, M., and Barral, Y. (2002). Septins: a ring to part mother and daughter. Curr Genet *41*, 123-131.

Fehrenbacher, K.L., Davis, D., Wu, M., Boldogh, I., and Pon, L.A. (2002). Endoplasmic reticulum dynamics, inheritance, and cytoskeletal interactions in budding yeast. Mol Biol Cell *13*, 854-865.

Feng, D., Zhao, X., Soromani, C., Toikkanen, J., Romisch, K., Vembar, S.S., Brodsky, J.L., Keranen, S., and Jantti, J. (2007). The transmembrane domain is sufficient for Sbh1p function, its association with the Sec61 complex, and interaction with Rtn1p. J Biol Chem *282*, 30618-30628.

Feske, S. (2010). CRAC channelopathies. Pflugers Arch *460*, 417-435.

Franke, W.W., and Kartenbeck, J. (1971). Outer mitochondrial membrane continuous with endoplasmic reticulum. Protoplasma *73*, 35-41.

Frolov, A., Woodford, J.K., Murphy, E.J., Billheimer, J.T., and Schroeder, F. (1996). Spontaneous and protein-mediated sterol transfer between intracellular membranes. J Biol Chem *271*, 16075-16083.

Fruman, D.A., Meyers, R.E., and Cantley, L.C. (1998). Phosphoinositide kinases. Annu Rev Biochem *67*, 481-507.

Fukasawa, M., Nishijima, M., and Hanada, K. (1999). Genetic evidence for ATP-dependent endoplasmic reticulum-to-Golgi apparatus trafficking of ceramide for sphingomyelin synthesis in Chinese hamster ovary cells. J Cell Biol *144*, 673-685.

Funato, K., and Riezman, H. (2001). Vesicular and nonvesicular transport of ceramide from ER to the Golgi apparatus in yeast. J Cell Biol *155*, 949-959.

Furuta, N., Fujimura-Kamada, K., Saito, K., Yamamoto, T., and Tanaka, K. (2007). Endocytic recycling in yeast is regulated by putative phospholipid translocases and the Ypt31p/32p-Rcy1p pathway. Mol Biol Cell *18*, 295-312.

Gadella, B.M., and Harrison, R.A. (2000). The capacitating agent bicarbonate induces protein kinase A-dependent changes in phospholipid transbilayer behavior in the sperm plasma membrane. Development *127*, 2407-2420.

Garcia, G., 3rd, Bertin, A., Li, Z., Song, Y., McMurray, M.A., Thorner, J., and Nogales, E. (2011). Subunit-dependent modulation of septin assembly: budding yeast septin Shs1 promotes ring and gauze formation. J Cell Biol *195*, 993-1004.

Gaspar, M.L., Aregullin, M.A., Jesch, S.A., Nunez, L.R., Villa-Garcia, M., and Henry, S.A. (2007). The emergence of yeast lipidomics. Biochim Biophys Acta *1771*, 241-254.

Gavin, A.C., Bosche, M., Krause, R., Grandi, P., Marzioch, M., Bauer, A., Schultz, J., Rick, J.M., Michon, A.M., Cruciat, C.M., *et al.* (2002). Functional organization of the yeast proteome by systematic analysis of protein complexes. Nature *415*, 141-147.

Gawrisch, K., Stibenz, D., Mops, A., Arnold, K., Linss, W., and Halbhuber, K.J. (1986). The rate of lateral diffusion of phospholipids in erythrocyte microvesicles. Biochim Biophys Acta *856*, 443-447.

Gaynor, P.M., and Carman, G.M. (1990). Phosphatidylethanolamine methyltransferase and phospholipid methyltransferase activities from Saccharomyces cerevisiae. Enzymological and kinetic properties. Biochim Biophys Acta *1045*, 156-163.

Georgiev, A.G., Sullivan, D.P., Kersting, M.C., Dittman, J.S., Beh, C.T., and Menon, A.K. (2011). Osh proteins regulate membrane sterol organization but are not required for sterol movement between the ER and PM. Traffic *12*, 1341-1355.

Giorgi, C., De Stefani, D., Bononi, A., Rizzuto, R., and Pinton, P. (2009). Structural and functional link between the mitochondrial network and the endoplasmic reticulum. Int J Biochem Cell Biol *41*, 1817-1827.

Gladfelter, A.S., Kozubowski, L., Zyla, T.R., and Lew, D.J. (2005). Interplay between septin organization, cell cycle and cell shape in yeast. J Cell Sci *118*, 1617-1628.

Gohil, V.M., and Greenberg, M.L. (2009). Mitochondrial membrane biogenesis: phospholipids and proteins go hand in hand. J Cell Biol *184*, 469-472.

Gomes, E.R., Jani, S., and Gundersen, G.G. (2005). Nuclear movement regulated by Cdc42, MRCK, myosin, and actin flow establishes MTOC polarization in migrating cells. Cell *121*, 451-463.

Graham, L.A., Flannery, A.R., and Stevens, T.H. (2003). Structure and assembly of the yeast V-ATPase. J Bioenerg Biomembr *35*, 301-312.

Griac, P. (2007). Sec14 related proteins in yeast. Biochim Biophys Acta *1771*, 737-745.

Han, G.S., O'Hara, L., Carman, G.M., and Siniossoglou, S. (2008). An unconventional diacylglycerol kinase that regulates phospholipid synthesis and nuclear membrane growth. J Biol Chem *283*, 20433-20442.

Han, G.S., Siniossoglou, S., and Carman, G.M. (2007). The cellular functions of the yeast lipin homolog PAH1p are dependent on its phosphatidate phosphatase activity. J Biol Chem *282*, 37026-37035.

Han, G.S., Wu, W.I., and Carman, G.M. (2006). The Saccharomyces cerevisiae Lipin homolog is a Mg2+-dependent phosphatidate phosphatase enzyme. J Biol Chem *281*, 9210-9218.

Hanada, K., Kumagai, K., Tomishige, N., and Kawano, M. (2007). CERT and intracellular trafficking of ceramide. Biochim Biophys Acta *1771*, 644-653.

Hanada, K., Kumagai, K., Yasuda, S., Miura, Y., Kawano, M., Fukasawa, M., and Nishijima, M. (2003). Molecular machinery for non-vesicular trafficking of ceramide. Nature *426*, 803-809.

Hayashi, T., and Su, T.P. (2007). Sigma-1 receptor chaperones at the ER-mitochondrion interface regulate Ca(2+) signaling and cell survival. Cell *131*, 596-610.

Heil-Chapdelaine, R.A., Oberle, J.R., and Cooper, J.A. (2000). The cortical protein Num1p is essential for dynein-dependent interactions of microtubules with the cortex. J Cell Biol *151*, 1337-1344.

Helenius, A., and Aebi, M. (2004). Roles of N-linked glycans in the endoplasmic reticulum. Annu Rev Biochem *73*, 1019-1049.

Henry, S.A., Kohlwein, S.D., and Carman, G.M. (2012). Metabolism and regulation of glycerolipids in the yeast Saccharomyces cerevisiae. Genetics *190*, 317-349.

Henry, S.A., and Patton-Vogt, J.L. (1998). Genetic regulation of phospholipid metabolism: yeast as a model eukaryote. Prog Nucleic Acid Res Mol Biol *61*, 133-179.

Hetz, C., and Glimcher, L.H. (2009). Fine-tuning of the unfolded protein response: Assembling the IRE1alpha interactome. Mol Cell *35*, 551-561.

Ho, C.H., Magtanong, L., Barker, S.L., Gresham, D., Nishimura, S., Natarajan, P., Koh, J.L., Porter, J., Gray, C.A., Andersen, R.J., *et al.* (2009). A molecular barcoded yeast ORF library enables mode-of-action analysis of bioactive compounds. Nat Biotechnol *27*, 369-377.

Hogan, P.G., Lewis, R.S., and Rao, A. (2010). Molecular basis of calcium signaling in lymphocytes: STIM and ORAI. Annu Rev Immunol *28*, 491-533.

Holthuis, J.C., and Levine, T.P. (2005). Lipid traffic: floppy drives and a superhighway. Nat Rev Mol Cell Biol *6*, 209-220.

Holtta-Vuori, M., and Ikonen, E. (2006). Endosomal cholesterol traffic: vesicular and non-vesicular mechanisms meet. Biochem Soc Trans *34*, 392-394.

Honlinger, A., Bomer, U., Alconada, A., Eckerskorn, C., Lottspeich, F., Dietmeier, K., and Pfanner, N. (1996). Tom7 modulates the dynamics of the mitochondrial outer membrane translocase and plays a pathway-related role in protein import. EMBO J *15*, 2125-2137.

Hope, M.J., Bally, M.B., Webb, G., and Cullis, P.R. (1985). Production of large unilamellar vesicles by a rapid extrusion procedure: characterization of size distribution, trapped volume and ability to maintain a membrane potential. Biochim Biophys Acta *812*, 55-65.

Huisman, S.M., and Segal, M. (2005). Cortical capture of microtubules and spindle polarity in budding yeast - where's the catch? J Cell Sci *118*, 463-471.

Hummasti, S., and Hotamisligil, G.S. (2010). Endoplasmic reticulum stress and inflammation in obesity and diabetes. Circ Res *107*, 579-591.

Hwang, E., Kusch, J., Barral, Y., and Huffaker, T.C. (2003). Spindle orientation in Saccharomyces cerevisiae depends on the transport of microtubule ends along polarized actin cables. J Cell Biol *161*, 483-488.

Im, Y.J., Raychaudhuri, S., Prinz, W.A., and Hurley, J.H. (2005). Structural mechanism for sterol sensing and transport by OSBP-related proteins. Nature *437*, 154-158.

Ishinaga, M., and Kito, M. (1974). Participation of soluble phosphatidylserine synthetase in phosphatidylethanolamine biosynthesis in Escherichia coli membrane. Eur J Biochem *42*, 483-487.

Janssen, M.J., de Jong, H.M., de Kruijff, B., and de Kroon, A.I. (2002). Cooperative activity of phospholipid-N-methyltransferases localized in different membranes. FEBS Lett *513*, 197-202.

Jesch, S.A., Zhao, X., Wells, M.T., and Henry, S.A. (2005). Genome-wide analysis reveals inositol, not choline, as the major effector of Ino2p-Ino4p and unfolded protein response target gene expression in yeast. J Biol Chem *280*, 9106-9118.

Johnston, G.C., Prendergast, J.A., and Singer, R.A. (1991). The Saccharomyces cerevisiae MYO2 gene encodes an essential myosin for vectorial transport of vesicles. J Cell Biol *113*, 539-551.

Jonikas, M.C., Collins, S.R., Denic, V., Oh, E., Quan, E.M., Schmid, V., Weibezahn, J., Schwappach, B., Walter, P., Weissman, J.S., *et al.* (2009). Comprehensive characterization of genes required for protein folding in the endoplasmic reticulum. Science *323*, 1693-1697.

Kagiwada, S., and Zen, R. (2003). Role of the yeast VAP homolog, Scs2p, in INO1 expression and phospholipid metabolism. J Biochem (Tokyo) *133*, 515-522.

Kahana, J.A., Schlenstedt, G., Evanchuk, D.M., Geiser, J.R., Hoyt, M.A., and Silver, P.A. (1998). The yeast dynactin complex is involved in partitioning the mitotic spindle between mother and daughter cells during anaphase B. Mol Biol Cell *9*, 1741-1756.

Kandutsch, A.A., and Thompson, E.B. (1980). Cytosolic proteins that bind oxygenated sterols. Cellular distribution, specificity, and some properties. J Biol Chem *255*, 10813-10821.

Kanno, K., Wu, M.K., Scapa, E.F., Roderick, S.L., and Cohen, D.E. (2007). Structure and function of phosphatidylcholine transfer protein (PC-TP)/StarD2. Biochim Biophys Acta *1771*, 654-662.

Kaplan, M.R., and Simoni, R.D. (1985). Transport of cholesterol from the endoplasmic reticulum to the plasma membrane. J Cell Biol *101*, 446-453.

Kato, U., Emoto, K., Fredriksson, C., Nakamura, H., Ohta, A., Kobayashi, T., Murakami-Murofushi, K., and Umeda, M. (2002). A novel membrane protein, Ros3p, is required for phospholipid translocation across the plasma membrane in Saccharomyces cerevisiae. J Biol Chem *277*, 37855-37862.

Kaufman, R.J. (2002). Orchestrating the unfolded protein response in health and disease. J Clin Invest *110*, 1389-1398.

Kelley, M.J., Bailis, A.M., Henry, S.A., and Carman, G.M. (1988). Regulation of phospholipid biosynthesis in Saccharomyces cerevisiae by inositol. Inositol is an inhibitor of phosphatidylserine synthase activity. J Biol Chem *263*, 18078-18085.

Kent, C., and Carman, G.M. (1999). Interactions among pathways for phosphatidylcholine metabolism, CTP synthesis and secretion through the Golgi apparatus. Trends Biochem Sci *24*, 146-150.

Kersting, M.C., Choi, H.S., and Carman, G.M. (2004). Regulation of the yeast EKI1-encoded ethanolamine kinase by inositol and choline. J Biol Chem *279*, 35353-35359.

Khelef, N., Soe, T.T., Quehenberger, O., Beatini, N., Tabas, I., and Maxfield, F.R. (2000). Enrichment of acyl coenzyme A:cholesterol O-acyltransferase near trans-golgi network and endocytic recycling compartment. Arterioscler Thromb Vasc Biol *20*, 1769-1776.

Kieran, D., Hafezparast, M., Bohnert, S., Dick, J.R., Martin, J., Schiavo, G., Fisher, E.M., and Greensmith, L. (2005). A mutation in dynein rescues axonal transport defects and extends the life span of ALS mice. J Cell Biol *169*, 561-567.

Kimata, Y., and Kohno, K. (2011). Endoplasmic reticulum stress-sensing mechanisms in yeast and mammalian cells. Curr Opin Cell Biol *23*, 135-142.

Koc, A., Wheeler, L.J., Mathews, C.K., and Merrill, G.F. (2004). Hydroxyurea arrests DNA replication by a mechanism that preserves basal dNTP pools. J Biol Chem *279*, 223-230.

Kodaki, T., and Yamashita, S. (1987). Yeast phosphatidylethanolamine methylation pathway. Cloning and characterization of two distinct methyltransferase genes. J Biol Chem *262*, 15428-15435.

Kornmann, B., Currie, E., Collins, S.R., Schuldiner, M., Nunnari, J., Weissman, J.S., and Walter, P. (2009). An ER-mitochondria tethering complex revealed by a synthetic biology screen. Science *325*, 477-481.

Kornmann, B., and Walter, P. (2010). ERMES-mediated ER-mitochondria contacts: molecular hubs for the regulation of mitochondrial biology. J Cell Sci *123*, 1389-1393.

Kozminski, K.G., Alfaro, G., Dighe, S., and Beh, C.T. (2006). Homologues of oxysterol-binding proteins affect Cdc42p- and Rho1p-mediated cell polarization in Saccharomyces cerevisiae. Traffic *7*, 1224-1242.

Krick, R., Muhe, Y., Prick, T., Bredschneider, M., Bremer, S., Wenzel, D., Eskelinen, E.L., and Thumm, M. (2009). Piecemeal microautophagy of the nucleus: genetic and morphological traits. Autophagy *5*, 270-272.

Kusch, J., Meyer, A., Snyder, M.P., and Barral, Y. (2002). Microtubule capture by the cleavage apparatus is required for proper spindle positioning in yeast. Genes Dev *16*, 1627-1639.

Kvam, E., Gable, K., Dunn, T.M., and Goldfarb, D.S. (2005). Targeting of Tsc13p to nucleus-vacuole junctions: a role for very-long-chain fatty acids in the biogenesis of microautophagic vesicles. Mol Biol Cell *16*, 3987-3998.

Kvam, E., and Goldfarb, D.S. (2004). Nvj1p is the outer-nuclear-membrane receptor for oxysterol-binding protein homolog Osh1p in Saccharomyces cerevisiae. J Cell Sci *117*, 4959-4968.

Kvam, E., and Goldfarb, D.S. (2006). Structure and function of nucleus-vacuole junctions: outer-nuclear-membrane targeting of Nvj1p and a role in tryptophan uptake. J Cell Sci *119*, 3622-3633.

Kvam, E., and Goldfarb, D.S. (2007). Nucleus-vacuole junctions and piecemeal microautophagy of the nucleus in S. cerevisiae. Autophagy *3*, 85-92.

Ladinsky, M.S., Mastronarde, D.N., McIntosh, J.R., Howell, K.E., and Staehelin, L.A. (1999). Golgi structure in three dimensions: functional insights from the normal rat kidney cell. J Cell Biol *144*, 1135-1149.

Lai, E., Teodoro, T., and Volchuk, A. (2007). Endoplasmic reticulum stress: signaling the unfolded protein response. Physiology (Bethesda) *22*, 193-201.

Lands, W.E., and Merkl, I. (1963). Metabolism of glycerolipids. III. Reactivity of various acyl esters of coenzyme A with alpha'-acylglycerophosphorylcholine, and positional specificities in lecithin synthesis. J Biol Chem *238*, 898-904.

Larsson, K.E., Kjellberg, J.M., Tjellstrom, H., and Sandelius, A.S. (2007). LysoPC acyltransferase/PC transacylase activities in plant plasma membrane and plasma membrane-associated endoplasmic reticulum. BMC Plant Biol *7*, 64.

Lavieu, G., Orci, L., Shi, L., Geiling, M., Ravazzola, M., Wieland, F., Cosson, P., and Rothman, J.E. (2010). Induction of cortical endoplasmic reticulum by dimerization of a coatomer-binding peptide anchored to endoplasmic reticulum membranes. Proc Natl Acad Sci U S A *107*, 6876-6881.

Lee, L., Tirnauer, J.S., Li, J., Schuyler, S.C., Liu, J.Y., and Pellman, D. (2000). Positioning of the mitotic spindle by a cortical-microtubule capture mechanism. Science *287*, 2260-2262.

Lee, W.L., Oberle, J.R., and Cooper, J.A. (2003). The role of the lissencephaly protein Pac1 during nuclear migration in budding yeast. J Cell Biol *160*, 355-364.

Lehto, M., and Olkkonen, V.M. (2003). The OSBP-related proteins: a novel protein family involved in vesicle transport, cellular lipid metabolism, and cell signalling. Biochim Biophys Acta *1631*, 1-11.

Lenoir, G., Williamson, P., Puts, C.F., and Holthuis, J.C. (2009). Cdc50p plays a vital role in the ATPase reaction cycle of the putative aminophospholipid transporter Drs2p. J Biol Chem *284*, 17956-17967.

Lev, S. (2004). The role of the Nir/rdgB protein family in membrane trafficking and cytoskeleton remodeling. Exp Cell Res *297*, 1-10.

Lev, S. (2010). Non-vesicular lipid transport by lipid-transfer proteins and beyond. Nat Rev Mol Cell Biol *11*, 739-750.

Lev, S., Ben Halevy, D., Peretti, D., and Dahan, N. (2008). The VAP protein family: from cellular functions to motor neuron disease. Trends Cell Biol *18*, 282-290.

Levine, T. (2004). Short-range intracellular trafficking of small molecules across endoplasmic reticulum junctions. Trends Cell Biol *14*, 483-490.

Levine, T., and Loewen, C. (2006). Inter-organelle membrane contact sites: through a glass, darkly. Curr Opin Cell Biol *18*, 371-378.

Levy, J.R., and Holzbaur, E.L. (2006). Cytoplasmic dynein/dynactin function and dysfunction in motor neurons. Int J Dev Neurosci *24*, 103-111.

Lewis, J.A., and Tata, J.R. (1973). A rapidly sedimenting fraction of rat liver endoplasmic reticulum. J Cell Sci *13*, 447-459.

Li, X., Rivas, M.P., Fang, M., Marchena, J., Mehrotra, B., Chaudhary, A., Feng, L., Prestwich, G.D., and Bankaitis, V.A. (2002). Analysis of oxysterol binding protein homologue Kes1p function in regulation of Sec14p-dependent protein transport from the yeast Golgi complex. J Cell Biol *157*, 63-77.

Li, Y., and Prinz, W.A. (2004). ATP-binding cassette (ABC) transporters mediate nonvesicular, raft-modulated sterol movement from the plasma membrane to the endoplasmic reticulum. J Biol Chem *279*, 45226-45234.

Li, Z., Agellon, L.B., Allen, T.M., Umeda, M., Jewell, L., Mason, A., and Vance, D.E. (2006). The ratio of phosphatidylcholine to phosphatidylethanolamine influences membrane integrity and steatohepatitis. Cell Metab *3*, 321-331.

Li, Z., Agellon, L.B., and Vance, D.E. (2005). Phosphatidylcholine homeostasis and liver failure. J Biol Chem *280*, 37798-37802.

Li, Z., and Vance, D.E. (2008). Phosphatidylcholine and choline homeostasis. J Lipid Res *49*, 1187-1194.

Liakopoulos, D., Kusch, J., Grava, S., Vogel, J., and Barral, Y. (2003). Asymmetric loading of Kar9 onto spindle poles and microtubules ensures proper spindle alignment. Cell *112*, 561-574.

Linton, K.J., Zolnerciks, J.K., and Schmitt, L. (2011). General Introduction, Structure and Likely Mechanism of Action of ABC Transport Proteins. In Genetics and Biochemistry of ATP Binding Cassette Transporters, K.J. Linton, I.B. Holland, and W.S. Publishing, eds.

Loewen, C.J., Gaspar, M.L., Jesch, S.A., Delon, C., Ktistakis, N.T., Henry, S.A., and Levine, T.P. (2004). Phospholipid metabolism regulated by a transcription factor sensing phosphatidic acid. Science *304*, 1644-1647.

Loewen, C.J., Moritz, O.L., Tam, B.M., Papermaster, D.S., and Molday, R.S. (2003a). The role of subunit assembly in peripherin-2 targeting to rod photoreceptor disk membranes and retinitis pigmentosa. Mol Biol Cell *14*, 3400-3413.

Loewen, C.J., Roy, A., and Levine, T.P. (2003b). A conserved ER targeting motif in three families of lipid binding proteins and in Opi1p binds VAP. Embo J *22*, 2025-2035.

Loewen, C.J., Young, B.P., Tavassoli, S., and Levine, T.P. (2007). Inheritance of cortical ER in yeast is required for normal septin organization. J Cell Biol *179*, 467-483.

Luedeke, C., Frei, S.B., Sbalzarini, I., Schwarz, H., Spang, A., and Barral, Y. (2005). Septin-dependent compartmentalization of the endoplasmic reticulum during yeast polarized growth. J Cell Biol *169*, 897-908.

Maass, K., Fischer, M.A., Seiler, M., Temmerman, K., Nickel, W., and Seedorf, M. (2009). A signal comprising a basic cluster and an amphipathic alpha-helix interacts with lipids and is required for the transport of Ist2 to the yeast cortical ER. J Cell Sci *122*, 625-635.

Madden, K., and Snyder, M. (1998). Cell polarity and morphogenesis in budding yeast. Annu Rev Microbiol *52*, 687-744.

Manford, A., Xia, T., Saxena, A.K., Stefan, C., Hu, F., Emr, S.D., and Mao, Y. (2010). Crystal structure of the yeast Sac1: implications for its phosphoinositide phosphatase function. EMBO J *29*, 1489-1498.

Manford, A.G., Stefan, C.J., Yuan, H.L., Macgurn, J.A., and Emr, S.D. (2012). ER-to-Plasma Membrane Tethering Proteins Regulate Cell Signaling and ER Morphology. Dev Cell *23*, 1129-1140.

Martin, S.W., and Konopka, J.B. (2004). Lipid raft polarization contributes to hyphal growth in Candida albicans. Eukaryot Cell *3*, 675-684.

Massey, J.B., Hickson, D., She, H.S., Sparrow, J.T., Via, D.P., Gotto, A.M., Jr., and Pownall, H.J. (1984). Measurement and prediction of the rates of spontaneous transfer of phospholipids between plasma lipoproteins. Biochim Biophys Acta *794*, 274-280.

McLean, L.R., and Phillips, M.C. (1981). Mechanism of cholesterol and phosphatidylcholine exchange or transfer between unilamellar vesicles. Biochemistry *20*, 2893-2900.

McMillan, J.N., and Tatchell, K. (1994). The JNM1 gene in the yeast Saccharomyces cerevisiae is required for nuclear migration and spindle orientation during the mitotic cell cycle. J Cell Biol *125*, 143-158.

Merida, I., Avila-Flores, A., and Merino, E. (2008). Diacylglycerol kinases: at the hub of cell signalling. Biochem J *409*, 1-18.

Michot, C., Hubert, L., Brivet, M., De Meirleir, L., Valayannopoulos, V., Muller-Felber, W., Venkateswaran, R., Ogier, H., Desguerre, I., Altuzarra, C., *et al.* (2010). LPIN1 gene mutations: a major cause of severe rhabdomyolysis in early childhood. Hum Mutat *31*, E1564-1573.

Miller, R.K., Cheng, S.C., and Rose, M.D. (2000). Bim1p/Yeb1p mediates the Kar9p-dependent cortical attachment of cytoplasmic microtubules. Mol Biol Cell *11*, 2949-2959.

Miller, R.K., and Rose, M.D. (1998). Kar9p is a novel cortical protein required for cytoplasmic microtubule orientation in yeast. J Cell Biol *140*, 377-390.

Milligan, S.C., Alb, J.G., Jr., Elagina, R.B., Bankaitis, V.A., and Hyde, D.R. (1997). The phosphatidylinositol transfer protein domain of Drosophila retinal degeneration B protein is essential for photoreceptor cell survival and recovery from light stimulation. J Cell Biol *139*, 351-363.

Morash, S.C., McMaster, C.R., Hjelmstad, R.H., and Bell, R.M. (1994). Studies employing Saccharomyces cerevisiae cpt1 and ept1 null mutants implicate the CPT1 gene in coordinate regulation of phospholipid biosynthesis. J Biol Chem *269*, 28769-28776.

Morre, D.J., Merritt, W.D., and Lembi, C.A. (1971). Connections between mitochondria and endoplasmic reticulum in rat liver and onion stem. Protoplasma *73*, 43-49.

Moseley, J.B., and Goode, B.L. (2006). The yeast actin cytoskeleton: from cellular function to biochemical mechanism. Microbiol Mol Biol Rev *70*, 605-645.

Moseley, J.B., Sagot, I., Manning, A.L., Xu, Y., Eck, M.J., Pellman, D., and Goode, B.L. (2004). A conserved mechanism for Bni1- and mDia1-induced actin assembly and dual regulation of Bni1 by Bud6 and profilin. Mol Biol Cell *15*, 896-907.

Mostowy, S., and Cossart, P. (2012). Septins: the fourth component of the cytoskeleton. Nat Rev Mol Cell Biol *13*, 183-194.

Mousley, C.J., Yuan, P., Gaur, N.A., Trettin, K.D., Nile, A.H., Deminoff, S.J., Dewar, B.J., Wolpert, M., Macdonald, J.M., Herman, P.K., *et al.* (2012). A sterol-binding protein integrates endosomal lipid metabolism with TOR signaling and nitrogen sensing. Cell *148*, 702-715.

Muhua, L., Karpova, T.S., and Cooper, J.A. (1994). A yeast actin-related protein homologous to that in vertebrate dynactin complex is important for spindle orientation and nuclear migration. Cell *78*, 669-679.

Munchow, S., Sauter, C., and Jansen, R.P. (1999). Association of the class V myosin Myo4p with a localised messenger RNA in budding yeast depends on She proteins. J Cell Sci *112 (Pt 10)*, 1511-1518.

Murase, K., Fujiwara, T., Umemura, Y., Suzuki, K., Iino, R., Yamashita, H., Saito, M., Murakoshi, H., Ritchie, K., and Kusumi, A. (2004). Ultrafine membrane compartments for molecular diffusion as revealed by single molecule techniques. Biophys J *86*, 4075-4093.

Nakamichi, S., Yamanaka, K., Suzuki, M., Watanabe, T., and Kagiwada, S. (2011). Human VAPA and the yeast VAP Scs2p with an altered proline distribution can phenocopy amyotrophic lateral sclerosis-associated VAPB(P56S). Biochem Biophys Res Commun *404*, 605-609.

Nayak, R.R., Kearns, M., Spielman, R.S., and Cheung, V.G. (2009). Coexpression network based on natural variation in human gene expression reveals gene interactions and functions. Genome Res *19*, 1953-1962.

Neupert, W., and Herrmann, J.M. (2007). Translocation of proteins into mitochondria. Annu Rev Biochem *76*, 723-749.

Ng, D.T., Spear, E.D., and Walter, P. (2000). The unfolded protein response regulates multiple aspects of secretory and membrane protein biogenesis and endoplasmic reticulum quality control. J Cell Biol *150*, 77-88.

Nguyen, T., Lewandowska, A., Choi, J.Y., Markgraf, D.F., Junker, M., Bilgin, M., Ejsing, C.S., Voelker, D.R., Rapoport, T.A., and Shaw, J.M. (2012). Gem1 and ERMES do not directly affect phosphatidylserine transport from ER to mitochondria or mitochondrial inheritance. Traffic.

Nichols, J.W., and Pagano, R.E. (1981). Kinetics of soluble lipid monomer diffusion between vesicles. Biochemistry *20*, 2783-2789.

Nikawa, J., Murakami, A., Esumi, E., and Hosaka, K. (1995). Cloning and sequence of the SCS2 gene, which can suppress the defect of INO1 expression in an inositol auxotrophic mutant of Saccharomyces cerevisiae. J Biochem (Tokyo) *118*, 39-45.

Nikawa, J., and Yamashita, S. (1997). Phosphatidylinositol synthase from yeast. Biochim Biophys Acta *1348*, 173-178.

Nishimura, A.L., Mitne-Neto, M., Silva, H.C., Richieri-Costa, A., Middleton, S., Cascio, D., Kok, F., Oliveira, J.R., Gillingwater, T., Webb, J., *et al.* (2004). A mutation in the vesicle-trafficking protein VAPB causes late-onset spinal muscular atrophy and amyotrophic lateral sclerosis. Am J Hum Genet *75*, 822-831.

Novikoff, A.B., Spater, H.W., and Quintana, N. (1983). Transepithelial endoplasmic reticulum in rat proximal convoluted tubule. J Histochem Cytochem *31*, 656-661.

Nunnari, J., Wong, E.D., Meeusen, S., and Wagner, J.A. (2002). Studying the behavior of mitochondria. Methods Enzymol *351*, 381-393.

Osman, C., Voelker, D.R., and Langer, T. (2011). Making heads or tails of phospholipids in mitochondria. J Cell Biol *192*, 7-16.

Ouellet, J., and Barral, Y. (2012). Organelle segregation during mitosis: lessons from asymmetrically dividing cells. J Cell Biol *196*, 305-313.

Ozaki-Kuroda, K., Yamamoto, Y., Nohara, H., Kinoshita, M., Fujiwara, T., Irie, K., and Takai, Y. (2001). Dynamic localization and function of Bni1p at the sites of directed growth in Saccharomyces cerevisiae. Mol Cell Biol *21*, 827-839.

Pagac, M., de la Mora, H.V., Duperrex, C., Roubaty, C., Vionnet, C., and Conzelmann, A. (2011). Topology of 1-Acyl-sn-glycerol-3-phosphate Acyltransferases SLC1 and ALE1 and Related Membrane-bound O-Acyltransferases (MBOATs) of Saccharomyces cerevisiae. J Biol Chem *286*, 36438-36447.

Palade, G.E. (1956). The endoplasmic reticulum. J Biophys Biochem Cytol *2*, 85-98.

Pan, X., Roberts, P., Chen, Y., Kvam, E., Shulga, N., Huang, K., Lemmon, S., and Goldfarb, D.S. (2000). Nucleus-vacuole junctions in Saccharomyces cerevisiae are formed through the direct interaction of Vac8p with Nvj1p. Mol Biol Cell *11*, 2445-2457.

Parks, L.W., Bottema, C.D., Rodriguez, R.J., and Lewis, T.A. (1985). Yeast sterols: yeast mutants as tools for the study of sterol metabolism. Methods Enzymol *111*, 333-346.

Patton-Vogt, J.L., Griac, P., Sreenivas, A., Bruno, V., Dowd, S., Swede, M.J., and Henry, S.A. (1997). Role of the yeast phosphatidylinositol/phosphatidylcholine transfer protein (Sec14p) in phosphatidylcholine turnover and INO1 regulation. J Biol Chem *272*, 20873-20883.

Peterfy, M., Phan, J., and Reue, K. (2005). Alternatively spliced lipin isoforms exhibit distinct expression pattern, subcellular localization, and role in adipogenesis. J Biol Chem *280*, 32883-32889.

Pichler, H., Gaigg, B., Hrastnik, C., Achleitner, G., Kohlwein, S.D., Zellnig, G., Perktold, A., and Daum, G. (2001). A subfraction of the yeast endoplasmic reticulum associates with the plasma membrane and has a high capacity to synthesize lipids. Eur J Biochem *268*, 2351-2361.

Poburko, D., Kuo, K.H., Dai, J., Lee, C.H., and van Breemen, C. (2004). Organellar junctions promote targeted Ca2+ signaling in smooth muscle: why two membranes are better than one. Trends Pharmacol Sci *25*, 8-15.

Porter, K.R., and Palade, G.E. (1957). Studies on the endoplasmic reticulum. III. Its form and distribution in striated muscle cells. J Biophys Biochem Cytol *3*, 269-300.

Preuss, D., Mulholland, J., Kaiser, C.A., Orlean, P., Albright, C., Rose, M.D., Robbins, P.W., and Botstein, D. (1991). Structure of the yeast endoplasmic reticulum: localization of ER proteins using immunofluorescence and immunoelectron microscopy. Yeast *7*, 891-911.

Prinz, W.A. (2010). Lipid trafficking sans vesicles: where, why, how? Cell *143*, 870-874.

Prinz, W.A., Grzyb, L., Veenhuis, M., Kahana, J.A., Silver, P.A., and Rapoport, T.A. (2000). Mutants affecting the structure of the cortical endoplasmic reticulum in Saccharomyces cerevisiae. J Cell Biol *150*, 461-474.

Proszynski, T.J., Klemm, R., Bagnat, M., Gaus, K., and Simons, K. (2006). Plasma membrane polarization during mating in yeast cells. J Cell Biol *173*, 861-866.

Pruyne, D., Legesse-Miller, A., Gao, L., Dong, Y., and Bretscher, A. (2004). Mechanisms of polarized growth and organelle segregation in yeast. Annu Rev Cell Dev Biol *20*, 559-591.

Rambourg, A., Jackson, C.L., and Clermont, Y. (2001). Three dimensional configuration of the secretory pathway and segregation of secretion granules in the yeast Saccharomyces cerevisiae. J Cell Sci *114*, 2231-2239.

Raturi, A., and Simmen, T. (2013). Where the endoplasmic reticulum and the mitochondrion tie the knot: The mitochondria-associated membrane (MAM). Biochim Biophys Acta *1833*, 213-224.

Raychaudhuri, S., Im, Y.J., Hurley, J.H., and Prinz, W.A. (2006). Nonvesicular sterol movement from plasma membrane to ER requires oxysterol-binding protein-related proteins and phosphoinositides. J Cell Biol *173*, 107-119.

Raychaudhuri, S., and Prinz, W.A. (2008). Nonvesicular phospholipid transfer between peroxisomes and the endoplasmic reticulum. Proc Natl Acad Sci U S A *105*, 15785-15790.

Raychaudhuri, S., Young, B.P., Espenshade, P.J., and Loewen, C.J. (2012). Regulation of lipid metabolism: a tale of two yeasts. Curr Opin Cell Biol.

Reue, K., and Brindley, D.N. (2008). Thematic Review Series: Glycerolipids. Multiple roles for lipins/phosphatidate phosphatase enzymes in lipid metabolism. J Lipid Res *49*, 2493-2503.

Ridgway, N.D. (2010). Oxysterol-binding proteins. Subcell Biochem *51*, 159-182.

Riekhof, W.R., Wu, J., Gijon, M.A., Zarini, S., Murphy, R.C., and Voelker, D.R. (2007a). Lysophosphatidylcholine metabolism in Saccharomyces cerevisiae: the role of P-type ATPases in transport and a broad specificity acyltransferase in acylation. J Biol Chem *282*, 36853-36861.

Riekhof, W.R., Wu, J., Jones, J.L., and Voelker, D.R. (2007b). Identification and characterization of the major lysophosphatidylethanolamine acyltransferase in Saccharomyces cerevisiae. J Biol Chem *282*, 28344-28352.

Ring, G., Khoury, C.M., Solar, A.J., Yang, Z., Mandato, C.A., and Greenwood, M.T. (2008). Transmembrane protein 85 from both human (TMEM85) and yeast (YGL231c) inhibit hydrogen peroxide mediated cell death in yeast. FEBS Lett *582*, 2637-2642.

Rizzuto, R., Duchen, M.R., and Pozzan, T. (2004). Flirting in little space: the ER/mitochondria Ca2+ liaison. Sci STKE *2004*, re1.

Rizzuto, R., Pinton, P., Carrington, W., Fay, F.S., Fogarty, K.E., Lifshitz, L.M., Tuft, R.A., and Pozzan, T. (1998). Close contacts with the endoplasmic reticulum as determinants of mitochondrial Ca2+ responses. Science *280*, 1763-1766.

Roberts, P., Moshitch-Moshkovitz, S., Kvam, E., O'Toole, E., Winey, M., and Goldfarb, D.S. (2003). Piecemeal microautophagy of nucleus in Saccharomyces cerevisiae. Mol Biol Cell *14*, 129-141.

Robinson, M.D., Grigull, J., Mohammad, N., and Hughes, T.R. (2002). FunSpec: a web-based cluster interpreter for yeast. BMC Bioinformatics *3*, 35.

Ron, D., and Walter, P. (2007). Signal integration in the endoplasmic reticulum unfolded protein response. Nat Rev Mol Cell Biol *8*, 519-529.

Rosenbluth, J. (1962). Subsurface cisterns and their relationship to the neuronal plasma membrane. J Cell Biol *13*, 405-421.

Rossi, D., Barone, V., Giacomello, E., Cusimano, V., and Sorrentino, V. (2008). The sarcoplasmic reticulum: an organized patchwork of specialized domains. Traffic *9*, 1044-1049.

Rouser, G., Fkeischer, S., and Yamamoto, A. (1970). Two dimensional then layer chromatographic separation of polar lipids and determination of phospholipids by phosphorus analysis of spots. Lipids *5*, 494-496.

Saarikangas, J., and Barral, Y. (2011). The emerging functions of septins in metazoans. EMBO Rep *12*, 1118-1126.

Saito, K., Fujimura-Kamada, K., Furuta, N., Kato, U., Umeda, M., and Tanaka, K. (2004). Cdc50p, a protein required for polarized growth, associates with the Drs2p P-type ATPase implicated in phospholipid translocation in Saccharomyces cerevisiae. Mol Biol Cell *15*, 3418-3432.

Saito, K., Fujimura-Kamada, K., Hanamatsu, H., Kato, U., Umeda, M., Kozminski, K.G., and Tanaka, K. (2007). Transbilayer phospholipid flipping regulates Cdc42p signaling during polarized cell growth via Rga GTPase-activating proteins. Dev Cell *13*, 743-751.

Santos-Rosa, H., Leung, J., Grimsey, N., Peak-Chew, S., and Siniossoglou, S. (2005). The yeast lipin Smp2 couples phospholipid biosynthesis to nuclear membrane growth. EMBO J *24*, 1931-1941.

Sasser, T., Qiu, Q.S., Karunakaran, S., Padolina, M., Reyes, A., Flood, B., Smith, S., Gonzales, C., and Fratti, R.A. (2011). The Yeast Lipin 1 orthologue Pah1p regulates vacuole homeostasis and membrane fusion. J Biol Chem.

Schaaf, G., Ortlund, E.A., Tyeryar, K.R., Mousley, C.J., Ile, K.E., Garrett, T.A., Ren, J., Woolls, M.J., Raetz, C.R., Redinbo, M.R., *et al.* (2008). Functional anatomy of phospholipid binding and regulation of phosphoinositide homeostasis by proteins of the sec14 superfamily. Mol Cell *29*, 191-206.

Schnabl, M., Daum, G., and Pichler, H. (2005). Multiple lipid transport pathways to the plasma membrane in yeast. Biochim Biophys Acta *1687*, 130-140.

Schneiter, R., Brugger, B., Sandhoff, R., Zellnig, G., Leber, A., Lampl, M., Athenstaedt, K., Hrastnik, C., Eder, S., Daum, G., *et al.* (1999). Electrospray ionization tandem mass spectrometry (ESI-MS/MS) analysis of the lipid molecular species composition of yeast subcellular membranes reveals acyl chain-based sorting/remodeling of distinct molecular species en route to the plasma membrane. J Cell Biol *146*, 741-754.

Schubert, U., Anton, L.C., Gibbs, J., Norbury, C.C., Yewdell, J.W., and Bennink, J.R. (2000). Rapid degradation of a large fraction of newly synthesized proteins by proteasomes. Nature *404*, 770-774.

Schuck, S., Prinz, W.A., Thorn, K.S., Voss, C., and Walter, P. (2009). Membrane expansion alleviates endoplasmic reticulum stress independently of the unfolded protein response. J Cell Biol *187*, 525-536.

Schuiki, I., Schnabl, M., Czabany, T., Hrastnik, C., and Daum, G. (2010). Phosphatidylethanolamine synthesized by four different pathways is supplied to the plasma membrane of the yeast Saccharomyces cerevisiae. Biochim Biophys Acta *1801*, 480-486.

Schuller, C., Mamnun, Y.M., Wolfger, H., Rockwell, N., Thorner, J., and Kuchler, K. (2007). Membrane-active compounds activate the transcription factors Pdr1 and Pdr3 connecting pleiotropic drug resistance and membrane lipid homeostasis in saccharomyces cerevisiae. Mol Biol Cell *18*, 4932-4944.

Schulz, T.A., Choi, M.G., Raychaudhuri, S., Mears, J.A., Ghirlando, R., Hinshaw, J.E., and Prinz, W.A. (2009). Lipid-regulated sterol transfer between closely apposed membranes by oxysterol-binding protein homologues. J Cell Biol *187*, 889-903.

Schulz, T.A., and Prinz, W.A. (2007). Sterol transport in yeast and the oxysterol binding protein homologue (OSH) family. Biochim Biophys Acta *1771*, 769-780.

Schumacher, M.M., Choi, J.Y., and Voelker, D.R. (2002). Phosphatidylserine transport to the mitochondria is regulated by ubiquitination. In J Biol Chem, pp. 51033-51042.

Schwartz, K., Richards, K., and Botstein, D. (1997). BIM1 encodes a microtubule-binding protein in yeast. Mol Biol Cell *8*, 2677-2691.

Shamu, C.E., Cox, J.S., and Walter, P. (1994). The unfolded-protein-response pathway in yeast. Trends Cell Biol *4*, 56-60.

Shcheprova, Z., Baldi, S., Frei, S.B., Gonnet, G., and Barral, Y. (2008). A mechanism for asymmetric segregation of age during yeast budding. Nature *454*, 728-734.

Sheff, M.A., and Thorn, K.S. (2004). Optimized cassettes for fluorescent protein tagging in Saccharomyces cerevisiae. Yeast *21*, 661-670.

Shen, H., and Dowhan, W. (1996). Reduction of CDP-diacylglycerol synthase activity results in the excretion of inositol by Saccharomyces cerevisiae. J Biol Chem *271*, 29043-29048.

Shepard, K.A., Gerber, A.P., Jambhekar, A., Takizawa, P.A., Brown, P.O., Herschlag, D., DeRisi, J.L., and Vale, R.D. (2003). Widespread cytoplasmic mRNA transport in yeast: identification of 22 bud-localized transcripts using DNA microarray analysis. Proc Natl Acad Sci U S A *100*, 11429-11434.

Shibata, Y., Shemesh, T., Prinz, W.A., Palazzo, A.F., Kozlov, M.M., and Rapoport, T.A. (2010). Mechanisms determining the morphology of the peripheral ER. Cell *143*, 774-788.

Shibata, Y., Voeltz, G.K., and Rapoport, T.A. (2006). Rough sheets and smooth tubules. Cell *126*, 435-439.

Shields, D.J., Altarejos, J.Y., Wang, X., Agellon, L.B., and Vance, D.E. (2003a). Molecular dissection of the S-adenosylmethionine-binding site of phosphatidylethanolamine N-methyltransferase. J Biol Chem *278*, 35826-35836.

Shields, D.J., Lehner, R., Agellon, L.B., and Vance, D.E. (2003b). Membrane topography of human phosphatidylethanolamine N-methyltransferase. J Biol Chem *278*, 2956-2962.

Shields, D.J., Lingrell, S., Agellon, L.B., Brosnan, J.T., and Vance, D.E. (2005). Localization-independent regulation of homocysteine secretion by phosphatidylethanolamine N-methyltransferase. J Biol Chem *280*, 27339-27344.

Sikorski, R.S., and Hieter, P. (1989). A system of shuttle vectors and yeast host strains designed for efficient manipulation of DNA in Saccharomyces cerevisiae. Genetics *122*, 19-27.

Siller, K.H., and Doe, C.Q. (2009). Spindle orientation during asymmetric cell division. Nat Cell Biol *11*, 365-374.

Siniossoglou, S. (2009). Lipins, lipids and nuclear envelope structure. Traffic *10*, 1181-1187.

Skinner, H.B., McGee, T.P., McMaster, C.R., Fry, M.R., Bell, R.M., and Bankaitis, V.A. (1995). The Saccharomyces cerevisiae phosphatidylinositol-transfer protein effects a ligand-dependent inhibition of choline-phosphate cytidylyltransferase activity. Proc Natl Acad Sci U S A *92*, 112-116.

Sopko, R., Huang, D., Preston, N., Chua, G., Papp, B., Kafadar, K., Snyder, M., Oliver, S.G., Cyert, M., Hughes, T.R., *et al.* (2006). Mapping pathways and phenotypes by systematic gene overexpression. Mol Cell *21*, 319-330.

Spellman, P.T., Sherlock, G., Zhang, M.Q., Iyer, V.R., Anders, K., Eisen, M.B., Brown, P.O., Botstein, D., and Futcher, B. (1998). Comprehensive identification of cell cycle-regulated genes of the yeast Saccharomyces cerevisiae by microarray hybridization. Mol Biol Cell *9*, 3273-3297.

Sprong, H., van der Sluijs, P., and van Meer, G. (2001). How proteins move lipids and lipids move proteins. Nat Rev Mol Cell Biol *2*, 504-513.

Stalberg, K., Neal, A.C., Ronne, H., and Stahl, U. (2008). Identification of a novel GPCAT activity and a new pathway for phosphatidylcholine biosynthesis in S. cerevisiae. J Lipid Res *49*, 1794-1806.

Stefan, C.J., Manford, A.G., Baird, D., Yamada-Hanff, J., Mao, Y., and Emr, S.D.Z. (2011). Osh proteins regulate phosphoinositide metabolism at ER-plasma membrane contact sites. Cell *144*, 389-401.

Summers, E.F., Letts, V.A., McGraw, P., and Henry, S.A. (1988). Saccharomyces cerevisiae cho2 mutants are deficient in phospholipid methylation and cross-pathway regulation of inositol synthesis. Genetics *120*, 909-922.

Surma, M.A., Klose, C., Klemm, R.W., Ejsing, C.S., and Simons, K. (2011). Generic sorting of raft lipids into secretory vesicles in yeast. Traffic *12*, 1139-1147.

Szabadkai, G., and Duchen, M.R. (2009). Mitochondria mediated cell death in diabetes. Apoptosis *14*, 1405-1423.

Tada, T., Simonetta, A., Batterton, M., Kinoshita, M., Edbauer, D., and Sheng, M. (2007). Role of Septin cytoskeleton in spine morphogenesis and dendrite development in neurons. Curr Biol *17*, 1752-1758.

Takeshima, H., Komazaki, S., Nishi, M., Iino, M., and Kangawa, K. (2000). Junctophilins: a novel family of junctional membrane complex proteins. Mol Cell *6*, 11-22.

Takizawa, P.A., DeRisi, J.L., Wilhelm, J.E., and Vale, R.D. (2000). Plasma membrane compartmentalization in yeast by messenger RNA transport and a septin diffusion barrier. Science *290*, 341-344.

Tanaka, K., Fujimura-Kamada, K., and Yamamoto, T. (2011). Functions of phospholipid flippases. J Biochem *149*, 131-143.

Tang, X., Germain, B.S., and Lee, W.L. (2012). A novel patch assembly domain in Num1 mediates dynein anchoring at the cortex during spindle positioning. J Cell Biol *196*, 743-756.

Tarassov, K., Messier, V., Landry, C.R., Radinovic, S., Serna Molina, M.M., Shames, I., Malitskaya, Y., Vogel, J., Bussey, H., and Michnick, S.W. (2008). An in vivo map of the yeast protein interactome. Science *320*, 1465-1470.

Tehlivets, O., Malanovic, N., Visram, M., Pavkov-Keller, T., and Keller, W. (2013). S-adenosyl-L-homocysteine hydrolase and methylation disorders: Yeast as a model system. Biochim Biophys Acta *1832*, 204-215.

Teuling, E., van Dis, V., Wulf, P.S., Haasdijk, E.D., Akhmanova, A., Hoogenraad, C.C., and Jaarsma, D. (2008). A novel mouse model with impaired dynein/dynactin function develops amyotrophic lateral sclerosis (ALS)-like features in motor neurons and improves lifespan in SOD1-ALS mice. Hum Mol Genet *17*, 2849-2862.

Thibault, G., Shui, G., Kim, W., McAlister, G.C., Ismail, N., Gygi, S.P., Wenk, M.R., and Ng, D.T. (2012). The membrane stress response buffers lethal effects of lipid disequilibrium by reprogramming the protein homeostasis network. Mol Cell *48*, 16-27.

Toikkanen, J.H., Miller, K.J., Soderlund, H., Jantti, J., and Keranen, S. (2003). The beta subunit of the Sec61p endoplasmic reticulum translocon interacts with the exocyst complex in Saccharomyces cerevisiae. J Biol Chem *278*, 20946-20953.

Tong, A.H., and Boone, C. (2006). Synthetic genetic array analysis in Saccharomyces cerevisiae. Methods Mol Biol *313*, 171-192.

Toulmay, A., and Prinz, W.A. (2011). Lipid transfer and signaling at organelle contact sites: the tip of the iceberg. Curr Opin Cell Biol *23*, 458-463.

Toulmay, A., and Prinz, W.A. (2012). A conserved membrane-binding domain targets proteins to organelle contact sites. J Cell Sci *125*, 49-58.

Travers, K.J., Patil, C.K., Wodicka, L., Lockhart, D.J., Weissman, J.S., and Walter, P. (2000). Functional and genomic analyses reveal an essential coordination between the unfolded protein response and ER-associated degradation. Cell *101*, 249-258.

Treves, S., Franzini-Armstrong, C., Moccagatta, L., Arnoult, C., Grasso, C., Schrum, A., Ducreux, S., Zhu, M.X., Mikoshiba, K., Girard, T., *et al.* (2004). Junctate is a key element in calcium entry induced by activation of InsP3 receptors and/or calcium store depletion. J Cell Biol *166*, 537-548.

Trivedi, D., and Padinjat, R. (2007). RdgB proteins: functions in lipid homeostasis and signal transduction. Biochim Biophys Acta *1771*, 692-699.

Trotter, P.J., Pedretti, J., and Voelker, D.R. (1993). Phosphatidylserine decarboxylase from Saccharomyces cerevisiae. Isolation of mutants, cloning of the gene, and creation of a null allele. J Biol Chem *268*, 21416-21424.

Trotter, P.J., and Voelker, D.R. (1995). Identification of a non-mitochondrial phosphatidylserine decarboxylase activity (PSD2) in the yeast Saccharomyces cerevisiae. J Biol Chem *270*, 6062-6070.

Tsai, Y.C., and Weissman, A.M. (2010). The Unfolded Protein Response, Degradation from Endoplasmic Reticulum and Cancer. Genes Cancer *1*, 764-778.

Urbani, L., and Simoni, R.D. (1990). Cholesterol and vesicular stomatitis virus G protein take separate routes from the endoplasmic reticulum to the plasma membrane. J Biol Chem *265*, 1919-1923.

Vaden, D.L., Gohil, V.M., Gu, Z., and Greenberg, M.L. (2005). Separation of yeast phospholipids using one-dimensional thin-layer chromatography. Anal Biochem *338*, 162-164.

van Meer, G., and Holthuis, J.C. (2000). Sphingolipid transport in eukaryotic cells. Biochim Biophys Acta *1486*, 145-170.

van Meer, G., and Lisman, Q. (2002). Sphingolipid transport: rafts and translocators. J Biol Chem *277*, 25855-25858.

van Meer, G., Voelker, D.R., and Feigenson, G.W. (2008). Membrane lipids: where they are and how they behave. Nat Rev Mol Cell Biol *9*, 112-124.

Vance, D.E., Walkey, C.J., and Cui, Z. (1997). Phosphatidylethanolamine N-methyltransferase from liver. Biochim Biophys Acta *1348*, 142-150.

Vance, J.E. (1990). Phospholipid synthesis in a membrane fraction associated with mitochondria. J Biol Chem *265*, 7248-7256.

Vance, J.E. (1991). Newly made phosphatidylserine and phosphatidylethanolamine are preferentially translocated between rat liver mitochondria and endoplasmic reticulum. J Biol Chem *266*, 89-97.

Vance, J.E. (2003). Molecular and cell biology of phosphatidylserine and phosphatidylethanolamine metabolism. Prog Nucleic Acid Res Mol Biol *75*, 69-111.

Vance, J.E., Aasman, E.J., and Szarka, R. (1991). Brefeldin A does not inhibit the movement of phosphatidylethanolamine from its sites for synthesis to the cell surface. J Biol Chem *266*, 8241-8247.

Vance, J.E., and Steenbergen, R. (2005). Metabolism and functions of phosphatidylserine. Prog Lipid Res *44*, 207-234.

Vashist, S., and Ng, D.T. (2004). Misfolded proteins are sorted by a sequential checkpoint mechanism of ER quality control. J Cell Biol *165*, 41-52.

Venable, R.M., Zhang, Y., Hardy, B.J., and Pastor, R.W. (1993). Molecular dynamics simulations of a lipid bilayer and of hexadecane: an investigation of membrane fluidity. Science *262*, 223-226.

Verfaillie, T., Rubio, N., Garg, A.D., Bultynck, G., Rizzuto, R., Decuypere, J.P., Piette, J., Linehan, C., Gupta, S., Samali, A., *et al.* (2012). PERK is required at the ER-mitochondrial contact sites to convey apoptosis after ROS-based ER stress. Cell Death Differ *19*, 1880-1891.

Versele, M., and Thorner, J. (2005). Some assembly required: yeast septins provide the instruction manual. Trends Cell Biol *15*, 414-424.

Villasmil, M.L., Bankaitis, V.A., and Mousley, C.J. (2012). The oxysterol-binding protein superfamily: new concepts and old proteins. Biochem Soc Trans *40*, 469-473.

Voelker, D.R. (1991). Organelle biogenesis and intracellular lipid transport in eukaryotes. Microbiol Rev *55*, 543-560.

Voelker, D.R. (2005). Bridging gaps in phospholipid transport. Trends Biochem Sci *30*, 396-404.

Voelker, D.R. (2009). Genetic and biochemical analysis of non-vesicular lipid traffic. Annu Rev Biochem *78*, 827-856.

Voeltz, G.K., Prinz, W.A., Shibata, Y., Rist, J.M., and Rapoport, T.A. (2006). A class of membrane proteins shaping the tubular endoplasmic reticulum. Cell *124*, 573-586.

Voeltz, G.K., Rolls, M.M., and Rapoport, T.A. (2002). Structural organization of the endoplasmic reticulum. EMBO Rep *3*, 944-950.

Vorvis, C., Markus, S.M., and Lee, W.L. (2008). Photoactivatable GFP tagging cassettes for protein-tracking studies in the budding yeast Saccharomyces cerevisiae. Yeast *25*, 651-659.

Voss, C., Lahiri, S., Young, B.P., Loewen, C.J., and Prinz, W.A. (2012). ER-shaping proteins facilitate lipid exchange between the ER and mitochondria in S. cerevisiae. J Cell Sci *125*, 4791-4799.

Wachtler, V., Rajagopalan, S., and Balasubramanian, M.K. (2003). Sterol-rich plasma membrane domains in the fission yeast Schizosaccharomyces pombe. J Cell Sci *116*, 867-874.

Wagenknecht, T., Hsieh, C.E., Rath, B.K., Fleischer, S., and Marko, M. (2002). Electron tomography of frozen-hydrated isolated triad junctions. Biophys J *83*, 2491-2501.

Wagner, W., Brenowitz, S.D., and Hammer, J.A., 3rd (2011). Myosin-Va transports the endoplasmic reticulum into the dendritic spines of Purkinje neurons. Nat Cell Biol *13*, 40-48.

Walkey, C.J., Shields, D.J., and Vance, D.E. (1999). Identification of three novel cDNAs for human phosphatidylethanolamine N-methyltransferase and localization of the human gene on chromosome 17p11.2. Biochim Biophys Acta *1436*, 405-412.

Wang, F., Zhao, Y., and Wang, P. (2003). Separation and determination of phospholipids in biological samples by high-performance liquid chromatography. J Chromatogr Sci *41*, 142-144.

Watanabe, R., Funato, K., Venkataraman, K., Futerman, A.H., and Riezman, H. (2002). Sphingolipids are required for the stable membrane association of glycosylphosphatidylinositol-anchored proteins in yeast. J Biol Chem *277*, 49538-49544.

Waterman-Storer, C.M., and Salmon, E.D. (1998). Endoplasmic reticulum membrane tubules are distributed by microtubules in living cells using three distinct mechanisms. Curr Biol *8*, 798-806.

Wera, S., Bergsma, J.C., and Thevelein, J.M. (2001). Phosphoinositides in yeast: genetically tractable signalling. FEMS Yeast Res *1*, 9-13.

West, M., Zurek, N., Hoenger, A., and Voeltz, G.K. (2011). A 3D analysis of yeast ER structure reveals how ER domains are organized by membrane curvature. J Cell Biol *193*, 333-346.

Wicky, S., Schwarz, H., and Singer-Kruger, B. (2004). Molecular interactions of yeast Neo1p, an essential member of the Drs2 family of aminophospholipid translocases, and its role in membrane trafficking within the endomembrane system. Mol Cell Biol *24*, 7402-7418.

Wiederkehr, A., Du, Y., Pypaert, M., Ferro-Novick, S., and Novick, P. (2003). Sec3p is needed for the spatial regulation of secretion and for the inheritance of the cortical endoplasmic reticulum. Mol Biol Cell *14*, 4770-4782.

Wiedmer, T., Zhou, Q., Kwoh, D.Y., and Sims, P.J. (2000). Identification of three new members of the phospholipid scramblase gene family. Biochim Biophys Acta *1467*, 244-253.

Wilcox, L.J., Balderes, D.A., Wharton, B., Tinkelenberg, A.H., Rao, G., and Sturley, S.L. (2002). Transcriptional profiling identifies two members of the ATP-binding cassette transporter superfamily required for sterol uptake in yeast. J Biol Chem *277*, 32466-32472.

Williamson, R. (2012). Scientists complete miRNA profiling of carcinogen-induced and spinach-fed colon tumors. Epigenomics *4*, 480.

Wolf, W., Kilic, A., Schrul, B., Lorenz, H., Schwappach, B., and Seedorf, M. (2012). Yeast Ist2 recruits the endoplasmic reticulum to the plasma membrane and creates a ribosome-free membrane microcompartment. PLoS One *7*, e39703.

Wu, W.I., and Voelker, D.R. (2001). Characterization of phosphatidylserine transport to the locus of phosphatidylserine decarboxylase 2 in permeabilized yeast. J Biol Chem *276*, 7114-7121.

Xiang, X. (2003). LIS1 at the microtubule plus end and its role in dynein-mediated nuclear migration. J Cell Biol *160*, 289-290.

Xie, W., and Ng, D.T. (2010). ERAD substrate recognition in budding yeast. Semin Cell Dev Biol *21*, 533-539.

Xie, Y., Vessey, J.P., Konecna, A., Dahm, R., Macchi, P., and Kiebler, M.A. (2007). The GTP-binding protein Septin 7 is critical for dendrite branching and dendritic-spine morphology. Curr Biol *17*, 1746-1751.

Xu, Z., Su, W.M., and Carman, G.M. (2012). Fluorescence spectroscopy measures yeast PAH1-encoded phosphatidate phosphatase interaction with liposome membranes. J Lipid Res *53*, 522-528.

Yeh, E., Skibbens, R.V., Cheng, J.W., Salmon, E.D., and Bloom, K. (1995). Spindle dynamics and cell cycle regulation of dynein in the budding yeast, Saccharomyces cerevisiae. J Cell Biol *130*, 687-700.

Yoshida, H., Matsui, T., Yamamoto, A., Okada, T., and Mori, K. (2001). XBP1 mRNA is induced by ATF6 and spliced by IRE1 in response to ER stress to produce a highly active transcription factor. Cell *107*, 881-891.

Young, B.P., Shin, J.J., Orij, R., Chao, J.T., Li, S.C., Guan, X.L., Khong, A., Jan, E., Wenk, M.R., Prinz, W.A., *et al.* (2010). Phosphatidic acid is a pH biosensor that links membrane biogenesis to metabolism. Science *329*, 1085-1088.

Zachowski, A. (1993). Phospholipids in animal eukaryotic membranes: transverse asymmetry and movement. Biochem J *294 (Pt 1)*, 1-14.

Zinser, E., Sperka-Gottlieb, C.D., Fasch, E.V., Kohlwein, S.D., Paltauf, F., and Daum, G. (1991). Phospholipid synthesis and lipid composition of subcellular membranes in the unicellular eukaryote Saccharomyces cerevisiae. J Bacteriol *173*, 2026-2034.

Zurek, N., Sparks, L., and Voeltz, G. (2011). Reticulon short hairpin transmembrane domains are used to shape ER tubules. Traffic *12*, 28-41.